

2011

# HYDROGEN PRODUCTION FROM BIOMASS BY INTEGRATING THERMO-CHEMICAL AND BIOLOGICAL PROCESSES

Rafael Orozco-Pulido

A thesis submitted to  
The University of Birmingham  
for the degree of  
DOCTOR OF PHILOSOPHY

School of biosciences

The University of Birmingham, UK



UNIVERSITY OF  
BIRMINGHAM

**University of Birmingham Research Archive**

**e-theses repository**

This unpublished thesis/dissertation is copyright of the author and/or third parties. The intellectual property rights of the author or third parties in respect of this work are as defined by The Copyright Designs and Patents Act 1988 or as modified by any successor legislation.

Any use made of information contained in this thesis/dissertation must be in accordance with that legislation and must be properly acknowledged. Further distribution or reproduction in any format is prohibited without the permission of the copyright holder.

## ***Abstract***

The purpose of this research was to contribute to the development of H<sub>2</sub> production technologies from biomass. The study integrated thermochemical processes to achieve biomass hydrolysis with biological methods to then obtain H<sub>2</sub> by the fermentation of these hydrolysates using *E. coli*.

Different strains of *E. coli* were tested under controlled conditions in 3 L scale fermentations with the aim to find the most useful strain for the fermentation process in terms of H<sub>2</sub> produced and the subsequent hydrogen production potential of the organic acid co-products in a downstream photofermentation. Among the strains tested FTD89, FTD67 and RL009 gave the best results, however ethanol was successfully abolished by strain RL009 making this strain more suitable for long term fermentations.

Model polysaccharide compounds such as starch and cellulose, and representative food and lignocellulosic wastes were hydrolysed in hot compressed water in the presence of CO<sub>2</sub> under pressure and various temperatures to produce hydrolysates with high sugar content suitable for fermentation for H<sub>2</sub> production. Optimum hydrolysis conditions for maximum sugar yields for each compound were determined. Fermentation of the obtained hydrolysates yielded acceptable amounts of H<sub>2</sub> after their 'detoxification' with activated carbon (AC), comparable to H<sub>2</sub> yielded by the glucose controls in all cases. The maximum yield of glucose after HCW treatment was obtained from starch at 200 °C yielding 548 g C.kg C initial starch<sup>-1</sup>; maximum glucose yield from cellulose was 225 g C.Kg C initial cellulose<sup>-1</sup> obtained from cellulose hydrolysis at 250 °C, and the glucose yield from food waste was 45.5 g.g food waste<sup>-1</sup>. The main degradation product (DP) from these hydrolysates was 5-Hydroxymethylfurfural (5-HMF), whereas the main DP obtained from the lignocellulosic wastes was Furfural. Both were successfully removed by AC treatment.

The best hydrolysate obtained from wastes was evaluated for H<sub>2</sub> production at 3 L scale. Despite obtaining low H<sub>2</sub> yields improvements would be possible and are discussed. Fermentations for H<sub>2</sub> production at pilot plant scale were also trialled, indicating key areas for future development for successful scale up.

**Dedicated to:**

God,

To Rocio<sup>†</sup>

And, very specially to my wife Marycarmen and my children Rafael, Dulcenary and Fermin.

## *Acknowledgements*

Very special thanks to my supervisor Professor Lynne E. Macaskie for all her invaluable support, patience, guidance and understanding throughout my PhD.

To Professor Gary Leeke for all his help and collaboration and Professor Regina Santos.

Also I appreciate and thank the invaluable help, collaboration and friendship of Dr. Mark D. Redwood at all times throughout my PhD. His support helped me to improve and add value to my PhD.

Special thanks to all my lab mates who I owe a great debt: Dr. Kevin D. Planche, Dr. Claire Mennan, Dr. Ping Yong, Dr. Marion Petterson, Dr. Neil Crammer, Dr. Inina Mihkeenko, Miss Angela Murray for their collaboration, willingness and enthusiasm always available to help.

All my colleagues from other departments and Universities who also provided help with valuable discussions and assistance: Dr. Ali Bahari, Mr. Ricardo Roque, Professor Xu-Zhang.

Thanks to my parents for all their support at all times.

Thanks to CONACYT for funding my throughout my study.

Thanks to the University of Birmingham, staff and other institutions (BBSRC, EPSRC) for all their collaboration during my studies.

And last but not least, to the Staff House and everyone who worked there during my PhD. This was the place where every Friday I met with friends to share great moments (and some pints) and to discuss important diverse topics, it became a meaningful part of my social life at the University.

## ***Statement***

I declare that this thesis contains no material which has been accepted for the award of any other degree or diploma in any University and that, to the best of my knowledge, this thesis contains no materials written by any person except where due reference is given in the text of this thesis.

Rafael L Orozco

## ***Layout of the thesis***

Each chapter is presented in form of a scientific paper; beginning with an abstract/introduction which defines the focus of the chapter and present information relevant to the work, followed by a method and analysis section, a results and discussion section and conclusions. Additional methodology is described in the appendices. Participations in seminars, conferences and other relevant work is also in the appendix section. References were added at the end of the thesis.

## TABLE OF CONTENTS

<b>I.</b>	<b>INTRODUCTION .....</b>	<b>1</b>
I.1	CLIMATE CHANGE.....	1
I.2	WASTE DISPOSAL .....	4
I.3	ENERGY .....	6
I.4	THE CHALLENGE, ACTIONS AND POLICIES. ....	11
I.5	TOWARDS THE HYDROGEN ECONOMY.....	14
<b>II.</b>	<b>HYDROGEN PRODUCTION TECHNOLOGIES.....</b>	<b>19</b>
II.1	HYDROGEN FROM STEAM REFORMING OF METHANE .....	19
II.2	HYDROGEN FROM WATER ELECTROLYSIS.....	21
II.3	HYDROGEN FROM BIOMASS UTILISATION .....	23
II.3.1	<i>Thermochemical processes.....</i>	<i>28</i>
II.4	BIOLOGICAL METHODS.....	39
II.4.1	<i>Biophotolysis of water.....</i>	<i>40</i>
II.4.2	<i>Photo fermentative processes.....</i>	<i>41</i>
II.4.3	<i>Dark fermentation.....</i>	<i>43</i>
II.4.4	<i>Hybrid systems for H<sub>2</sub> production.....</i>	<i>50</i>
<b>III.</b>	<b>BIOMASS HYDROLYSIS METHODS .....</b>	<b>56</b>
<b>IV.</b>	<b>AIMS AND OBJECTIVES .....</b>	<b>62</b>
<b>V.</b>	<b>LAYOUT OF THE THESIS.....</b>	<b>64</b>
<b>VI.</b>	<b>RESULTS AND DISCUSSIONS.....</b>	<b>68</b>
VI.1	<i>E. COLI</i> STRAIN EVALUATION FOR H <sub>2</sub> PRODUCTION.....	69
VI.1.1	<i>E. coli</i> strains evaluation for H <sub>2</sub> , OA and ethanol production.....	70
VI.1.2	<i>Strains RL007 and RL009 in comparison to parent strain MC4100.....</i>	<i>86</i>
VI.1.3	<i>Towards an integrated system for bio-energy.....</i>	<i>97</i>
VI.2	HYDROGEN FROM STARCH.....	117
VI.3	HYDROGEN FROM CELLULOSE.....	139
VI.3.1	<i>Paper on HCW hydrolysis of cellulose .....</i>	<i>139</i>
VI.3.2	<i>Comparison between HCW cellulose hydrolysis set 1 and set 2 experiments.....</i>	<i>159</i>
VI.4	HYDROGEN FROM BIOWASTES.....	163
VI.5	HYDROGEN FROM BIOMASS BY HCW AND EXTRACTIVE FERMENTATION.....	190
VI.5.1	<i>Electroextractive fermentation for efficient biohydrogen production.....</i>	<i>190</i>
VI.5.2	<i>An integrated biohydrogen refinery: Synergy of photofermentation, extractive fermentation and hydrothermal hydrolysis of food wastes.....</i>	<i>210</i>
VI.6	PILOT PLANT .....	213
<b>VII.</b>	<b>GENERAL DISCUSSION: OUTCOMES WITH RESPECT TO OBJECTIVES .....</b>	<b>226</b>
VII.1	FINAL DISCUSSION AND CONCLUSIONS .....	227
<b>VIII.</b>	<b>APPENDICES .....</b>	<b>233</b>
VIII.1	APENDIX I. METHODS OF CELL GROWTH AND TESTING .....	233
VIII.1.1	<i>Aerobic pre-growth in flask and harvesting of cells (for chapter VI.1).....</i>	<i>233</i>

VIII.1.2	<i>Aerobic pre-growth in fermenter (EF media) (for chapter VI.4)</i> .....	233
VIII.1.3	<i>Fermentation media formula (for chapter VI.1)</i> .....	234
VIII.1.4	<i>15 mL H<sub>2</sub> fermentation tests (for chapters VI.2, VI.3 and VI.4)</i> .....	234
VIII.1.5	<i>Media for growth tests (for chapters VI.3 and VI.4)</i> .....	235
VIII.2	APPENDIX II. GAS ANALYSIS AND MEASUREMENTS.....	236
VIII.2.1	<i>Combustible gas meter (CGM)</i> .....	236
VIII.2.2	<i>Water height displacement column (WHDC)</i> .....	238
VIII.2.3	<i>Low flow gasmeters (LFG)</i> .....	238
VIII.3	APPENDIX III. DETOXIFICATION METHOD .....	241
VIII.4	APPENDIX IV. QUANTITATIVE CHEMICAL ANALYSIS .....	242
VIII.4.1	<i>DNSA assay for glucose quantification</i> .....	242
VIII.4.2	<i>Total Organic Carbon (TOC)</i> .....	243
VIII.4.3	<i>Lignin determination</i> .....	244
VIII.4.4	<i>Saccharification of cellulose</i> .....	246
VIII.5	APPENDIX V. CONFERENCES AND ADDITIONAL PUBLICATIONS .....	247
VIII.5.1	<i>An Integrated biohydrogen refinery: Synergy of photofermentation, extractive fermentation and hydrothermal hydrolysis of food wastes</i> .....	247
VIII.5.2	<i>Conference posters</i> .....	271
VIII.5.3	<i>Conference presentations</i> .....	271
VIII.6	APPENDIX VIII.6 PARTICIPATION IN OTHER RELATED PROJECTS .....	272
VIII.6.1	<i>Biowaste2energy research base</i> .....	272
VIII.6.2	<i>Growth of <i>Spirulina plantensis</i></i> .....	278
<b>IX.</b>	<b>REFERENCES</b> .....	<b>301</b>

## List of figures

FIG. 1 GHG EMISSIONS BY SOURCE IN TERMS OF CO <sub>2EQ</sub> BY 2004.....	3
FIG. 2 TRENDS AND PROJECTIONS ON CO <sub>2</sub> ATMOSPHERIC CONCENTRATIONS AND TEMPERATURE CHANGE .....	3
FIG. 3 WORLD MARKETED ENERGY CONSUMPTION. ....	7
FIG. 4 A) WORLD ENERGY USE (WEU) BY TYPE AND B) WORLD ENERGY GENERATION (WEG) .....	8
FIG. 5 OIL PRICES; HISTORY (BEFORE 2009) AND PROJECTIONS (AFTER 2009). ....	8
FIG. 6 ENERGY CONSUMPTION BY SECTOR A) IN US; B) IN UK.. ....	10
FIG. 7 DAILY AVERAGE OIL WORLD PRODUCTION, THE DASHED LINES ARE PROJECTIONS FROM 2010. ....	10
FIG. 8 DIAGRAM OF THE DIFFERENT ELEMENTS CONTEMPLATED BY THE STRATEGIC PLANS TO SUPPORT THE DEVELOPMENT OF H <sub>2</sub> ENERGY INFRASTRUCTURE. ....	16
FIG. 9 A) H <sub>2</sub> POWERED CAR SHOWN AT THE WORLD HYDROGEN ENERGY CONVENTION, GERMANY 2010.....	18
FIG. 10 A) AMYLOPECTIN MOLECULE STRUCTURE AND B) AMYLOSE .....	25
FIG. 11 MOLECULAR STRUCTURE OF CELLULOSE.....	26
FIG. 12 STRUCTURE OF HEMICELLULOSE .....	27
FIG. 13 SHOWS A MODEL OF A LIGNIN MOLECULE .....	28
FIG. 14 THERMAL DEGRADATION SEQUENCE OF MAIN COMPONENTS OF BIOMASS .....	37
FIG. 15 METABOLIC PATHWAYS INVOLVED IN MIXED ACID FERMENTATION. ....	48
FIG. 16 WASTE WATER TREATMENT FACILITY FOR CH <sub>4</sub> AND H <sub>2</sub> GENERATION LOCATED IN ESSEN, GERMANY.....	53
FIG. 17 SIMPLIFIED REPRESENTATION OF THE ED CELL .....	55
FIG. 18 ILUSTRATION OF AN EXTRACTIVE FERMENTATION UNIT IN OPERATION WITH IMPORTANT PARTS LABELLED. ....	56
FIG. 19 IN TOP PICTURE HIGH PRESSURE REACTOR SYSTEM FOR HCW HYDROLYSIS EXPERIMENTS .....	61
FIG. 20 DIAGRAM OUTLINING THIS RESEARCH PROJECT.....	67
FIG. 21 HYDROGEN YIELDS FOR STRAINS (●) HD701; (X) FTD89; (◇) FTD67; AND PARENT STRAIN (Δ) MC4100. ....	79
FIG. 22 RATES OF H <sub>2</sub> PRODUCTION BY STRAINS: (A) MC4100; (B) HD701; (C) FTD89; (D) FTD67. ....	80
FIG. 23 OA YIELDS BY STRAIN HD701.....	83
FIG. 24 OA YIELDS BY STRAINS (×) FTD89, (◇) FTD67 AND PARENT STRAIN (Δ) MC4100 .....	83
FIG. 25 DIAGRAM OF CENTRAL METABOLIC NETWORK TO ACETATE/ACETYL COA MADE BY <i>E. COLI</i> . ....	88
FIG. 26 HYDROGEN YIELDS BY STRAINS (Δ) MC4100; (O) RL007; (■) RL009.....	93
FIG. 27 RATES OF H <sub>2</sub> PRODUCTION BY STRAINS: (A) MC4100; (B) RL007; (C) RL009. ....	94
FIG. 28 ORGANIC ACID BY STRAINS: (Δ) MC4100; (O) RL007; (□) RL009.....	94
FIG. 29 MC4100 LACTATE-BUTYRATE RELATIONSHIP; RL007 & RL009 PYRUVATE-BUTYRATE RELATIONSHIP. ....	95
FIG. 30 DEGRADATION PATHWAY OF LIGNOCELLULOSIC COMPOUNDS .....	169
FIG. 31 <i>E. COLI</i> HD701 GROWTH VS. INHIBITOR CONCENTRATION.....	174
FIG. 32 YIELDS OF <i>E. COLI</i> HD701 H <sub>2</sub> FERMENTATION AT DIFFERENT DP CONCENTRATIONS .....	175
FIG. 33 SHOWS YIELDS OF PRODUCTS IN BG HYDROLYSATES BEFORE AC AT DIFFERENT REACTION TEMPERATURES. ....	179
FIG. 34 HPLC CHROMATOGRAPH FOR BG HYDROLYSATE AT 220 °C BEFORE AC.....	180
FIG. 35 SHOWS YIELDS OF PRODUCTS IN FW HYDROLYSATE BEFORE AC AT DIFFERENT REACTION TEMPERATURES.....	181
FIG. 36 SHOW YIELDS OF PRODUCTS OF WS HYDROLYSATE BEFORE AC AT 220 AND 240 °C.....	182
FIG. 37 SHOWS HPLC CHROMATOGRAPHS FOR BG HYDROLYSATE AT 220 °C A) BEFORE AND B) AFTER AC .....	184
FIG. 38 SHOWS THE THREE STAGES OF THE FERMENTATION WITH <i>E. COLI</i> HD701 AND PRODUCT DISTRIBUTION OF FW HYDROLYSATES OBTAINED AT 220 °C AFTER AC .....	188
FIG. 39 SHOWS A MODEL OF A FERMENTATION SYSTEM.....	214
FIG. 40 TWIN FERMENTATION SYSTEM AT THE UNIVERSITY OF BIRMINGHAM. ....	215
FIG. 41 HD701 GROWTH AND pH DURING FERMENTATION TIME.....	224
FIG. 42 OA PRODUCED AND GLUCOSE CONSUMPTION BY HD701 WITH FERMENTATION TIME .....	224
FIG. 43 SCHEMATIZATION OF A BIO REFINERY PROCESS.....	232
FIG. 44 LOW FLOW GASMETER.....	239

FIG. 45 SHOWS THE DIFFERENCE IN (A) H<sub>2</sub> PRODUCTION (VERTICAL AXIS: MOL H<sub>2</sub> .MOL GLUCOSE<sup>-1</sup>) AND (B) H<sub>2</sub> RATES (VERTICAL AXIS: mL H<sub>2</sub>.H<sup>-1</sup>) PATHWAYS BY STRAIN MC4100.....240

FIG. 46 SHOWS THE DIFFERENCE IN (A) H<sub>2</sub> PRODUCTION (VERTICAL AXIS: mL H<sub>2</sub>) AND (B) H<sub>2</sub> RATES (VERTICAL AXIS: mL H<sub>2</sub>.H<sup>-1</sup>) PATHWAYS BY STRAIN HD701 .....240

## List of tables

TABLE 1 FOSSIL FUEL RESERVES (OIL, NATURAL GAS AND COAL) AND CONSUMPTION AS OF 2009.....	11
TABLE 2 COMMITMENTS IN REDUCTION OF CO <sub>2</sub> EMISSIONS AND IN UTILIZATION OF RENEWABLE SOURCES (RS) OF ENERGY IN TRANSPORT AND AS A SHARE OF TOTAL ENERGY PRODUCTION .....	12
TABLE 3 THE PROJECTED SCENARIO FOR THE INTRODUCTION OF H <sub>2</sub> FUEL CELL VEHICLES INTO THE EU MARKET.....	17
TABLE 4 MAIN GENES INVOLVED IN THE MIXED ACID FERMENTATION OF <i>E. COLI</i> FOR H <sub>2</sub> PRODUCTION. ....	49
TABLE 5 FORMULAS OF MAIN ORGANIC ACIDS GENERATED BY <i>E. COLI</i> .....	71
TABLE 6 <i>E. COLI</i> STRAINS UTILIZED IN THIS STUDY. ....	73
TABLE 7 A. SUMMARY TABLE SHOWING PRODUCT DISTRIBUTION PER STRAIN OF <i>E. COLI</i> .....	76
TABLE 8 FORMATE AND ETHANOL YIELDS BY <i>E. COLI</i> STRAINS IN 0.1 L FERMENTATIONS TESTS AND 3 L FERMENTATIONS .....	77
TABLE 9 ACETATE, LACTATE AND SUCCINATE BY <i>E. COLI</i> STRAINS IN 0.1 L FERMENTATION TESTS AND 3 L FERMENTATIONS.....	77
TABLE 10 HYDROGEN PRODUCTION POTENTIAL (HPP) IN MOL H <sub>2</sub> .MOL OA <sup>-1</sup> AFTER 45 H FERMENTATION TIME UNDER IMPROVED GROWTH REGIME .....	85
TABLE 11 PRODUCTS FORMED BY STRAINS RL007 AND RL009 COMPARED TO PARENT STRAIN MC4100. FOR RL007 AND RL009.....	86
TABLE 12 COMPARATIVE OF HYDROGEN PRODUCTION POTENTIAL (HPP) (MOL H <sub>2</sub> .MOL OA <sup>-1</sup> ) AFTER 45 H FERMENTATION PERIOD .....	89
TABLE 13 H <sub>2</sub> YIELDS AND HPP BY STRAIN AFTER TOTAL FERMENTATION PERIOD (55-66 H) .....	91
TABLE 14 BREAK EVEN CURRENT EFFICIENCY EXPECTED BY EACH OA PRODUCED AFTER PHOTOFERMENTATION. ....	91
TABLE 15 A COMPARATIVE OF REACTION PARAMETERS BETWEEN 1 <sup>ST</sup> AND 2 <sup>ND</sup> SET; STARTING MATERIAL IS CELLULOSE. ....	160
TABLE 16 A COMPARATIVE IN PRODUCT YIELD [G C (G C INITIAL CELLULOSE) <sup>-1</sup> ] BETWEEN BOTH SETS OF EXPERIMENTS.....	161
TABLE 17 CHARACTERIZATION OF FOOD WASTE, BREWERY GRAIN AND WHEAT STRAW. ....	177
TABLE 18 REACTION PARAMETERS FOR THE TESTED WASTES AT DIFFERENT TEMPERATURES. ....	178
TABLE 19 SHOWS HEXOSES (GLUCOSE, GALACTOSE AND FRUCTOSE) CONCENTRATION (MM) AND YIELDS [MG (G STARTING MATERIAL) <sup>-1</sup> ] IN THE HYDROLYSATES AFTER AC; CELL CONCENTRATION ON GROWTH TEST FOR FW, FOOD WASTE; BG, BREWERY GRAIN AND WS, WHEAT STRAW .....	183
TABLE 20 SAMPLES AND REAGENT PROPORTIONS ACCORDING TO ASSAY RANGE. ....	242

## ***List of abbreviations***

AC (Activated Carbon)  
ADP (Adenosin Tri-Phosphate)  
ATP (Adensione Tri-Phospahte)  
BTU (British thermal Unit)  
CHP (Combined Heat and Power)  
CCS (Carbon Capture and Storage)  
DB (Dried Biomass)  
DOE (Department of Energy)  
DECC (Department of Energy and Climate Change)  
DEFRA (Department for Environment, Food and Rural Affairs)  
ED (Electro Dialysis)  
EIA (Energy Information Administration)  
EU (European Union)  
FC (Fuel Cell)  
FHL (Formic hydrogen Lyase)  
FW (food waste)  
GHG (Green House Gas)  
GDP (Gross Domestic Product)  
gge (gallon gasoline equivalent)  
HCW (Hot Compressed Water)  
HHV (Higher heating value)  
HPLC (High Pressure Liquid Chromatography)  
LDH (Lactate Dehydrogenase)  
LHV (Lower heating Value)  
M (Million)  
MSW (Municipal Solid Waste)  
MBW (Municipal Biodegradable Waste)  
NAD<sup>+</sup> (Nicotinamide Adenine Dinucleotide)  
NADH (Hydrogen Nicotinamide Adenine Dinucleotide)  
OA (Organic Acid)

PEM (Proton Exchange Membrane)

PHB (Poly- $\beta$ -Hydroxybutyrate)

PFL (Pyruvate Formate Lyase)

PNS (Purple Non Sulphur)

SCW (Super Critical Water)

SMR (Steam Methane Reforming)

SOFC (Solid Oxide Fuel Cell)

SOEC (Solid Oxide Electrolyser Cells)

SG (Spent Grain)

US (United States)

UK (United Kingdom)

UNEP (United Nations Environment Programme)

WMO (World Meteorological Organization)

WB (Wet Biomass)

WE (Water Electrolysis)

WGS (Water Gas Shift)

# I. INTRODUCTION

The interaction between Earth and Human systems is more intense than ever before due to an accelerated socio economic development involving population growth, technology, trade, production and consumption patterns, and governance among others. As a consequence our natural resources on Earth are being rapidly consumed; varied land use practices are employed across the world as a result of urban sprawl while food security, desertification, soil erosion and degradation and looming consumption and exhaustion of our fossil fuel reserves to produce ~90 % of the energy we need are contemporary and increasing problems. Three major interconnected problems that seriously threaten our world and civilization arise from this global scenario: Climate change due to accumulation of greenhouse gases in the atmosphere, waste disposal and the need of renewable and environment friendly sources of energy [1]. In addition energy demand is increasing rapidly according to world population which is estimated to grow from 6 to 9 billion by 2050, number of light-duty vehicles is expected to increase from 1 to 2.8 billion cars by 2050 [2] and highly populated developing countries will become more energy intensive as they expand their economies[3, 4]. World Gross Domestic Product (GDP) (an indicator of world's economy) has been increasing from 21.9 Trillion US dollars in 1990 to 58.3 Trillion US dollars in 2009.

## I.1 Climate change

Climate change from global warming is evident from observations in global average air and ocean temperatures, widespread melting of snow and ice and rising of sea levels. The earth's surface temperature has been increasing 0.1 – 0.16 °C per decade during the last 50 years, arctic sea ice extent has shrunk by 2.7 % per decade with larger decreases in summer of 7.4 % with the first access by boat to the North Pole in open water reported in summer 2011; sea levels rose at an average of 1.8 mm.yr<sup>-1</sup> (1961- 2003) to 3.1 (1993 – 2003) [5]. Oceans have been taking up over 80 % of the heat being added to the climate system which could be associated with an increase in intense tropical cyclone activity in the North Atlantic since 1970 [1, 5]. In some recent events the unprecedented and devastating tornado activity in 7 southern states in US (2011), Pakistan floods (2010), China floods (2011) and the 50 mile wide dust storm that engulfed Arizona state in US (2011) among others.

A wide number of studies demonstrate that global warming and climate change are likely to be caused by the accumulation of green house gases (GHG) in the atmosphere [1, 6]. Main GHGs are CO<sub>2</sub>, methane (CH<sub>4</sub>), nitrous oxide (N<sub>2</sub>O) and halocarbons (gases containing chlorine, fluorine or bromine). The global atmospheric concentration of CO<sub>2</sub> increased from a preindustrial (1750) value ~ 280 ppm to 379 ppm in 2005, CH<sub>4</sub> increased from 715 ppb to 1732 ppb and N<sub>2</sub>O from 270 to 319 ppb [5, 6].

As can be observed, CO<sub>2</sub> is the most abundant anthropogenic GHG in the atmosphere and therefore the main contributor to climate change [5, 6]. It results from burning of fossil fuels and as of June 2011 CO<sub>2</sub> levels reached 390 ppm ([7-9] an average increase of 3.3 ppm.yr<sup>-1</sup> during the last 6 years which is 1.7 fold the average increase from 1995 – 2005 (Fig.1). The earth has warmed 0.7 °C since 1900, it has been projected that if no action is taken to control mainly CO<sub>2</sub> emissions, the concentration of GHG in the atmosphere could double its preindustrial level reaching 560 ppm as early as 2035 with a consequent temperature rise that could exceed 5 °C with severe major impacts in earth physical geography and peoples' lives (Fig. 2) and notably loss of the world's major coastal cities [6]. In efforts to define a level of danger caused by a GHG interference with the climate system in terms of global mean surface temperature change, a maximum of 2 °C above preindustrial levels is the most widely accepted climate policy target, at temperatures higher than 2 °C ecosystems will become extremely vulnerable [6, 10] . In terms of economics, what we do now will have an effect in the next 40 to 50 years. The risks of not taking action today will translate in costs (and risk of climate change) as high as 5 – 20 % of the global gross domestic product (GDP).yr<sup>-1</sup>. The poorest countries and populations will suffer earliest and most (floods, droughts, storms, etc). Instead, the cost of action would imply an estimated 1 % of global GDP.yr<sup>-1</sup> and bring stabilization [6]. The Stern report was ground-breaking being the first to show in clear economic terms the necessity to invest heavily now in CO<sub>2</sub> mitigation technologies and reduction in fossil fuel consumption by alternative approaches to energy production. The quest for alternative energy is no longer merely an attractive option but is inescapable goal of human civilization.

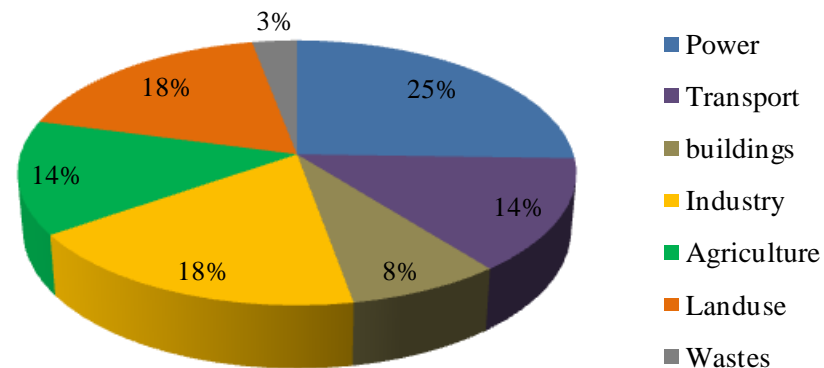


**Fig.1** GHG emissions by source in terms of CO<sub>2eq</sub> by 2004. Adapted from: IPCC 2007 report fig. 2.1 [5].

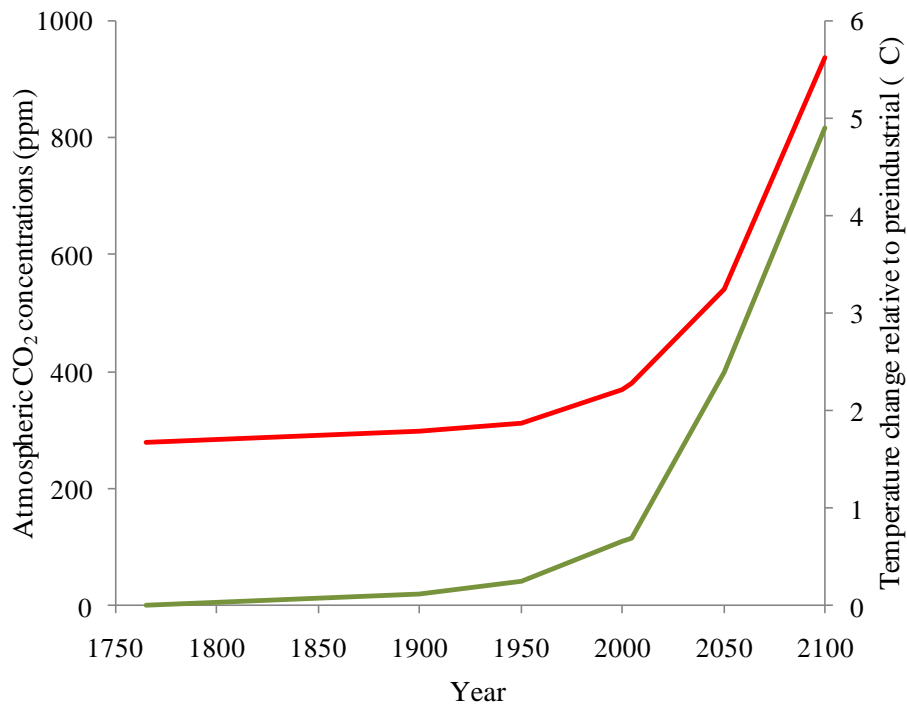


**Fig. 2** Trends and projections on CO<sub>2</sub> atmospheric concentrations (red) and temperature change (green) associated with the increase in CO<sub>2</sub> emissions, relative to preindustrial levels (1750). Adapted from Manuscript RCP GHG concentrations [11].

## I.2 Waste disposal

Waste is generated at all stages of the materials cycle (from extraction to consumption and waste treatment) in urban and rural areas. The amount of waste generated and the way it is managed influence their environmental impacts, for example through the emission of pollutants and the demand for energy or land, and on human health, especially in the case of poor waste management. Important waste streams of special focus in this work are municipal solid wastes (MSW) and agricultural wastes. These wastes are rich in organic biodegradable materials, therefore having potentially high environmental impacts compared to other types, especially if poorly managed since they are capable of undergoing anaerobic or aerobic decomposition (biodegradability) generating methane ( $\text{CH}_4$ ),  $\text{CO}_2$  and toxic leachate (liquid of varying composition that drains from a landfill into the ground water contaminating water springs and flushes). Emissions of methane from landfill sites make a contribution to global warming due the fact that methane is a 25 times more potent greenhouse gas than  $\text{CO}_2$  [6, 12].

*Solid wastes* are generally disposed in landfills which have been classified according to the type of waste generated as: Inert (mining, quarrying, white glass, construction and demolition wastes); Non hazardous (generated household and commercial waste) and Hazardous (solvents, chemical products, pharmaceuticals, batteries, radioactive materials wastes among others). Each carries a financial penalty for its disposal to landfill (see section I.4) and in response biodegradable waste is now generally segregated for composting or anaerobic digestion (AD) and many materials can be regulated due to development in recycling technologies in parallel with development of clean technologies such as biodegradable plastics.

*Inert wastes* represent a significant portion of the waste generated, it accounted for ~57- 61 % of the waste generated in EU in 2006.

*Non-hazardous wastes* include MSW which contain municipal biodegradable waste (MBW) (food, paper, wood, and yard trimmings); and plastics, metals, textiles, leather among others. MBW represented approximately 64.5 % of the MSW generated in US (243 M tones, approx. 820 Kg per person per annum) and as such is an abundant renewable resource that guarantees sustainability for industrial applications through recycling, incineration for energy recovery or biological reprocessing (composting or anaerobic digestion). In US in 2009, 82 M tonnes of MSW recycled provided an annual benefit of 178 M metric tonnes of  $\text{CO}_{2\text{eq}}$  reduced that is comparable to the annual GHG emissions from almost 33 M vehicles [13]. In Europe 258 M tonnes of municipal waste were

generated in 2010 and 280 M tonnes projected by 2020, recycling would increase from 40 % in 2008 to 49 % by 2020 [14]. Adequate waste management is necessary for the reduction of landfill and GHG emissions.

**Sewage** is water carrying waste in solution or in suspension from residences or institutions containing body wastes, washing water, food preparation wastes, laundry wastes, and other waste products of normal living which are classed as domestic or sanitary sewage. They also include liquid carried wastes from stores and service establishments (commercial waste) and industry (industrial wastes). Surface runoff (mainly rain water) flows also to defined channels; this water contains absorbed gases and particles from the atmosphere, dissolved and leached materials from vegetation and soil, washed spills and debris from urban streets and highways carrying these pollutants as wastes in its flow to a collection point which is often a river [15]. Such run-offs are in fact a resource since they contain high levels of precious and scarce metals (Pd, Pt, Rh) which are shed from automotive catalysts from today's cars but which are vital resources for the clean H<sub>2</sub> fuel cell propelled vehicles of tomorrow.

**Agricultural waste** is waste produced at agricultural sites as a result of agricultural and farming activity, this includes:

**Manure** from a variety of livestock and poultry which is the largest problem as shown: Farm yard manure ~54%; Slurry (water and animal waste) ~39 %; straw ~ 3%; traditional ways to reprocess these wastes are: as fertilizers, biological treatment, gasification and also burning (no longer acceptable). A regular practice is to spread manure wastes at the place of production for the benefit of agriculture (as fertilizers) however manure management is a critical component in improving environment and water quality [16].

**Agricultural residues** (wheat, rice and corn straw, corn stover, grass, etc) are the biomass materials remaining after harvesting agricultural crops; they constitute an important biomass resource. Because of its abundance and availability, wheat straw (WS) is an opportunity feedstock for biotechnology plants in the intermediate future. Potential products include bioethanol, biohydrogen, biogas, polymers and a wide range of high value pharmaceuticals, nutraceuticals and chemicals. In 2000 the availability of WS in the EU was ~44 M tonnes.yr<sup>-1</sup> [17], up 7-fold on 2007. Total agricultural waste including manure and agricultural residues in the UK is ~ 110 M tonnes per year [17-20].

**Spent grains** (SG) are the by-products of the mashing process in brewing and, depending on the separation process, the amount of brewers' SG would be 85 % of the total by products [21, 22].

About 3.4 M tonnes of brewery SG are produced in the EU every year and UK contributes with 0.5 M tonnes annually. Brazil, the 4<sup>th</sup> largest beer producer, generated 1.7 M tonnes of SG in 2002 [23]. Therefore, brewery SG is a high volume low cost by-product valuable for bio-processing. Brazil also produces very large amounts of waste from sugar cane processing ('bagasse' ~ 50 M tonnes dry basis in 2000 [24] ) since the Brazilian bioethanol industry from cane sugar has led the world's in development of biofuel ('gasohol') powered vehicles.

**Food waste** (FW) includes food materials discarded before or during food preparation and 'plate wastes'. Approximately one third of the food we buy is thrown away, the majority being sent to landfill. The largest producers of FW are domestic and commercial kitchens. FW has an important social, economic and environmental impact especially in countries such as US and UK, FW in UK is ~ 16 M tonnes per annum [25, 26].

Dumping food waste in landfill causes severe environmental damage; it is an important contributor to anthropogenic release of CH<sub>4</sub> [12, 13, 27, 28]. Hence favourable options are to intercept waste and turn it into CH<sub>4</sub> controllably for combined heat and power (CHP) use (with carbon capture) or by H<sub>2</sub> production (see section II.4.4.1.).

### **I.3 Energy**

Energy is the driving force that sustains our lifestyle. All our activities, economic, social and physical welfare depend on energy. Its uninterrupted supply with an increasing worldwide demand constitutes a significant challenge for our society. Fig. 3 shows that the world energy consumption in quadrillion of British Thermal unit (Btu), energy demand is expected to increase by 49 % from 2007 to 2035, the largest projected increase demand is for emerging economies such as China, Brazil, Russia and India.

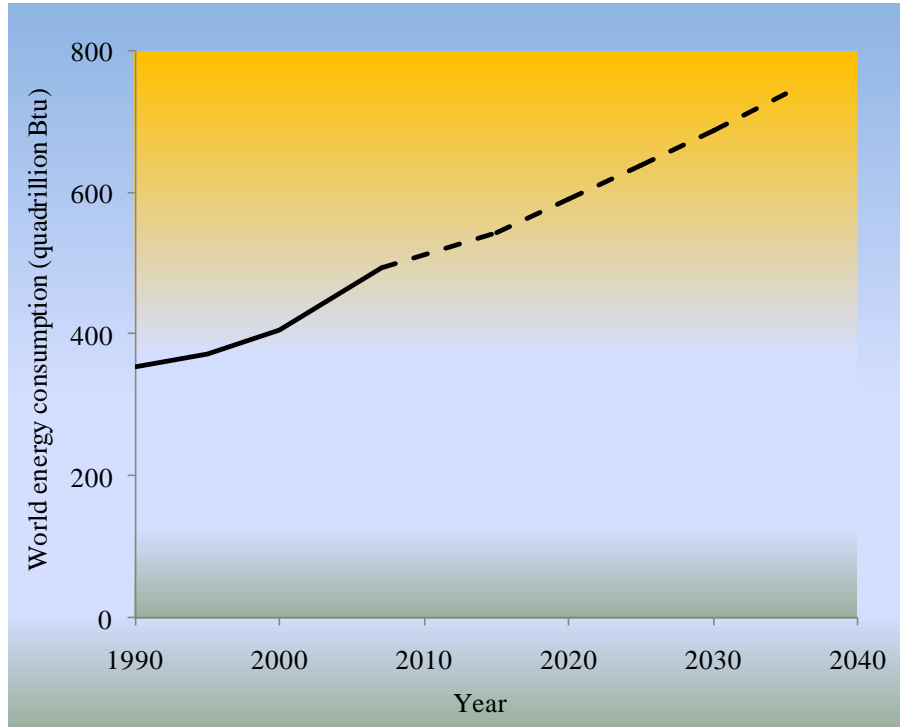


**Fig. 3** World marketed energy consumption. Dashed line is projections from 2009 to 2035. Adapted from EIA [29].

This demand (78-87 %) has been met mainly by the exploitation of our enormous natural reserves of fossil fuels (oil, coal, gas) that in addition emit GHG when burnt and other pollutants which significantly contaminate our planet [6, 29]. Fig. 4A shows the different world energy utilization (WEU) by fuel and Fig. 4B shows the world energy generation (WEG) by fuel which comprises liquid, coal, natural gas, renewable and nuclear. The utilisation of all of them increases over the time horizon. Liquids (gasoline, diesel, kerosene) consumption is increasing at an average annual rate of 0.9 % from 2007 – 2035 whereas renewable (see section I.4), the fastest growing source of world energy, increases 2.6 % per year. Oil prices as well as concern about environmental impacts of fossil fuel use are incentives for increasing the use of renewable energy throughout the world. Oil prices has been on an upward path for more than six years and continue reaching record levels in 2008 as shown in Fig. 5 with huge economic impact mostly on industrialized countries. As can be noticed oil prices are expected to remain high through the projection period. As of July, 2011 the price per barrel was US\$ 94.56 (£ 59.1) [29].

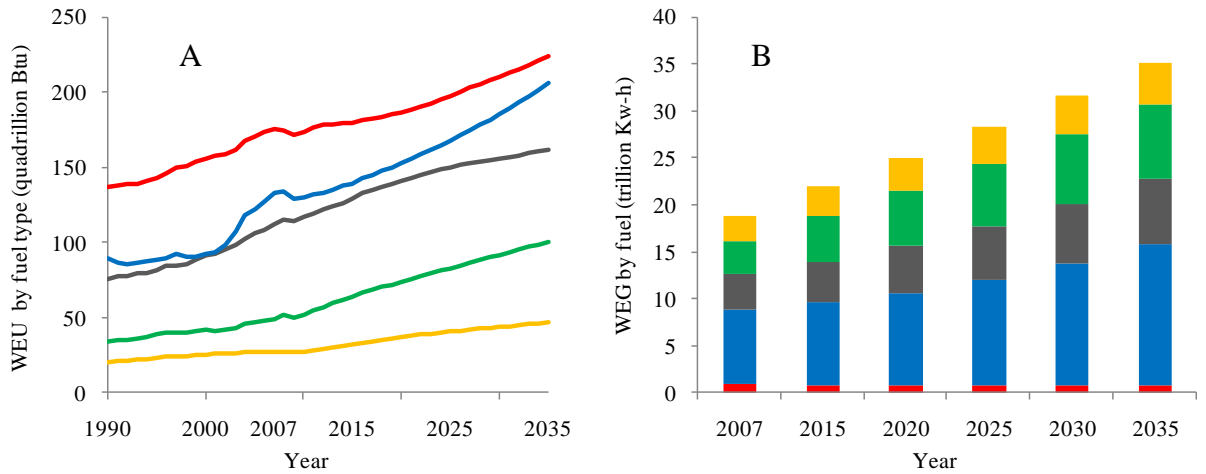


**Fig. 4** A) world energy use (WEU) by type and B) world energy generation (WEG); (—) Liquids; (—) Coal; (—) Natural Gas; (—) Renewables; (—) Nuclear. Source EIA [29].

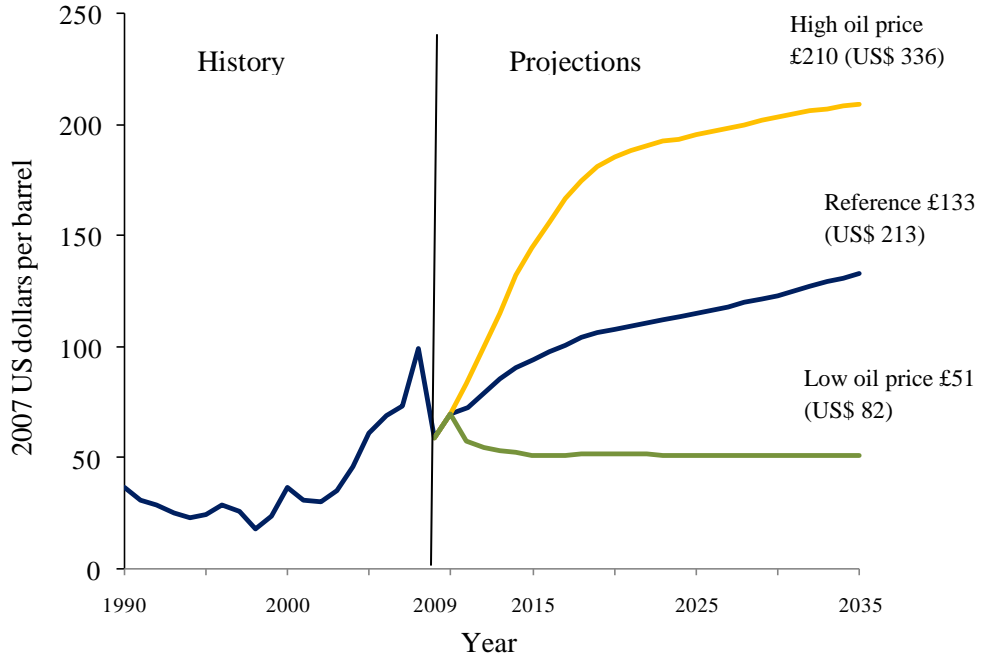


**Fig. 5** Oil prices; history (before 2009) and projections (after 2009) contemplating three scenarios: high oil price, reference (most likely) and low oil price. Source EIA.

Oil prices are subject to geopolitical regions (e.g. Middle East) but new sources of fossil fuels are being developed e.g. a new large Norwegian gas field in the North Sea and development of the heavy 'oil sands' of the Athabasca region in Canada.

Natural gas remains an important fuel for electricity production worldwide given that is cheaper than oil and natural gas electricity generating plants and being less capital intensive than those using coal, nuclear or most renewable energy sources. World natural gas consumption is projected to increase by 1.3 % per year from 108 trillion ft<sup>3</sup> in 2007 to 156 trillion ft<sup>3</sup> in 2035 [29]. Petrol cars can be easily converted to run on natural gas.

World coal consumption increases by an average 1.6 % from 2007 to 2035 but demand will escalate after 2020. China accounts for 78 % of the net increase of coal consumption. Fig. 4B shows that coal provides the largest share of world electricity generation which was 42 % in 2007 and remains unchanged through 2035 [29].

In developing nations, hydroelectric power is a major source of renewable energy growth. Brazil, China and India in combination account for 83 % for the total increase in hydroelectric production. Also growth rates for wind powered electricity production are high in developing nations, especially in China where total generation from wind power plants is projected to increase from 6 B Kw.h in 2007 to 374 B Kw.h in 2035; however the total increase in China's wind power will be less than half the projected increase in its hydroelectric generation. World nuclear power will increase from 2.6 Trillion Kw.h in 2007 to an estimated 4.5 Trillion Kw.h in 2035, although there is now considerable uncertainty about the future of nuclear power since plant safety, radioactive waste disposal and nuclear material proliferation concerns have been paramount, and the recent events in Fukushima, Japan have intensified the safety debate. Despite this, China, India and Russia account for the largest increment in world installed nuclear power between 2007-2035 with 114 Gigawatts of nuclear capacity of which 60 % belongs to China alone [29].

With regards to energy consumption by sector, the industrial and transportation sectors account for more than 50 % of the total energy consumption in 2007 for the US and UK as shown in Fig. 6. Note that the residential and commercial sectors together exceed industrial energy consumption [29, 30].

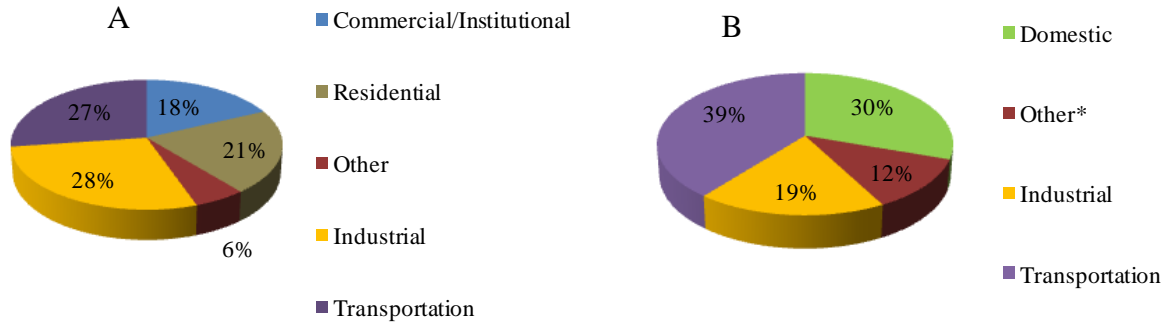


**Fig. 6** Energy consumption by sector A) in US; B) in UK. Sources US EIA and UK department of energy and climate change (DECC) [30].

The transportation sector accounted for 27 % of world energy consumption in 2007 and its demand will increase more rapidly than in any other fuel end-use sector (>1.3 % per year) (2007-2035). By 2035 world liquid fuel consumption in the transportation sector is projected to be 61 % of the world total liquid fuel consumption (assuming reference price of oil) this implies approximately 67.2 M of oil barrels per day (Fig. 7). This is associated with the expected increase in population, economic growth and 1 billion cars, projected to be 2.8 billion in 2050 [31].

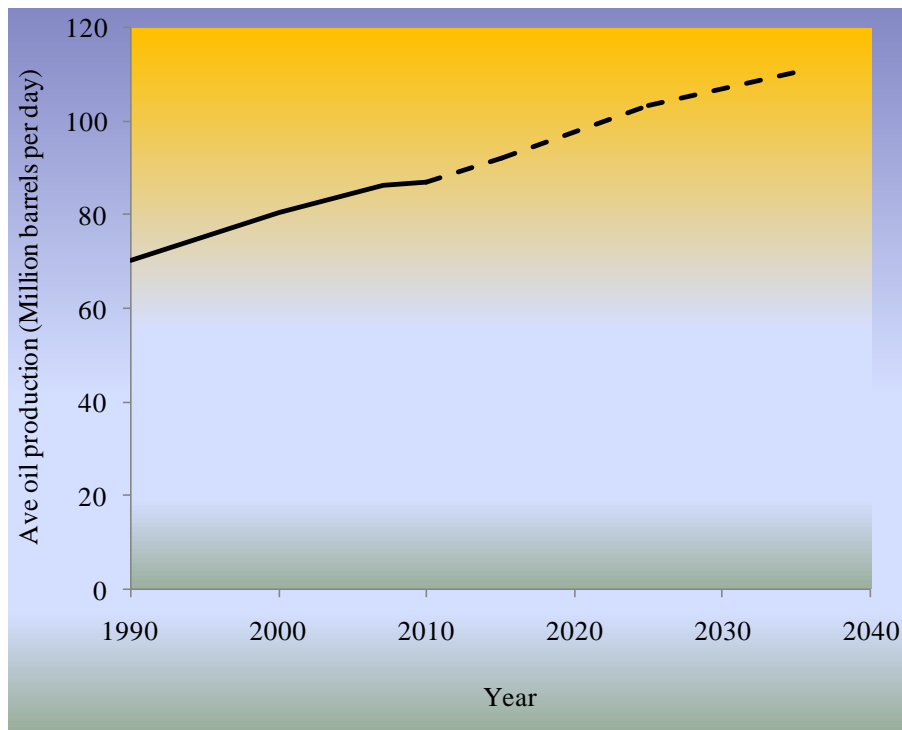


**Fig. 7** Daily average oil world production, the dashed lines are projections from 2010. Source British Petroleum (BP).

Global energy consumption is expected to increase by 49 % from 2007 to 2035 (considering oil prices in reference case Fig. 5) with the most rapid growth in energy demand by developing nations (84 %) compared to an increase of only 14 % by developed nations. About 78 to 87 % of the world energy is derived from fossil fuels; therefore the ongoing growth in fossil fuel consumption also suggests that CO<sub>2</sub> emissions will continue to rise with the aforementioned consequences.

## I.4 The Challenge, actions and policies.

Table 1 shows the fossil fuel identified world reserves and consumption as of 2009. Reserve/Production (R/P) ratio indicates our reserves in years under the assumption that energy consumption remains constant which will not be the case due to the projected increase in global energy demand as explained in section I.3.

**Table 1** Fossil fuel reserves (oil, natural gas and coal) and consumption as of 2009. Source BP [32].

	Oil	Natural Gas	Coal
World reserves	(M barrels) 1.3331 x 10 <sup>12</sup>	(T m <sup>3</sup> ) 187.5	(M tonnes) 826001
Consumption	(M barrels per day) 84.1	(B m <sup>3</sup> per year) 2940.4	(M tonnes per year) 3278.3
R/P	45.7	Years 62.8	~ 240

As all sources of energy are expected to increase in utilisation, more efforts should be made to increase particularly renewable resources in order to reverse the continuing tendency towards fossil fuels.

Natural gas and coal are used to produce heat and electricity whereas oil is not only being rapidly consumed by the transportation sector but is also an important and irreplaceable resource for the manufacture of a huge range of high value chemicals with great demand that simply burning it constitutes an appalling waste.

Organizations like the United Nations Framework Convention on Climate Change (UNFCCC) created an international treaty more than a decade ago, to begin to consider what can be done to reduce global warming and to cope with the causes of temperature increase. More recently, a number of nations approved the addition to the treaty the Kyoto protocol, which has more powerful and legally required measures. The UNFCCC supports all institutions involved in the

mitigation of climate change process. As of March, 2011 there were 195 parties to the UNFCCC and 193 parties to its Kyoto protocol. However in 2012 the Kyoto Protocol will come to an end. In 2009 the parties of the UNFCCC met in Copenhagen in preparation for a new climate agreement; this time the Intergovernmental Panel on Climate Change (IPCC) provided an objective source of information about climate change. IPCC is a scientific intergovernmental body established by the World Meteorological Organization (WMO) and the United Nations Environment Programme (UNEP), IPCC was awarded the Nobel Peace Prize in 2007. During these meetings the US and China, the two major contributors to CO<sub>2</sub> emissions to the atmosphere, announced their commitment to the reduction of CO<sub>2</sub> emissions. Table 2 summarizes some of the most important milestones:

**Table 2** Commitments in reduction of CO<sub>2</sub> emissions and in utilization of renewable sources (RS) of energy in transport and as a share of total energy production by some industrialized countries and one of the biggest growing economies (China). Sources WMO and UNEP.

Country	Energy from RS share	Energy from RS in transport	Reduction in CO <sub>2</sub> emissions
United Kingdom	20%	10%	
Germany	25 - 30 %	20% by 2020 and 30% by 2030	≥ 20 % 2020 and ≥ 80 % by 2050
Europe	20%	10%	
Japan	> 20 %	50 % in passenger cars by 2020 and 70 % by 2030	25 % 2020
United States	80% from clean energy sources by 2035		17 % 2020 and 83 % 2050
China	15%		40 to 45 % reduction per unit of GDP by 2020

The GHG balance may be also affected by land use changes and corresponding emissions and removals. Land use, land-use change and forestry is defined by the UN as "A greenhouse gas inventory sector that covers emissions and removals of greenhouse gases resulting from direct human land use, land-use change and forestry activities". Bioenergy can lead to avoided GHG emissions from residues and wastes in landfill disposals and co products; the combination of bioenergy with carbon capture and storage (CCS) may provide for further significant reductions.

Proper governance of land use, zoning, and choice of biomass production systems are key considerations for policy makers. Policies are in place that aim to ensure that the benefits from bioenergy, such as rural development, overall improvement of agricultural management and the contribution to climate change mitigation, are realized even though their effectiveness has not been assessed [33]. For example, to stimulate alternative waste treatment options gate fees and landfill taxes were introduced in some countries, in the UK the latter was introduced in 1996 and started at £ 7 per tonne of active waste (wastes that decay like household wastes) and annually increased to a current £ 56 and projected £ 72 per tonne by 2013. Since the introduction of the tax, the proportion of waste sent to landfill fell by ~ 30 % by 2009, with a subsequent similar increase in recycling [34].

In front of this entire scenario, a vital strategic challenge is to transform our current fossil fuel dependent energy systems to new *clean* renewable energy sources to protect our planet and ourselves from the negative effects of excessive CO<sub>2</sub> emissions and to anticipate an imminent non renewable fossil fuel shortage and energy crisis. For such strategy to be effective and long lasting, it should embrace the following goals:

- Environmental quality:
  - Reduction of CO<sub>2eq</sub> emissions
  - Solution to pollution problems.
  - Solution to waste disposal problems.
- Energy security
  - Secure energy supply
  - Reduce dependence by diversification
- Economic Competitiveness
  - Innovative technologies and products
  - Economic wealth

Renewable sources of energy as considered in the IPCC report, 2011 include: Bioenergy, direct solar, geothermal, hydropower, wave and wind energy. A new clean fuel that can be obtained from renewable resources for use in the transportation sector is necessary to save the world from the consequences of burning an increasing amount of 60 M barrels of oil per day.

Hydrogen has been recognized globally as an energy carrier that complies with all the environmental quality, energy security and economic competitiveness demands. Hydrogen roadmaps to the transition to the “Hydrogen economy” have already been developed by countries

and regions, among them: The ‘Hyways Roadmap Europe’ by the European Commission (EC); The National Hydrogen Energy Roadmap and the Hydrogen Posture Plan by the US Department of Energy (DOE); The Hydrogen Technology Roadmap by the Australian Government Department of Resources, Energy and Tourism and the Future Fuels for the Asia Pacific Economic Cooperation (APEC) region roadmap [3, 35]. All of these roadmaps contemplate the vision, goals, resources, opportunities, risk and challenges, milestones, strategies, investments and incentives, and economic implications derived from the introduction of hydrogen into the energy system. The steps to this transition have already been initiated as will be discussed in section I.5.

## **I.5 Towards the hydrogen economy**

Hydrogen ( $H_2$ ) is the most abundant element in the universe and the third most abundant element on Earth [36]. Under ordinary conditions  $H_2$  is an invisible, nontoxic light gas that is very rare in the atmosphere ( $\sim 1$  ppm by volume). Because of its high reactivity  $H_2$  is always combined with other elements; it is present in water, hydrocarbons, in every living organism and in natural and artificial compounds. The energy content of  $H_2$  ( $285.9 \text{ KJ.mol}^{-1}$ ) is 2.7 times higher than the energy content of gasoline and, when used in fuel cells, the combination of  $H_2$  and oxygen ( $O_2$ ) generates electricity, heat and water. The efficiency of a fuel cell to produce power or electricity is not limited by the Carnot cycle as the case for fossil fuels (which is  $\sim 27\%$  efficient for most automotive engines); it is determined by the ratio of the free energy change ( $\Delta G^\circ$ ) and the enthalpy change ( $\Delta H^\circ$ ) of the chemical reaction between  $H_2$  and  $O_2$ , typical efficiencies of hydrogen fuel cells are between 50-70% [37]. This implies that the efficiency of a  $H_2$  fuel cell vehicle is 2-3 times greater than that of conventional gasoline vehicle and 1.5-2 times greater than diesel-electric hybrids [4]. Based on these considerations  $H_2$ -fuel cell systems constitute a solution for oil saving and power generation in the transport sector.

Actually about 50 M tonnes of  $H_2$  with a market value of £ 120 Billion are produced annually to meet world demand, which has 6-15% annual growth [38, 39]; the main uses and applications of  $H_2$  are currently in the chemical and petrochemical industry specially to produce ammonia and in the hydro cracking process. The most important  $H_2$  production technologies will be discussed in chapter II.

The utilization of  $H_2$  as a source of power for mobile and stationary applications implies major challenges in the development of new and clean  $H_2$  production technologies to meet the

increasing demand. The transition to the H<sub>2</sub> economy will require several decades to be accomplished (estimated by 2050); this is demanding intensive research and development activities, learning and commercial demonstrations to overcome the barriers to making hydrogen and fuel cell technologies competitive with alternative technologies: the ultimate goal considered in any plan towards the H<sub>2</sub> economy is to develop low cost methods for H<sub>2</sub> production and delivery. Technologies for low cost CC and containment for fossil based H<sub>2</sub> production; compact, safe and efficient storage systems, and advanced fuel cell technologies would enable the automobile and energy companies to opt for commercial availability of fuel cell vehicles and a H<sub>2</sub> fuel infrastructure by 2020.

Two of the most important roadmaps prepared to support the development of H<sub>2</sub> based energy systems are The Hydrogen Posture Plan prepared in 2006 by the US DOE and the HyWays action plan developed in 2007 by the EU. These plans explore the wide range of activities required to recognize the potential of H<sub>2</sub> in resolving energy security, diversity, and environmental needs as schematized in Fig. 8. They seek to motivate and support organizations that invest in H<sub>2</sub> energy systems either public, private, state, federal or interest groups to become involved in a coordinated effort to reduce risk, improve performance, decrease cost, and implement a secure, clean, and reliable energy future.

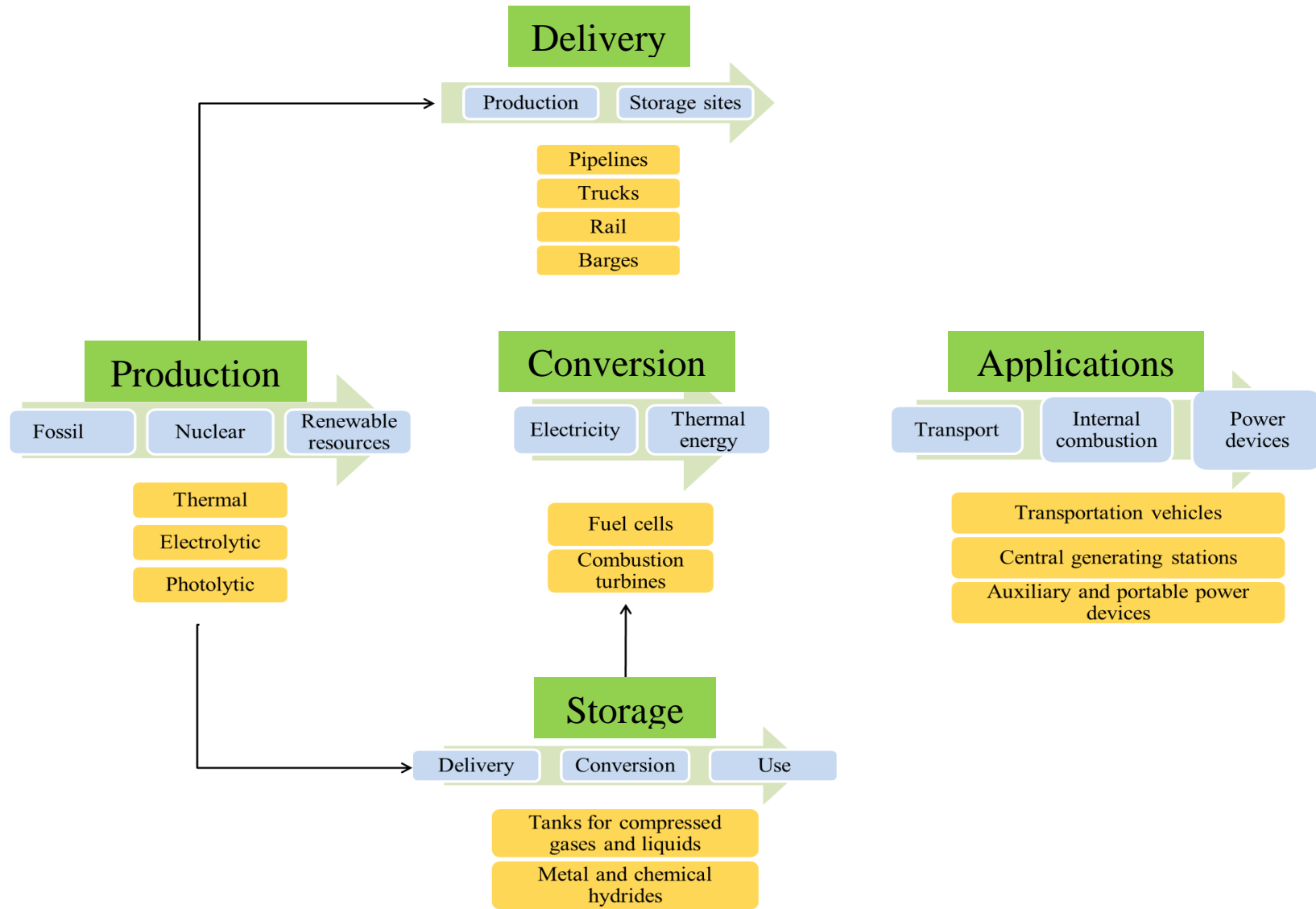


**Fig. 8** Diagram of the different elements contemplated by the strategic plans to support the development of H<sub>2</sub> energy infrastructure. Green boxes represent main areas under development. Source: US DOE Hydrogen Posture Plan

Key questions are: how much H<sub>2</sub> will be needed, how will it be produced and how much it will cost ?. The US produces 9 M tonnes of H<sub>2</sub> annually (DOE, 2006). The US department of transportation (DOT) estimates that an additional 40 M tonnes of H<sub>2</sub> per year will be needed to power 100 M fuel cell powered cars, or to provide electricity to about 25 M homes. According to the US DOE the H<sub>2</sub> cost goal by 2015 is \$2.00-\$3.00 per gallon of gasoline equivalent (GGE) based on the EIA forecast of gasoline cost. This ensures that consumers' operating cost (\$.mile<sup>-1</sup>) in a H<sub>2</sub> fuel cell vehicle will be equal to or less than the gasoline vehicle in 2015. In comparison the EU scenario is summarized in Table 3.

**Table 3** The projected scenario for the introduction of H<sub>2</sub> fuel cell vehicles into the EU market. Source: HyWays, 2007.

		Year			
		2015	2020	2030	2050
Vehicles			2.5 M fleet	25 M fleet	
Cost					80 % of light duty vehicles and city buses fuelled with CO <sub>2</sub> free H <sub>2</sub> ; > 80 % CO <sub>2</sub> reduction in passenger car transport; In stationary applications H <sub>2</sub> is used in remote locations
	H <sub>2</sub>	Start commercialization of H <sub>2</sub> -fuel cell vehicles	4 - 5 €.Kg <sup>-1</sup> (50 € per oil barrel)	3 - 4 €.Kg <sup>-1</sup> (50 € per oil barrel)	
	FC		100 €.KW <sup>-1</sup>	50 €.KW <sup>-1</sup>	
	Storage		10 €.KWh <sup>-1</sup>	5 €.KWh <sup>-1</sup>	
Sales of H <sub>2</sub> -fuel cell vehicles			> 5 % of new car sales	> 20 % of new car sales	

According to this picture, it is easy to forecast that the current world H<sub>2</sub> demand could at least triplicate between 2030 and 2050. The US DOE through the national H<sub>2</sub> energy roadmap; established a production “mosaic” that includes a combination of distributed (electrolysis, small reformers) and centralized (coal and biomass gasification plants, oil and natural gas refinery) to produce 40 M tonnes of H<sub>2</sub> per year and satisfy immediate demand; one scenario is shown below:

- 100,000 neighbourhood electrolyzers (with electricity from renewables): 4 M tonnes
- 15,000 small reformers in refuelling stations: 8 M tonnes
- 30 coal/biomass gasification plants: 8M tonnes
- 10 nuclear water splitting plants: 4 M tonnes
- 7 large oil and gas SMR/gasification refineries: 16 M tonnes

Advanced methods that are not yet available include direct H<sub>2</sub> production from renewables (carbon free) which will eventually dominate by 2050, while the next generation of nuclear reactors

will couple waste heat to drive water electrolysis to make storable  $H_2$ . The key feature of  $H_2$  is that it is an energy vector that can be stored as compressed gas or in e.g. solid hydride stores, whereas electrical power can only be stored in batteries that have a shut life.

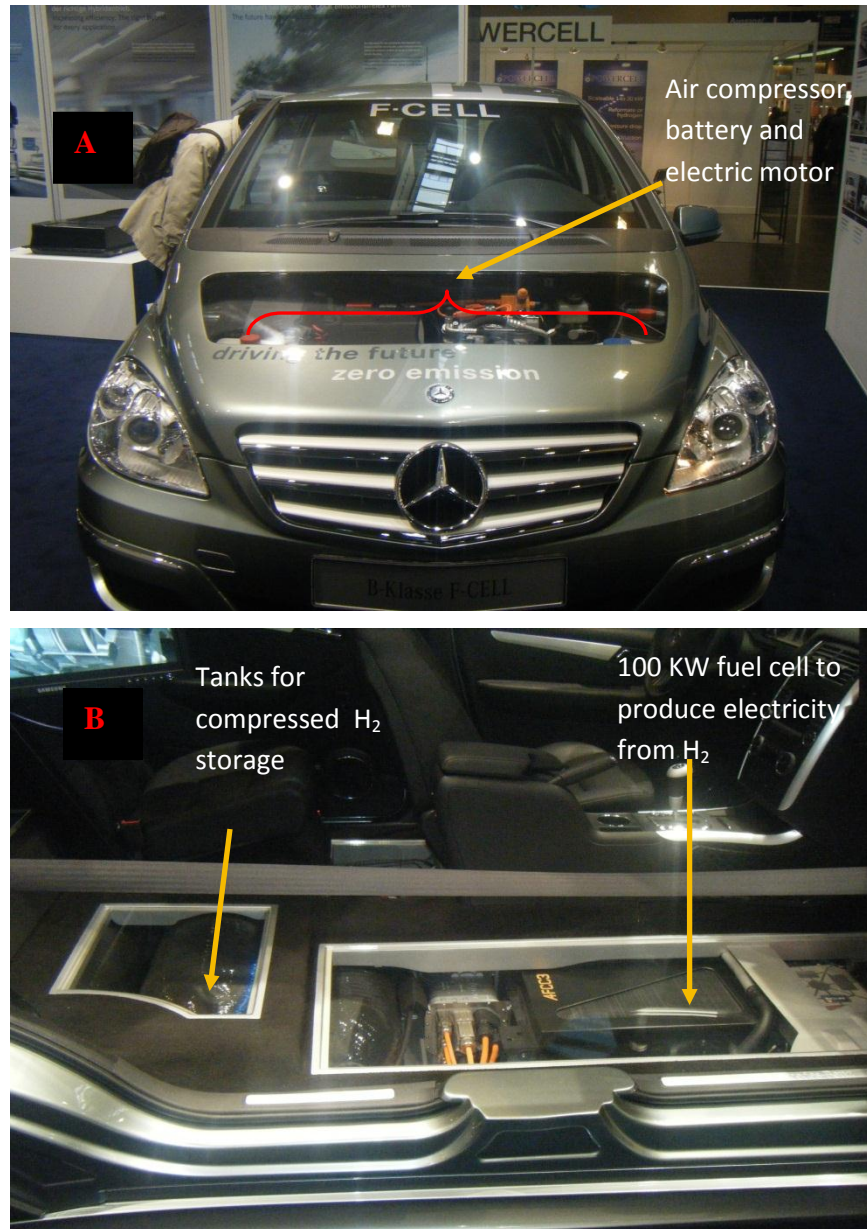


**Fig. 9** A)  $H_2$  powered car shown at the World Hydrogen Energy Convention, Germany 2010, it can reach a speed of  $\sim 170 \text{ km.h}^{-1}$ ; the battery is a Lithium Polymer Battery; the target price for this car will be  $\sim \text{£ } 28\text{-}35,000$  by 2015. B) distribution of the  $H_2$  storage tanks and fuel cell inside the car. There are three tanks with a total storage capacity of 3 kgs of  $H_2$  gas compressed at 700 bars enough for  $\sim 300$  miles, tanks filling time is  $\sim 3$  min. The fuel cell is a proton exchange membrane fuel cell (PEM FC), 100 KW; PEM FC estimated duration is  $\sim 5$  years.

## II. HYDROGEN PRODUCTION TECHNOLOGIES

In response to the environmental, energy and economic security needs, international attention towards the development of new H<sub>2</sub> technologies has emerged especially in developed nations like US, Japan, UK and many European countries with Germany playing a leading role. The technologies for H<sub>2</sub> production will be briefly described in this section. Major attention will be given to those related to biological methods especially an alternative which integrates both, thermochemical pre-treatment of biomass and biological hybrid system approaches to H<sub>2</sub> since they constitute the basis of this research project.

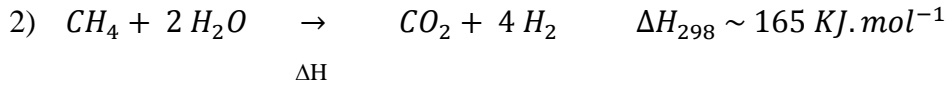
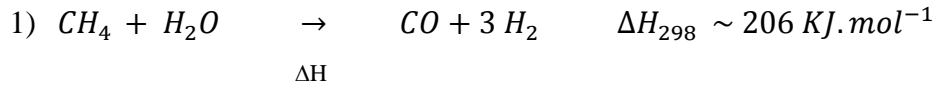
- a) Hydrogen from steam methane reforming (SMR).
- b) Hydrogen from water electrolysis (WE).
- c) Hydrogen from biomass.
- d) Hydrogen from biological methods.
- e) Hydrogen from biomass by integration of thermochemical and biological methods.

### II.1 Hydrogen from steam reforming of methane

Nearly 96 % of global H<sub>2</sub> production is obtained from steam reforming of fossil fuels, with natural gas or methane (CH<sub>4</sub>) being the most important source of H<sub>2</sub> production (49 %), liquid hydrocarbons (29 %) and coal (18 %) [37, 40]. Steam methane reforming (SMR) is the preferred current technology for H<sub>2</sub> and syngas production since it is highly efficient (65-75 %). It involves the reaction of steam and CH<sub>4</sub> in the presence of heat ( $\Delta H$ ) and catalyst in a fired reactor, “the tubular reformer” in which catalyst tubes are placed in a fired furnace that supplies the heat for the reaction and the heat for arriving at the exit temperature required for the desired conversion according to the following reactions:

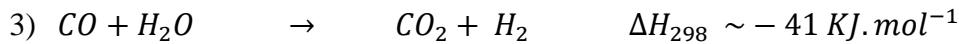
➤ Steam reforming reactions:

Ni/ceramic support catalyst



➤ Water shift gas reaction

Copper catalyst



Reactions (1) and (2) are highly endothermic; reaction (3) is exothermic. The first step is the steam reforming at 750 – 800 °C; it produces synthesis gas which is a mixture of CO and H<sub>2</sub>. The second step is the water gas shift (WGS) reaction (3) that is a catalytic reaction of CO with steam to produce more H<sub>2</sub> and CO<sub>2</sub>. To achieve high energy efficiency, separation of CO<sub>2</sub> to increase the equilibrium conversion and efficient heat process integration are important factors to consider [40].

Hydrogen for fuel cells applications (especially low temperature fuel cells) requires pure H<sub>2</sub> as CO is a poison for the platinum anode. The integration of reaction/separation membranes to the SMR process help to overcome thermodynamic limitations can also achieve almost 100 % CH<sub>4</sub> conversion to H<sub>2</sub> at lower temperatures. The main issues regarding membrane reactors involve the selection of a suitable membrane material (for stability), its mass transport characteristics, purity of the H<sub>2</sub> required (selectivity), factors affecting membrane fouling, cost, etc. Parameters that affect the performance of membrane reactors are operating pressure, temperature, membrane reactor length and thickness, the latter as the most important construction parameter. Typical membranes used for H<sub>2</sub> separation are Pd based due to its high selectivity towards H<sub>2</sub>; however they are very expensive for industrial applications. Other options that have proved to be successful are composite membranes with a thin Pd based layer supported on a porous substrate such as porous glass, alumina and other metals; however mechanical strength and different thermal expansion coefficients could represent a problem. Tong et al. (2005) prepared a thin and dense Pd/CeO<sub>2</sub>/MPSS (macro porous stainless steel) membrane that overcame these difficulties and achieved 97 % CH<sub>4</sub> conversion at 500 °C [41]; mixed ceramic-metal membranes are also of potential use. Membrane reactor

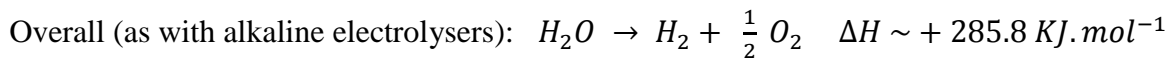
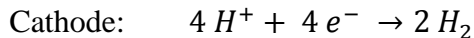
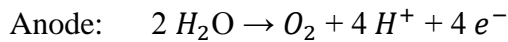
technology is advancing fast towards more efficient approaches and process integration that are required for the SMR to produce H<sub>2</sub> for utilization in fuel cells.

Another issue associated with SR of fossil fuels is CO<sub>2</sub> footprint. According to stoichiometry the CO<sub>2</sub> footprint of a SMR process is 0.25 CO<sub>2</sub>:H<sub>2</sub> yet in a modern CH<sub>4</sub> based plant is about 0.3-0.4. CO<sub>2</sub> capture and storage (CCS) may well dictate the acceptance of fossil fuel technologies to produce H<sub>2</sub> in the future. CCS is seen as a way to reduce CO<sub>2</sub> emissions into the atmosphere and thereby decrease the threat of global warming. It involves the capture of CO<sub>2</sub>, transportation of CO<sub>2</sub> to a store location (which requires diesel fuel) and storing and maintaining the CO<sub>2</sub> however experience in CCS is currently limited and in need of more research and demonstration projects to develop efficient and economic methods for its capture, transport and storage.

As SMR with ultimate CCS is projected to be the main source of H<sub>2</sub> to cover immediate increasing demand it is important to keep in mind that CH<sub>4</sub> from fossil reserves is a non renewable resource with its consequent depletion and price tendency to increase. The tendency to reduce dependence on fossil fuel hastens the utilization of other sources of CH<sub>4</sub> (anaerobic digestion) and the development of H<sub>2</sub> technologies from renewable resources such as biomass and water which are expected to dominate H<sub>2</sub> production by 2050. 'Green' methods, such as those described in this thesis (sections 0VI.3 and VI.4) utilise CO<sub>2</sub> as a catalyst, giving scope for in-process conversion and a zero waste process.

## II.2 Hydrogen from water electrolysis

Hydrogen production via water electrolysis (WE) consists of splitting water to H<sub>2</sub> and O<sub>2</sub> by passing electrical current through an aqueous electrolyte hereby achieving the conversion of electrical energy into chemical energy [42], which is more convenient for storage. The reactions at the anode and cathode of the electrolyser are as follows :



The electrical energy is later recovered by reacting H<sub>2</sub> with O<sub>2</sub> in a fuel cell (reverse reaction) or combustion engine, therefore the efficiency of an electrolysis system can be calculated as the heating value of the H<sub>2</sub> produced divided by the electrical energy input:

$$\text{electrical efficiency}_{(LHV \text{ or } HHV)} = \frac{\text{LHV or HHV of H}_2 \text{ produced}}{\text{electricity used}}$$

Where,

*HHV=Higher Heating Value*, which is determined by bringing all the products of combustion back to the original pre-combustion temperature (25 °C), and considering the condensation of any vapor produced.

*LHV=Lower Heating Value*, which is determined by subtracting the heat of vaporization of the water vapor from the HHV.

However it takes both electricity and heat to split water electrochemically and heat is not included in the above equation. Splitting 1 mol of H<sub>2</sub>O to produce 1 mol of H<sub>2</sub> at 25 °C requires 285.8 KJ of energy of which 237.2 KJ as electricity and 48.6 KJ as heat and this is the minimum energy required to split water in electrolysis cells. This translates into a cell voltage (E<sub>0</sub>) of 1.481 V and this is the voltage at which an electrolysis cell at 25 °C can operate without producing excess heat; this voltage also corresponds to the HHV of H<sub>2</sub> representing a more reasonable value to use when calculating cell and stack voltage efficiency. The equation for calculating such voltage efficiency now becomes [37]:

$$\text{voltage efficiency} = \frac{\text{thermal neutral voltage } (E)}{\text{cell operating voltage } (V)}$$

Conventional electrolysis technologies are alkaline based and with PEM FC electrolysis [43] but they are limited in energy efficiency to 60-80 %. Hydrogen production via WE could play an increasingly important role in the future if the electrical power needed to drive the reaction is provided by a renewable resource such as wind, solar, geothermal, or low emission generators such as hydro or next generation nuclear generators and if a higher energetic efficiency can be reached; currently about 4 % of the H<sub>2</sub> produced worldwide comes from WE. WE at high temperature using protonic or ionic conducting electrolytes is an advanced concept aimed at increased electrical to chemical energy conversion efficiency; in recent years there has been special interest towards the reversible operation of solid oxide fuel cells (SOFC) as H<sub>2</sub>O electrolyser cells (SOEC). Cell voltages under operation of around 1.0-1.3 V at 800 °C are achieved which translates into substantial saving

of electrical energy compared with low temperature electrolysis but start up energy consumption is an issue and highly effective thermal insulation is required to maintain 800 °C.

The H<sub>2</sub> produced by WE is pure and can be used for fuel cell vehicles, electricity generation, or industrial applications. In addition, during periods of low electrical demand, many renewable power generators, such as wind turbines, produce excess electricity, which is lost. Electrolysis enables the storage of this excess energy as H<sub>2</sub> that can be later converted to electrical energy on demand.

Costs of H<sub>2</sub> vary depending on technology, scale of production and form of delivery. In 2009 the cost of decentralized electrolysis varied from \$ 3.5 per gallon of gasoline equivalent (gge) using non-renewable electricity from the grid to \$ 4.1-6.1 per gge using 100 % renewable electricity from the grid to \$ 19.4 per gge for using electricity from solar driven photovoltaic (PV) cells since sunlight is free it is clear that the cost of solar-PV is a major limitation at current grid electricity prices. Other costs (as of 2009) including transport are \$ 7.2, \$ 4.4 and \$ 11.30 per gge for distributed electrolysis, central wind electrolysis and central solar electrolysis respectively [37]. Even though these costs are still significantly higher than the \$ 2.6 per gge cost of H<sub>2</sub> from central SMR process and from the set goal of \$ 2.0-3.0 per gge set by the US DOE by 2015 (section I.5), WE costs are expected to drop significantly in the near future as it is expected to be an important source of H<sub>2</sub>.

## **II.3 Hydrogen from biomass utilisation**

Biomass is an abundant renewable resource capable of supporting the future H<sub>2</sub> economy [2, 4, 39]. In recent studies made by the Biomass R&D Technical Advisory Committee (BTAC) of the US Department of Energy and Agriculture it is reported that biomass now exceeds hydropower as the largest potential domestic source of renewable energy. It currently provides over 3% of the total energy consumption in the United States where the total annual consumption of biomass feedstock for bioenergy and bioproducts together currently approaches 190 million dry tons.

Hydrogen from biomass is an emerging technology that offers a feasible and potentially more attractive alternative for bio-hydrogen production since biomass resources are abundant, renewable and quite diverse. In general biomass includes agricultural residues, forest resources, perennial grasses, woody energy crops, wastes (municipal solid waste, urban wood waste, and food waste), and algae. Its distinctive characteristic among renewable energy resources is that it can be

converted to carbon based fuels and chemicals, in addition to power. Biomass is the only renewable resource with the potential to replace petroleum based fuels used for transportation and approach carbon neutrality; it is estimated that the US alone has over a billion tons of sustainable biomass resources that can provide fuel for cars, trucks, and jets; make chemicals; and produce power to supply the grid, while creating new economic opportunities and jobs throughout the country in agriculture, manufacturing, and service sectors [44, 45].

The Office of Energy Efficiency and Renewable Energy (EERE) at the U.S. Department of Energy (DOE) developed the Biomass Program, 2011 [44, 45]. This plan identifies the research, development, demonstration, and deployment activities on which the program will focus on over the next five years, and its mission is to develop and transform the renewable biomass resources into cost competitive, high performance biofuels, bioproducts, and biopower through targeted research, development, demonstration, and deployment supported through public and private partnerships. The program main goals are to enable the production of biofuels in the US and reduce its dependence on oil through the creation of a new domestic bioenergy industry supporting the goal of 36 B gallons per year of renewable transportation fuels by 2022 and to increase biopower's contribution to the national renewable energy goals (Table 3) through increasing biopower generating capacity.

Examples of similar programs for the transformation of renewable biomass developed by other nations and regions are the UK renewable energy roadmap and the Europe renewable energy technology roadmap. Among the main challenges contemplated by the programs are:

- Feedstock supply: Produce large, sustainable supplies of regionally available biomass and implement cost-effective biomass feedstock infrastructure, equipment, and systems for biomass harvesting, collection, storage, preprocessing, and transportation.
- Bioenergy production: Develop and deploy cost effective, integrated biomass conversion technologies for the production of biofuels, bioproducts and biopower.
- Bioenergy distribution: Implement biofuels distribution infrastructure (storage, blending, transportation both before and after blending, and dispensing).
- Bioenergy end use: Assess impact of fuel blends on end-user vehicles.

Biomass composition varies depending on its nature. Starch, cellulose, hemicelluloses and lignin are the most important components of biomass and as such are also among the most abundant

renewable resources on earth. From these, starch, cellulose and hemicelluloses are polymers of sugars and consequently a valuable potential source of fermentable hydrolysates into products such as H<sub>2</sub>, ethanol, butanol among others. Biomass hydrolysis methods will be presented in chapter III.

Agricultural food and food waste biomass is usually rich in starch whereas wood, plants, grass, agricultural crop wastes (typically known as lignocellulosic biomass) mainly consists of cellulose 25-50 %, hemicelluloses 20-40 % and lignin 15-35 % [46].

Other components of biomass include organic compounds that perform different functions such as intermediates in metabolism, energy reserves and protection against microbial and insect attack; these compounds may be extracted using polar or nonpolar solvents as part of a pretreatment to hydrolysis ([47, 48]. Small amount of inorganic substances such as potassium, sodium, calcium among others are also present as a result of nutrients uptake during growth.

*Starch*, a main constituent of biomass, is one of the most abundant renewable organic compound on Earth, being present in a wide variety of agricultural and staple food wastes such as potatoes, corn, rice, wheat, pasta and wastes from textile industries [49, 50]. Starch molecule exhibits two types of linkage: 1,4- $\alpha$ -linked glucosyl units in the form of linear, water insoluble amylose (20-25%) (Fig. 10 A) and 1,6- $\alpha$ -linked branched, water soluble amylopectin (75-80%) (Fig. 10 B). Starch molecules form semicrystalline structures which, as a consequence of its linkages are highly amorphous making it more susceptible to enzyme and other hydrolysis systems to be broken down into glucose units [51, 52].

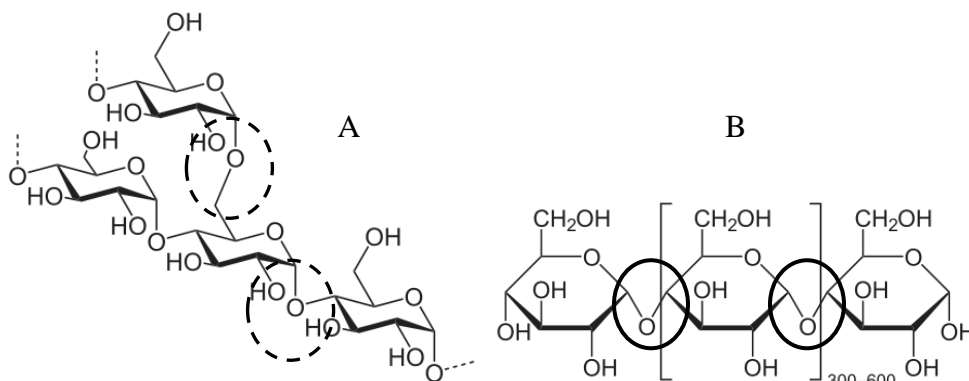


**Fig. 10** A) Amylopectin molecule structure with glucose units held together by 1,6- $\alpha$ -glucosyl bonds shown by the dotted circle; B) Amylose with 1,4- $\alpha$ -linked glucosyl units shown by the solid circle. Source: Wikipedia images.

*Cellulose* is also one of the most abundant renewable organic compound on earth being a major component of agri-food wastes; cellulose is a homopolymer comprising 7000 to 15000 D-glucose units linked by  $\beta$  (1,4) glucosidic bonds, with a molecular weight within the range of

300,000 to 500,000 units depending of the length of the cellulose chain (Fig. 11) [53]. Due to intermolecular and intramolecular hydrogen linkages through the hydroxyl groups, cellulose molecules form crystalline strong structures with low surface area that are insoluble in water under normal conditions and are strongly resistant to enzymatic attack and chemicals such as acid compounds. As a consequence of its structure, cellulose is more difficult to hydrolyse into glucose units than starch [54, 55].

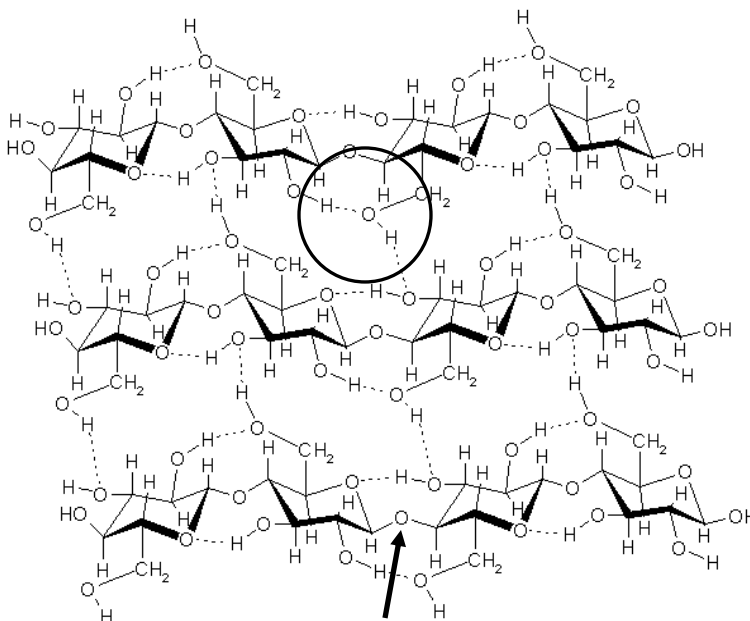


**Fig. 11** Molecular structure of cellulose with D-glucose units linked by  $\beta$  (1,4) glucosidic bonds (filled arrow pointing at one) and H<sub>2</sub> bonds (dotted lines, one is indicted by the circle). Source: Wikipedia images.

*Hemicellulose* is a heteropolymer containing many different sugar monomers (xylose, galactose, mannose, arabinose, etc) with xylose always present in the largest amounts linked at the 1 and 4 positions, hemicellulose has a random amorphous structure usually comprising from less than 100 to 200 units and with little strength that is more easily hydrolysed than cellulose [54, 56]. See Fig. 12.

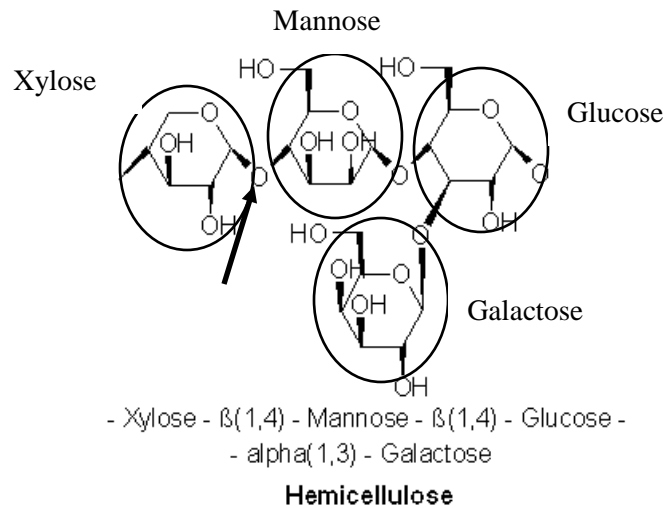


**Fig. 12** Structure of hemicellulose; in this figure units of xylose, mannose, glucose and galactose held together by glucosidic bonds (see arrow). Source: Wikipedia images.

*Lignin* is a highly branched polyphenolic compound with different amorphous polymeric complex structures formed by very stable *p*-hydroxyphenylpropane units that are connected together by ether and carbon-carbon linkages and some percentages of other substances such as minerals and proteins [46, 54]. The three general monomeric phenylpropane units exhibit the *p*-coumaryl, coniferyl, and sinapyl structures (Fig. 13); the amorphous structure of lignin guides to a huge number of interlinkages between these individual units with ether bonds predominating, Fig. 13 shows a model of lignin structure [54].

Lignin serves as cement between wood fibres due to the existence of covalent linking between lignin and polysaccharides hereby assuming an important structural role as are responsible for the longevity of standing trees due to its relatively high resistance to enzymatic attack (decay) [57].

Lignin is usually present with cellulose and hemicellulose constituting lignocellulosic compounds which must be broken down to make the cellulose or hemicellulose accessible to hydrolysis systems.

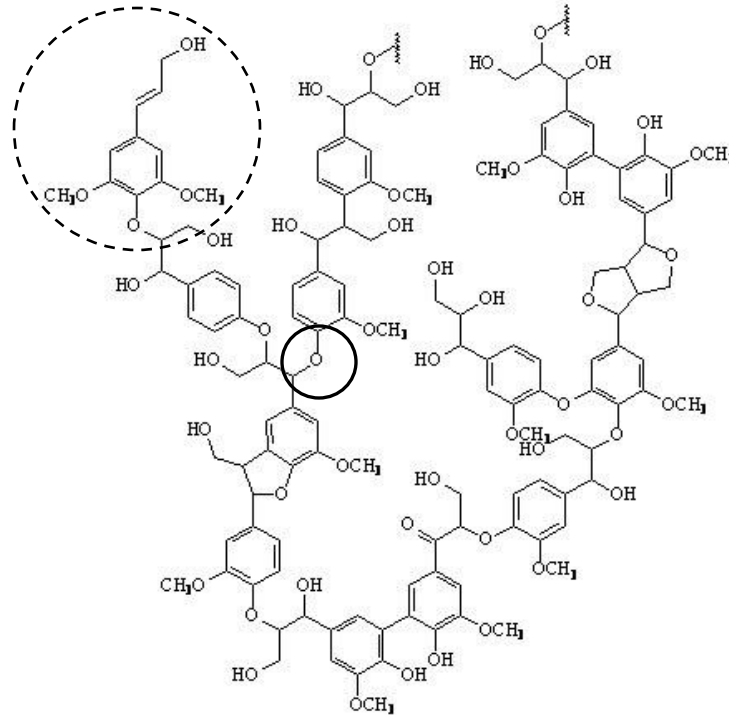


**Fig. 13** Shows a model of a lignin molecule. The ether bond is indicated by the circle; The dotted circle shows a sinapyl unit as a part of the complex structure Source: Wikipedia images.

The available technologies to produce H<sub>2</sub> from biomass can be divided in two general categories: thermochemical and biological processes.

### II.3.1 Thermochemical processes

Thermochemical processes consist of the conversion of biomass into a gaseous mixture of fuel gases or liquids and other compounds by applying heat under pressure and steam; the products obtained can be used for the production of electric power, heat, chemicals or fuels [49]. The two most feasible thermochemical technologies for biomass conversion to H<sub>2</sub> are: biomass gasification (section II.3.1.1) and biomass pyrolysis (section II.3.1.2) [43, 58].

#### II.3.1.1 Biomass gasification

Gasification is an efficient method to convert biomass into gaseous products with a usable heating/power value. Gasification is achieved by partial oxidation of biomass under heat and pressure to form a gaseous mixture of H<sub>2</sub>, CO<sub>2</sub>, CO and CH<sub>4</sub>, and light and heavy hydrocarbons and char. The gas mixture is called synthesis gas (syngas) and has important applications in synthesis

reactions in the chemical industry and for the production of  $H_2$ . Technologies for biomass gasification can be classified based on the moisture content of the biomass as: dry biomass (DB) and wet biomass (WB) (moisture content  $> 70\%$ ) gasification technologies; operating conditions and reactor types depend strongly on these two biomass conditions and have also strong influence in the product distribution in the syngas generated [37, 49, 58].

At present, about 90 % of the biomass used worldwide for energy supply is combusted by firing and less than 1 % is used in CHP plants. Efficiency for electricity generation obtained from biomass combustion is in the order of 20-40 %, however modern biomass gasification plants can preserve between 75 and 88 % of the heating value of the original fuel and achieve efficiencies 35-50 % based on the lower heating value [37].

A variety of processes for different products are currently being tested at pilot plant scale and recently technologies for gasification of dry biomass have approached commercialization for some applications. In the near future, biomass gasification processes could provide a significant contribution for the sustainable production of syngas and  $H_2$  to be used as energy carrier for mobile or stationary applications; however these technologies are under intensive research and development before large scale plants are in operation [37].

Another problem to be addressed with the use of this technology is the tremendous amount of resources and transportation needed to concentrate large amounts of biomass to central processing plants. Alternatives to develop smaller efficient gasification plants deployed in strategic locations may be required for this technology to be cost effective for  $H_2$  production.

#### *II.3.1.1.1 Dry biomass (DB) gasification*

DB gasification is applicable to biomass having moisture content less than 35 % [37, 58]; examples of such biomass are: coal, wood, bagasse and saw dust, as a consequence the gasification process usually suffers from low thermal efficiency with less so than with wet gasification (see II.3.1.1.2) since moisture contained in the biomass must also be vaporized.

Gasification proceeds at high temperatures (800-1000 °C) with or without catalyst and in a fixed bed or fluidized bed reactor; a variety of oxidation agents can be used: air, oxygen, steam and  $CO_2$ . Air is the cheapest and most widely used, however it introduces  $N_2$  in large concentrations in the syngas (about 50%) hereby reducing its heat value. Oxygen is expensive whereas steam provides a feasible alternative to increase the heating value of the syngas. One of the major issues in biomass

gasification is to deal with the tar and char formation that occurs during the process, several approaches are available to minimize this problem, in one of them it has been found that utilization of CO<sub>2</sub> as an oxidant is an interesting option since it is one of the products of the syngas obtained and CO<sub>2</sub> with a catalyst such as Ni/Al can convert char, tar and CH<sub>4</sub> into H<sub>2</sub> and CO [59-61]. When steam or CO<sub>2</sub> is used as the oxidant, an external heat supply has to be provided. Superheated steam (900 °C) has been used to reform DB using a fluidized bed gasifier and suitable catalysts achieving, high syngas yields (~0.95 g gas. g initial source material<sup>-1</sup>) with ~ 60 % vol. H<sub>2</sub> [43, 58] which is ~ two fold higher than typical thermal biomass decomposition yields.

Catalysts not only help to reduce the tar content, they also improve the gas product quality and biomass-gas conversion efficiency. Dolomite, Ni based catalysts and alkaline metal oxides are amongst the most widely used [58].

The optimization process of biomass gasification involves tests with different biomass types at various operating conditions in gasifiers (reactors). Reactors are classified into fixed bed, fluidized bed and entrained flow process [37]. In fixed bed reactors the biomass moves slowly downwards due to gravity during gasification either in co-current (same direction) or counter-current (opposite direction) with the oxidants. Fixed bed reactors have high thermal efficiency, require minimal biomass pretreatment and are economically feasible on a scale smaller than 1 MW [58].

In fluidized bed reactors a high flow rate of a bed material (which may act as a catalyst) is evenly fluidized by the gasification agent providing optimal heat and mass transfer conditions. Superficial velocities of the mass may vary from slow (1-2 m.s<sup>-1</sup>) to fast (6 m.s<sup>-1</sup>); in this case the bed material is fed to the reactor via a cyclone delivering particles of average size between 0.2-4 mm. Fluidized bed reactors are suitable for plants larger than 10 MW for economic reasons and are mostly applied for biomass gasification [37, 61-63].

Currently, some teams are focussing research on three possible combinations of dual fluidized bed reactors, specifically two fixed bed, one fixed bed and one fast fluidized bed, or two fluidized beds [37, 64]. By using two fluidized bed reactors, gasification is carried out by steam in the first reactor, whereas in the other bed combustion takes place to generate the heat for endothermic gasification, heat pipes are used to transport heat between the dual fluidized bed systems. Industrial application of this technology has been implemented successfully [37, 65].

In recent years another interesting approach namely, Hydrogen Production by Reaction Integrated Novel Gasification (HyPr-RING) was proposed by Lin et al., 2001 [66]. This method consists of an integration of the water hydrocarbon reaction, water-gas shift reaction and absorption

of CO<sub>2</sub> and other pollutants in a single reactor under both sub critical and super critical water conditions. This is an exothermic process and a high yield of H<sub>2</sub> can be obtained at relatively low temperature (650-700 °C) as compared with conventional gasification processes. This novel technology can be conducted in a simpler manner as the reaction for H<sub>2</sub> production and gas separation occur in one single reactor at a lower temperature; the method has been analyzed theoretically and demonstrated experimentally to be a very efficient technique for H<sub>2</sub> production from biomass.

The costs of H<sub>2</sub> production by biomass gasification are competitive with SMR [37, 58, 67] and taking into account the environmental benefit it constitutes a promising option based on both economic and environmental considerations. As gasification technologies develop, they will integrate systems with solid oxide fuel cells (SOFCs) which are attractive due to their higher electrical efficiency and lower requirements of gas quality.

#### *II.3.1.1.2 Wet biomass (WB) gasification*

The technologies applicable for DB gasification are not suitable for wet biomass (WB) gasification (moisture above 35 %). A large proportion of biomass wastes contain up to 95 % water therefore the drying costs will prohibit classical gasification processes. Supercritical water (SCW) gasification of wet biomass is a very promising alternative to transform WB into a pressurized clean mixture of gases (CH<sub>4</sub>, H<sub>2</sub> and CO<sub>2</sub>) with high calorific value and high H<sub>2</sub> content. The term *critical condition* or *critical point* of a material usually denotes its vapor-liquid critical point. The vapor-liquid critical point defines the conditions above which liquid and gas phases do not exist or become indistinguishable (absence of phase boundaries). The critical point of water occurs at its critical temperature (T<sub>c</sub>) of 374 °C and critical pressure (P<sub>c</sub>) of 218 atm. Water at or above critical conditions (SCW) has organic solvent-like behaviour and provides a single fluid phase chemistry since gases are also miscible in SCW; hereby serving as an excellent solvent for homogeneous reactions of organic compounds with gases (e.g. the oxidation of organic compounds with oxygen and air) [68]. SCW gasification of WB can advantageously avoid high drying costs and at the same time has been shown to achieve high gasification efficiency (total mass of the product gas/total mass of the dry feed<sup>-1</sup>), high molar fraction of hydrogen content and the availability of the products at high pressure (HP) which is wanted for most applications (Lu et al., 2006, Yoshida et al, 2004) [69, 70]. However, this would require the application process to be co-located with the WB gasification,

and, due to the complexity of plant, small localised processes are unlikely and WB transportation costs to the plant would be incurred. There are also several other problems to solve, among them reactor plugging by accumulation of tar and reactor wall deposits in typical tubular reactors utilized for WB gasification that are caused by degradation of products such as furfural and phenols; for this different reactor configurations have been proposed (fluidized bed reactors) along with extensive studies of the reaction pathways of the different constituents of biomass (cellulose, lignin, hemicelluloses, protein, etc) [71-74] and studies of the parametric effects such as pressure, temperature, residence time, reactor sizes and types, heating rate, reactor wall properties, biomass types, particle size, catalysts and solution concentration on the WB gasification in SCW [75].

Matsumura et al., 2005 contemplated two approaches to biomass gasification in SCW: the first proceeds at low temperature (350 to 600 °C) in the presence of metal catalysts and the second at high temperature (500 to 750 °C) without catalyst or with non-metallic catalysts [70]. SCW oxidation is, however, highly corrosive and hence high capital investment in corrosion resistant materials is required.

*WB SCW gasification reactor systems:* As SCW gasification takes place at high temperature and pressure the reactor setup needs special consideration; for experimental purposes quartz capillary batch reactors, fluidized bed microreactors and process development unit (PDU) tubular reactors have been widely utilized to generate data on reaction kinetics under well-defined conditions and develop models of the dominant steps [70, 76]. However for commercial SCW gasification a proper reactor design has yet to be defined. Tubular and series of stirred tank reactors among many others may be suitable but these should also incorporate heat exchange systems between the reactor outlet and inlet streams to achieve high thermal efficiency. Pre heating of the incoming biomass slurry through the inlet tube of a reactor is likely to cause plugging problems due to the thermal decomposition of the biomass starts at ~ 260 °C which is far below the gasification temperature (~ 600 °C). It is also possible that the feed stream may reach the supercritical point in the heat exchanger with unknown consequences.

*Low temperature catalytic gasification of biomass:* In low temperature (350-600 °C) catalytic gasification complete gasification of feedstock is difficult despite catalysts being employed. Studies with regards to the role of catalysts, reaction mechanisms using model compounds, interaction between components, batch and continuous reactors and partial oxidation in an attempt to improve gasification efficiency has been also studied by various authors.

A limited range of metal catalysts can be used for low temperature gasification due to the oxidation of metal components in the hot water environment [70, 77]. Combinations of Ruthenium and Nickel supported on Carbon or Titania have shown to be valuable in this process environment.

Minowa and his group [77, 78] investigated the effect of catalyst on cellulose and glucose (model compounds) under hot compressed water (HCW) using an alkali catalyst ( $\text{Na}_2\text{SO}_4$ ) and a Nickel (Ni) metal catalyst. They found that the alkali catalyst lowered the onset temperature of cellulose degradation but also promoted sugar degradation since higher yields of gas and oil were obtained. The alkali catalyst also showed inhibition of char formation resulting in high oil yield even at temperatures as high as  $350^\circ\text{C}$ .

The metal catalyst also catalysed the gasification of water soluble products to syngas.  $\text{CO}_2$  and  $\text{H}_2$  were produced first and then  $\text{CH}_4$  was formed by methanation; oil and char were minimal. Minowa found that the gas yield also increased with the Ni catalyst loading and that the oil materials produced were no longer gasified.

Another important factor to consider in the course of SCW gasification is the interaction between components and its effect on  $\text{H}_2$  production. Yoshida et al., 2001 [70, 74] studied this interaction by preparing different mixtures of cellulose, xylan (model compound for hemicellulose) and lignin with a Ni catalyst and treating them by SCW using a 4-ml tubing bomb reactor. Their results indicated that a mixture of cellulose and hemicellulose is summative in the production of  $\text{H}_2$ . Conversely, when lignin was present in any of the mixtures, the production of  $\text{H}_2$  was suppressed. In further studies, Yoshida and his co-workers showed that this effect depends on the species of lignin [50]. This result shows the importance of component interactions during the gasification process.

Batch processing tests to provide comparative low temperature gasification results with different biomass feedstocks and catalysts have been performed by several research groups. Yanik et al., 2008 [79] tested trona ( $\text{NaHCO}_3 \cdot \text{Na}_2\text{CO}_3 \cdot 2\text{H}_2\text{O}$ ) and red mud (Fe-oxide containing residue from Al-production) as catalysts besides the commonly used  $\text{K}_2\text{CO}_3$  and Raney-Ni catalysts to perform SCW gasification of cotton stalk, corncob and a tannery waste using an Inconel 625-lined, tumbling batch autoclave (volume of 1 L), with three thermocouples inserted internally into the reactor. They found that the effect of catalysts on gasification varied with the type of biomass. In general, the results showed that the tested catalysts significantly increased the  $\text{H}_2$  yield in comparison to catalyst free gasification and showed similar or better activity than  $\text{K}_2\text{CO}_3$  and Raney-Ni. All of the catalysts used enhanced the water-gas shift reaction and reformation of methane due to the  $\text{H}_2$  production rather than methanation.

Matsumura et al., 2005 [70] tested a variety of high moisture feedstocks suitable for wet gasification varying from fermentation ethanol beverage distillation residue to cattle manure solids. The reactor was a stirred 1 L vessel and the catalysts employed are described as follows:

- Ru/TiO<sub>2</sub> = 3 % Ru on rutile titania (by Degussa).
- Ru/C = 7 % Ru on carbon (by Engelhard).
- Ru/Ni = 1 % Ru on GI-80 Ni methanation catalyst (by BASF).
- Cu/Ni = 1 % Cu on GI-80 Ni methanation catalyst (by BASF).
- No catalyst.

The gasification was very limited with the catalyst un-supplemented test. The Ru on titania catalyst exhibited the lowest activity whereas the Ru/Ni catalysts showed the highest conversion activity especially on the manure solids followed by the lightly processed grains. The effect of temperature was eminent since higher conversions were achieved at the critical point of water (374 °C), however at higher temperature there was no noticeable difference.

It is believed that partial oxidation, which is commonly used in gasification technology, will enhance the gasification efficiency of SCW gasification. Matsumura et al., 2002 tested this effect by adding hydrogen peroxide (2.5 wt %) to 6 wt % cabbage slurry; the reaction temperature was 400 °C and the pressure applied was 25 MPa. The gasification efficiency was successfully improved to 0.87 ( 87 %).

*High temperature catalytic gasification of biomass:* The temperature range for this process is between 500 to 750 °C; high gasification efficiencies are achieved due to the reactivity of biomass at these temperatures however such efficiencies are highly dependent on biomass concentration. In reactions performed on glycerol and glucose at concentration (1-20 wt%) without catalyst at reaction temperatures of 500-800 °C and at pressure of 5-45MPa it was found that concentrations higher than 5-10 wt% lead to significant reduction of the H<sub>2</sub> yield and gasification efficiency. It was found also that upon increasing the reaction temperatures above 650 °C, the yields of H<sub>2</sub> and CO<sub>2</sub> sharply increased reaching 100 % (complete gasification) with small biomass concentration (< 3 %), while CO decreases, indicating strong water-gas shift reaction activity at T > 650 °C.

In addition to research conducted on model compounds like glucose or cellulose which provided a good understanding of the main reaction pathways detected by key compounds [80, 81], a real model biomass of reproducible composition and similar to potential feedstocks such as residues from the food industry was also needed. Baby food (by Hipp) consisting of mainly cooked potatoes and carrots with water content of 89.2 % and 6.2 g.kg<sup>-1</sup> ash content (mainly K and Na salts)

was selected for long term WB gasification investigations. In these experiments, the role of alkali salts during biomass gasification, changes of product composition as a function of temperature and heating rate and the influence of dry matter content were studied. Two different reactors were used; a tumbling batch reactor (up to 500 °C and 50 MPa, 1 L internal volume) and a stirred vessel used in continuous or batch mode (up to 700 °C and 100 MPa, 0.190 L internal volume) [71]. In both modes of the stirred vessel heating of the biomass was achieved by injecting the biomass into heated water and mixing. The tumbling batch reactor was used with a low heating rate of 1 to 3 °K.min<sup>-1</sup> from room temp. to 500 °C. Key compounds belonging to the following categories: sugars, aldehydes, acids, furfurals, phenols and gases were selected to elucidate different reaction pathways.

Experiments in the tumbling reactor revealed that the presence of KHCO<sub>3</sub> leads to an increased amount of aqueous products, less coke/char formation, a lower concentration of furfurals and higher concentration of phenols ([70, 71]. This is important considering that salts can influence a number of reaction mechanisms and that real biomass includes salts, which would mean high H<sub>2</sub> yield and low yields of CO.

Biomass conversion is also strongly dependent on temperature. Slow heating up leads to the formation of coke and char which was found in the tumbling reactor in every reaction but never in the stirred vessels. A decrease of heating rate also led to a decrease in H<sub>2</sub> yield [71]. One explanation for the formation of coke and char in the tumbling reactor is that when the wet biomass spends long time in subcritical temperatures, furfurals and other compounds may polymerize when free radicals are formed above the critical temperature. Another interesting finding was an increased yield of phenols with temperature, suggesting that the degradation rate of phenols is slower than that of furfurals; in this respect phenols can be considered the last obstacle before complete gasification.

The dry matter content (carbon input) is of special interest. In a tubular reactor, the higher the dry matter or carbon input the lower the gasification efficiency; conversely in a stirred vessel an increased gasification rate was achieved at increasing dry matter input. Thus the type of reactor was determinant in the results; the stirred vessel reactor had fast heating-up and back mixing of the products, therefore one possible explanation could be that due to the back mixing, the H<sub>2</sub> present inhibited unwanted polymerization through the saturation of the free radicals which would lead to less coke or tar and high gas yields [70].

Due to the difficulty to recover alkali catalysts from the reactor effluent metal oxide catalysts have been also tested but in contrast with low temperature catalytic gasification of biomass the gasification efficiencies using these catalysts is low, mostly due to deactivation of the catalyst. For

example when Ni/MgO catalyst was used the deactivation of the catalyst was attributed to: a) lack of regeneration treatments by the presence of char-like carbonaceous products and the formation of  $\text{Mg}(\text{OH})_2$  and b) with regeneration treatments to a change in Ni structure resulting in a decrease of surface area [70, 74, 79, 82].

Yoshida et al., 2004 investigated the effects of Ni catalyst amounts in the gasification of five different lignin species using a microreactor made of 316 stainless steel tubing with an outer diameter of 9.53 mm and inner diameter of 6.53 mm at 653 °K, 25 MPa and reaction time of 20 min. The gasification efficiencies were very low possibly due to a deactivation of Ni catalyst by tarry products; when the amounts of catalyst were increased higher gasification efficiencies were observed despite deactivation of the catalyst. They also found that different lignin showed different gasification characteristics due to different lignin structure [50].

Furuzawa et al., 2007 also investigated the gasification of lignin with 10 wt % Ni/MgO catalyst prepared by impregnating MgO with aqueous solution of  $\text{Ni}(\text{NO}_3)_2$  and calcined in air at temperatures of 773 and 1173 °K in SCW using a stainless steel tube bomb reactor at 673 °K and 30-37 MPa. The best results were obtained with 10 wt % Ni/MgO(873 °K) with a carbon yield of gas products ( $\text{CH}_4$ ,  $\text{CO}_2$  and  $\text{C}_2\text{H}_6$ ) of 30 % which, despite the low conversion, is an improvement and further research is necessary [83].

The need for new catalysts with high activity, high stability and scope for regeneration of catalytic performance is necessary for significant improvements on WB SCW gasification.

With respect to the engineering of SCW gasification process, several technological challenges arise due to the high temperature and high pressure (HP) conditions of the reactor [70]. Among these are: feedstock pre-treatment and pumping equipment to continuously feed a HP reactor; a heat recovery unit which is essential for SCW gasification to be energy efficient; a depressurization system and a gas recovery unit which may involve unit operations for the separation of the gas mixture ( $\text{CH}_4$ ,  $\text{H}_2$  and  $\text{CO}_2$ ) if  $\text{H}_2$  is to be used for fuel cell applications.

The VERENA test facility located in Karlsruhe, Germany apparently is the largest SCW gasification plant with a throughput of  $100 \text{ Kg}\cdot\text{h}^{-1}$  [37]. In this pilot plant different types of biomass have been used successfully and converted with heat transfer efficiency greater than 80 % whereas typical energy efficiencies for different SCW gasification processes vary from 44 to 65 % [37, 84]. Yoshida et al., 2003 [37, 85] found that SCW gasification was the most energy efficient technology for biomass with water content  $> 30 \%$ ; commercialization of gasification plants is in its initial stage.

### II.3.1.2 Biomass pyrolysis

Pyrolysis can be defined as the thermal degradation of biomass by heat in the absence of oxygen, which results in the production of charcoal (solid), bio-oil (liquid), and fuel gas products. In this process biomass is heated at low pressure (1 to 5 bars) at temperatures within the range of 280 °C and 780 °C in the absence of air [49, 58, 86]. The product distribution depends on the type of biomass, heating rate, residence time and type of catalyst. Depending on these operating conditions, the pyrolysis process can be divided into three subclasses: slow pyrolysis (carbonization), fast pyrolysis, and flash pyrolysis. Slow pyrolysis is not considered for H<sub>2</sub> production as the products are mainly charcoal and oils [58]. Fast pyrolysis is the preferred technology for the production of liquid and gaseous products from biomass, in this process biomass feedstock (particle size < 1 mm) is heated rapidly (10-200 °C.s<sup>-1</sup>) at temperatures of 580-980 °C and a short residence time (0.5-10 s) in the absence of air. Gaseous products include H<sub>2</sub>, CH<sub>4</sub>, CO and CO<sub>2</sub> and possibly other gases depending on the biomass composition; liquid products include tar and oils; and solid products are mainly char, carbon and other inert materials [87].

Fast pyrolysis proceeds at temperatures above 780 °C at much higher heating rates than fast pyrolysis (> 1000 °C.s<sup>-1</sup>), a particle size < 0.2 mm is therefore necessary and low residence time (< 0.5 s) also in the absence of air. Recently this technology has attracted great interest for maximizing liquid yields. [58, 86, 87].

The mechanisms of biomass pyrolysis have been studied based on the major components of biomass (hemicellulose, cellulose and lignin). In essence the thermal degradation process of these components can be summarized as shown in Fig. 14:

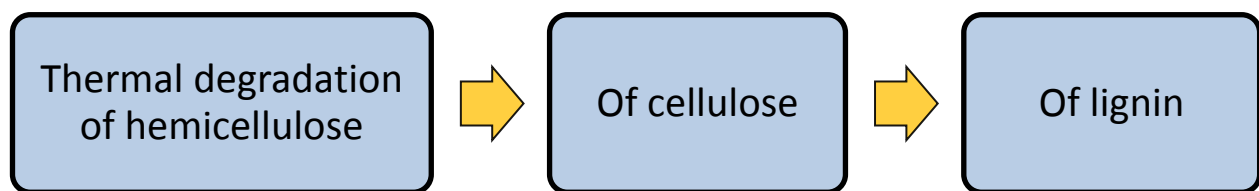


**Fig. 14** Thermal degradation sequence of main components of biomass from lowest to highest temperature. This indicates that hemicellulose is degraded first, then cellulose and finally lignin.

Even though H<sub>2</sub> can be obtained from biomass by pyrolysis processes, this technology is mainly seen to have great promise as a means for converting biomass into chemicals and higher value liquid fuels and in that sense it differs from gasification. It is said that pyrolysis lies at the heart of all thermochemical fuel conversion processes and is assumed to become an avenue to petroleum type products from biomass resources, for example pyrolytic oil may be used directly as a liquid fuel, added to petroleum refinery feedstocks, or catalytically upgraded to transport grade fuels [88].

## II.4 Biological methods

Biological methods for H<sub>2</sub> production (biotechnologies) provide an alternative that is more environmentally friendly and less energy intensive than thermochemical and electrochemical processes due to the capacity of these systems to utilize sunlight and organic wastes (biomass) as substrates for bio H<sub>2</sub> conversions. In addition, bio H<sub>2</sub> does not contain CO and H<sub>2</sub>S which are catalyst poisons for fuel cells applications [89]. Biological methods for H<sub>2</sub> have formed the subject of several recent reviews [90-92].

As described in sections I.2 and II.3 biomass suitable for biotechnologies are abundant and guarantee sustainability, they can be found in agricultural residues [93], food wastes [94] and effluents specially from food and farming industrial processes such as manure [95] sugar mills [96], olive processing [97], dairy products [98] among others. Consequently biotechnologies could provide a valuable contribution to reduce organic waste disposal and environmental damage, and saving increasing costs associated when disposed in landfill (section I.2) which in UK are currently in £56 and expected to increase to £72 per tonne by April 2013 (WRAP gate fees report 2010, [http://www.wrap.org.uk/recycling\\_industry/market\\_information/](http://www.wrap.org.uk/recycling_industry/market_information/)).

Hence biotechnologies for H<sub>2</sub> production are expected to grow in importance in the near future as research and laboratory scale work develops for demonstration and practical applications.

Biological H<sub>2</sub> production occurs through the active use of different microorganisms under the appropriate conditions; it is controlled by the action of hydrogen-producing enzymes such as hydrogenase and nitrogenase following specific metabolic pathways. The main bio-process technologies for bio-hydrogen production can be classified as follows:

- Biophotolysis of water
- Photobiological hydrogen production
- Dark hydrogen fermentation
- Hybrid systems using photosynthetic and fermentative bacteria
- Hybrid system using Bio methane production followed by steam methane reforming (SMR)

It is not the purpose of this overview to provide a thorough review of these technologies (see review papers) [90-92] but a brief description of them will be provided.

#### II.4.1 Biophotolysis of water

Photosynthesis is a chemical process utilized by plants, algae and many species of bacteria that converts CO<sub>2</sub> into organic compounds especially carbohydrates using the energy from sunlight. Photosynthetic organisms are called photoautotrophs since they can create their own food.

Biotechnologies involving microorganisms that harness light (solar or artificial) for growth and that are useful for H<sub>2</sub> production are all photosynthetic. Biophotolysis of water utilizes microorganisms (microalgae and cyanobacteria) capable to use photosynthesis processes for the generation of H<sub>2</sub> gas instead of carbon containing biomass. Microalgae and cyanobacteria, like plants, possess two photosynthetic systems for light absorption (Photosystem I and II: PSI and PSII) that operate in series (direct photolysis) and can decompose water to release H<sub>2</sub> and O<sub>2</sub> (oxygenic photosynthesis) [90, 91, 99].

*Direct photolysis:* In general by this mechanism microalgae and cyanobacteria convert solar energy into chemical energy in the form of H<sub>2</sub>. In this process water is split evolving O<sub>2</sub> (PSII) and PSI generates the reductant for CO<sub>2</sub> fixation. In this sequential process, two photons (one per photosystem) are used for each electron removed from water and used whether in CO<sub>2</sub> reduction or H<sub>2</sub> (2e<sup>-</sup> & 2H<sup>+</sup>) formation. In green plants only CO<sub>2</sub> reduction takes place as the enzymes that catalyze H<sub>2</sub> generation (hydrogenase and nitrogenase) are absent, however microalgae and cyanobacteria have such enzymes and can produce H<sub>2</sub> under defined conditions. The mechanisms involved in H<sub>2</sub> production by these two types of microorganisms are more detailed in various reviews [90, 99, 100].

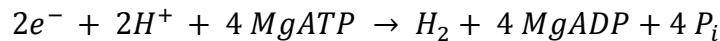
An important limitation for obtaining sustained H<sub>2</sub> production from biophotolysis of water is the sensitivity of the hydrogenase enzymes to O<sub>2</sub>. Oxygen irreversibly inactivates H<sub>2</sub> producing systems. Recent attempts to increase H<sub>2</sub> production by direct photolysis involve nutrient deprivation; under sulphate limitation PSII subunits can not be maintained and PSII activity ceases, thereby reducing O<sub>2</sub> production, while respiration rates remain high causing anoxia, this allows hydrogenase (or nitrogenase) to express and therefore H<sub>2</sub> production [90].

*Indirect photolysis:* In this process the CO<sub>2</sub> generated is fixed via the Calvin cycle to synthesise polycarbohydrates (starch in microalgae and glycogen in cyanobacteria) which can be subsequently metabolised by fermentation to produce H<sub>2</sub> indirectly [90].

## II.4.2 Photo fermentative processes.

Photofermentative processes utilize photoheterotrophs (microorganisms that use light for energy and organic compounds for carbon source) for H<sub>2</sub> production under anaerobic conditions in the presence of light in a process known as photofermentation. Purple non-sulphur (PNS) bacteria are the preferred microorganisms for photofermentations; they are anoxygenic photosynthetic bacteria (bacteria that capture light energy and store it as ATP without the production of O<sub>2</sub>) with a single photosystem (PSI) which prevents these microorganisms from producing O<sub>2</sub>, thereby making sustained H<sub>2</sub> production possible [90]. Also PNS bacteria do not produce H<sub>2</sub>S (a catalyst poison). PNS bacteria are capable of converting organic acids (OA) to clean H<sub>2</sub> appropriate for use in PEM-fuel cells [100]. They evolve H<sub>2</sub> through the action of the nitrogenase enzyme whose primary function is to fix N<sub>2</sub> gas into NH<sub>4</sub><sup>+</sup> ion for assimilation in an irreversible process [101] which is activated anaerobically under nitrogen limitation according to Equation 1 [102].

### Equation 1



The nitrogenase complex has to be saturated with ATP and NADH for optimal activity. For this reason H<sub>2</sub> photo production rates are favored under light saturating intensity, a fermentation media with mineral components and organic substrates in anaerobic conditions with optimal temperature and pH [90, 91].

Nitrogenase expression and activity are strongly inhibited by O<sub>2</sub> which damages the photo pigments needed to maintain ATP flux for nitrogenase activity. Therefore sustained H<sub>2</sub> photo fermentative processes are possible as PNS bacteria are unable to generate O<sub>2</sub> due to their single PSI as explained.

Hydrogen production capabilities of some species of PNS bacteria have been investigated, among them species belonging to the genera *Rhodobacter*, *Rhodopseudomonas* and *Rhodospirillum* [90]. Some major benefits of these species include: high theoretical conversion yields, lack of O<sub>2</sub> evolving activity, use of light, possibility to consume organic acids derived from bio-wastes and therefore the utilization of bio-wastes as resources [100].

Two important H<sub>2</sub> producing and metabolizing enzymes found in PNS bacteria are the membrane-bound uptake hydrogenases and the nitrogenase enzymes.

Nitrogenase enzymes re-oxidise electron carriers to reduce  $2\text{H}^+$  to  $\text{H}_2$  but also compete with other reductive process detracting from  $\text{H}_2$  production; the formation of poly- $\beta$ -hydroxybutyrate (PHB) from acetate [100]. Mutagenesis of the PHB synthase gene produced PHB deficient mutants. These mutants produced  $\text{H}_2$  in conditions that would normally support PHB synthesis [100, 103]. Mutants lacking both uptake hydrogenases and also PHB synthase produced  $\sim 2.5$  fold higher  $\text{H}_2$  rates compared to parent strain [100, 104].

In regards to substrate utilization which includes mainly OA from dark fermentation (e.g. lactate, acetate, butyrate and succinate) the substrate range is strain specific [90, 105]. The metabolic pathways are still undefined for many substrates except for acetate which, in most bacteria, is assimilated via the glyoxylate cycle whereas in other microorganisms lacking the glyoxylate cycle enzyme (*Rhodobacter sphaeroides* and *Rhodospirillum rubrum*) an alternative citramalate cycle is thought to operate [90, 106].

Ethanol, another common fermentation product, might be also utilized by some *Rhodopseudomonas* species and was rapidly removed from an *E. coli* fermentation effluent by *R. sphaeroides* O.U.001 after 96 h [107]. It is possible then that other PNS bacteria would be capable of ethanol utilization [90].

Factors affecting the performance of photofermentation include the light intensity. An increase of light intensity has a stimulatory effect on  $\text{H}_2$  production but an adverse effect on light conversion efficiency (LCE) to  $\text{H}_2$  in which important improvements have to be made [90]. LCE is variable for PNS bacteria with an average value of 4 % whereas the theoretical maximum photosynthetic efficiency is considered to exceed 10 % under these circumstances the photosystems of PNS bacteria saturate at low light intensity causing low light conversion efficiency even under high light intensity (e. g. in solar photobioreactors) [90, 100].

Alternatives for improving light conversion efficiency include genetic manipulation to reduce the size of light harvesting antennae and simultaneously reducing the amount of antenna pigment [91], increasing the concentration of cells in the photobioreactor without causing decay in light intensity, and improvements in photoreactor design.

As previously mentioned industrial waste streams can make suitable feeds for photofermentation to produce  $\text{H}_2$ , however one important requirement is that these streams possess high C/N ratio which limits  $\text{H}_2$  production by PNS bacteria due to the incompatibility of nitrogenase activity and the presence of  $\text{NH}_4^+$  [90, 100] and see above.

PNS bacteria are potentially capable of efficient conversion of OA to H<sub>2</sub> providing also a valuable solution for the remediation of wastes rich in OA, alcohols or aromatics; but the problems of working in a N<sub>2</sub>-free environment are challenging, for example until sufficient H<sub>2</sub> is produced to fill the headspace sparging with e.g. argon is needed.

### **II.4.3 Dark fermentation.**

As mentioned in section II.4 feeds for biological processes are available in large quantities and guaranteed sustainability. Fermentative bacteria enable the utilization of biomass as sources for energy production through the generation of H<sub>2</sub> as an energy carrier while at the same time contributing to minimize organic waste disposal and environmental damage.

Fermentative H<sub>2</sub> production technologies depend on either hydrogenase or nitrogenase mediated metabolisms for H<sub>2</sub> production and derive energy either from light/sun or by consuming photosynthetically derived carbon compounds (carbohydrates)[108]. In fermentative processes from carbohydrates hydrogenase-mediated metabolisms are preferred over nitrogenase-mediated due to their higher fermentative H<sub>2</sub> yields and lower metabolic cost (no light energy is required and higher theoretical H<sub>2</sub> yields of 4 mol H<sub>2</sub>.mol hexose<sup>-1</sup>) can be achieved [90, 98, 109].

Dark fermentation is a biological process performed in anoxic conditions with bacteria grown in the absence of light sources under appropriate conditions to produce H<sub>2</sub> from carbohydrate rich substrates. The anaerobic degradation of such carbohydrates by heterotrophic microorganisms (bacteria that use organic matter synthesized by other organisms for energy and growth) has several important advantages such as high rates of H<sub>2</sub> production and constant H<sub>2</sub> production (during day and night). Fermentative bacteria have a good growth rate to supply the H<sub>2</sub>-production system and the utilization of agricultural and food industry wastes as resources provides a valuable way to divert these wastes from landfill [90, 109, 110].

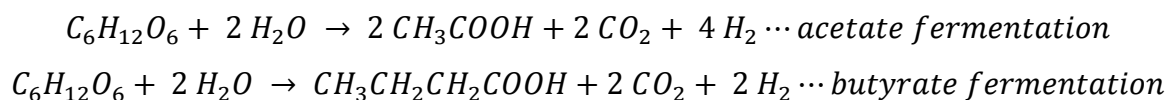
In anoxic environments protons act like an electron acceptor to produce molecular hydrogen [111]. When glucose is used as substrate for fermentative H<sub>2</sub> production, it is transported into the cell by the phosphotransferase system and then catabolised by the H<sub>2</sub> producing bacteria via the glycolytic pathway to NADH and pyruvate [90, 92]. The metabolic pathway of mixed acid fermentation will be presented in section II.4.3.1 (Fig. 15).

Most microbial H<sub>2</sub> production is driven by the anaerobic metabolism of pyruvate [98, 100]. Pyruvate is oxidized to acetyl-CoA recycling NAD<sup>+</sup> from NADH by the competing action of three

enzymes: pyruvate formate lyase (PFL), pyruvate-ferredoxin oxidoreductase (PFOR) and fermentative lactate dehydrogenase (LDH). The H<sub>2</sub> produced depends on the fate of pyruvate, which is a very complex process influenced by many factors such as culture species, substrate, reactor type, nutrients, temperature and pH. Acetyl-CoA is finally converted to ATP and soluble end products such as acetate, butyrate, ethanol, etc. [92, 100, 112].

Axenic cultures (pure cultures) had been exploited to produce H<sub>2</sub> using a variety of substrates. The most widely used are members of *Clostridium* and *Enterobacter*. Species of *Clostridium* are Gram negative, rod shaped strict anaerobes and endospore formers, whereas *Enterobacter* are gram negative, rod shaped facultative anaerobes (can grow in aerobic or anaerobic conditions) [90, 111]. Most studies involving axenic cultures were performed in batch mode and used glucose as substrate. Facultative anaerobic bacteria gave 2 mol of H<sub>2</sub> per mol of glucose whereas strict anaerobic bacteria gave 4 mol of H<sub>2</sub> per mol of glucose [111]. The normal pathway used by *E. coli* goes to 2 mol H<sub>2</sub>.mol glucose<sup>-1</sup> and is irreversible, as a consequence H<sub>2</sub> can accumulate to high pressure in the head space. Using the 'NADH pathway' (enterobacter) you can get the 4 mol H<sub>2</sub>.mol hexose<sup>-1</sup> but the NADH pathway is freely reversible as H<sub>2</sub> accumulates so to realise the yield H<sub>2</sub> must not accumulate. A positive pressure is needed to fill a H<sub>2</sub>-store or run a fuel cell.

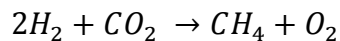
Facultative anaerobes are less sensitive to O<sub>2</sub> and are able to recover H<sub>2</sub> production activity after O<sub>2</sub> exposure by rapidly depleting O<sub>2</sub> present in the broth. For this reason, facultative anaerobes are considered better microorganisms than strict anaerobes for fermentative H<sub>2</sub> production processes. One of the main restrictions of dark fermentation is the low H<sub>2</sub> yield (2-4 mol H<sub>2</sub>.mol glucose<sup>-1</sup>) which proceeds according to the following reactions [98, 111]:



These theoretical yields are sufficient to permit economic viability compared to existing chemical or electrochemical processes [90, 108, 113] and even to theoretical yields of photofermentations [90, 100] therefore research and development activities for dark fermentation focuses on attaining the highest yields of H<sub>2</sub> from a wide variety of carbohydrate rich substrates which include complex waste streams through the development of two stage fermentation process,

metabolic engineering and the utilization of mixed cultures of microorganisms as inocula obtained from waste water, sludge and soil [108, 114].

The use of mixed cultures for dark fermentation offer more practical advantages over axenic cultures since this mode can utilize a broader source of feedstocks without sterilization, is more easy to operate and easier to control. However several problems arise when using mixed cultures, one of these being the coexistence in nature of H<sub>2</sub> producing and H<sub>2</sub> consuming bacteria (e.g. methanogens) which oxidise H<sub>2</sub> and reduce CO<sub>2</sub> according to the following reaction:



It has been found that when mixed cultures are treated under harsh conditions, H<sub>2</sub> producing bacteria have more chance of survival than H<sub>2</sub> consuming activity from non H<sub>2</sub> producers [115]; as a consequence pretreatments for enriching H<sub>2</sub> producing bacteria in mixed cultures include: heat shock, acid-base treatment, aeration, freezing and thawing, and chemical treatments e.g. with chloroform. Such pre-treatment can be monitored using microbial analysis methods such as the spread plate method [116]. Since most pre-treatment methods have been conducted in batch mode, research in continuous mode has been proposed [108, 115] since microorganisms in general have good adaptive stress responses.

Temperature is one of the most important operational parameters that affects the growth rate and metabolic activity of microorganisms in fermentative H<sub>2</sub> production. Fermentative reactions can be operated at mesophilic (25-40 °C), thermophilic (40-65 °C) or hyperthermophilic (> 80 °C) temperatures. It has been demonstrated thermodynamically that increasing the temperature of glucose fermentation while maintaining reactant concentrations constant would enhance H<sub>2</sub> concentration [98, 108, 117].

Thermophilic and hyperthermophilic fermentation reactions utilize thermatogales (thermophilic or hyperthermophilic microorganisms whose enzymes remain active at high temperatures) and various studies investigating the effect of temperature on fermentative H<sub>2</sub> production using glucose and sucrose as substrates. Optimum temperatures were not always the same, in the mesophilic range optimum values were around 37 °C and in the thermophilic range around 55 °C. In addition one of the studies reported that the volumetric H<sub>2</sub> production rate (VHPR) was 60 % greater under thermophilic conditions than mesophilic conditions which was attributed to the optimum temperature for the enzyme hydrogenase present in thermophilic *clostridia* [118], also a yield of 3.2-3.7 (mol H<sub>2</sub>.mol glucose<sup>-1</sup>) was reported for *Caldicellulosiruptor saccharolyticus* [119]. Contrary to this, high temperatures can induce thermal denaturation of proteins in some cases

affecting the microorganism activity, for example higher values of H<sub>2</sub> production (VHPR) were reported at mesophilic temperatures in the case of *Citrobacter* CDN1 and *Clostridium saccharoperbutylaceticum* ATCC27021 (maximum H<sub>2</sub> production at 30 °C in both cases), it was inferred that high temperature induced thermal denaturation of proteins affecting the microbial activity [120]. Thermophiles are specially adapted to life at high temperatures with various modifications to their proteins and cell membranes to enable maintenance of activity at high temperatures. One important disadvantage of thermophilic processes is the increased energy cost of fermentations and the building partial pressure of 10-20 KPa (0.0-0.2 bar) caused by the accumulation of H<sub>2</sub> in the fermentation process that inhibits H<sub>2</sub> production [90, 121].

The pH is another important parameter that has a profound effect on the hydrogenase activity and the metabolic pathways of H<sub>2</sub> producing bacteria, thereby on fermentative H<sub>2</sub> production potential and H<sub>2</sub> production rate [122]. On several studies conducted in batch mode without pH control, only the effect of initial pH was investigated on fermentative H<sub>2</sub> production. From these studies the optimal pH in most cases lies in between 6 and 8. In some cases where mixed inocula were used a low pH of 4.2-5.0 supported the maximum H<sub>2</sub> production. In pure cultures *Citrobacter* CDN1 gave maximum H<sub>2</sub> production at pH 5 [92, 108]. Different studies reported that fermentative H<sub>2</sub> production was best supported in slight acidic condition. The initial pH has an influence on the extent of log phase in batch fermentations. Research revealed that an initial pH of 4-4.5 causes longer lag periods than an initial pH around 9 but causes a decrease in the yield of H<sub>2</sub> production [122]. This effect was attributed to a rapid H<sub>2</sub> production (high rates) with a consequent fast acid production to inhibitory levels that also depleted the buffering capacity of the fermentation media. Conversely at lower initial pH, bacteria produces H<sub>2</sub> gradually at a moderate rate due to an adaptation period but for longer [108, 122]. The specific H<sub>2</sub> production rate was highest for the pH range of 5.5-5.7 where also the ratio of acetate/butyrate produced was in the range of 3-4 indicating a tendency towards acetate type fermentation (see acetate and butyrate fermentation reactions above). It is concluded then that pH and intermediate products especially OA drive the hydrogenase reaction during dark H<sub>2</sub> fermentation.

The effect of nitrogen, phosphate, metal ions and magnesium also influence the fermentative biological process. Nitrogen is a very important component for proteins, nucleic acids and enzymes that are indispensable to the growth of H<sub>2</sub> producing bacteria; essential micronutrients for bacterial metabolism during fermentation such as Na, Mg, Zn and Fe are also needed due to the fact that these

elements play an important task in bacterial enzyme cofactors, transport processes and dehydrogenases [92, 100, 108]

#### ***II.4.3.1 Mixed acid dark fermentations***

Mixed-acid fermentation is performed under mesophilic anaerobic conditions using sugars as substrates by facultative anaerobes such as *Enterobacter* and *Escherichia coli* (*E. coli*) producing gaseous products in substantial amounts ( $H_2$  and  $CO_2$ ) and a mixture of OA (lactate, acetate, butyrate and succinate), in addition to ethanol.

*E. coli* is facultative anaerobe attractive as a model organism for such biotechnological application because it is fast and easy to grow, non-sporulating, and well characterized in physiological and biochemical terms as well as having a very well defined molecular biology and hence being the laboratory ‘workhorse’ for studies in molecular engineering. As a facultative anaerobe *E. coli* can grow in aerobic or anaerobic conditions by using sugars (glucose) as sole carbon and energy source [123]. As explained in section II.4.3 during fermentation glucose is converted to pyruvate and is in the subsequent metabolism of pyruvate that differences between aerobic and anaerobic growth conditions take place [123] (oxidative phosphorylation or fermentation respectively).

The key enzymes involved in mixed acid fermentations by facultative anaerobes are pyruvate formate lyase (PFL) and the formic hydrogen lyase (FHL) complex (containing a specific formate dehydrogenase and hydrogenase). In simple terms, PFL converts pyruvate to acetyl-CoA and formate, which is then transformed to  $H_2$  and  $CO_2$  by FHL; acetyl-CoA is split into acetate (which generates ATP) and ethanol (which oxidises NADH to regenerate NAD) [123]. The  $H_2$  produced during mixed acid fermentation by facultative anaerobes is performed exclusively by the formate hydrogenlyase (FHL) complex which is located on the inner membrane of the bacterial cell and having formate as a unique precursor for  $H_2$  production in an irreversible process; the metabolic pathway is illustrated in Fig. 15.

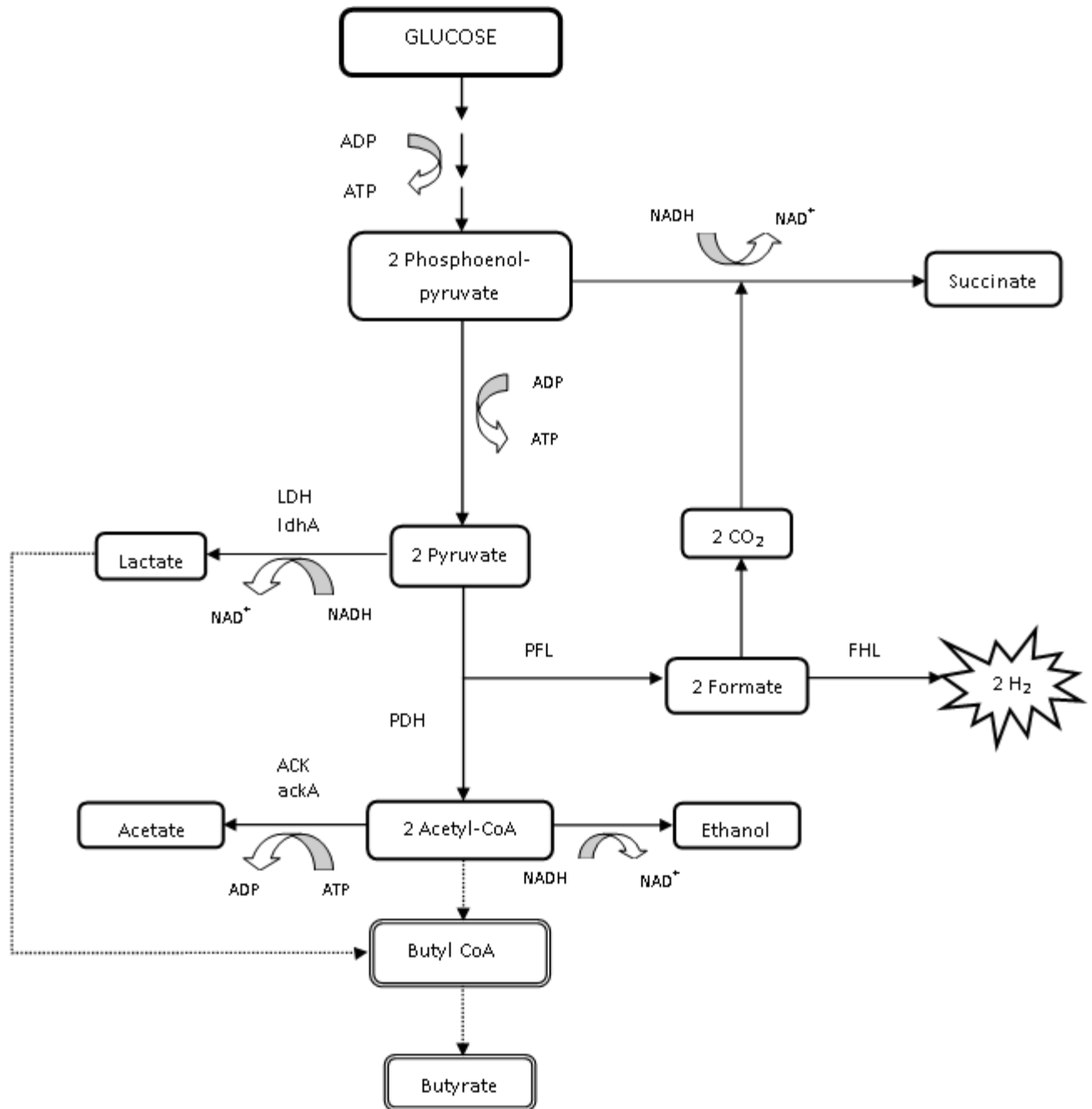


**Fig. 15** Metabolic pathways involved in mixed acid fermentation. The solid lines show pathways to H<sub>2</sub> production; (.....) represent a possible pathway to butyrate usually involved in *Clostridium*. LDH: Lactate dehydrogenase, gene: ldhA; ACK: acetate kinase. Gene: ack A; FHL: formate hydrogenlyase complex. Reactions shown as (\*) are biochemical mechanisms to ‘dump’ H<sub>2</sub> on to metabolic intermediates to regenerate the H carrier NAD<sup>+</sup> which is key to continued metabolism in the absence of O<sub>2</sub>; lactate, ethanol and succinate are produced.

**Table 4** Main genes involved in the mixed acid fermentation of *E. coli* for H<sub>2</sub> production. Source Clark, 1989.

Gene	Description	Role
PFL	pyruvate formate lyase	Generates formate from pyruvate, formate is H <sub>2</sub> precursor
PDH	Pyruvate dehydrogenase	Transforms pyruvate into Acetyl-CoA by pyruvate decarboxilation
<i>ackA</i>	acetate kinase	makes acetate from acetyl CoA and generates ATP
<i>fdhF</i>	formate dehydrogenase	part of the formate dehydrogenase H <sub>2</sub> lyase complex (FHL) responsible for H <sub>2</sub> and CO <sub>2</sub> generation from formate
<i>hyd_1, hyd_2</i>	Hydrogenase	catalyses cell respiratory H <sub>2</sub> oxidation (H <sub>2</sub> recycling activity)
<i>hyd_3</i>	Hydrogenase	catalyses fermentative H <sub>2</sub> production
<i>ldhA</i>	lactate dehydrogenase	forms lactate, regenerates NAD <sup>+</sup>

A maximum yield of 2 mol H<sub>2</sub> / mol glucose can be achieved in mixed acid fermentations, but typical yields in batch mode are in the order of 50 % due to several factors such as diversion of pyruvate to the formation of lactate (which also regenerates NAD<sup>+</sup> from NADH) and also to competing respiratory H<sub>2</sub> oxidation e.g. where H<sub>2</sub> is oxidised as a source of electrons which is catalyzed by two uptake hydrogenases *Hyd-1* and *Hyd-2* (see Table 4). These effects were minimized by the utilization of genetic techniques to remove *Hyd-1* and *Hyd-2* as well as optimization of culture conditions to improve bio-hydrogen generation [124].

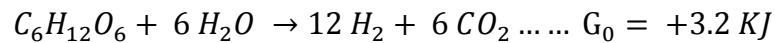
For example, while formate cleaves into H<sub>2</sub> and CO<sub>2</sub> in an irreversible process, H<sub>2</sub> uptake for cell respiratory H<sub>2</sub> oxidation was resolved by removing the hydrogenase *Hyd-2* responsible for H<sub>2</sub> uptake resulting in a 37 % increased H<sub>2</sub> yield [124]. The rate of H<sub>2</sub> formation was also increased through the up-regulation of FHL unable to synthesise the FHL complex repressor *HycA* [125]. One important limitation of dark fermentation is that the formation and accumulation of OA in the fermentation system can inhibit the H<sub>2</sub> production therefore a way to remove these organic molecules has to be implemented for continuous and more efficient H<sub>2</sub> production.

H<sub>2</sub> production through biological processes is an exciting new opportunity for technology development for bioenergy generation, however significant improvements are still to be made through rapid gas removal and separation, the development of effective hybrid systems considering the disadvantages of the dark and photofermentation while maximising H<sub>2</sub> yield and by metabolic

engineering of metabolic pathways through genetic engineering; genomic technology may contribute to make biological H<sub>2</sub> production more economical, practical and commercially feasible.

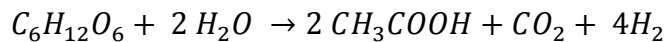
#### II.4.4 Hybrid systems for H<sub>2</sub> production

Even after optimizing all possible factors for fermentative H<sub>2</sub> production, production of H<sub>2</sub> beyond 4 mol H<sub>2</sub>.mol hexose<sup>-1</sup> is not possible by a single stage system [90, 108]. Complete oxidation of glucose into H<sub>2</sub> and CO<sub>2</sub> can not be achieved as the reaction is thermodynamically unfavourable:

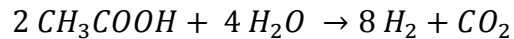


A strategy to surpass this thermodynamic limitation is by combining H<sub>2</sub> production via dark fermentation followed by H<sub>2</sub> production through photo fermentation. This system, known as a hybrid system or two stage fermentation process utilizes the OA (acetic, butyric, lactic, succinic acids) generated during the dark fermentation stage as feedstock for the photosynthetic bacteria to be converted into more H<sub>2</sub> in a second photo fermentation step. The overall process is represented as follows:

Stage 1: Dark fermentation by facultative anaerobes.



Stage 2: Photo fermentation by photosynthetic bacteria.



Ideally then, 12 moles of H<sub>2</sub>.mole of glucose<sup>-1</sup> could be expected by integration of these two fermentation stages.

Another strategy consists in producing bio-CH<sub>4</sub> which can be generated from biomass using anaerobic digesters (anaerobic digestion), then bio-CH<sub>4</sub> is subjected to steam methane reforming (SMR) for H<sub>2</sub> production as explained in section II.1. In addition to bio-CH<sub>4</sub>, organic compounds such as ethanol, methanol and organic acids derived from biomass can also be used to generate more H<sub>2</sub> via SR or biological methods (section II.4).

Both strategies will be briefly explained in sections II.4.4.1 and II.4.4.2

#### **II.4.4.1 Anaerobic digestion coupled to SMR for H<sub>2</sub> production**

Waste treatment consists of a combination of aerobic processes for organic matter to obtain a solid residue (digestate) similar to compost, then under oxygen free conditions in a sealed reactor (anaerobic digester) anaerobic biological degradation of the digestate occurs using a mixed microbial population to allow the production of a gas mixture (biogas) consisting of methane (60-70 %) and carbon dioxide (30-40 %).

AD comprises 2 stages in the same vessel:

Stage 1 acetogenesis:  $Glucose \rightarrow Acetate + other\ OAs + CO_2 + H_2 + cell\ growth$

Stage 2 methanogenesis:  $Acetate + OAs + H_2 + CO_2 \rightarrow CH_4 + CO_2 + cell\ growth$

Essentially stage 1 is a dark fermentation just like *E. coli*, therefore the effluent from a dark fermentation process can be used as a substrate for a methanogenic stage of anaerobic digestion (AD) while at the same time reducing the chemical oxygen demand (COD) and solids content of the effluent. By combining the H<sub>2</sub> and the CH<sub>4</sub> produced in both stages we achieved an important integrative approach from two separate reactors each subjected to different operating conditions and to individual optimization [126]. Among the advantages of this integration is the maximization of energy produced as a number of studies confirm that not only more energy can be produced through the combined process, but also the gas mixture produced has superior combustion properties and reduced emissions of air pollutants. For example DiStefano and Palomar et al., 2010 showed that using fodder maize, the two step anaerobic process can produce 121,522 MJ.ha<sup>-1</sup> compared to 24,185 and 77,264 MJ.ha<sup>-1</sup> as biodiesel from oil seed rape and bioethanol from wheat grain respectively [127].

Some commercial AD plants produce CH<sub>4</sub> and H<sub>2</sub> from food wastes and from waste water treatment. Fig. 16 illustrates important units of an AD pilot plant operating in Essen, Germany for CH<sub>4</sub>, H<sub>2</sub> and energy production. This facility offers the opportunity of economic feasibility study of the H<sub>2</sub> production from renewable energy sources and provides the infrastructure for mobile fuel cell application (H<sub>2</sub> filling stations).

AD has low carbon footprint and no overall environmental impact (“carbon neutral”) since the greenhouse gases generated may be burnt for energy and originates from organic material with a short carbon cycle (fixed CO<sub>2</sub>). This technology is in growing demand; according to the Waste

Resources Action Programme (WRAP), treating 5.5 million tons per annum (tpa) of food waste by AD could generate between 470 and 760 Giga Watt (GW) of electricity per year which could supply electricity to 164 000 houses and save 0.20 to 0.35 million tonnes of CO<sub>2</sub> equivalent [128, 129].

Waste water effluent ( $4.5 \text{ m}^3 \cdot \text{sec}^{-1}$ )



Three digesters, total volume  $60,000 \text{ m}^3$  (20,000 each)



Reformer and advance gas treatment  
for the production of  $100 \text{ m}^3 \cdot \text{h}^{-1}$  of  $\text{H}_2$



Rig of  $\text{H}_2$  store, 65 cylinders with 100  
Kg capacity (50 L of  $\text{H}_2$  per cylinder)  
at 200 bars as part of a filling station



**Fig. 16** Waste water treatment facility for  $\text{CH}_4$  and  $\text{H}_2$  generation located in Essen, Germany. Pictures taken by the author.

#### ***II.4.4.2 Dark fermentation coupled to photo fermentation processes for $\text{H}_2$ production.***

Studies on two stage fermentation processes have been implemented through a variety of strategies alongside the choice of microorganisms. One of the key issues lies in the nature of the bridge connecting these two stages. One simple approach consists in a co-culture where the different microorganisms act simultaneously under the same conditions; however this is not practical since

the selection of microorganisms is based on compatibility rather than optimal individual performance. The utilization of sequential reactors, despite complexity, permits the support of different optimal conditions for each individual microorganism as well as permitting N<sub>2</sub> exclusion from the PBR in separate apparatus as part of a dual system, however this sort of system requires a mode of transportation of the products from the 1<sup>st</sup> reactor to the 2<sup>nd</sup> reactor while retaining the biomass. This major challenge has been addressed using different strategies, for continuous processes the most utilized are continuous centrifugation and the utilization of membrane systems [130] (both are costly methods). Centrifugation utilizes size and density of the particles and therefore high degree of resolution is difficult to obtain [131].

A novel technique named electrodialysis (ED) was applied by Mark Redwood at the University of Birmingham [100]. ED is an electrochemical method for separating an aqueous electrolyte feed solution into an ion concentrated and ion depleted solution by electrical driving force and ion-selective membranes. Under direct current the migration of ions is unidirectional and rapid. The ED configuration consists of four chambers (C, M, MA and A) divided by three membranes: A cation selective membrane (CSM) carrying a (-) charge that attracts and passes (+) charged ions (cations), while retarding negative ions (e.g.  $-\text{SO}_3^-$ ,  $-\text{COO}^-$ ,  $-\text{PO}_3^{3-}$ ). An anion selective membrane (ASM) carrying a (+) charge attracts and allows passage of negative ions (anions) retarding positive ions (e.g.  $-\text{NH}_4^+$ ,  $-\text{NRH}_2^+$ ,  $-\text{NR}_3^+$ ). A bi-polar membrane is also employed (BP) consisting of a CSM-ASM bilayer, Fig. 17. CSM and BP membranes avoid direct contact between bacterial cells and the electrodes which will be harmful for the bacteria; in addition the BP membrane lyses water providing pH control during extractive fermentations; the CSM also transports Na<sup>+</sup> from the C chamber forming sodium salts in the MA chamber.

The use of ED in the dual system is an innovative feature that offers the potential to efficiently and selectively separate the OA without transfer of any ammonium ion generated during the dark fermentation and delivery of OAs into the photobioreactor permitting continuous production of H<sub>2</sub> with the maximum utilization of feed and feed fermentation products [100]. Also, although electricity is consumed (4 V; current density of 2 mA.cm<sup>2</sup>), this is partly offset by the generation of H<sub>2</sub> gas cathodically; this H<sub>2</sub> can be combined with the two bio-H<sub>2</sub> streams for utilization in a fuel cell.

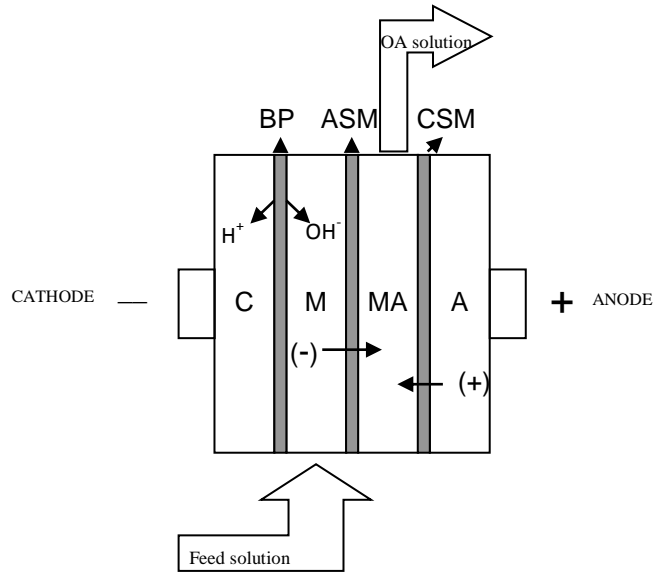


**Fig. 17** Simplified representation of the ED cell showing BP, bi-polar membrane; ASM, anion-selective membrane; CSM, cation selective membrane; C, cathode chamber; M, main chamber; MA, permeate chamber; A, anode chamber; -, cathode; +, anode. Feed solution consisting of *E. coli* culture rich in organic acids is circulated through the M chamber and the permeate was collected for use by *R. sphaeroides* (photo-fermentation) through the MA chamber. Adapted from [100].

The application and productivity of ED to integrate both fermentation stages and their integration in principle was tested by Dr. Mark Redwood in his doctoral work. The results obtained show that ED was successful in the transfer of OA while successfully achieving the retention of biomass and  $\text{NH}_4^+$  permitting continuous production of  $\text{H}_2$  by *E. coli* and *R. sphaeroides*. Yet this novel system needs significant improvements especially in the ED and photofermentation process to fully achieve the efficiency levels in terms of  $\text{H}_2$  production and economic viability. However constitutes a promising alternative for integrating dark and photofermentation in a continuous fermentation process. This novel process called extractive fermentation was tested by Redwood et al., 2011 using different food wastes with great success as described in chapter VI.5 [132].

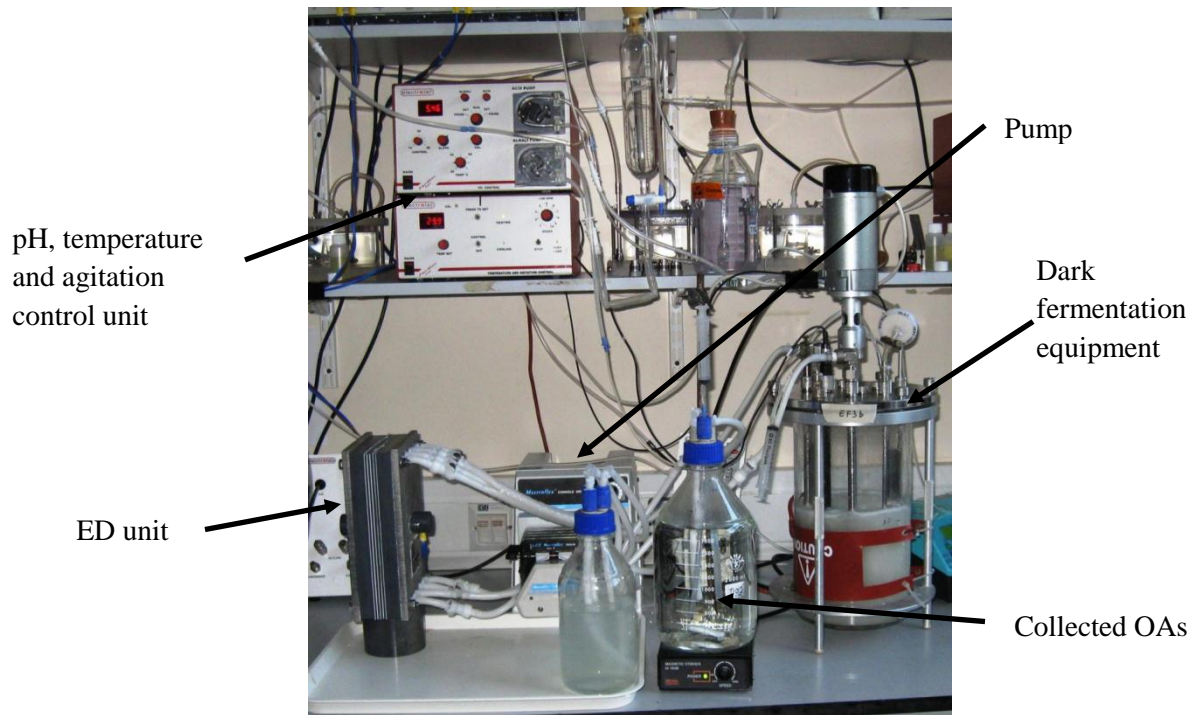


**Fig. 18** Illustration of an extractive fermentation unit in operation with important parts labelled. Picture from M.D. Redwood.

### III. BIOMASS HYDROLYSIS METHODS

In situations where complete biomass degradation is not required; eg in order to create a feedstock for microbial fermentation, a more benign form of biomass degradation can be employed that achieves partial breakdown (hydrolysis) of biomass.

Biomass is not readily fermented by microorganisms due to its complex structure; therefore biomass hydrolysis is a valuable step to produce a feedstock which is highly suitable for microbial conversion into useful products. In this section we will discuss the different hydrolysis methods available that can be applied to hydrolyse biomass.

In general hydrolysis of biomass can be achieved by several methods including acid and alkaline hydrolysis, microbial and enzymatic hydrolysis, and hydrothermal hydrolysis; the effectiveness of each of these methods depends greatly on biomass composition.

*Acid hydrolysis* has been commonly used to hydrolyse cellulose and it can be divided in dilute acid hydrolysis and concentrated acid hydrolysis. Dilute acid hydrolysis traditionally converts

cellulose to glucose with yields of about 50-70 % using  $\text{H}_2\text{SO}_4$  (< 3 %) at high temperature (250-300 °C) and pressure (100 bar); however further degradation of glucose to other unwanted products such as furfurals also occurs. Hemicellulose derived sugars ( $\text{C}_5$ ) suffer even faster degradation than cellulose derived sugars ( $\text{C}_6$ ) and, under less severe conditions, high yields of xylan (main component of hemicelluloses) to xylose can be achieved which would enhance the overall process economics as hemicelluloses could account for up to 30 % of the total carbohydrate fraction in some lignocellulosic biomass [46]. Acid hydrolysis of starch was widely used in the past but has been replaced mainly by microorganisms or enzymes (biological processes) as starch is more accessible to enzymatic attack than cellulose, however a relatively long treatment time is required in biological processes [133, 134]. Hydrothermal processes offer a viable alternative for cellulose and starch hydrolysis as will be described in sections 0 and VI.3.

Other important considerations regarding acid hydrolysis besides environmental and corrosion problems include high operating cost for acid consumption and high power demand and utility costs for operation at elevated temperatures.[53, 135].

Concentrated acid hydrolysis is a more aggressive method that decrystallizes cellulose via concentrated  $\text{H}_2\text{SO}_4$  ( $\geq 70$  %) forming homogeneous gelatine which is easily hydrolyzed by diluting with water at lower temperatures (120 °C). This method gives low sugar degradation and yields in the order of 100% but with strong environmental and corrosion problems as well as high cost associated to the high consumption of  $\text{H}_2\text{SO}_4$  and product recovery [136].

*Alkaline hydrolysis:* The  $\text{OH}^-$  cleaves the ether bridge of the cellulose glycosidic bonds hereby liberating glucose. Alkaline hydrolysis has higher reaction rate than acid hydrolysis and hydrothermal degradation methods however glucose produced is severely attacked by  $\text{OH}^-$  at temperatures below 100 °C affecting sugar yields considerably. Glucose degradation also yields OA whose reaction with the alkali is also a problem [46, 54].

When used in lignocellulosic biomass the effect of alkaline hydrolysis depends on the lignin content of the biomass. The mechanism of alkaline hydrolysis usually leads to a myriad of problems associated with high cost, environmental degradation and product degradation.

*Enzymatic hydrolysis* is based on the same principles of biomass microbial hydrolysis in which both bacteria and fungi can produce enzymes necessary for cellulose, hemicellulose and in some cases lignin degradation. These microorganisms can be anaerobic or aerobic, mesophilic or thermophilic. For example, brown, white and soft fungi are used to degrade lignin and hemicellulose

in waste materials as they produce the necessary degradative enzymes [46, 137-139] whereas *Clostridium*, *Cellulomonas*, *Bacillus*, *Thermomonospora* among others can produce cellulases [46, 140]. The understanding of these principles has led to the conceptual structure for enzymatic conversion. When compared to microbial hydrolysis, enzymatic hydrolysis using synthesized enzymes usually delivers higher monosaccharide yields and hydrolysis efficiency [141].

Enzymatic hydrolysis of cellulose is achieved via three major classes of cellulose enzymes acting synergistically to decrystallize and then hydrolyze cellulose: *endoglucanases*, which act randomly on soluble and insoluble glucose chains; *exoglucanases*, which preferentially liberate glucose monomers from the end of the cellulose chain; and  *$\beta$ -glucosidases*, which release D-glucose from cellobiose dimers and soluble cellodextrins. Recently genetically modified organisms have been developed that produce large amounts of cellulose enzymes that can digest cellulose efficiently, however the enzymatic hydrolysis of native cellulose is still a slow process and the costs of enzymes is high due to high dosages (0.1 g enzyme.g cellulose<sup>-1</sup>) [46, 53, 142].

Enzymatic hydrolysis of hemicellulose is mainly performed by xylanase, which is the generic name of enzymes that degrade the linear  $\beta$ -1,4-xylan into xylose. These enzymes are abundant in nature and produced by members of the genus *Aspergillus*, *Trichodema*, *Streptomyces* and *Clostridium* among others, however to achieve complete degradation of hemicellulose, branched xylan and mannose have to be hydrolysed by the synergistic action of different enzymes (such as *Thermomyces lanuginous*). As with cellulose, the rate of enzymatic hydrolysis is low and costly [141].

Enzymatic hydrolysis of starch (by  $\alpha$ -amylase, glucoamylases, etc) is more practical than cellulose due to its lack of crosslinking hydrogen bonds and hence crystalline structure. Of the two components of starch, amylopectin is more resistant to enzymic attack due to the  $\alpha$ -1,6 glucosidic branch ends which accounts for 4-6 % of the glucose present that must be cleaved for complete enzymatic hydrolysis of amylopectin to glucose. The majority of the existing enzymes are specific for  $\alpha$ -1,4-glucosidic bonds (amylose portion) [143]. Therefore research efforts are focusing on the development of new debranching enzymes for the amylopectin portion. Fermentative H<sub>2</sub> production from untreated potato peels has been achieved at yields comparable to pure glucose by extreme thermophilic bacteria *C. saccharolyticus* and *T. neapolitana* [52]. Although, reportedly effective in-fermentation hydrolysis of starch has not yet been applied commercially.

*Hydrothermal hydrolysis* using hot compressed water (HCW) has been recognized as an excellent alternative for biomass hydrolysis [54, 68, 144-147]. HCW is an environmentally benign

method that recently has been the object of extensive research since the process only requires water and heat [16,17].

HCW can be defined as water at temperatures above 200 °C under pressure. Under these conditions, water exhibits very interesting and extraordinary properties that can be used to support a wide variety of chemical reactions. The critical point is defined as the temperature and pressure where liquid and gaseous phases become indistinguishable and the properties of both phases are identical, in water the critical point occurs at  $T_c = 374$  °C and  $P_c = 22.1$  MPa. Water at conditions  $\geq$  than the critical point is known as supercritical water (SCW).

The properties of water change with temperature and pressure, below the critical point, the ionic product of HCW is up to three times higher than under standard conditions (25 °C; 0.1 MPa) which means that water can act as an acid/base catalyst. In addition, its relative dielectric constant [ $\epsilon$ ], a measure of its polarity, e.g. n-hexane, non-polar, has a  $\epsilon$  of 1.89 at 20 °C whereas water, very polar, has a  $\epsilon$  of 80] apparently enhances ionic reaction. The properties of HCW in this sub-critical region are suitable for a variety of synthesis and hydrolysis reactions in which water is the solvent, reactant, and catalyst. The structure of water molecule remains unchanged and its polarity is still high enough to interact, e.g. with ions. Depending on temperature and pressure, HCW can support free radical or ionic reactions implying that HCW is an “adjustable” solvent [68].

HCW is, therefore, an excellent solvent suitable for the solvolysis of complex polysaccharides such as cellulose, hemicellulose and starch [54, 68]. Its increasing miscibility with gases which increases with temperature and pressure favours homogeneous reactions of organic compounds with gases, e.g. the addition of CO<sub>2</sub> which forms carbonic acid acting as an environmentally benign acid catalyst effective for polysaccharide hydrolysis under HCW [144].

Regarding the hydrolysis of lignocellulosic biomass, the complex nature of its structure requires a pretreatment step necessary for the biological conversion of lignocellulosic biomass into bio-products such as H<sub>2</sub> and ethanol. Pretreatment of lignocellulosic biomass has two main purposes: one is to remove lignin, hemicellulose or any other compositional factor that impedes the hydrolysis of cellulose present in biomass to sugars, the other is to alter structural factors such as reduction of the crystallinity of cellulose, and increase of its porosity to make it more accessible to hydrolysis treatments, thereby improving sugar yields while preventing the generation of DP.

Pretreatment varies according to biomass composition and goals pursued, it could be one of the most expensive processing steps in lignocellulosic biomass conversion to sugars, therefore the appropriate selection of pretreatment or combination of pretreatment methods is important. As

mentioned in section II.3, cellulose, hemicellulose and lignin have different hydrolysis characteristics associated to their different structures. Therefore a strategy should be developed to obtain an efficient use of lignin, hemicellulose and cellulose for maximal sugar recovery.

A two-step process is then suggested for lignocellulosic biomass hydrolysis: first, a pretreatment to remove the lignin and hemicellulose fraction and second, a hydrolysis step to obtain sugars from cellulose.

HCW is a suitable process for biomass pretreatment [141]. Lignin and hemicellulose can be removed efficiently at lower temperatures (200 °C) before cellulose hydrolysis occurs, and then the cellulose fraction remaining will be more accessible to either further HCW hydrolysis or enzymatic hydrolysis which will be the preferred step since it has been shown that glucose yields can be considerably improved by this process after HCW pre-treatment [46, 141, 142].

HCW hydrolysis is considered as being a potentially cost-effective method for biomass pretreatment and hydrolysis [141, 148].

HCW hydrolysis constitutes the backbone of this research and the fermentability of HCW hydrolysis products from model compounds such as starch and cellulose, as well as from selected biowastes to produce H<sub>2</sub> will be studied and reported in sections 0, VI.3, VI.4 and VI.5. Fig. 19 illustrates the reactor system utilized for the experiments.

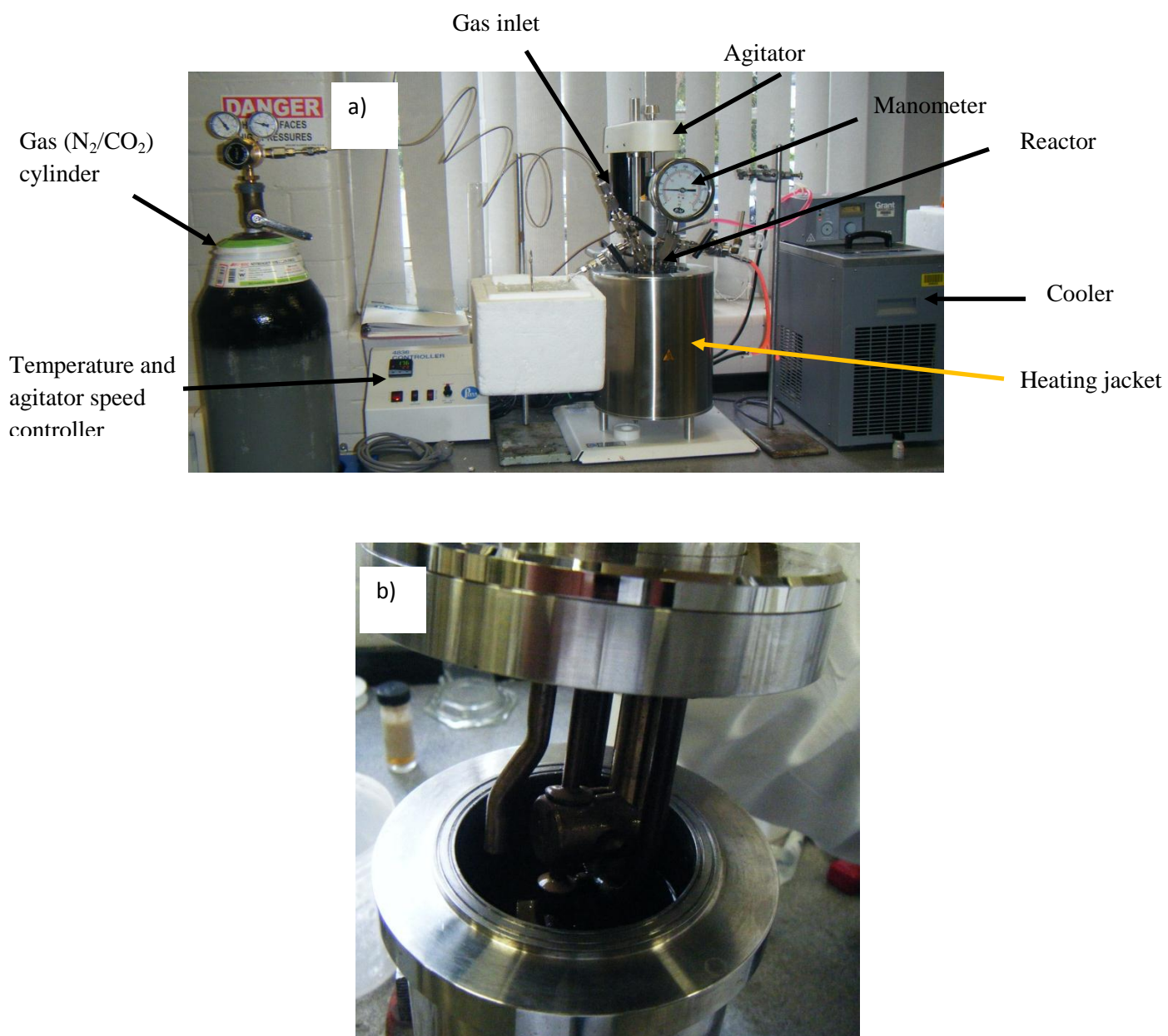


**Fig. 19** In a) the high pressure reactor system for HCW hydrolysis experiments with important parts labelled. Picture b) shows the reactor vessel.

## IV. AIMS AND OBJECTIVES

The overall purpose of this work was to advance in the development of bio-H<sub>2</sub> production technologies from biomass through the integration of thermochemical and biological processes.

Four important considerations guided the realization of this work at all times:

- 1) Utilization of environmental friendly technologies/processes.
- 2) Utilization of abundant renewable resources.
- 3) The envisioning of economical process escalation within the context a bio-refinery process.
- 4) Towards waste minimization and ultimately a zero waste process

### **Thermochemical process**

As will be explained later, the utilization of biomass for the biological process requires the selection of a suitable method of pre-treatment to achieve biomass hydrolysis and produce a hydrolysate rich in sugar, then the development of a further ‘detoxification’ step necessary to remove degradation by-products that are known microbial inhibitors, to deliver a hydrolysate suitable for downstream processing. Overall the thermochemical upstream process consisted of:

- A. Evaluation of the hot compressed water (HCW) treatment under N<sub>2</sub> and CO<sub>2</sub> for cellulose hydrolysis to hydrolysis products (sugars, sugar degradation products (DP) and organic acids (OA)) under various temperatures.
- B. Evaluation of the HCW treatment under CO<sub>2</sub> for starch hydrolysis to hydrolysis products under various temperatures and concentrations.
- C. Evaluation of the HCW treatment under CO<sub>2</sub> for food and lignocellulosic wastes under various temperatures.
- D. Evaluation of a “detoxification” technique based on activated carbon (AC) to remove potential inhibitors from the hydrolysates obtained by HCW treatments. The “detoxified” hydrolysates in each case will be fermented for H<sub>2</sub> production and H<sub>2</sub> yields will be compared to those obtained using glucose.

### **Biological process**

This step involves first, the selection of the best *E. coli* mutant for the downstream process, the evaluation was done based on the performance of the *E. coli* strains, under appropriate controlled conditions and utilizing glucose as feedstock, to:

- A. Generate the least possible amounts of inhibitory co-products (ethanol) resulting from the dark fermentation of sugars.
- B. Generate the best rate and yield of H<sub>2</sub> production.
- C. Make the “best” organic acids (OA) for the downstream photobioreactor step with respect to:
  - C.1. The highest ratio of Hydrogen Production Potential (HPP)/ionic charge (to minimize the electrodialysis power input and generate the best net energy profit).
  - C.2. The availability of purple-non-sulphur (PNS) bacterial species able to convert the OA to more H<sub>2</sub>.
- D. Ability to make an effective Bio-Pd/Pt catalyst from the waste biomass for use in:
  - D.1. Hydrogen fuel cell (downstream).
  - D.2. Upstream thermochemical processing (Pt is a catalyst often used).

Second, an evaluation of the effectiveness of an extractive fermentation process to produce H<sub>2</sub> utilizing bio-wastes from the food industry as feedstocks.

Third, a first incursion to a pilot plant scale of the dark fermentation process utilizing bio-waste substrate as feedstock.

### **Thermochemical-biological integration**

This is an integrative approach consisting of two independent steps:

- A. Pre-treatment of food wastes rich in hexoses followed by fermentation of the juices and HCW hydrolysis of the residues with subsequent H<sub>2</sub> fermentation test of the detoxified hydrolysates.
- B. The best hydrolysate (in terms of sugar content and H<sub>2</sub> yield) obtained from the HCW treatment of the food and lignocellulosic wastes will be fermented at a 5 L scale dark-fermentation, under appropriate controlled conditions (pH, temperature and agitation) for bio-H<sub>2</sub> production.

## V. LAYOUT OF THE THESIS

This research project is outlined in Fig. 20; each of the following chapters represents a sub-project. Following the introduction and general methods the results chapters are presented as follows:

### **Biological process:**

*Chapter VI.1 E. coli strain evaluation for bio H<sub>2</sub> production.* The aim of this subproject is to evaluate different *E. coli* strains available for their ability to produce H<sub>2</sub> and end products using glucose as a substrate in 3 L scale “dark” fermentation under appropriate controlled parameter (pH, temperature, agitation). Results are compared to those obtained at smaller scale (100 mL) obtained without adequate controls. Comparisons are made in terms of H<sub>2</sub> production yields and rates and OA yields with the aims cited in chapter IV.

This section includes a published paper: “Towards an integrated system for bio-energy: hydrogen production by *Escherichia coli* and use of palladium-coated waste cells for electricity generation in a fuel cell” and a subchapter describing the behaviour of various engineered *E. coli* strains.

*Chapter VI.6 Pilot plant fermentations.* Glucose and the best fruit waste juice for bio H<sub>2</sub> production will be utilized in 140 L dark fermentations using *E. coli* HD701. The aim is to begin to gain experience in the scalation of bench bank equipment (5 L fermenter system) to pilot plant scale (140 L fermentation system). The results were discussed and confirmed that more work needs to be done in order to obtain similar results to smaller scale fermentations.

### **Thermochemical process:**

*Chapter 0 Hydrogen from starch.* Starch, a model compound, was hydrolysed in HCW/CO<sub>2</sub>. The obtained hydrolysates were detoxified and tested for their ability to produce H<sub>2</sub> using the overproducing strain *E. coli* HD701. The aim was to determine conditions that maximize bio-H<sub>2</sub> production from starch. The results obtained in this work were submitted for publication in the International Journal of Hydrogen Energy (IJHE), the submitted paper: “Hydrothermal hydrolysis of starch with CO<sub>2</sub> and detoxification of the hydrolysates with activated carbon for bio-hydrogen fermentation.”

*Chapter VI.3 Hydrogen from cellulose.* Cellulose, another important model compound, was hydrolysed in HCW under CO<sub>2</sub> and N<sub>2</sub>, the advantages of using CO<sub>2</sub> vs. N<sub>2</sub> were established in terms of reaction parameters, product distribution and fermentability of the products for H<sub>2</sub> production using *E. coli* HD701. Optimum reaction conditions were established for the production of hydrolysates suitable for fermentation. The results from this work are submitted as a paper to Journal of Chemical Technology and Biotechnology “Bio-hydrogen production by *E. coli* HD701 following hot compressed water hydrolysis of cellulose under N<sub>2</sub> and CO<sub>2</sub>.”

An additional section (section VI.3.2) discusses possible reactor wall catalysed reactions that influence the product distribution and that was found in one set of experiments.

*Chapter VI.4 Hydrogen from biowastes.* Two abundant lignocellulosic compounds; wheat straw and spent brewery grain and starch rich food waste were pre treated and hydrolysed in HCW/CO<sub>2</sub>, the product distribution of the hydrolysates obtained from each of these wastes under different conditions was established and the hydrolysates were detoxified and evaluated for bio H<sub>2</sub> production using *E. coli* HD701. The effect on bio H<sub>2</sub> production and on *E. coli* growth of some potential fermentation inhibitors usually found in these hydrolysates was also studied. The aim was to utilise the experience gained with model compounds in the utilization of HCW/CO<sub>2</sub> as a hydrolysis method incorporating AC as a detoxification agent to produce hydrolysates from example of wastes suitable for bio H<sub>2</sub> production and to test at 3 L fermentation scale the most promising option. A paper is in preparation to publish the results obtained from these experiments: “Hydrothermal Bio-H<sub>2</sub> production from agricultural and kitchen wastes: impact of degradation products on *E. coli* HD701 growth and H<sub>2</sub> fermentation.”

### **Thermochemical-biological integration**

*Chapter VI.5 Hydrogen from biomass by HCW and extractive fermentation.* Wastes (pear, mango, foodwaste) rich in hexoses (glucose, fructose, sucrose) content were pre-treated. The final solid residue was hydrolysed in HCW/CO<sub>2</sub> followed by detoxification of the hydrolystes with AC and tested for bio H<sub>2</sub> production with *E. coli* HD701. The hexose rich juices were fermented for H<sub>2</sub> production by electro-extractive fermentation; the extracted organic acids (OAs) were tested for bio-H<sub>2</sub> production in small photo fermentation tests using *R. capsulatus*.

This work combined the results obtained jointly with Dr M.D. Redwood and presented as papers authored by Dr Redwood submitted to Bioresource Technology: “Electroextractive

fermentation for efficient biohydrogen production” and Environmental Science and Technology: “An integrated biohydrogen refinery: Synergy of photofermentation, extractive fermentation and hydrothermal hydrolysis of food wastes.” And the specific contribution of this author to these joint works is noted as appropriate.

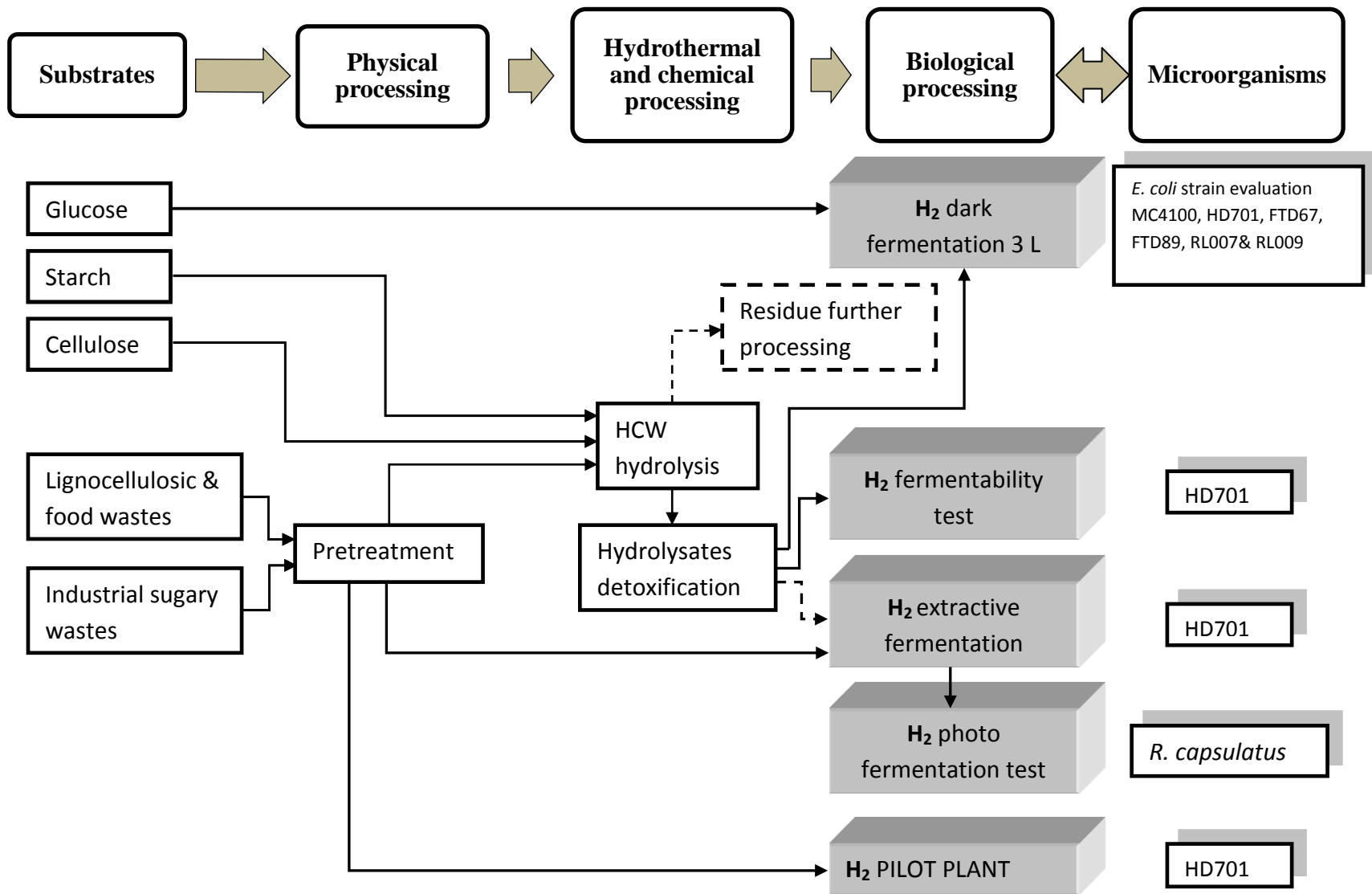


Fig. 20 Diagram outlining this research project

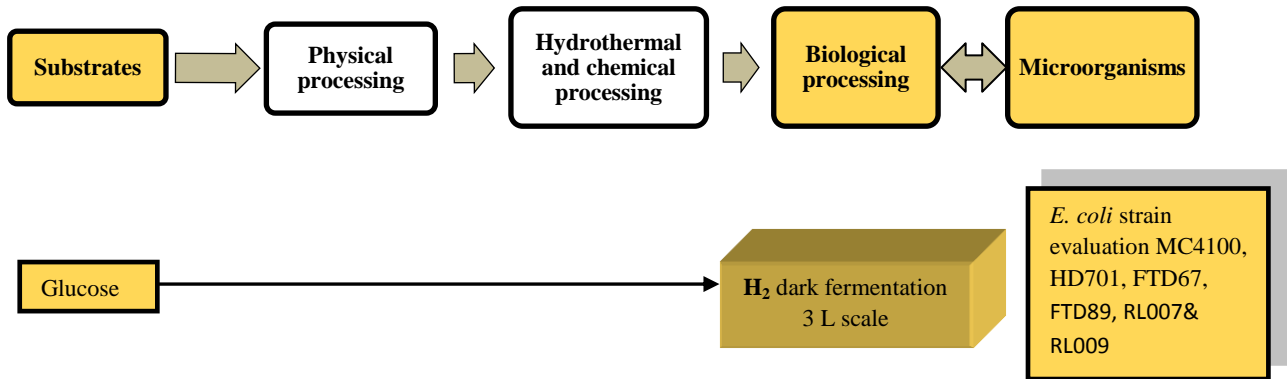
## **VI. RESULTS AND DISCUSSIONS.**

The results obtained from each subproject will be presented and discussed in this chapter. Some of the subprojects are presented in the form of papers that were already published, in review or in preparation for publication. To avoid duplicity and when appropriate; methods were referred to a method section in the appendices chapter of this thesis, with the same purpose and where appropriate some parts of the texts were also referred to the corresponding section contained in this document.

## VI.1 *E. coli* strain evaluation for H<sub>2</sub> production

This section comprises two parts:

- Section 0 *E. coli* strains MC4100, HD701, FTD67 and 89 evaluation for H<sub>2</sub>, OA and ethanol production presented in a traditional part-chapter.
- Section VI.1.3 Evaluation of H<sub>2</sub> production by strains devoided of *ldhA* compared to parent strain MC4100 and use of waste bacteria in fuel cell catalyst including a paper submitted to Biotechnology Letters.



## VI.1.1 *E. coli* strains evaluation for H<sub>2</sub>, OA and ethanol production

### Introduction

*E. coli* was the microorganism selected for the biological processing stage. Despite its low theoretical H<sub>2</sub> yield of a maximum of 2 mol H<sub>2</sub>.mol glucose<sup>-1</sup> *E. coli* provides important advantages over other microorganisms that are suitable for our biotechnological applications since it is fast and easy to grow (aerobically), non-sporulating, less sensitive to O<sub>2</sub> than strict anaerobes, can tolerate a higher H<sub>2</sub> partial pressure (pH<sub>2</sub>) than thermophiles, strict anaerobes or facultative anaerobes of the genus *enterobacter*, and is well characterized in physiological and biochemical terms (section II.4.3).

Formate is the only precursor of H<sub>2</sub> in *E. coli* mixed acid fermentations of sugars ([124, 149] being cleaved to H<sub>2</sub> and CO<sub>2</sub> by the formate hydrogenlyase complex (FHL) [150]. The full pathway of the mixed acid fermentation by *E. coli*; together with the ADP/ATP and NAD/NADH balances is shown in section II.4.3.1 (Fig. 15).

Compared to aerobic growth with an ATP yield of 38 mol ATP.mol glucose<sup>-1</sup> [151] via oxidative phosphorylation with O<sub>2</sub> as the terminal electron acceptor, the yield of ATP anaerobically are much lower (2 mol ATP.mol glucose<sup>-1</sup>) obtained by substrate level phosphorylation at two key points: 1) the formation of pyruvate and 2) the formation of acetate (Fig. 15). As a consequence, both the growth rates and yields of biomass anaerobically are much lower than those obtained aerobically and for bio H<sub>2</sub> production aerobic pre-growth was employed followed by transfer to anaerobic conditions which, when pre-induced with formate, gave cultures of *E. coli* producing H<sub>2</sub> comparable to those grown anaerobically throughout [100].

A main objective of this investigation was to develop a linked fermentation system for maximum bio-H<sub>2</sub> production that relies on the electro-dialytic transfer of OAs from a dark fermentation by *E. coli* FTD67 (this section) and subsequent photofermentation by *Rhodobacter spp* (see section II.4.2); the coupled dual system was shown in principle by Redwood [100]. Key to success is the maximum formation of charged OAs (formate, lactate, acetate, succinate, butyrate) and not ethanol as, having no charge, the latter is not transported by electro-dialysis, and thus accumulates to high levels in the dark fermentation; eventually causing inhibition and limiting the potential for a continuous extractive fermentation process (see section II.4.4.2). Hence the first objective of this study was to apply molecular engineering to develop a strain deficient in ethanol production and to evaluate the ability of this strain to make bio-H<sub>2</sub>.

Of the various OAs that are produced fermentatively (structural formula shown in Table 5) two factors are important: the number of carbons and the charge. Hence formate and acetate (1 and 2

carbons, one negative charge) are unattractive; similarly succinate is unattractive (comparable to acetate) it consumes the same electrical energy per carbon to transport electro dialytically [100].

**Table 5** Formulas of main organic acids generated by *E. coli*. Only succinic acid has a double negative charge (divalent), the rest is monovalent as only possess one negative charge. Formic acid has 1 carbon, acetic acid has 2 carbons, pyruvic acid 3 carbons whereas lactic, butyric and succinic acids have 4 carbons each.

Organic acid	Formula	Comments
Formic acid	$\text{HCOO}^- \text{H}^+$	Monovalent
Acetic acid	$\text{H}_3\text{COO}^- \text{H}^+$	Monovalent
Lactic acid	$\text{HO CO CH}_2 \text{CH}_2 \text{COO}^- \text{H}^+$	Monovalent
Butyric acid	$\text{H}_3\text{C CH}_2 \text{CH}_2 \text{COO}^- \text{H}^+$	Monovalent
Pyruvic acid	$\text{H}_3\text{C CO COO}^- \text{H}^+$	Monovalent
Succinic acid	$\text{H}^+ \text{OOC CH}_2 \text{CH}_2 \text{COO}^- \text{H}^+$	Divalent

Butyrate is the ideal end product (four carbons, one negative charge) giving the best carbon transfer for the least consumption of ‘parasitic energy’ (see section II.4.4.2) and although butyrate production is very poorly described in *E. coli* (prior to the study of Redwood (thesis) only early and superficial reports existed it was nevertheless a significant fermentation end product in *E. coli* cells grown for bio  $\text{H}_2$  production [100] (this section). Hence the second objective of this study was to examine two strains described previously [124] and the putative ethanol-deficient strain (above) for their ability to produce butyrate. Finally an energy balance is presented to ‘trade off’ a diversion of ethanol production (unavailable to the downstream Rhodobacter) versus other resultant charges from OA production, in the context of an increased substrate availability for bio  $\text{H}_2$  production in the dual system versus other factors that emerge as consequences of the loss of metabolic freeness consequent on the loss of ackA which diverts metabolic flux away from ethanol but at the expense of ATP production via acetate synthesis (Fig. 15). Several strains of *E. coli* that have been genetically modified from the parent strain MC4100 to enhance  $\text{H}_2$  production were provided by F. Sargent as shown in Table 6 and some were initially tested by Dr. M. D. Redwood [100] of the University of Birmingham for their ability to produce  $\text{H}_2$ . In his experiments 0.120 L anaerobic bottles containing 0.100 L test medium (buffered) were utilized, the initial cell concentration was 0.5 g dry weight.L<sup>-1</sup>. The pH was not externally controlled (buffered medium was used). Degassed glucose 2M (to 20 mM) was added to the test medium. The  $\text{H}_2$  produced was measured over a solution of 2M NaOH with universal indication for 45 h. Test medium consisted of 0.1 M MES buffer [2-(N-Morpholino) ethanesulfonic acid], pH 6.80 supplemented with 6.96 g.L<sup>-1</sup> NaCl (final concentration), 0-100  $\mu\text{l}$  2 M  $\text{NH}_4\text{Cl}$  and 0.3

ml trace elements solution given in [152]. Unless otherwise stated the final concentration of  $\text{NH}_4\text{Cl}$  was 1 mM.

In this work, fermentations were scaled up using 5 L fermentation vessels containing 3 L of formulated media. The fermentation system employed provides adequate control over important parameters such as pH, temperature and stirring. This enabled controlled comparison of the performance of the *E. coli* strains in these scaled up experiments under more sophisticated controlled conditions. The strains utilized are listed and described in Table 6, the previous strains used by Redwood et al., 2007 [124] and two additional strain: RL007 and RL009.

**Table 6** *E. coli* strains utilized in this study.

E. coli strain	Genotype	Comments/references	Source
MC4100	Parental strain	<i>E. coli</i> strains cited below were derived from this strain.	J.A. Cole, University of Birmingham
HD701	$\Delta hycA$	Up regulated Formate hydrogenlyase (FHL) system regulates H <sub>2</sub> production from <i>E. coli</i> , this strain can not synthesise HycA, which is a FHL repressor	A. Böck (Lehrstuhl für Mikrobiologie der Universität, Munich, Germany)
FTD67	$\Delta hyd-2$	Hyd-2 is an uptake hydrogenase that contributes to H <sub>2</sub> recycling activity during fermentation. Its deletion improves H yield and rate	F. Sargent, university of Dundee
FTD89	$\Delta hyd-1$ & 2	Hyd-1 is also an uptake hydrogenase that recycles H <sub>2</sub> produced	F. Sargent, university of Dundee
RL007	$\Delta focA$ , $\Delta focB$ , $\Delta hycA$ , $\Delta ldhA$ , $\Delta nirC$ , $\Delta tatABC::apra$	Devoided of lactate dehydrogenase A ( <i>ldhA</i> ). There are three lactate dehydrogenase (LDH) enzymes in <i>E. coli</i> that interconvert lactic acid and pyruvic acid, there is a second locus, <i>ldhB</i> (so far unmapped) while the third, <i>ldh</i> is responsible for lactate assimilation for gluconeogenesis. $\Delta focA$ , $\Delta focB$ are formate transporter genes, its deletion increases intracellular formate reducing excreted formate. $\Delta nirC$ a formate-nitrite transporter gene. $\Delta tatABC$ is a protein transportation system, its deletion inactivates the uptake dehydrogenases 1 and 2 and the Tat-dependent respiratory formate dehydrogenases, FdHN and FdHO.	F. Sargent, university of Dundee
RL009	$\Delta focA$ , $\Delta focB$ , $\Delta nirC$ , $\Delta ackA$ , $\Delta hycA$ $\Delta ldhA$ $\Delta N-fhlA$ , $\Delta tatABC::apra$	Devoided of lactate dehydrogenase A ( <i>ldhA</i> ) and acetate kinase ( <i>ackA</i> ); can not make ATP by substrate level phosphorylation via acetate synthesis.	F. Sargent, university of Dundee

## Materials and methods

Bacterial strains were sourced as described in Table 6 and maintained according to the appendix section VIII.1.1, as well as a description of the chemicals utilized. *E. coli* was pre-grown aerobically and in the presence of formate to cause pre-adaptation to anaerobic H<sub>2</sub> production (by inducing the expression of FHL) [150] as described in appendix section VIII.1.1

Fermentations were done in 5 L fermentation vessels containing 3 L of formulated media as described in appendix section VIII.1.3.

The initial concentration of glucose usually was within  $23 \pm 2$  mM. H<sub>2</sub> evolution was measured for about 65 h or until H<sub>2</sub> production ceased.

H<sub>2</sub> production was quantified in two different ways: water column displacement (WCD) and low flow gas meters (FGM), both methods described in appendix sections 0VIII.2.3. Unless otherwise stated, fermentations were performed utilizing WCD method.

### Chemical analysis

Samples withdrawn from the fermentation vessel were filtered using a 0.2 μm supor membrane and the filtrates were kept at  $-20^{\circ}\text{C}$  before analysis. Glucose was assayed using the dinitrosalicylic acid assay (DNSA) ([153] (appendix VIII.4.1). Organic acids were measured by anion HPLC using a Dionex 600 series system as described in (Redwood&Macaskie, 2006). Ethanol was determined by HPLC (Agilent 1100 series) as described in chapter 0. The carbon fermentation balance (C. bal.) was estimated according to Equation 2 to Equation 4 [124], with values in mol product.mol glucose<sup>-1</sup> from Table 7. These equations are based on the methabolic pathway of *E. coli* according to Fig. 15 [154]

#### Equation 2

$$\text{C. bal. (\%)} = \frac{3.lact+2.acet+2.ethanol+4.succ+form+3.pyruv+4.butyr+CO_2+0.044.biomass}{6} \cdot 100$$

CO<sub>2</sub> is derived from the decomposition of formate (HCOOH = CO<sub>2</sub> + H<sub>2</sub>) and succinate formation requires the incorporation of CO<sub>2</sub> (Fig. 15). Therefore, the production of CO<sub>2</sub> was estimated (CO<sub>2est</sub>) by subtracting the succinate formed from the theoretical formate decomposed (Equation 3):

#### Equation 3

$$CO_{2est} = acetate + ethanol - formate - succinate$$

H<sub>2</sub> uptake was estimated as the according to Equation 4 and is the difference between the expected H<sub>2</sub> and measured H<sub>2</sub>:

#### Equation 4

$$H_2 \text{ uptake} = acetate + ethanol - formate - H_2 \text{ formed}$$

The carbon gained by the cells during fermentation growth was calculated from the increase in dry weight and considering 53.1 % as the C fraction of *E. coli* biomass [124, 155, 156]. From this, a factor of 0.044 was utilized to convert g biomass.mol glucose<sup>-1</sup> to mol carbon.mol glucose<sup>-1</sup> (Equation 2) [124].

Experiments were repeated at least twice for each strain and mean values are reported, reproducibility between experiments performed twice was usually within 10 %.

## Results and discussion

A summary of the results obtained in this work involving strains MC4100, HD701, FTD67 and FTD89 are shown in (a) together with the results obtained by Redwood [124] in (b) after 45 h of fermentation period in both cases. Strains RL007 and RL009 in comparison to the parent strain (MC4100) will be discussed separately in the subsequent section. H<sub>2</sub> yielded by strains in 3 L fermentations (3LF) exceeds by a range of 22-35 % those obtained in 0.1 L fermentations (0.1LF) with the exception of HD701 where H<sub>2</sub> produced was 76 % higher (b); however this strain was upregulated and so was not a true comparison. This higher H<sub>2</sub> production by the strains has two possible implications. The first is that better control conditions (pH, mixing, temperature) in larger scale fermentation is favourable for increasing H<sub>2</sub> yield, for example in the 0.1 L fermentations the pH dropped from initial 6.80 to final 5.93 whereas in this study the pH was kept at 5.5 + 0.2 throughout, which is optimal for H<sub>2</sub> production by *E. coli* according to work performed by Redwood [100]. Strains HD701, FTD89 and FTD67 reached levels up to 65 % of the maximum theoretical yield of 2 mol H<sub>2</sub>.mol glucose<sup>-1</sup>; parent strain MC4100 only reached ~ 50 % of the maximum yield. The second is that the biochemical features of the strains benefit from the better control conditions, for example in the case of strain HD701 (whose H<sub>2</sub> production was 76 % higher) has the particular biochemical feature that it lacks the FHL repressor but it is not a clean mutation in the sense that this is a control function which may have other effects (a pleiotropic mutation) that relate to low pH tolerance of the cells and better pH tolerance by having removed the repressor, in a way which is not clear. Growth yields and H<sub>2</sub> uptake are shown in (a) and (b). For MC4100, HD701, FTD89 and 67 growth yield is the same in both studies, uptake of H<sub>2</sub> is halved by the 3 LF pH controlled regime but is abolished in the strain via  $\Delta$  foc (Table 6).

**Table 7 a.** Summary table showing product distribution per strain of *E. coli*; (a) this study and (b) Redwood et al., 2007 [124].

Strain ID	Genotype	Hyd			Products formed (mol.mol glucose)										Growth g.mol glucose <sup>-1</sup>	Carbon balance (%)	
		1	2	3	H <sub>2</sub> formed	Form	Acet	Ethanol	Lact	Succin	Butyr	Pyruv	Glucose	CO <sub>2est</sub>			H <sub>2</sub> uptake
MC4100	Parental strain	+	+	+	0.976	0.046	0.22	0.926	0.51	0.18	0.21	0	0	0.92	0.124	3.95	109
HD701	<i>ΔhycA, FHL upregulated</i>	+	+	+	1.3	0.032	0.355	0.985	0.200	0.277	0.236	0	0	1.031	0.008	2.53	108
FTD67	<i>ΔhybC</i>	+	-	+	1.25	0.034	0.38	0.834	0.37	0.247	0.23	0	0	0.933	-0.07	2.56	109
FTD89	<i>ΔhyaB, ΔhybC</i>	-	-	+	1.3	0.032	0.375	0.89	0.37	0.21	0.24	0	0	1.023	-0.067	2.5	110
RL007	<i>ΔfocA, ΔfocB, ΔhycA, ΔldhA</i>				1.03	0.118	0.91	0.225	0.01	0.7	0.095	0.12	0	0.317	-0.013	4	107
RL009	<i>ΔfocA, ΔfocB, ΔackA, ΔhycA, ΔldhA</i>				1.1	0.048	0.87	0.12	0.02	0.084	0.118	0.13	0.31	0.858	-0.158	12.95	110

**Table 7 b.**

Strain ID	Genotype	Hyd			Products formed (mol.mol glucose <sup>-1</sup> )										Growth g.mol glucose <sup>-1</sup>	Carbon balance (%)
		1	2	3	H <sub>2</sub> formed			Form	Acet	Ethanol	Lact	Succin	CO <sub>2est</sub>	H <sub>2</sub> uptake		
					0.1 L	3 L	Dif (%)									
MC4100	Parental strain	+	+	+	0.764	1.03	34.7	0.149	0.499	0.649	0.318	0.494	0.504	0.236	2.61	100
HD701	<i>ΔhycA, FHL upregulated</i>	+	+	+	0.737	1.3	76.4	0.132	0.363	0.667	0.359	0.47	0.422	0.162	2.57	95
FTD67	<i>ΔhybC</i>	+	-	+	1.024	1.25	22.1	0.214	0.686	0.539	0.383	0.432	0.674	-0.001	2.52	104
FTD89	<i>ΔhyaB, ΔhybC</i>	-	-	+	1.043	1.3	24.6	0.176	0.64	0.583	0.372	0.436	0.611	0.004	3.62	104

*Detailed study of mutants HD701, FTD67 and FTD89.*

As previously mentioned, of special interest is the generation of ethanol (toxic with no HPP) and OA (toxic but with HPP). Ideally, ethanol generation should be abolished as it is not harvestable via ED, while OAs are potentially valuable by-products due to their high HPP in a downstream photofermentation. Table 8 shows formate and ethanol production by *E. coli* strains, from this table we appreciate that the residual formate is considerably reduced to negligible levels under the 3 LF growth regimes but ethanol production increased by ~42-55%. By comparing parent strain MC4100 with FTD 89 and 67 (the two  $\Delta hybC$  mutants) formate and ethanol are 28% and 7% less in the mutants.

**Table 8** Formate and ethanol yields by *E. coli* strains in 0.1 L fermentations tests and 3 L fermentations without and with external pH control respectively. Values in mol.mol glucose<sup>-1</sup>.

Strain ID	Formate		Ethanol	
	0.1 L	3 L	0.1 L	3 L
MC4100	0.149 ± 0.011	0.046 ± 0.002	0.649 ± 0.012	0.926 ± 0.084
HD701	0.132 ± 0.013	0.032 ± 0.001	0.667 ± 0.015	0.985 ± 0.088
FTD67	0.214 ± 0.026	0.034 ± 0.002	0.539 ± 0.005	0.834 ± 0.075
FTD89 <sup>a</sup>	0.176 ± 0.012	0.032	0.583 ± 0.028	0.89
<sup>a</sup> Experiments done twice in 3 LF with variations within 10%				

Regarding acetate, lactate and succinate we notice from Table 9 that their yields in strains FTD89 and 67 are very similar under the 3 L regime whereas variations in comparison with the parent strain are 71.5 and 27% higher for acetate and succinate respectively in the  $\Delta hybC$  mutants; yields of lactate are 27% lower in the mutants.

**Table 9** Acetate, lactate and succinate by *E. coli* strains in 0.1 L fermentation tests and 3 L fermentations with external pH control and variations (%) between both fermentations with respect to 3 L fermentations. Values in mol.mol glucose<sup>-1</sup>.

Strain ID	Acetate		Lactate		Succinate	
	0.1 L	3 L	0.1 L	3 L	0.1 L	3 L
MC4100	0.499 ± 0.036	0.22 ± 0.019	0.318 ± 0.012	0.51 ± 0.041	0.494 ± 0.008	0.18 ± 0.007
HD701	0.363 ± 0.036	0.355 ± 0.028	0.359 ± 0.009	0.2 ± 0.010	0.47 ± 0.009	0.277 ± 0.005
FTD67	0.686 ± 0.016	0.38 ± 0.019	0.383 ± 0.030	0.37 ± 0.026	0.432 ± 0.030	0.247 ± 0.074
FTD89 <sup>a</sup>	0.64 ± 0.057	0.375	0.372 ± 0.029	0.37	0.436 ± 0.021	0.21
<sup>a</sup> Experiments done twice in 3 LF with variations within 10%						

Average ethanol production by all these strains in 0.1LF was  $0.609 \pm 0.051$  mol.mol glucose<sup>-1</sup> whereas ethanol production was  $0.909 \pm 0.055$  mol.mol glucose<sup>-1</sup> by the same strains in 3LF (~50 %

higher). The average production of formate, acetate and succinate by all the strains in 3LF was  $0.036 \pm 0.006$ ,  $0.333 \pm 0.066$  and  $0.229 \pm 0.036$  mol.mol glucose<sup>-1</sup> respectively which is 78, 39 and 50 % lower compared to 0.1 LF respectively. In 3LF the production of lactate was 60 % higher by strain MC4100, 44 % lower by strain HD701 and very similar by strains FDT89 and 67. Butyrate was also found in 3LF after 24 h fermentation period Table 7 (a); however its metabolic pathway has been little studied. H<sub>2</sub> yields were limited by glucose depletion and accumulation of OA and ethanol in the fermentation media.

The causes of these differences can be attributable to the two possible implications earlier discussed in this section.

In his doctoral work, Redwood [100] was able to sustain H<sub>2</sub> production from glucose by *E. coli* HD701 in 3LF scale (fed-batch mode) for 20 days with a yield of 1.6 mol H<sub>2</sub>.mol glucose<sup>-1</sup> (80 % of theoretical maximum) where OA were continuously removed from the system through ED hereby avoiding limitation due to substrate availability and accumulation of these inhibitory end-products.

In addition to the aforementioned findings, the results obtained also exhibit two very interesting and distinctive behaviors identified for all strains (as was also found by Redwood [100]). The first behavior occurs during the period of time in which glucose is totally consumed and encompasses the initial 20-24 h after inoculation (“stage 1”). The second behavior takes place during the remaining time after first 22-24 h and corresponds to the time subsequent to glucose consumption by *E. coli* (“stage 2”). In this stage the cellular metabolism turns over (although no growth occurs) with the cells obtaining energy via assimilation of stored carbon sources and their channeling into central metabolism.

### *Stage 1*

More than 95 % of the added glucose was consumed by the strains. H<sub>2</sub> yielded by the strains during this stage accounted for 66 % of the total H<sub>2</sub> produced after a prolonged 65 h fermentation period by MC4100, 80 % by HD701, 82 % by FTD89 and 75 % by FTD67 (Fig. 21).

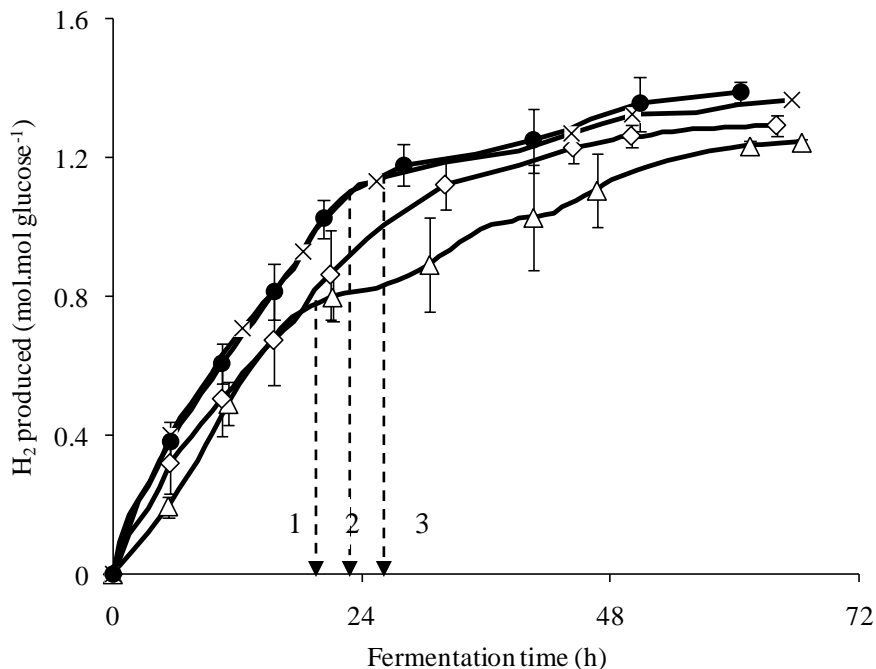


**Fig. 21** Hydrogen yields for strains (●) HD701; (X) FTD89; (◇) FTD67; and parent strain (Δ) MC4100. The broken arrows indicates the point where glucose was totally consumed by strain (1) MC4100 (~20 h), (2) by HD701 (~ 22 h) and (3) by FTD89 and 67 (~ 24-25 h).

The progress of H<sub>2</sub> rates by these strains is shown in Fig. 22 and during this stage was as follows:

Strain HD701 (Fig. 22 B) immediately started to evolve hydrogen reaching a peak of about ~ 120 mL H<sub>2</sub>.h<sup>-1</sup> within the first 3 h of fermentation. Between 3 – 22 h period production rate was fairly constant (70-80 mL H<sub>2</sub>.h<sup>-1</sup>).

Strains FTD89 and FTD67 (Fig. 22 C and D) showed similar rate trends having the highest values between 2-3 h of fermentation period from an initial of ~ 200 mL H<sub>2</sub>.h<sup>-1</sup>. After that (6-22 h) H<sub>2</sub> rates decreased gradually and became steady at ~ 50-60 mL H<sub>2</sub>.h<sup>-1</sup>.

Strain MC4100 (Fig. 22 A) H<sub>2</sub> production rate increased to ~ 110 mL H<sub>2</sub>.h<sup>-1</sup> during the first 10 h of fermentation; then rate decreased and became steady at ~ 30 mL H<sub>2</sub>.h<sup>-1</sup> for the next 14 h. Overall, the H<sub>2</sub> production profile was similar between the strains except that HD701 produced more H<sub>2</sub> before glucose depletion and little thereafter. Both FTD 89 and 67 showed a peak in H<sub>2</sub> production approximately 5 h before glucose depletion (Fig. 22 C and D).

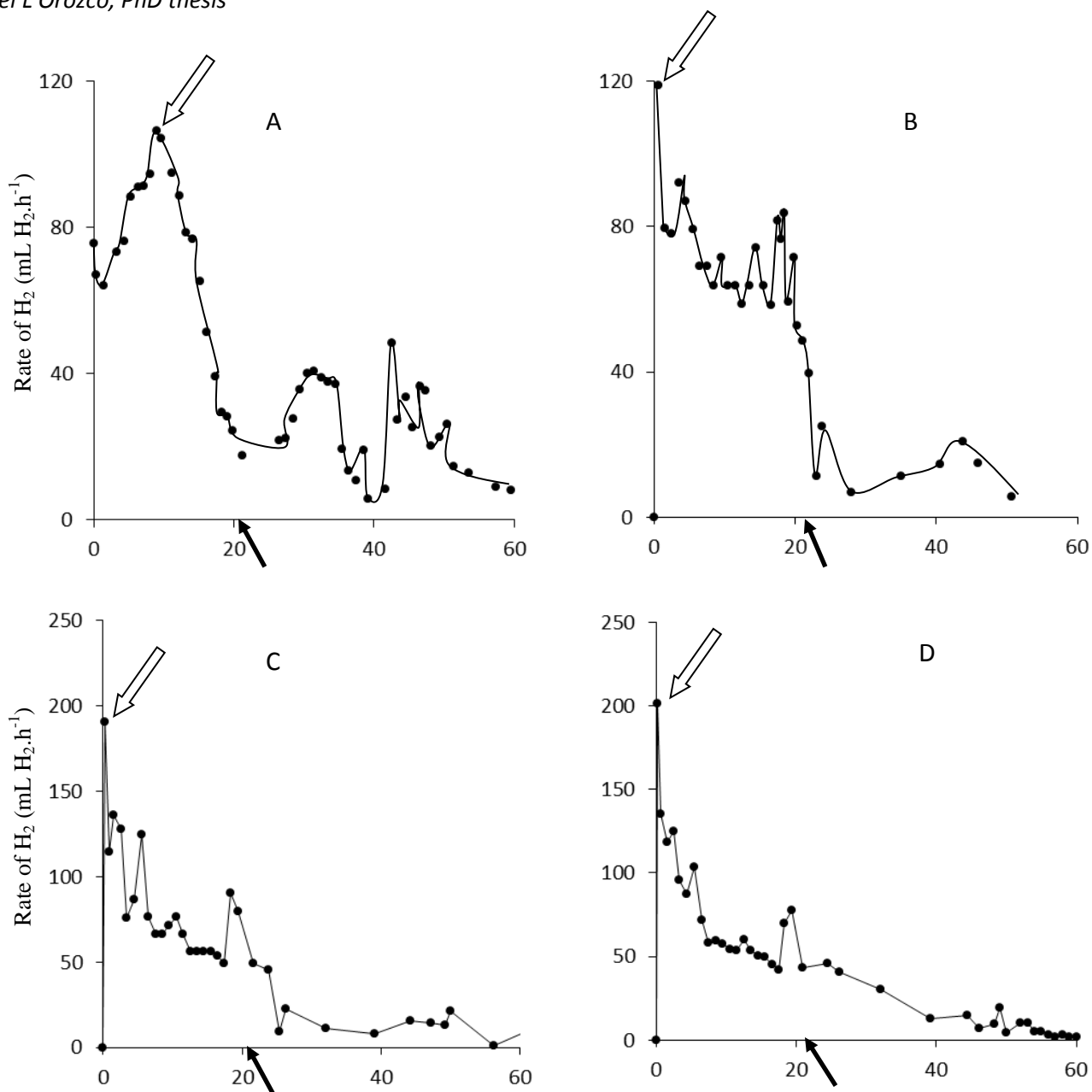


**Fig. 22** Rates of H<sub>2</sub> production by strains: (A) MC4100; (B) HD701; (C) FTD89; (D) FTD67. In all graphs horizontal axis represents fermentation time (h). Solid arrows represent the point of glucose depletion; open arrows show maximum rates.

OA produced in this stage were lactate, succinate and acetate (Fig. 23 and Fig. 24).

### Stage 2

Glucose was totally consumed and the fermentation pattern changed for all strains. Succinate and acetate remained steady in strain HD701 (Fig. 23 B); for MC4100, FTD89 and 67 succinate remained steady and small decrease in acetate was observed (Fig. 23 B and Fig. 24 B) whereas butyrate began to accumulate at the expense of lactate in all strains (Fig. 23 A and Fig. 24 A). H<sub>2</sub> was produced at much lower rates (< 30 mL H<sub>2</sub>.h<sup>-1</sup>) and its generation may be attributed to the re-assimilation of lactate and its metabolism into a H<sub>2</sub> production pathway [100], it is thought that after glucose depletion the cells switched to gluconeogenesis. In this process they will re-assimilate lactate, acetate and feed them into synthetic pathways which consume energy. The cells go to a 'resting' period in that they are continuing to ferment the synthesized glucose (to make energy) that has been made by re-using fermentation end products (consume energy), hence there is no net cell growth but turnover with a second stage of H<sub>2</sub> production. After 50-65 h the fermentation products accumulated to yields shown in Fig. 21, Fig. 23 and Fig. 24.

The generation of butyrate by *E. coli* at the expense of lactate during stage 2 was unexpected as butyrate is not a characteristic product usually found and is scarcely reported in *E. coli* fermentations [100]. As seen in Fig. 23 A and Fig. 24 A, butyrate became a major product in long term fermentations. Not much information has been reported regarding the metabolic pathways leading from lactate-butyrate in *E. coli* fermentations. It was hypothesized by Redwood [100] that the depletion of glucose, the accumulation of lactate and the decreased rate of acetate accumulation in the medium, possibly attributable to acetate re-assimilation, triggered the butyrate metabolism, as butyrate did not detract from H<sub>2</sub> production. The precursor of butyrate is a product of pyruvate formate lyase (PFL). Acetyl-CoA is a product from PFL and a precursor to ethanol, acetate and Aceto acetyl Co-A which is a precursor to Butyl-CoA that generates butyrate in the metabolic pathway of *Clostridium* strains (Fig. 15) [108, 157]. In his hypothesis Redwood suggested that the enzymes necessary for the operation of this pathway are: acetoacetyl-CoA thiolase (ACT), 3-hydroxyacyl-CoA dehydrogenase (HCDH) fructuronate reductase (FR), enoyl-CoA hydratase (ECH, MaoC), butyryl-CoA dehydrogenase (BCAD) and acetate CoA-transferase (ACT) which can be found in *E. coli* K-12, but more investigation is required to establish the operation of this pathway and confirm the enzymes involved. Butyrate is a desirable product with respect to its high ratio of potential H<sub>2</sub> production in the downstream photo-fermentation process to its charge [100]; less energy is expected for its electro-dialytic transfer as compared to e.g. acetate; four carbons and one charge and two carbons and one charge respectively.

Strain MC4100 produces twice as much lactate as HD701 (Fig. 23 A) but butyrate yield is the same ( $\sim 0.3 \text{ mol.mol glucose}^{-1}$ ) after the fermentation period ( $\sim 54 \text{ h}$ ). Lactate profiles are also very similar. HD701 produces more acetate ( $\sim 20 \%$ ) and more succinate ( $\sim 25 \%$ ) than MC4100 (which makes more lactate) (Fig. 23 B). It can be also noticed that the decrease amount of acetate is higher in strain MC4100 than in HD701 after glucose depletion.

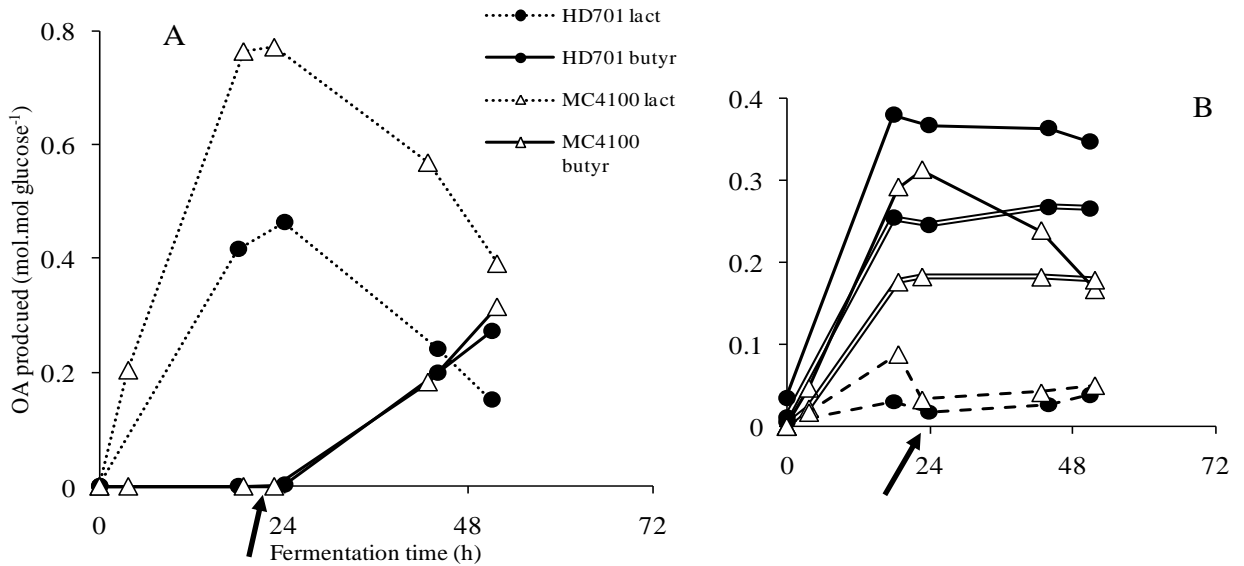


**Fig. 23** OA yields by strain HD701; A) shows lactate-butyr relationship compared to parent strain MC4100; B) shows (●) HD701 and (△) Mc4100 yields of (—) acetate; (- - -) formate and (====) succinate. Arrows indicate the point of glucose deletion.

Strains FTD89 and 67 exhibit a very similar lactate-butyr pattern (Fig. 24 A). After a prolonged fermentation period of ~84 h all lactate was depleted from strain FTD89 and the butyrate yield by both strains was very similar reaching a maximum of ~ 0.55 mol.mol glucose<sup>-1</sup>. FTD89 and 67 made more acetate (~ 0.43 mol.mol glucose<sup>-1</sup>) than MC4100 (~ 0.31 mol.mol glucose<sup>-1</sup>) before glucose depletion, afterwards acetate began to decrease at similar rates as in MC4100 (Fig. 23 B).

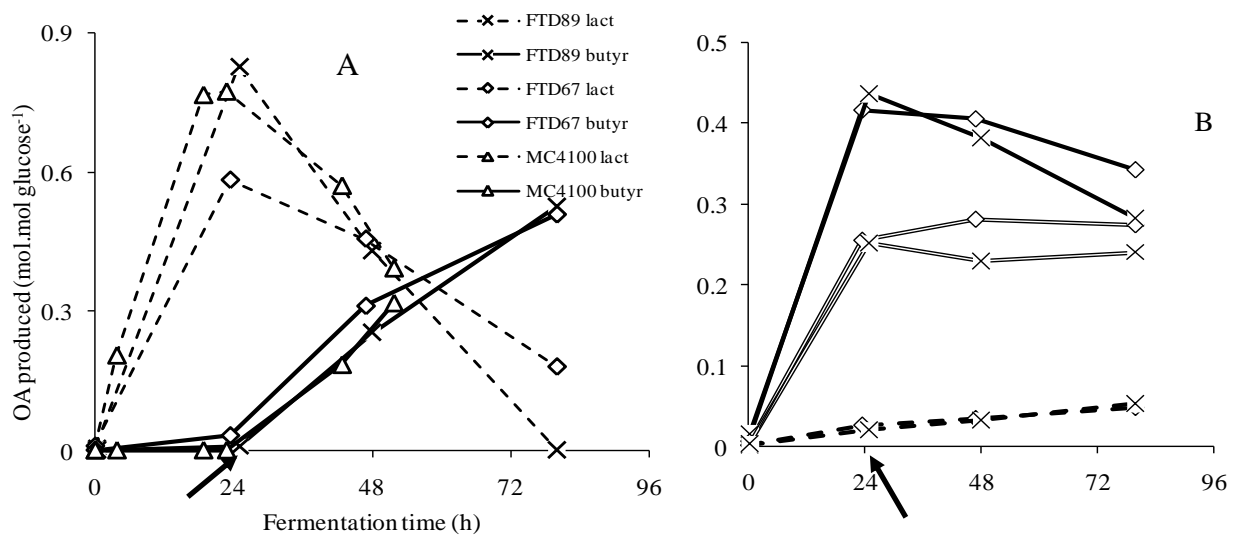


**Fig. 24** OA yields by strains (x) FTD89, (◇) FTD67 and parent strain (△) MC4100; A) shows FTD89 and FTD67 lactate-butyr relationship compared to parent strain MC4100; B) show yields of (—) acetate; (- - -) formate and (====) succinate, to avoid confusion MC4100 was left out from B. Arrows indicate the point of glucose depletion

## Conclusions

The effect of the *foc* lesions (uptake hydrogenases) is to have no effect in the sensitivity of the strains with respect to acetate and succinate production while the production of lactate is unaffected in the two *foc* mutants by the change in fermentation regime.

Redwood et al., 2007 showed increased H<sub>2</sub> by using FTD89 and FTD67 because they are devoid of uptake hydrogenases (the competing pathway has been removed). The previous fermentation tests were done at 0.1 L scale. This study shows that if the conditions are improved (3 L, pH control) the following things happen:

- 1) H<sub>2</sub> production is increased which confirms the previous paper by using the mutants. The increased H<sub>2</sub> production is by ~ 30 % by the mutants of the parent.
- 2) In all three cases the change of regime increases H<sub>2</sub> yields by 30 %, being lowest in MC4100 (0.976 mol H<sub>2</sub>.mol glucose<sup>-1</sup> vs. 0.764 mol H<sub>2</sub>.mol glucose<sup>-1</sup> in 0.1 LF). Highest H<sub>2</sub> (mutants) is 1.25-1.3 mol H<sub>2</sub>.mol glucose<sup>-1</sup>; hence overall H<sub>2</sub> is increased by > 60 % by a combination of new strains and better growth regime. H<sub>2</sub> production is now comparable to using the up-regulated strain HD701.
- 3) There is no advantage between strains with respect to butyrate production by means of changing the growth regime (at least during the 1<sup>st</sup> 45 h of fermentation period).
- 4) Lactate production has no advantage the new scale up way (3 LF) if we use the mutants. However the new method increases lactate production by 60 % if we use MC4100.
- 5) Butyrate production is an almost unreported phenomenon that has major implications of a future integrated H<sub>2</sub> production process.
- 6) Therefore we have to choose:
  - Option A use FTD89/67 with the advantage of 30 % more H<sub>2</sub> production (same lactate; no HPP gain)
  - Option B use of MC4100 with the advantage of 60 % more lactate (more HPP in the PBR) but less H<sub>2</sub> production.

From Table 10 we have that HPP for the downstream photobioreactor PBR from the mutant strains is ~ 5 % higher than the parent MC4100 and ~ 11 % higher than HD701 under 3 LF regimes. Considering ~30 % additional H<sub>2</sub> during the dark fermentation stage over the parent strain we conclude that strains FTD89 and/or FTD67 are more suitable for the hybrid system.

**Table 10** Hydrogen production potential (HPP) in mol H<sub>2</sub>.mol OA<sup>-1</sup> after 45 h fermentation time under improved growth regime. HPP as defined by Erglu et al., 2004 [97]; HPP (mol HPP.mol OA<sup>-1</sup>) succinate:7; butyrate: 10; lactate:6; acetate:4.

Strain	3 LF HPP				OA
	Acetate	Lactate	Succinate	Butyrate	Total HPP
MC4100	0.9	3.1	1.3	2.1	7.3
HD701	1.4	1.2	1.9	2.4	6.9
FTD67	1.5	2.2	1.7	2.3	7.8
FTD89	1.5	2.2	1.5	2.4	7.6

The mechanism of lactate-butyrate production detected in the second stage after glucose depletion remains unclear and requires further investigation.

## VI.1.2 Strains RL007 and RL009 in comparison to parent strain MC4100

### Results and discussion

In regards to strains RL007 and RL009 compared to parent strain MC4100 considering only the 3 LF experiments (pH controlled), fermentation products yields after 45 h period are shown in Table 11 and for the complete fermentation period (55-65 h) in Fig. 26-Fig. 29.

**Table 11** Products formed by strains RL007 and RL009 compared to parent strain MC4100. For RL007 and RL009 results are the average of two experiments with variations within 10 %.

Strain ID	Products formed (mol.mol glucose)									Carbon balance (%)
	H <sub>2</sub> formed	Form	Acet	Ethanol	Lact	Succin	Butyr	Pyruv	Glucose	
MC4100	0.976	0.046	0.22	0.926	0.51	0.18	0.21	0	0	109
RL007	1.03	0.118	0.91	0.225	0.006	0.7	0.095	0.12	0	107
RL009	1.1	0.048	0.87	<b>0.12</b>	<b>0.02</b>	0.084	<b>0.118</b>	0.13	0.31	110

From Table 11 we notice that H<sub>2</sub> is not improved whereas butyrate is halved during this period, the production of acetate increases ~ 4 fold, lactate production is lost completely and succinate is halved in RL009 compared to the parent strain, pyruvate is beginning to accumulate in both mutants and there is still > 30 % of the glucose residual in the fermentation medium for strain RL009. Ethanol production was successfully abolished in RL009. Ethanol production was halved in RL009 compared to RL007. Strains RL009 and 007 produced 6-fold more acetate than the parent strain.

Strain RL007 is devoid of the lactate dehydrogenase (*ldhA*) and strain RL009 is devoid of *ldhA* and in addition of the acetate kinase (*ackA*) enzyme. Hence the pathway to lactate for both strains is blocked which explains the lack of lactate production. Based on the metabolic pathway described in Fig. 15, *ldhA* deficient strains cannot recycle NAD<sup>+</sup> by “dumping” H<sub>2</sub> onto pyruvate to make lactate therefore they would tend to compensate by making more succinate/ethanol. Strain RL007 ( $\Delta$ *ldhA*) made this compensation by yielding more succinate and accumulating acetate with much lower yields of ethanol than the parent strain (Table 11) [158]. However for strain RL009 which in addition lacks *ackA*, it loses out a way to make ATP consequently needs to overcome this. As the acetate pathway is blocked, it would be expected to see no acetate synthesis, therefore the products should back-up pyruvate. The ‘down’ enzyme pyruvate dehydrogenase which makes acetyl CoA is subjected to tight regulation by NADH and acetyl CoA [159]. Accumulation of acetyl CoA

inhibits the PDH complex and therefore pyruvate accumulates; the down pathway stops and ethanol is considerably reduced (Fig. 15).

To get rid of excess pyruvate the cells would attempt to make lactate but can not as they lack *ldhA*, then the expected flux would be directed towards formate hereby increasing H<sub>2</sub> production while achieving the suppression of ethanol, as seen in Table 11, Fig. 26 and Fig. 28 C. This eventually occurred during the fermentation period. It was seen (Table 11) that strain RL009 still made important amounts of acetate, therefore another possible pathway to acetate might have been activated. It has been found that an elevated intracellular concentration of pyruvate activates the pyruvate oxidase complex (POX) which contains the *poxB* (an acetate producing enzyme) [159]; the pathway is described in Fig. 25. So if RL009 lacks *ackA* and pyruvate accumulates (as shown in Fig. 29) then POX will be activated and excess pyruvate will go to acetate by this route [159] which does not generate energy in the form of ATP. The down regulation of *adhE* and *poxB* contributes to explain the lower production of ethanol.

Based on this evidence we can suggest that POX is the means for RL009 to accumulate acetate from pyruvate.

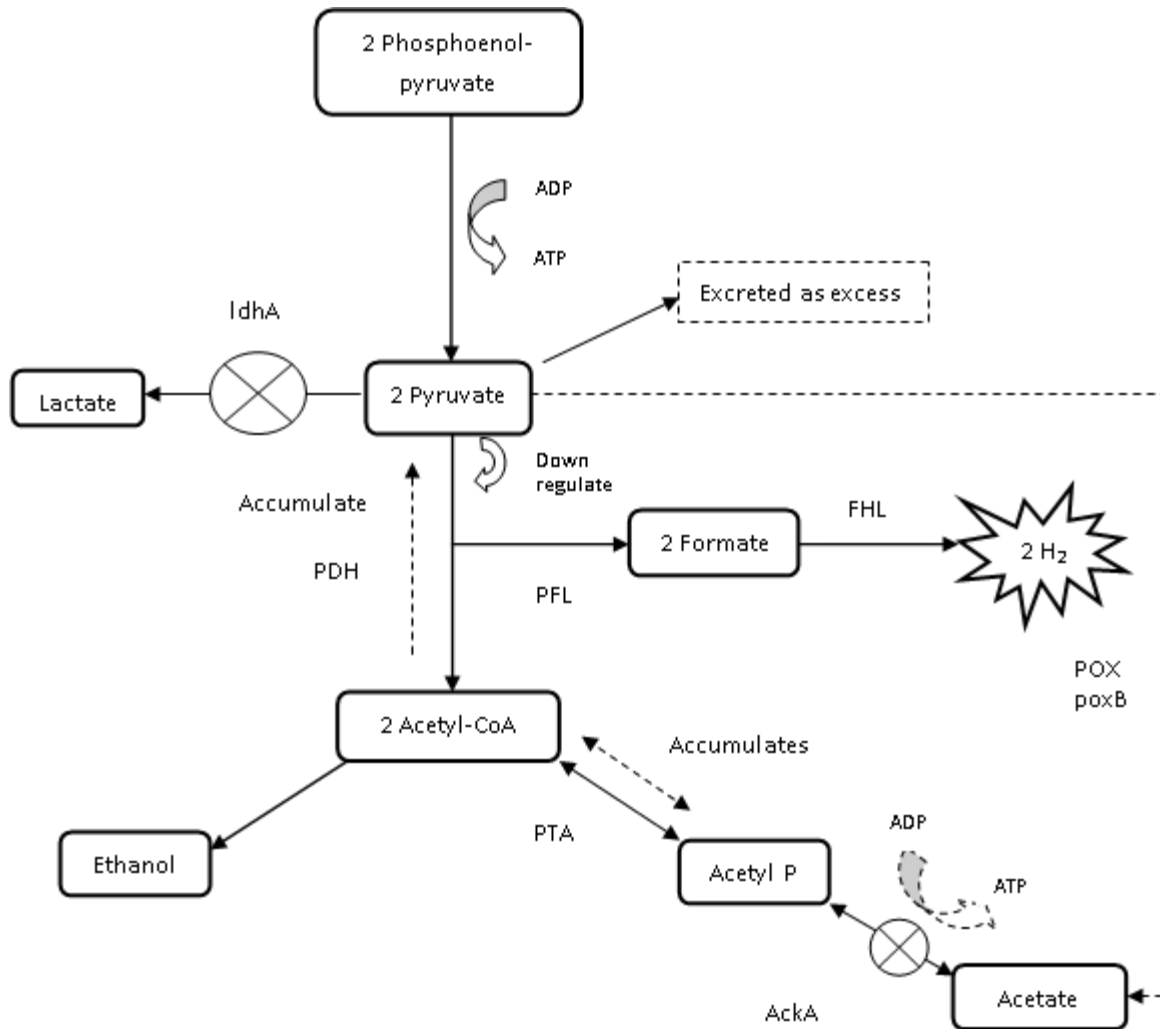


**Fig. 25** Diagram of central metabolic network to acetate/acetyl CoA made by *E. coli*. The circles with crosses represents blocked pathways, arrows going back to pyruvate are where products are assimilated. Adapted from Castano-Cerezo [159]. PTA is phosphotransacetylase enzyme.

The effect of the differential amounts in OA by strains RL007 and RL009 with respect to the parent strain MC4100 in terms of HPP is shown in Table 12 after 48 h of fermentation. RL007 exhibits the highest HPP with 9.6 mol H<sub>2</sub>.mol OA<sup>-1</sup>, the effect of halving butyrate and losing lactate by strain RL007 is highly surpassed by the changes in acetate and succinate resulting in a 31 % increase in HPP for the downstream process by strain RL007 whereas for strain RL009, 4.3 units of succinate were lost and as a consequence total HPP decreased ~ 74 % of the parent strain. The generation of succinate made the difference in HPP between both mutant strains. Succinate is usually generated by the condensation of the CO<sub>2</sub> produced with phosphoenol-pyruvate, and a subsequent reduction which consumes 4 H<sup>+</sup> per succinate (Fig. 15) [123]. This pathway is catalyzed by several enzymes such as phosphoenol-pyruvate carboxylase (*ppc*), malate hydrogenase (*mdh*),

fumarase and fumarate reductase (*frdABCD*); CO<sub>2</sub> is formed from the split of formate to H<sub>2</sub> and CO<sub>2</sub> by the FHL complex [123]. According to the carbon balance shown in Table 7, the estimated generation of CO<sub>2</sub> by strain RL007 is approximately one third of the other strains, it is therefore suggested that as the lactate pathway is blocked by  $\Delta$ ldhA, and not only pyruvate but also 2-phosphoenolpyruvate (which was not measured) accumulates, reacting in excess with CO<sub>2</sub> to overproduce succinate. This however does not occur for strain RL009 as H<sub>2</sub> production (and hence CO<sub>2</sub> co-production) by this strain was seen to be ‘delayed’ (Fig. 26) this strain also lacks ackA suggesting that the activation of the POX by the accumulation of acetyl CoA occurs rapidly, diverting pyruvate into acetate, for any accumulation of 2-phosphoenolpyruvate there is not any CO<sub>2</sub> available for the condensation reaction to form succinate to proceed. The differences in pyruvate accumulation can be seen in Fig. 29. The HPP of each strain at the 45 h stage is shown in Table 12.

**Table 12** Comparative of hydrogen production potential (HPP) (mol H<sub>2</sub>.mol OA<sup>-1</sup>) after 45 h fermentation period by the *E. coli* strains involved in this study.

Strain	3 LF HPP				OA
	Acetate	Lactate	Succinate	Butyrate	Total HPP
MC4100	0.9	3.1	1.3	2.1	7.3
RL007	3.6	0.1	4.9	1.0	9.6
RL009	3.5	0.1	0.6	1.2	5.4

Table 13 shows the H<sub>2</sub> yields and HPP after 55-66 h fermentation period for all the strains (compare with Table 10 and Table 12). As fermentation proceeds, butyrate and succinate are the main OA produced as they continue to accumulate in the system. Lactate decreases for all the strains and acetate remains constant for strains MC4100, HD701, FTD67 and FTD89 but increased for strains RL007 and 009. The overall balance results in an increase of HPP by strains FTD67 (+ 22 %); FTD89 (+ 43 %); RL007 (+ 64 %) and RL009 (+ 90 %), as a consequence the best strain would be RL007 which offers 50 % more HPP than strains FTD67 and RL009 and about 100 % more HPP than the parent strain MC4100 after 55-66 h fermentation period. In addition, strain RL007 makes ~ 4 fold less ethanol than the parent strain which is another important feature of this strain since it would allow the dark fermentation process to continue for more extended periods compared to the other strains before ethanol reaches inhibitory levels. Whilst total inhibition of ethanol (RL009) would be advantageous this must be offset against the HPP.

**Table 13** H<sub>2</sub> yields and HPP by strain after total fermentation period (55-66 h)

Strain	HPP 3 LF after fermentation period				HPP	H <sub>2</sub>	Ferm.
	Acetate	Lactate	Succinate	Butyrate	Total	(mol.mol gluc. <sup>-1</sup> )	(h)
MC4100	0.7	2.4	1.2	3.2	7.4	1.20	66
HD701	1.4	0.9	1.9	2.7	6.9	1.40	60
FTD67	1.4	1.1	1.9	5.1	9.5	1.30	65
FTD89	1.1	0.0	1.7	5.3	8.1	1.35	65
RL007	5.3	0.0	8.1	2.2	15.7	1.10	65
RL009	4.8	0.0	1.1	4.5	10.3	1.70	55

The separation of OA by electrodialysis needs the supply of electrical energy; for a profitable energy process this energy would have to be exceeded by the energy output of the dual system. This absolutely depends upon the current efficiency and the HPP from the transported OA to the downstream process. Redwood [100] calculated the break even current efficiency (BCE) for some OA, which denotes the relationship at which the energy output resulting from ED products balances the electrical energy supplied to ED expressed as (%). Table 14 summarizes some of these results:

**Table 14** Break even current efficiency expected by each OA produced after photofermentation. (Data from Mark D. Redwood doctoral thesis [100]). No.C: number of carbons.

Organic acid	No. C	Valence (C)	pK <sub>a</sub>	HPP	HPP.C <sup>-1</sup>	BCE (%)
Butyrate	4	1	4.81	10	10	13
Lactate	3	1	3.86	6	6	21.6
Acetate	2	1	4.76	4	4	32.5
Succinate	4	2	4.19, 5.57	7	3.5	37.1

Succinate and acetate have the highest BCE (37.1 and 32.5 % respectively) whereas butyrate has the lowest (13 %). This indicates that succinate and acetate are less likely to result in a net energy profit, whereas butyrate would be the most suitable substrate for the downstream process in terms of energy profit. This is a very important consideration in the selection of the most suitable strain for the upstream process in consideration of downstream process integration and energy generation for the integrated upstream and downstream bioreactors as a whole. From and comparing strains RL007 and RL009 in terms of energy balance strain RL007 despite having ~50 % higher HPP, it also has similar amounts of acetate, ~8 fold higher succinate and ~ half the butyrate than strain RL009 therefore strain RL007 is less likely to offer a more energy profit than strain RL009,

this would make strain RL009 preferable over strain RL007 and the parent strain MC4100, in addition the advantage conferred by the loss of ethanol production.

Of particular interest is the type of fermentation observed for RL007 and RL009. Instead of the lactate-butyrate type found in the parent strain MC4100 and the rest of the strains, these two mutants undergo a pyruvate-butyrate fermentation which developed as follows:

For strain RL007 H<sub>2</sub> production was very similar as in the parent strain, glucose was totally consumed between 23-25 h after inoculation (Fig. 26), during this stage ~ 65 % of its total H<sub>2</sub> has been produced reaching its highest rate (~ 150 mL H<sub>2</sub>.h<sup>-1</sup>; mean of two experiments with variations within 5 %) which was ~ 20 % higher than the parent, during the first 6 h of fermentation (Fig. 28). Rates rapidly decreased to become stable at 35-50 mL H<sub>2</sub>.h<sup>-1</sup> (mean ± 5 %) for the next 25 h and finally rates dropped to < 10 mL H<sub>2</sub>.h<sup>-1</sup> (mean ± 2 %) for the rest of the fermentation period.

Pyruvate began to accumulate reaching its maximum yield (0.42 mol.mol glucose<sup>-1</sup>; mean ± 6 %) after ~ 30 h of fermentation and then gradually decreased while at the same time butyrate began to accumulate. After ~55 h of fermentation the yields were 0.13 and 0.21 mol.mol glucose<sup>-1</sup> (mean ± 2.5 %) for pyruvate and butyrate respectively

However for strain RL009 in contrast with the parent strain and RL007, the stages were apparent by the time of glucose consumption and when H<sub>2</sub> production rates began to increase (Fig. 27 C). For this strain only 20-30 % of the added glucose has been consumed during the first 24 h, H<sub>2</sub> was only ~ 13 % of the total H<sub>2</sub> produced and its production began ~ 12 h after fermentation was initiated (Fig. 26). H<sub>2</sub> rate rapidly began to increase after the initiation of H<sub>2</sub> production reaching a maximum of ~ 450 ± 35 mL H<sub>2</sub>.h<sup>-1</sup> after ~ 17 h of fermentation, then rapidly decreased to ~ 110 ± 15 mL H<sub>2</sub>.h<sup>-1</sup> (Fig. 27) (1<sup>st</sup> stage), rates began to gradually increase again after 20 h reaching the same maximum rate achieved during the 1<sup>st</sup> stage after ~ 38 h of fermentation and gradually decreased to ~ 200 ± 21 mL H<sub>2</sub>.h<sup>-1</sup>, when glucose was completely consumed (after 48 h) the H<sub>2</sub> rates began to decrease until H<sub>2</sub> production completely ceased (after 55 h of fermentation) but total yield of H<sub>2</sub> produced reached 1.7 mol H<sub>2</sub>.mol of glucose<sup>-1</sup> which is 42 % higher than the achieved by the parent strain (Table 13). Pyruvate accumulated reaching a maximum yield of 0.25 mol.mol glucose<sup>-1</sup> after ~ 45 h of fermentation and butyrate began to accumulate after approximately 30 h of fermentation but at the expense of pyruvate reaching a maximum of 0.45 mol.mol glucose<sup>-1</sup> at the end of the fermentation period while pyruvate decreased to 0.07 mol.mol glucose<sup>-1</sup> (Fig. 29).

It was explained earlier in this section that as the downway path to acetate is blocked (due to the lack of *ackA*) the accumulation of pyruvate occurs and in an excess of pyruvate the POX

complex is activated opening another route to acetate (Fig. 25) while at the same time accumulation of formate and production of H<sub>2</sub> proceeds in a 1<sup>st</sup> stage associated with a slow rate of glucose consumption (Fig. 26 and Fig. 28 C), during the 2<sup>nd</sup> stage of H<sub>2</sub> production (with POX complex activated) glucose is more rapidly consumed and formate is rapidly metabolized to H<sub>2</sub>. It is possible that the accumulation of acetyl CoA during the activation of the POX complex also activates the enzymes involved in the formation of butyrate as explained in section VI.1.1 [100].

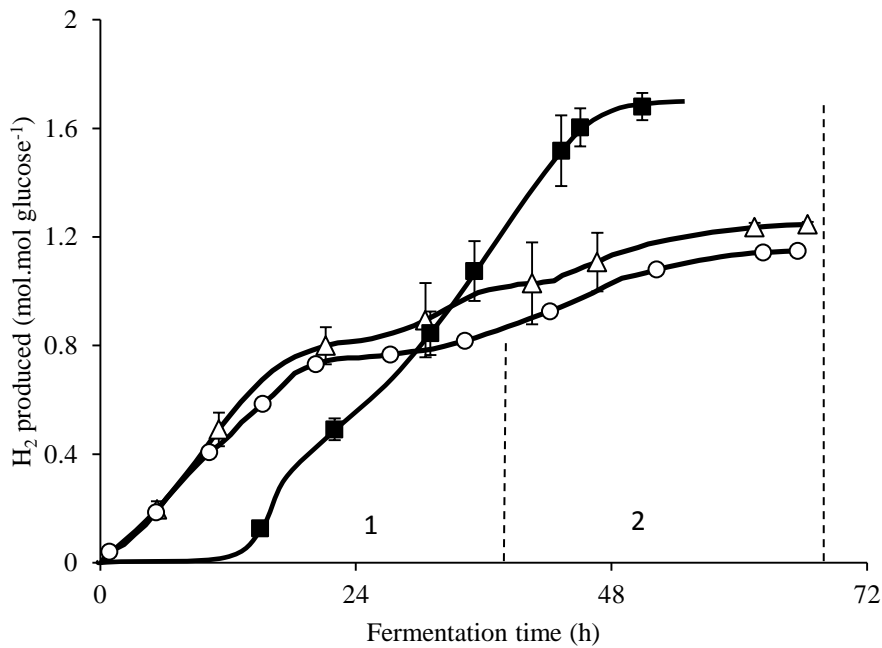


**Fig. 26** Hydrogen yields by strains ( $\Delta$ ) MC4100; (O) RL007; ( $\blacksquare$ ) RL009; dashed lines indicate the time where glucose was totally consumed (1) MC4100, RL007 and (2) RL009. Experiments were done in triplicate, where error bars are not shown these were within the dimensions of the symbols.

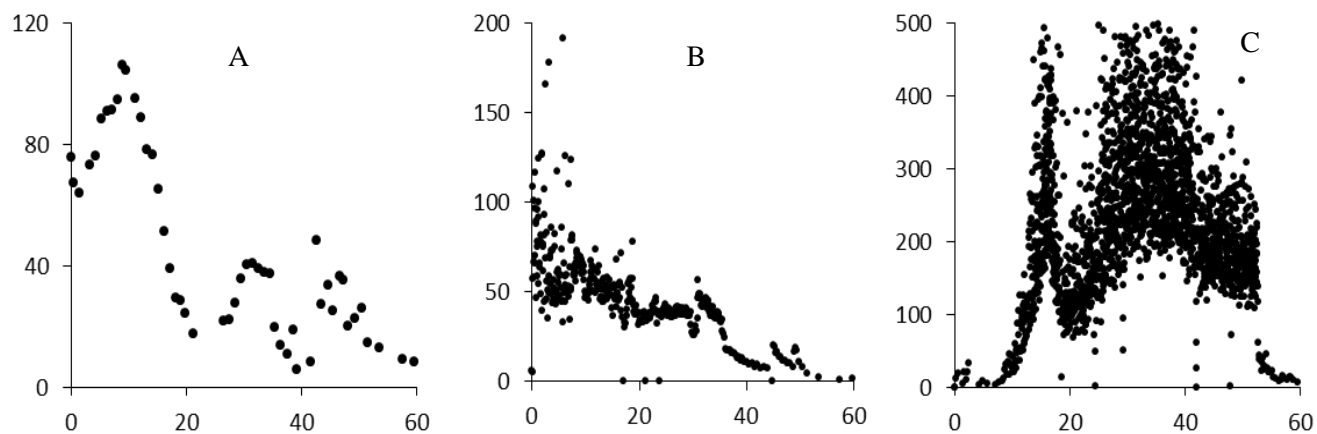


**Fig. 27** Rates of H<sub>2</sub> production by strains: (A) MC4100; (B) RL007; (C) RL009. In all graphs horizontal axis represents fermentation time (h) and vertical axis represent rate of H<sub>2</sub> production (mL H<sub>2</sub>.h<sup>-1</sup>)

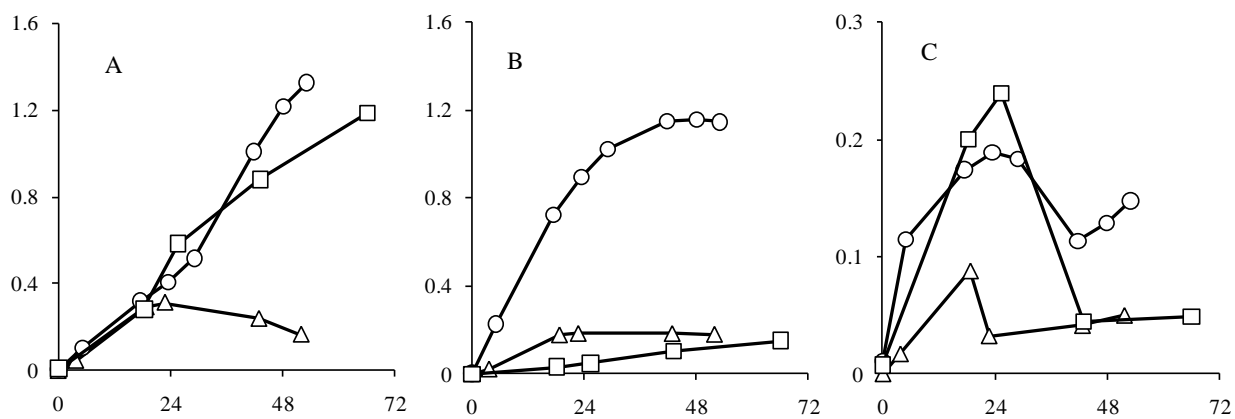


**Fig. 28** Organic acid by strains: ( $\Delta$ ) MC4100; (O) RL007; ( $\square$ ) RL009. A) acetate; B) succinate and C) formate. Horizontal axis represents fermentation time (h), vertical axis OA produced (mol.mol glucose<sup>-1</sup>).

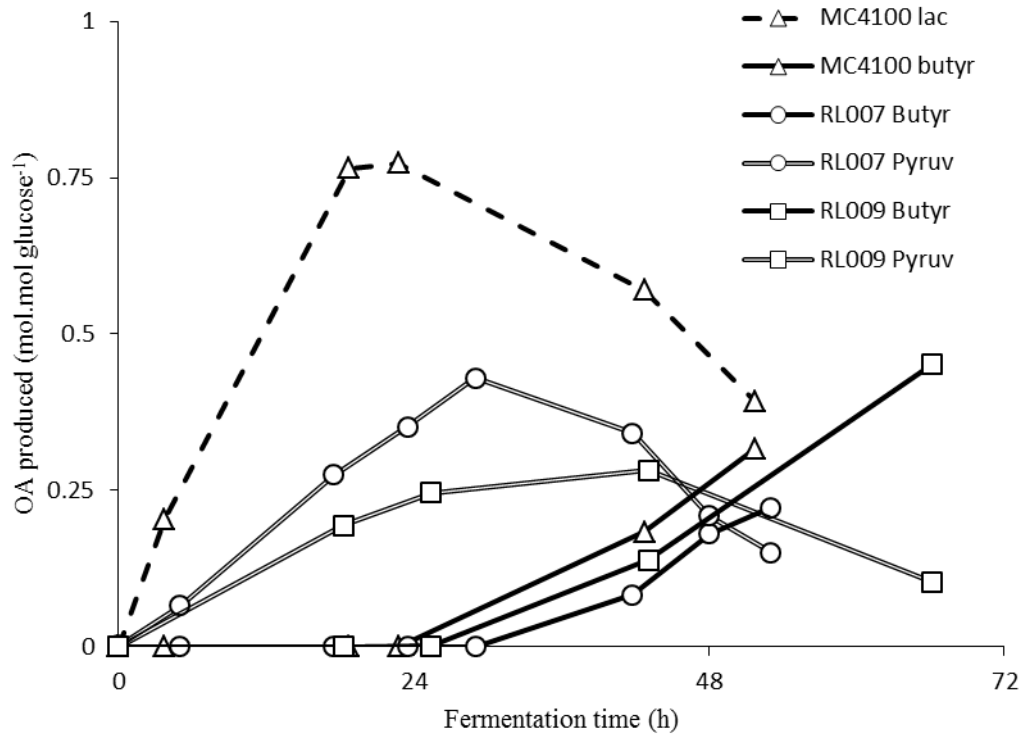


Fig. 29 MC4100 lactate-butyrate relationship; RL007 & RL009 pyruvate-butyrate relationship.

## Conclusions

Ethanol production was successfully abolished in RL009 but it was also reduced in strain RL007 which has a functional *ackA*. Ethanol was halved c.f. RL009 of RL007 which makes strain RL009 more suitable for long term dark fermentations.

In regards of HPP, strain RL007 reached 50 % more HPP than RL009 due to its excess of succinate but the penalty for the electric current necessary to transport succinate to the downstream process is highly likely to be equivalent to its contribution to energy output, therefore strain RL009 with higher content of butyrate and about 8 fold less succinate would be the preferable strain.

Overall, strain FTD67 offers more energy profit potential as its HPP (which is comparable to RL009) is less acetate dependent than in the case of strain RL009, however strain FTD67 makes more ethanol which will accumulate much faster to inhibit fermentation.

Strain RL009 produces the most H<sub>2</sub> in the dark fermentation; this, in conjunction with its lack of ethanol production and overall high HPP make it the strain of choice for integrated system.

In the next section which is reported in the form of a published paper, cells obtained from fermentation with strains RL007 and MC4100 were palladised and tested for electricity generation

in a fuel cell. This would be another factor to consider for the appropriate strain selection. Further experiments would test RL009 in a similar way.

### **VI.1.3 Towards an integrated system for bio-energy**

This section is presented in form of a paper that is in submission in the Journal mentioned below; it describes the role of *E. coli* strain RL007 in H<sub>2</sub> production and electricity generation.

“Towards an integrated system for bio-energy”.

Journal: Biotechnological Letters (2010) 32:1837-1845.

This paper was written by Rafael L. Orozco in collaboration with Dr. P. Yong, Professor F. Sargent and Dr. M. Redwood. All experiments and analysis related with H<sub>2</sub> and OA production were performed by Rafael L. Orozco. Cells coating and electricity generation experiments were performed by Dr. P. Yong. Professor Frank Sargent wrote on the construction of the strains.

### **VI.1.3 Towards an integrated system for bio-energy**

Towards an integrated system for bio-energy: Hydrogen production by *Escherichia coli* and use of palladium-coated waste cells for electricity generation in a fuel cell

R.L. Orozco<sup>1</sup>, M.D. Redwood<sup>1</sup>, P. Yong<sup>1</sup>, I. Caldelari<sup>2,\*</sup>, F. Sargent<sup>2</sup> and L.E. Macaskie<sup>1</sup>.

<sup>1</sup> Unit of Functional Bionanomaterials, School of Biosciences, University of Birmingham, Edgbaston, Birmingham B15 2TT, UK.

<sup>2</sup> Division of Molecular Microbiology, College of Life Sciences, University of Dundee, Dundee DD1 5EH, Scotland.

\*Present address: Institut de Biologie Moléculaire et Cellulaire, Centre National de la Recherche Scientifique Unité Propre de Recherche, Université Louis Pasteur, 67084 Strasbourg Cedex, France

## Abstract

*Escherichia coli* strains MC4100 (parent) and a mutant strain derived from this (RL007) were evaluated for their ability to produce hydrogen and organic acids (OAs) via fermentation. Following growth, each strain was coated with Pd(0) via bioreduction of Pd(II). Dried, sintered Pd-biomaterials ('Bio-Pd') were tested as anodes in a proton exchange membrane (PEM) fuel cell for their ability to generate electricity from hydrogen. Both strains produced hydrogen and OAs but 'palladized' cells of strain RL007 (Bio-Pd<sub>RL007</sub>) produced ~ 3-fold more power as compared to Bio-Pd<sub>MC4100</sub> (56 and 18 mW respectively). The power output using, for comparison, commercial Pd(0) powder and Bio-Pd made from *Desulfovibrio desulfuricans*, was ~100 mW. The implications of these findings for an integrated energy generating process are discussed.

Key words: biohydrogen, *Escherichia coli*, fuel cell, palladium

## Introduction

Hydrogen and fuel cell technologies offer a feasible alternative to fossil fuels that is consistent with environmental demands for low carbon energy and zero emissions. Hydrogen is currently produced mainly as a by-product from the petrochemical industry. This is unsustainable and, furthermore, commercial H<sub>2</sub> contains traces of CO, a fuel cell catalyst poison. Currently the life time of a proton exchange membrane fuel cell (PEMFC) is less than 4,000 h (~ 167 days) whereas that required for a commercial market launch is 40,000 h (5 years; Aki et al. 2005). Photovoltaically-driven water electrolysis produces clean H<sub>2</sub> but the requirement for solar energy, the large light capture area, and efficiency of photovoltaic materials are currently limiting factors (MacKay 2008). Use of H<sub>2</sub> as a storable energy vector can overcome the problems of intermittency of renewable power systems.

Clean H<sub>2</sub> can also be made via microbial fermentation of organic wastes (Davila-Vazquez et al. 2008; Redwood et al. 2009). Biomass (sugary, starchy, and ligno-cellulosic wastes) is an abundant renewable resource and is, therefore, potentially capable of supporting a future sustainable H<sub>2</sub> economy. The proportion of the energy demand which could be satisfied in this way is difficult to estimate, but it was reported that diverting landfill-destined cellulosic waste into bioH<sub>2</sub> production in the Netherlands would produce enough H<sub>2</sub> to meet 9% of the domestic energy demand (de Vrije and Claassen 2003). Furthermore it has been predicted that bioconversion of organic waste to biogas could provide up to 7.5% of the UK's 2020 renewable energy commitment (Anon 2009).

*Escherichia coli*, an example of a facultative anaerobe, converts sugar via the mixed acid fermentation to gaseous products (H<sub>2</sub> and CO<sub>2</sub>) and soluble products including the organic acids (OAs) acetate, lactate, formate and small amounts of succinate, and also ethanol (Clark 1989). H<sub>2</sub> production in *E. coli* is mediated by the formate hydrogenlyase (FHL) complex which is located on the inner cell membrane. FHL catalyses the release of H<sub>2</sub> and CO<sub>2</sub> from formate in response to an increase in intracellular formate, which signals the reduction in extracellular pH caused by OA formation (Penfold et al. 2003; Redwood 2007; Redwood et al. 2009). The bioH<sub>2</sub> is sufficiently clean (after CO<sub>2</sub> removal) to be used directly in a PEMFC without further purification (Macaskie et al. 2005).

Formate is the sole precursor of H<sub>2</sub> in *E. coli* with a maximum yield of 2 mol of H<sub>2</sub> per mol of glucose (Clark, 1989). Although other organisms such as *Enterobacter* and *Clostridium* can produce, maximally, 4 mol H<sub>2</sub>/mol glucose via redox carrier-linked reversible hydrogenases these systems are inhibited even at a very low partial pressure of H<sub>2</sub>, whereas *E. coli* is unaffected due to

the use of an irreversible formate-linked hydrogenase system (FHL). The H<sub>2</sub> yield was improved further by utilising the produced OAs in a downstream photobioreactor to make a second H<sub>2</sub> stream via nitrogenase activity; effectively here the *E. coli* fermentation has a dual function in both H<sub>2</sub> and OA production (Redwood 2007; Redwood et al. 2009).

Bio-hydrogen has additional potential due to its compatibility with fuel cells (Macaskie et al. 2005). These utilise precious metal catalyst to split the H<sub>2</sub> for electricity production; hence the second target for process improvement is the fuel cell itself since robustness is a major limitation for commercial development (Aki et al. 2005; above). Previous work showed that spent yeast biomass, coated with platinum nanoparticles can function as the anode material in a proton exchange membrane fuel Cell (PEMFC) (Dimitriadis et al. 2007) while a parallel study showed that *D. desulfuricans* could behave similarly when coated with either Pd(0) or Pt(0) nanoparticles fabricated via the hydrogenase-mediated reduction of Pd(II) or Pt(IV) (Yong et al. 2007). The PEMFC power output was comparable to commercial Pt(0) fuel cell catalyst under similar conditions (Yong et al. 2007). Cells of *E. coli* can fulfil a similar role but the power output using Bio-Pd<sub>*E. coli*</sub> was substantially lower than that obtained by using Bio-Pd<sub>*D. desulfuricans*</sub> (Yong et al. 2008). For economy and sustainability via re-use of the H<sub>2</sub>-producing biomass to make Bio-Pd/Pt and hence electricity ‘in process’, the power output from a PEMFC made with Bio-Pd<sub>*E. coli*</sub> must be increased, but without detriment to the production of either bioH<sub>2</sub> in the ‘dark’ fermentation or the organic acid co-products which provide the feedstock for the secondary-stage photofermentation to generate the second H<sub>2</sub> stream (Redwood 2008; Redwood et al. 2009). Hence, the dual objectives of this work were to compare hydrogen production and the ‘catalytic quality’ of Bio-Pd made from cells of *E. coli* strain MC4100 and its mutant RL007 developed within this study. The downstream photofermentation described elsewhere (Redwood et al. 2009) utilises *Rhodobacter sphaeroides* to make additional H<sub>2</sub> via rapid separation and utilisation of the organic acid products of the *E. coli* fermentation. Therefore, the opportunity was also taken to evaluate the potential to use Bio-Pd<sub>*R. sphaeroides*</sub> in a PEMFC.

## Materials and Methods

### *Bacterial strains and hydrogen production.*

*Desulfovibrio desulfuricans* was as described previously (Yong et al. 2007). *R. sphaeroides* OU001 was grown as described by Redwood (2007). For comparison of *E. coli* strains, *E. coli* HD701 (hydrogen overproducer; derived from the parental strain *E. coli* MC4100 via upregulation

of formate hydrogenlyase: Penfold et al. 2003) was also used. *E. coli* strain RL007 ( $\Delta focA$ ,  $\Delta focB$ ,  $\Delta nirC$ ,  $\Delta hycA$ ,  $\Delta ldhA$ ,  $\Delta tatABC::Apra^R$ ) was also derived from the parental strain MC4100. Construction of RL007 took advantage of the PCR-targeting approach of Datsenko and Wanner (2000) and the ‘Keio Collection’ of single, kanamycin resistance-marked *E. coli* deletion strains (Baba et al. 2006). First, for deletion of *focA* and *focB*, the apramycin resistance cassette and flanking FLP recombinase recognition sequences encoded on plasmid pIJ773 (Gust et al. 2003) were amplified using primers based on the FRT recognition sequences together with the *focA* or *focB* flanking sequences. In each case the PCR-amplified apramycin resistance cassette was transformed into electro-competent *E. coli* strain BW25113 harbouring plasmid pKD20 and double cross-overs were selected by plating the transformants onto LB plates containing apramycin. Disruption of the targeted gene was confirmed by PCR, and the marked deletions were subsequently transduced using P1 phage into MC4100 using the method of Miller (1992) The apramycin resistance cassette was subsequently ‘flipped out’ of the marked deletions using the method described by Datsenko and Wanner (2000) to give strains IC00A and IC00B. Loss of the apramycin-resistance cassette was confirmed by PCR and apramycin sensitivity. Using identical methods, the *focA* and *focB* mutant alleles were then combined to give a double mutant strain IC001 (as MC4100,  $\Delta focA$ ,  $\Delta focB$ ), which was used as a base to build additional mutations upon. The *nirC* gene was deleted first, using identical methods, to yield IC002 (as MC4100,  $\Delta focA$ ,  $\Delta focB$ ,  $\Delta nirC$ ). Next, the  $\Delta hycA::Kan^R$  allele from *E. coli* strain JW2695 was moved by P1 transduction into IC002 and flipped out using pCP20 ( $Amp^R$ ) to yield strain IC003 (as MC4100,  $\Delta focA$ ,  $\Delta focB$ ,  $\Delta nirC$ ,  $\Delta hycA$ ). Next, a  $\Delta ldhA::Cam^R$  allele, which was prepared by PCR, was introduced into IC003 and flipped out resulting in IC005 (as MC4100,  $\Delta focA$ ,  $\Delta focB$ ,  $\Delta nirC$ ,  $\Delta hycA$ ,  $\Delta ldhA$ ). Finally, a  $\Delta tatABC::Apra^R$  cassette was prepared by PCR and introduced into IC005 to yield RL007 (as MC4100,  $\Delta focA$ ,  $\Delta focB$ ,  $\Delta nirC$ ,  $\Delta hycA$ ,  $\Delta ldhA$ ,  $\Delta tatABC::Apra^R$ ). The genotypic identity of strain RL007 is summarised in Table 1.

Stocks of *E. coli* strains were maintained at -80 °C in 75% glycerol, plated on nutrient agar (Oxoid) and incubated overnight at 30 °C. For experiments, colonies were picked for pre-culture into nutrient broth (Oxoid, 5 mL), with sodium formate (0.5% w/v) pH 7, and shaken (6h, 30 °C). Cells were inoculated (10 µL) in two 2 L Erlenmeyer flasks containing 1 L of the same medium and shaken for 16 h (30 °C). Cell pellets, obtained by centrifugation, were washed twice in 100 mL phosphate buffered saline (PBS: 1.43 g  $Na_2HPO_4$  0.2 g  $KH_2PO_4$ , 0.8 g NaCl, 0.2 g KCl /L, pH 7.0)

and resuspended in 20 mL PBS to produce a concentrated inoculum for fermentation containing ~ 40—46 g dry weight/L ( $OD_{600nm}$  of 1 corresponded to a concentration of 0.48 g dry weight/L (a previously determined conversion factor).

Fermentations (two conditions, each in duplicate) were performed consisting of a 5 L fermenter (Fermac 200-series, Electrolab UK) with pH, temperature and agitation control, a “scrubber” column containing 2 M NaOH, a H<sub>2</sub> collector cylinder full of water and a N<sub>2</sub> gas supply. At least 99.5% of CO<sub>2</sub> was trapped in the scrubber solution as verified by GC (Redwood 2007) and H<sub>2</sub> was collected and quantified by water displacement in a graduated collector cylinder. All tubes and connectors were previously sterilized with 70% ethanol.

The fermentation vessels contained 3 L of fermentation medium (de-ionized water; in each 3 litre batch: 42.60 g Na<sub>2</sub>SO<sub>4</sub>, 10.46 g K<sub>2</sub>HPO<sub>4</sub>, 0.20 g KH<sub>2</sub>PO<sub>4</sub>, 0.20 g (NH<sub>4</sub>)<sub>2</sub>SO<sub>4</sub>, pH 5.8). All solutions were prepared using de-ionized water and analytical grade reagents. The following supplements were aseptically added to the fermenter just before inoculation: 1 M MgSO<sub>4</sub>·7H<sub>2</sub>O (6 mL), 2 M glucose (30 mL; 20 mM final concentration), trace elements solution (9 mL) and polyethylene glycol antifoam (PEG; 0.5 mL). Trace elements solution comprised (quantities in g/L): CaCl<sub>2</sub>·H<sub>2</sub>O (0.74); ZnSO<sub>4</sub>·7H<sub>2</sub>O (0.18); MnSO<sub>4</sub>·H<sub>2</sub>O (0.10); disodium-EDTA (20.1); FeCl<sub>3</sub>·6H<sub>2</sub>O (16.7); CuSO<sub>4</sub>·5H<sub>2</sub>O (0.10); CoSO<sub>4</sub>·7H<sub>2</sub>O (0.21).

The system was purged with oxygen free nitrogen (OFN), (through a 0.2 µm filter) for at least 30 min before inoculation. pH was maintained throughout the fermentation at pH 5.5-5.7 by dosing 2M NaOH and 2M H<sub>2</sub>SO<sub>4</sub> via an Electrolab Fermac260 pH controller, at 30 °C with stirring (300 rpm). To start each experiment the OFN was stopped, nitrogen tubes were depressurized and valves to the gas collector cylinder were opened to allow the system to equilibrate for at least 45 min.

### *Sampling and analysis.*

For glucose, organic acids and ethanol analysis, samples were periodically withdrawn from the culture, filtered (0.2 µm supor membrane syringe filter) and stored at -20°C before analysis. Glucose determination was by the colorimetric dinitrosalicylic acid assay [160]. Organic acids were measured by an anion HPLC (Dionex 600-series) as described previously (Redwood & Macaskie 2006). Ethanol was analysed using a Cecil Adept HPLC system equipped with Resex-RCM column (Phenomenex); RI detector; temperature 75 °C; eluate H<sub>2</sub>O; flow rate 0.5 ml/min; 30 min experiment time. Bacterial growth was monitored via the  $OD_{600}$  of withdrawn samples ( $OD_{600}:1 \equiv 0.482$  g DW/L; Ultrospec 3300 pro). H<sub>2</sub> production was monitored and measured by the

displacement of water from graduated cylinders with time-lapse photography for continuous monitoring. CO<sub>2</sub> was removed into 2M NaOH scrubber solution with universal indicator pH 9-13. Hydrogen in collectors was confirmed using a hydrogen sensor detector. Previous work (Sauter et al. 1992 and DW Penfold, unpublished) showed that CO<sub>2</sub> and H<sub>2</sub> are the only gases evolved under these conditions. The H<sub>2</sub> yield was calculated in relation to a theoretical maximum of 2 mol H<sub>2</sub>/mol glucose (Clark 1989); 90% of this yield was achieved previously under similar conditions (Redwood 2007).

*Preparation of fuel cell electrode materials.*

For experiments to test the utility of ‘palladised’ cells in a fuel cell *D. desulfuricans* (reference organism: Yong et al. 2007) and *E. coli* strains (this study) were grown as described by Yong et al. (2002) and Penfold et al. (2006), respectively. Cells were palladised as described previously (5% Pd by mass; Yong et al, 2007), washed in acetone dried and ground, and then transferred into 10 mL alumina ceramic crucibles for sintering (i.e. carbonising) in a programmable furnace. The temperature was increased from room temperature to 700 °C within 4 h and held at 700 °C for a further 4 h before cooling to room temperature in the furnace.

Commercial submicron Pd powder (C-Pd) (Sigma-Aldrich, Germany), and ‘Bio-Pds’ (20 mg of each, as metal) were mixed separately with pure activated carbon powder (80 mg; BDH Chemicals Ltd, UK). Nafion® perfluorinated ion-exchange resin (0.2 mL; 10 wt % in water, Sigma-Aldrich) and water (1.0 mL) were added to each sample containing 20% of Pd and 80% of C. The sample was mixed well, manually applied evenly onto 16 cm<sup>2</sup> teflon-treated carbon paper (Fuel Cell Scientific, USA), and dried at room temperature. The lab-made electrodes were tested for electricity production versus the commercial Pd powder in a small proton exchange membrane (PEM) fuel cell as described previously (Yong et al. 2007) and the maximum power output (mW) was recorded.

## Results and Discussion

### *Hydrogen and organic acid production by E. coli strains MC4100 and RL007.*

H<sub>2</sub> production (mL), biomass (g), glucose consumption (mmol), organic acid (OA) and ethanol production (mmol) were measured and quantified; reproducibility was usually within 10% between separate experiments. Hydrogen overproduction by *E. coli* strain HD701 (via derepression of the H<sub>2</sub>-producing formate hydrogen lyase complex (Penfold et al. 2003)) and by strains deficient in uptake hydrogenases (Penfold et al. 2006; Redwood et al. 2008) were described previously and production of OA by the latter was also quantified (Redwood & Macaskie 2006). A combination of the *hycA* and *tat* mutations did not increase hydrogen production over that obtained with one mutation alone (Penfold et al. 2006). Hence, in this work, further metabolic engineering of *E. coli* was performed. A new strain (RL007) was prepared that combined mutations additional to those in the *hycA* and *tatABC* genes previously studied (Table 1). Strain RL007 was rendered devoid its formate transporters (FocA and FocB), and the FocA/B homolog NirC, in an attempt to impair formate secretion during fermentation and utilise early and sustained formate hydrogenlyase (FHL) activity. In addition, strain RL007 lacks an active *ldhA* gene, which encodes an NADH-dependent lactate dehydrogenase that is normally active in the later stages of fermentative growth. The rationale in removing LdhA was to prevent the metabolism of pyruvate to lactate and, instead, shunt additional pyruvate towards formate and hence boost H<sub>2</sub> production.

The fermentation kinetics of strains MC4100 and RL007 are compared in Figure 1 and summarised in the fermentation balances shown in Table 2. During a 24h fermentation, both strains grew very slightly, limited by the low concentration of added nitrogen source; note that prior to the incubation the cells had been grown aerobically to high density, with formate as a FHL inducer (Redwood et al. 2008). The parent strain MC4100 consumed all of the initial added glucose within 24h, whereas the mutant strain RL007 consumed only 70% of the added glucose over 24h. Correspondingly, the MC4100 parent strain evolved H<sub>2</sub> more rapidly than strain RL007 (Fig. 1 a,b), the rate peaking at ~ 4.2 mmol H<sub>2</sub>/h during the initial 10h and gradually decreasing within 24h. The overall yields of H<sub>2</sub> produced were 41% and 37% for strains MC4100 and RL007, respectively, and not significantly different on the basis of the two experiments reported (Table 2).

Analysis of OA production (Fig 1 c,d and Table 2) showed that lactate was the main organic product of the parent strain MC4100 but the lactate yield was negligible in strain RL007 due to the *ldhA* mutation. However, the result of this was not an increase in H<sub>2</sub> production but in non-lactate by-products, especially pyruvate, succinate and ethanol. Despite the loss of lactate production, the

overall yield of H<sub>2</sub> in strain RL007 was not significantly different from the parent strain MC4100, which can be attributed to the accumulation of alternative byproducts (succinate) and H<sub>2</sub> precursors (pyruvate and formate). The inability of strain RL007 to reassimilate all of the formate initially secreted into the reaction medium may be attributed to the lack of dedicated formate transport machinery in this strain and partially accounts for the reduced H<sub>2</sub> yield observed. Clearly, lactate dehydrogenase is a major route for pyruvate dissimilation and recycling of NADH during fermentation. The loss of *ldhA* leads to the accumulation and ultimate secretion of pyruvate; the shortfall in NADH recycling via removal of lactate production is compensated by an increased production of ethanol and succinate.

Similar observations regarding different *ldh* mutants were made by Mat-Jan et al. (1989) and Zelic et al. (2004) in *ldh* mutants. However, we also observed that when strain IC700 was allowed to ferment for a further 24 h, the pyruvate was reassimilated, which is in accordance with the observations of Sode et al. (1999) where, likewise, the reaction was followed to completion.

We conclude that eliminating lactate production did not benefit the H<sub>2</sub> yield in this study as the additional intermediate either accumulated or gave enhanced production of alternative products, particularly succinate and ethanol. Eliminating succinate production would be difficult due to the key role of succinate-producing enzymes in central metabolism. Further, succinate is potentially useful in the downstream photobioreactor and hence could be re-used 'in process'. Jointly upregulating the activity of pyruvate formate lyase and FHL could hypothetically channel more pyruvate intermediate towards H<sub>2</sub> production, an approach to be addressed in future work. Work is currently in progress to reduce the production of ethanol since this product cannot be transferred easily into the downstream photobioreactor but this metabolic engineering will have implications in the ability of the cells to recycle NADH and such mutants may be highly impaired or non-viable.

#### *Electricity production by palladised cells of E. coli in a fuel cell.*

Cells of the *E. coli* strains MC4100 and RL007 (this study), together with strain HD701 (hydrogen production was as described previously: Penfold et al. 2003), *R. sphaeroides* (Redwood 2007) and *D. desulfuricans* (positive control) were coated with palladium nanoparticles as described previously (Yong et al. 2007) and tested for their ability to produce electricity as anodes in a PEM fuel cell. Sintering of palladised biomass was essential to obtain catalytic activity (P. Yong, unpublished) since biomass is predominantly water and sintering carbonises the biomass to make it electrically conductive. As shown in Fig. 2 and Table 3, Bio-Pd<sub>*D. desulfuricans*</sub> produced power

comparably to commercial finely-ground Pd(0) while Bio-Pd<sub>MC4100</sub> and Bio-Pd<sub>HD701</sub> produced little power (~18-28 mW). However Bio-Pd<sub>RL007</sub> produced ~ 56 mW, which was ~ three-fold higher than the parent strain (~18 mW) or Bio-Pd<sub>*R. sphaeroides*</sub>. (~ 20 mW). Representative data are shown, since the power output is critically dependent on the exact preparation of the electrode but in 3 replicate experiments the Bio-Pd(0) of the mutant outperformed that of the parent strain consistently as shown.

From these results it can be concluded that the catalytic activity of the palladium in a fuel cell relates to the enzymatic composition and localisation in the strain which produced it. A similar conclusion with respect to chemical catalysis was drawn (Rousset et al. 2006) using a mutant of *D. fructosovorans* which lacked its periplasmic hydrogenases; here, the Pd(0) relocated to the site of the remaining cytoplasmic hydrogenase (Mikheenko et al. 2008) and was catalytically more active in the reduction of Cr(VI) (Rousset et al. 2006). In the present case the key difference between strains HD701 and RL007 is that the Tat transport system is missing, and therefore there are no functional periplasm-facing hydrogenases. Therefore, strain RL007, like the *D. fructosovorans* mutant (above) may be location-modified with respect to making Pd-nanoparticles. However no obvious differences were observed in initial comparisons of the Bio-Pd produced by strains MC4100 and RL007 (Yong et al. 2010) and a high resolution TEM study is clearly warranted. Taken together, the two studies using *D. fructosovorans* and *E. coli* indicate that ‘relocating’ the Pd-nanoparticles may be beneficial to the ‘quality’ of the catalyst produced. Potential pleiotropic effects of the mutations introduced into strain RL007 were not investigated but warrant further investigation. The extent to which the ‘biochemical’ component of the Bio-Pd moderates the catalytic activity of its Pd(0) ‘partner’ after sintering of the material is a subject of current investigation.

## Conclusion

In terms of H<sub>2</sub> production strain RL007 offers little benefit over a 24 hour period as compared to its parent strain MC4100, although its ability to produce more succinate and pyruvate could be beneficial as secondary products. However, in terms of an integrated energy process, where biomass is re-used ‘in process’ the mutant strain offers more potential to make a better fuel cell although this still falls short (by ~ 50%) of the use of *D. desulfuricans* as a support for ‘Bio-Pd’ for this purpose. The extent to which further molecular engineering could improve the rates and yields of hydrogen production without compromising fuel cell catalyst performance is the subject of ongoing studies.

## **Acknowledgements**

The financial support of the BBSRC (Grant Nos BB/C516195/2 and BB/E003788/1), the EPSRC (Grant Nos EP/D05768X/1 and EP/E034888/1), the Royal Society (Industrial Fellowship to LEM), Advantage West Midlands (Grant ref. POC46) and the Government of Mexico (studentship no. 203186) to RLO is acknowledged, with thanks.

## References

Aki H, Murata A, Yamamoto S, Kondoh J, Maeda T, Yamaguchi H, Ishii, I (2005) Penetration of residential fuel cells and CO<sub>2</sub> mitigation – case studies in Japan my multi-objective models. *Int J Hyd Energy*, 30: 943-952.

Anon: Department of Food and Rural Affairs (Feb 2009) Anaerobic Digestion - Shared Goals. [www.defra.gov.uk](http://www.defra.gov.uk) Accessed May 2010.

Baba T, Ara T, Hasegawa T, Takai Y, Okumura Y, Baba M Datsenko KA, Tomita M, Wanner BL, Mori H (2006) Construction of *Escherichia coli* K-12 in-frame, single-gene knockout mutants: the Keio collection. *Mol Syst Biol* 2: 0008.

Berks BC, Palmer T & Sargent F (2003) The Tat protein translocation pathway and its role in microbial physiology. *Adv Microbial Physiol* 47: 187-254.

Bunch PK, Mat-Jan F, Lee N, Clark DP (1997) The *ldhA* gene encoding the fermentative lactate dehydrogenase of *Escherichia coli*. *Microbiology* 134: 187-195.

Chaplin MF (1986). Monosaccharides. In *Carbohydrate analysis: a Practical Approach*. Chaplin MF, Kennedy JF, (Eds). IRL Press at Oxford University press, UK: p.3

Clegg FYS, Griffiths L, Cole JA, (2002) The roles of the polytopic membrane proteins NarK, NarU and NirC in *E.coli* K-12- two nitrate and three nitrite transporters *Mol Microbiol* 44: 143-155.

Datsenko KA, Wanner BL (2000) One-step inactivation of chromosomal genes in *Escherichia coli* K-12 using PCR products. *Proc Natl Acad Sci U S A* 97:6640-6645

Davila-Vazquez G, Arriaga S, Alatraste-Mondragon F, de Leon-Rodriguez A, Rosales-Colunga LM, Razo-Flores E (2008) Fermentative biohydrogen production: trends and perspectives. *Rev Environ Sci Biotechnol* 7:27-45.

De Vrije T, Claassen PAM (2003) Dark hydrogen fermentations. in *Bio-methane and Bio-hydrogen*. Reith JH, Wijffels RH, Barten H, (Eds). Petten, Netherlands, Dutch Biological Hydrogen Foundation: 103-123.

Dimitriadis S, Nomikou N, McHale Biotechnology AP (2007) Pt-based electro-catalytic materials derived from biosorption processes and their exploitation in fuel cell technology. *Biotechnol Lett* 29: 545-551.

Gust B, Challis GL, Fowler K, Kieser T, Chater KF (2003) PCR-targeted *Streptomyces* gene replacement identifies a protein domain needed for biosynthesis of the sesquiterpene soil odor geosmin. *Proc Natl Acad Sci* 100:1541–1546

Macaskie LE, Baxter-Plant VS, Creamer NJ, Humphries AC, Mikheenko IP, Penfold DW, Yong P (2005) Applications of bacterial hydrogenases in waste decontamination, manufacture of novel bionanocatalysts and in sustainable energy. *Biochem Soc Trans* 33; 76-79.

MacKay DJC (2008) *Sustainable Energy - without the hot air.*, UIT Cambridge. Published online at [www.withouthotair.com](http://www.withouthotair.com). Accessed, June 2010.

Mat-Jan F, Alam KY, Clark DP (1989) Mutants of *Escherichia coli* deficient in the fermentative lactate dehydrogenase. *J Bacteriol* 171: 342-348.

Mikheenko I, Rousset M, Dementin S, Macaskie LE (2008) Bioaccumulation of palladium by *Desulfovibrio fructosovorans* and hydrogenase deficient strains. *Appl Environ Microbiol* 19: 61144-6146

Miller JH (1992) *A Short Course in Bacterial Genetics: A Laboratory Manual and Handbook for Escherichia coli and Related Bacteria*, Cold Spring Harbor Laboratory Press, New York, USA.

Miller M (2005) Twin-arginine specific protein export in *Escherichia coli* *Res Microbiol* 156: 131-136

Penfold DW, Forster CF, Macaskie LE (2003) Increased hydrogen production by *Escherichia coli* strain HD701 in comparison with the wild-type parent strain MC4100. *Enz Microbial Technol* 33:185-189.

Penfold DW Sargent F, Macaskie LE (2006) Inactivation of the *Escherichia coli* K-12 twin-arginine translocation system promotes increased hydrogen production *FEMS Microbiol Lett* 262: 135-137.

Redwood MD (2007) Bio-hydrogen and biomass supported palladium catalyst for energy production and waste minimisation. Ph.D. Thesis, University of Birmingham, UK

Redwood MD, Macaskie LE (2006). A two-stage, two-organism process for biohydrogen from glucose. *Int J Hydrogen Energy* 31:1514-1521.

Redwood, MD, Mikheenko IP, Sargent F and Macaskie LE. (2008) Dissecting the roles of *E. coli* hydrogenases in biohydrogen production. *FEMS Microbiol Letts* 278: 48-55.

Redwood MD, Paterson-Beedle M, Macaskie LE (2009) Integrating dark and light biohydrogen production strategies: towards the hydrogen economy. *Rev Environ Sci Bio/Technol* 8:149-185.

Rousset M L, Casalot P, de Philip A, Bélaich I, Mikheenko I, Macaskie LE (2006) Use of bacterium strains for the preparation of metallic biocatalysts, in particular for the preparation of

palladium biocatalysts. European Patent Application Number: WO/2006/087334. International Application No.: PCT/EP2006/05094.

Saier MH, Ford S, Garg J, Haggerty DA, Hutchinson WJ, Jack DL, Lai EC, Liu HJ, Nusinew DP, Omar AM, Pao SS, Paulsen IT, Quen JA, Sliwinski M, Tseng TT, Wachi S, Young GB, (1999) Phylogenetic characterization of novel transport protein families revealed by genome analysis. *Biochim Biophys Acta* 1422: 1-56.

Sauter M, Bohm R, Bock A (1992) Mutational analysis of the operon (*hyc*) determining hydrogenase-3 formation in *Escherichia coli*. *Mol Microbiol* 6:1523-1532.

Sode K, Yamamoto S, and Tomiyama M. (1999) Construction and characterisation of fermentative lactate dehydrogenase *E. coli* mutant and its potential for bacterial hydrogen production. *Appl Biochem Biotechnol* 77-79: 317-323.

Suppmann B, Sawers G (1994) Isolation and characterization of hypophosphite resistant mutants of *Escherichia coli*: identification of the FocA protein, encoded by the *pfl* operon, as a putative formate transporter. *Mol Microbiol* 11: 865-982.

Yong P, Rowson NA, Farr JP, Harris IR, Macaskie LE (2002) Bioreduction and biocrystallization of palladium by *Desulfovibrio desulfuricans* NCIMB 8307. *Biotechnol Bioeng* 80:369-379.

Yong P, Paterson-Beedle M, Mikheenko IP, Macaskie LE (2007) From biomineralization to fuel cells: biomanufacture of Pt and Pd nanocrystals for fuel cell electrode catalyst. *Biotechnol Lett* 29:539-544.

Yong P, Mikheenko I., Macaskie LE (2008) Manufacturing of fuel cell catalysts by biocrystallization. *J Biotechnol* 136S: S374-S375

Zelic B, Gostovic S, Vuorilehto K, Vasic-Racki D, and Takors R (2004) Process strategies to enhance pyruvate production with recombinant *Escherichia coli*: From repetitive fed-batch to in situ product recovery with fully integrated electrodialysis. *Biotechnol Bioeng* 85: 638-646

## Legends to Figures

**Figure 1.** Hydrogen production (a,b) and organic acid production (c,d) from *E. coli* MC4100 (a,c) and RL007 (b,d). Open and filled symbols represent two independent experiments. Hydrogen production and glucose utilization (a,b) are shown as total mmoles to aid comparison. Masses are shown in mmol: ( $\Delta$ ,  $\blacktriangle$ ) Glucose utilization; ( $\square$ ,  $\blacksquare$ ) Hydrogen production in a and b. Fermentation products in c and d are: ( $\square$ ,  $\blacksquare$ ) lactate; ( $\diamond$ ,  $\blacklozenge$ ) acetate; ( $\circ$ ,  $\bullet$ ) formate; ( $\triangle$ ,  $\blacktriangle$ ) succinate; ( $\times$ ,  $\boxtimes$ ) pyruvate.

**Figure. 2.** Power production in a PEM fuel cell using alternative anode catalysts: commercial Pd(0) ( $\square$ ) and palladised, sintered cells (Bio-Pd) made from *D. desulfuricans* ( $\blacksquare$ ) and *E. coli* strains MC4100 ( $\bullet$ ); HD701 ( $\blacktriangle$ ) and RL007 ( $\blacklozenge$ ).

Table 1 Genotypic identity of strain *E. coli* RL007

Deletion	Affected gene product ( <i>resultant phenotype</i> )
	Reference
$\square$ <i>focA</i>	Formate transporter Suppmann et al. 1994 <i>(impaired ability to secrete and take up formate)</i>
$\Delta$ <i>focB</i>	Formate transporter Saier et al. 1999 <i>(impaired ability to secrete and take up formate)</i>
$\square$ <i>hycA</i>	Formate hydrogen lyase (FHL) regulatory protein Sauter et al. 1992; Penfold et al. 2003 <i>(upregulated FHL; H<sub>2</sub> overproduction)</i>
$\Delta$ <i>ldhA</i>	NADH-linked fermentative lactate dehydrogenase Bunch et al. 1997 <i>( lactate not produced)</i>

$\Delta tatABC$  The twin arginine translocation system: transports folded proteins across membranes Berks et al. 2003; Miller 2005

(*tat* inactivation prevents uptake hydrogenase transport; increases  $H_2$  production) Penfold et al. 2006

□ *nirC* Nitrite transporter, paralogous with FocA/B

Clegg et al. 2002

(*impaired ability to secrete and take up formate*)

Strain RL007 was made from its parent MC4100 as described in Materials and Methods. It combines the ability to overproduce hydrogen via

deletion of the FHL regulator FhlA and the Tat system with impaired ability to transport formate. It does not make lactate, potentially

increasing the metabolic flux into the other fermentation products.

Table 2. Fermentation balance of *E. coli* strains MC4100 and RL007

Strain	Repeat	Time	Product yields (mol/mol glucose)*								Growth (g/mol glucose)	Carbon balance ***
			Lac	Pyr	Form	Succ	Ac	EtOH	H <sub>2</sub>	CO <sub>2</sub> **		
MC4100	Expt 1	22.75	0.892	0.000	0.048	0.200	0.354	0.405	0.788	0.51	3.99	99%
	Expt 2	22.75	0.789	0.000	0.024	0.196	0.326	0.438	0.849	0.54	4.49	93%
RL007	Expt 1	23.5	0.008	0.518	0.079	0.492	0.227	0.704	0.735	0.36	4.41	102%
	Expt 2	23.5	0.007	0.527	0.069	0.479	0.222	0.685	0.760	0.36	2.64	99%

\* Propionate and butyrate were not detected. Lac: lactate; Pyr: pyruvate; Form: formate; Succ: succinate; Ac: acetate; EtOH: ethanol

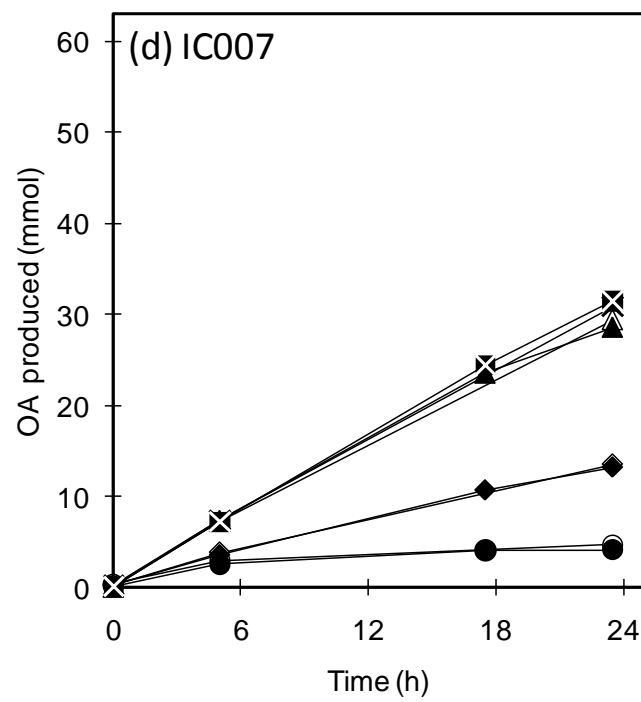
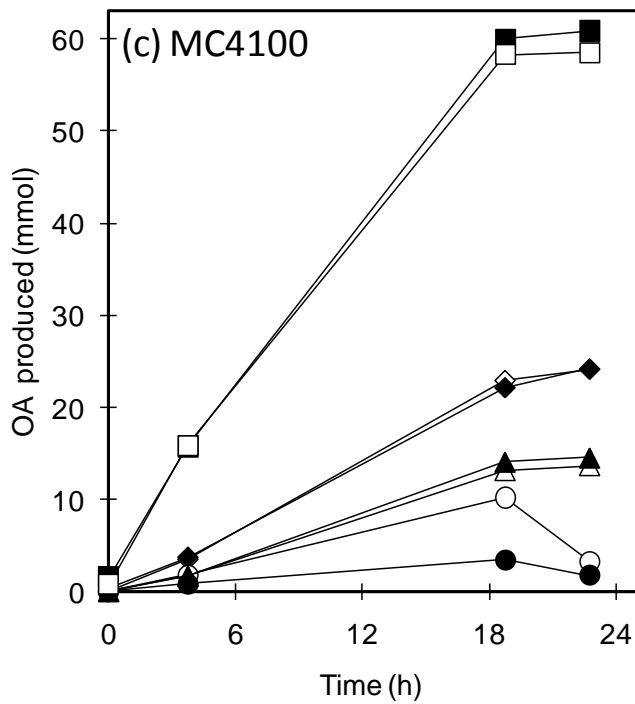
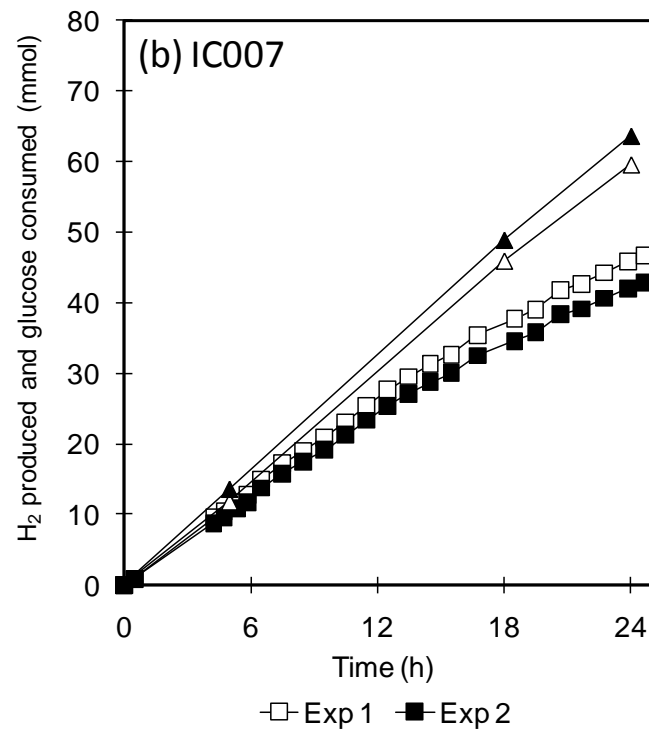
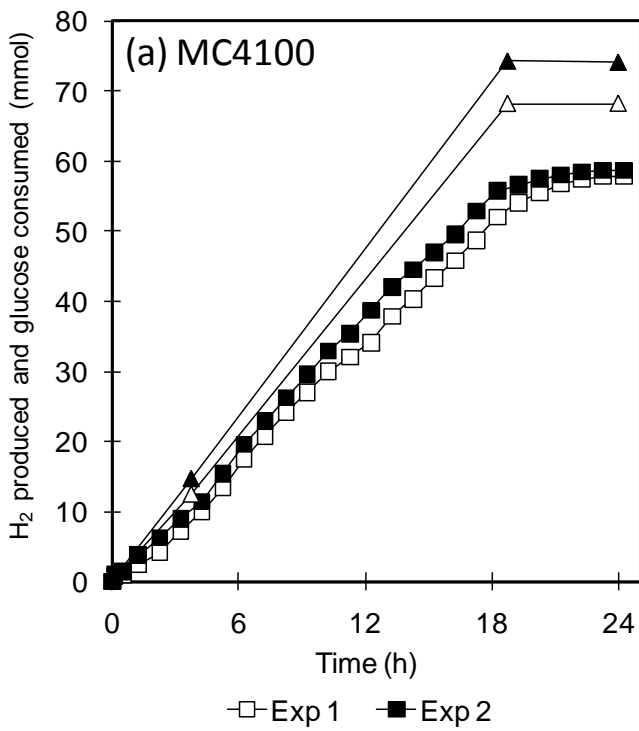
\*\* The yield of CO<sub>2</sub> was estimated as described by Redwood et al (2007), equation 2.

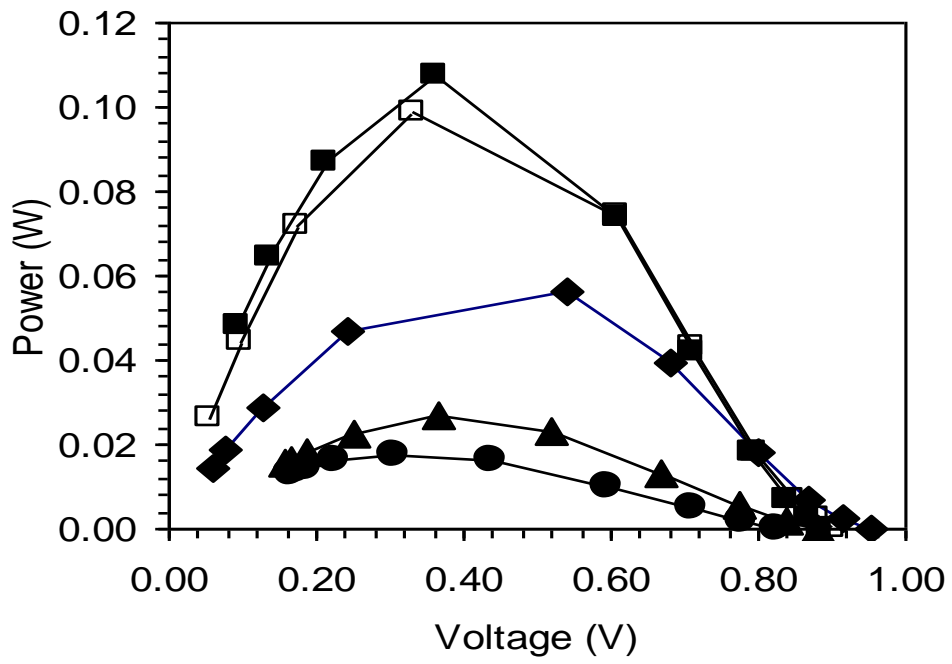
\*\*\* Carbon balance was calculated as Redwood et al (2007), but including pyruvate (3 carbon equivalents).

Table 3. Maximum power output ( $P_{\max}$ , mW) from a PEM fuel cell using anodes made from commercial precious metals and Bio-Pd..

Preparation	$P_{\max}$ (mW)	Reference
Commercial Pt(0)	170	Yong et al.
2007		
Bio-Pt <sub><i>D. desulfuricans</i></sub>	170	Yong et al.
2007		
Commercial Pd(0)	100	This study
Bio-Pd <sub><i>D. desulfuricans</i></sub>	108	This study
Bio-Pd <sub><i>E. coli</i> HD701</sub>	28	This study
Bio-Pd <sub><i>E. coli</i> MC4100</sub>	18	This study
Bio-Pd <sub><i>E. coli</i> RL007</sub>	56	This study
Bio-Pd <sub><i>R. sphaeroides</i> OU001</sub> *	19.5	Redwood
2007		

Native metallised biomass was inactive in a PEMFC. Samples (all 5% Pd w/w) were, therefore, sintered before use to carbonise the biomass, as described in Materials and Methods.





## **VI.2 Hydrogen from starch**

This section is presented in form of a paper that is in submission in the Journal mentioned below, it describes the hydrolysis of starch in HCW and the fermentability of the products.

“Hydrothermal hydrolysis of starch with CO<sub>2</sub> and detoxification of the hydrolysates with activated carbon for bio-hydrogen fermentation”.

Journal: International Journal of Hydrogen Energy, in submission.

This paper was written by Rafael L. Orozco. All experiments and analysis were performed by Rafael L. Orozco.

## **Hydrothermal hydrolysis of starch with CO<sub>2</sub> and detoxification of the hydrolysates with activated carbon for bio-hydrogen fermentation.**

R.L. Orozco<sup>1</sup>, M.D. Redwood<sup>1</sup>, G.A. Leeke<sup>2</sup>, A. Bahari<sup>2</sup>, R.C.D. Santos<sup>2</sup> and L.E. Macaskie<sup>1</sup>.

<sup>1</sup> Unit of Functional Bionanomaterials, School of Biosciences, University of Birmingham, Edgbaston, Birmingham B15 2TT, UK.

<sup>2</sup> School of Chemical Engineering, University of Birmingham, Edgbaston, Birmingham B15 2TT, UK.

### **Abstract**

The imminent use of hydrogen as an energy vector establishes the need for sustainable production technologies based on renewable resources. Starch is an abundant renewable resource suitable for bio-hydrogen generation. It was hypothesised that starch hydrolysates from a large (250 mL) hydrothermal reactor could support bioH<sub>2</sub> fermentation without inhibition by toxic byproducts.

Starch was hydrolysed at high concentrations (40-200 g.L<sup>-1</sup>) in hot compressed water (HCW) with CO<sub>2</sub> at 30 bar in a 250 mL reactor, the largest so far for polysaccharide hydrolysis, at 180-235 °C, 15 min. Hydrolysates were detoxified with activated carbon (AC) and tested in biohydrogen fermentations. The maximum yield of glucose was 548 g.kg starch<sup>-1</sup> carbon at 200 °C. 5-hydroxymethyl furfural, the main fermentation inhibitor, was removed by AC to support 70% more hydrogen production than the untreated hydrolysates. The potential utilization of starch hydrolysates from HCW treatment for upscaled fermentations is promising.

Keywords:

Hot Compressed Water, Hydrothermal hydrolysis, Detoxification, Biohydrogen, Starch.

### **1. Introduction**

The depletion of fossil fuel sources along with the greenhouse effect caused by increasing atmospheric CO<sub>2</sub> is driving the need for new clean energy alternatives to substitute for petroleum and meet increasing energy demand.

Hydrogen is an environmentally benign energy carrier that can be effectively utilized for power generation and it will play an important role in future energy technologies [1,2]. .

H<sub>2</sub> is a valuable commodity, its main uses being in the chemical industry, petroleum refining, ammonia production and as rocket fuel with a total world annual consumption of more than 50 million tonnes, with a market value of \$120 billion in 2010 and 15% annual growth [2-4]. The potential use of H<sub>2</sub> as a major power source for stationary applications and for the transportation industry will considerably increase its demand [1].

Currently, strong investment in infrastructure consisting of the production, storage, transportation and the strategic deployment of H<sub>2</sub> refuelling station networks is taking place in countries like Japan, Germany, USA, China, U.K. and Canada among others. [5,6].

The majority of the world's supply of H<sub>2</sub> comes from fossil fuels which is not sustainable. In light of this scenario new production technologies not based on fossil fuel to generate H<sub>2</sub> are required.

Biological H<sub>2</sub> production by the fermentation of agricultural products, by-products and organic wastes (biomass) is a sustainable low-carbon technology for H<sub>2</sub> production. This technology is based on the capabilities of various microorganisms to evolve H<sub>2</sub> from sustainable organic materials.

Biomass is an abundant renewable resource capable of supporting the future H<sub>2</sub> economy [2,4,7]. In recent studies made by the Biomass R&D Technical Advisory Committee (BTAC) of the US Department of Energy and Agriculture [8] it is reported that biomass now exceeds hydropower as the largest potential domestic source of renewable energy. It currently provides over 3% of the total energy consumption in the United States where the total annual consumption of biomass feedstock for bioenergy and bioproducts together currently approaches 190 million dry tons. This study also found that the combined forest and agriculture land resources (1.3 billion tonnes) have the potential to supply sustainably more than 30% of the US current petroleum consumption for fuels and chemicals.

Starch, a main constituent of biomass, is one of the most abundant renewable organic compounds on Earth, being present in a wide variety of agricultural and staple food wastes such as potatoes, corn, rice, wheat and pasta. Starch comprises 1,4- $\alpha$ -linked glucosyl units in the form of linear, water insoluble amylose (20-25%) and 1,6- $\alpha$ -linked branched, water soluble amylopectin (75-80%).

Strict anaerobes like the clostridia and thermatogales can utilise starch directly. However, the demand on the cells to perform enzymatic hydrolysis limits the rate of H<sub>2</sub> production. By analysing the data of four reviews [9-12] and excluding duplicates, it was determined that fermentations using simple sugars produced H<sub>2</sub> with 3-fold higher specific rates (mmol H<sub>2</sub> [g DW.h]<sup>-1</sup>) than fermentations using complex sugars. The analysis included 19 reports using

complex sugars (starch and cellulose) and 27 reports using simple sugars (glucose, sucrose) with mean values of 4.8 and 14.6 mmol H<sub>2</sub> [g DW.h]<sup>-1</sup>, respectively (t-test, P value: 0.030). Hence, for complex polysaccharides (i.e. sustainable starch resources) to support bio-H<sub>2</sub> production, a pre-fermentation hydrolysis may be advantageous over an in-fermentation hydrolysis.

Hydrolysis can be achieved by several methods including chemical hydrolysis, enzymatic hydrolysis and hydrothermal hydrolysis. Enzymatic hydrolysis of starch is currently the preferred method in industrial use with high hydrolysis yields and mild conditions, although it incurs the costs of enzyme production. Thermostable  $\alpha$ -amylases are highly attractive with high optimal temperatures (60-100 °C) and associated high reactivity [13] but this temperature range (and hence the potential reactivity) is well below that of hydrothermal hydrolysis (see below) while the  $\alpha$ -limit dextrin of amylopectin is inaccessible without the concerted action of a debranching enzyme. Chemical hydrolysis leads to environmental and equipment corrosion problems as well as the costs associated with concentrated acids and post-hydrolysis neutralisation [14,15]. In contrast, hydrothermal hydrolysis is an environmentally benign method that, recently, has been the object of extensive research since the process only requires water and heat [16,17], which could be obtained internally in a waste-to-hydrogen process or externally from other renewable resources.

Hydrothermal hydrolysis using hot compressed water (HCW) is considered an alternative option to thermophilic enzymatic hydrolysis. At high temperatures (180-240 °C) the starch granules swell and burst, the semi-crystalline structure is lost and hydrolysis proceeds. Under these conditions, water possesses very interesting and unique properties which make it a powerful solvent suitable for the solvolysis of complex polysaccharides [18]. It has been demonstrated that at least 93% of starch is converted to soluble products at temperatures ranging from 180 to 220 °C under various conditions [17,19]

However, at temperatures above 200 °C the degradation of sugars to other compounds, mainly 5-hydroxymethylfurfural (5-HMF) and furfural, is unavoidable. These compounds, when present in the hydrolysate, are potent inhibitors of growth and fermentation and, therefore, should be removed [20]. Activated carbon (AC) has been tested as an effective approach for this purpose [21-23]. This is also attractive since AC can be derived from biomass char, a low value by product of the thermochemical conversion of biomass by pyrolysis.

Starch may be contained in various biomasses and the conditions of hydrolysis require optimisation specific to each biomass (depending mainly on its composition) to maximise sugar yields at the lowest possible temperature, to minimise heating cost and sugar decomposition.

This study investigated hydrolysis in HCW in the presence of CO<sub>2</sub>. The addition of CO<sub>2</sub> into HCW hydrolysis was shown to enhance the yield of sugars from starch [24] and to reduce the concentrations of organic acids (fermentation inhibitors) in lignocellulose hydrolysates [25]. This effect was attributed to the action of CO<sub>2</sub> as an acid catalyst [26] unlike traditional acids CO<sub>2</sub> is extremely benign as it can be largely neutralised by the release of reactor pressure [25].

Table 1 summarises the five previous studies on starch hydrolysis in HCW, with and without CO<sub>2</sub>, showing that previous reactors had very small volumes (3-80 ml). This small volume enabled the precise control of reaction conditions with rapid heating and cooling through bath techniques, which would not be efficient at large scale because of limited heat transfer.

Rapid heating and cooling is advantageous as it minimises the degradation of monosaccharides and associated formation of degradation products (furans, phenolics and organic acids). Sugar degradation occurs rapidly at temperatures above 100 °C particularly in the presence of acids or amines [29], whereas starch hydrolysis occurs above 200 °C [19]. Therefore, cooling time should be minimised because very little starch hydrolysis occurs in this phase, whereas the degradation of formed sugars continues.

The practicality of rapid heating and cooling decreases with increasing reactor size and the reactors required for practical application will be much larger than those studied to date (Table 1). Therefore, the fermentability of hydrolysates is a direct consequence of reactor size. For practical application, the technique must be scaled up and the consequences for practical process control require assessment. This study investigates the byproduct formation and fermentability of starch hydrolysates using a larger HCW/CO<sub>2</sub> reactor than any reported previously (250 ml) and unlike previous studies the results can be extrapolated to practical scale because of the non-bath type heating mechanism employed.

To evaluate the effectiveness of starch hydrolysis in HCW/CO<sub>2</sub> the fermentability of starch hydrolysates produced under a range of conditions, was assessed by the anaerobic fermentation of *E. coli* HD701 (an MC4100 derivative derepressed for formate hydrogenlyase) [30] as a convenient model organism to indicate fermentability.

The objective of this study was to test the effectiveness and viability of fermentable hydrolysate production from starch using hydrolysis in HCW/CO<sub>2</sub>. Starch functions as a model system prior to extension of the approach to enable the effective use of lignocellulosic biomass as fermentation precursors. The hydrolysis of starch in HCW/CO<sub>2</sub> was examined at concentrations between 40-200 g.L<sup>-1</sup> in a 250 mL batch reactor which, as far as the authors are aware, is the largest reactor of this type reported for starch hydrolysis representing an important step towards scale-up of this technology. We also describe the consequences of scale-up for the practical control of reaction conditions, report the effects on product distribution and evaluate the product for its suitability as an *E. coli* fermentation substrate.

## 2. Materials and Methods

### 2.1. Materials.

All chemicals were analytical grade from (Sigma-Aldrich) and were used without purification. The activated carbon (AC) was colorsorb 5 steam activated powder from JACOBI (micropore, 0.19 cm<sup>3</sup>.g<sup>-1</sup>; mesopore, 0.37 cm<sup>3</sup>.g<sup>-1</sup>; macropore, 1.68 cm<sup>3</sup>.g<sup>-1</sup>; total surface area: 900 m<sup>2</sup>.g<sup>-1</sup>). *E. coli* HD701 was provided kindly by Prof. F. Sargent (University of Dundee).

### 2.2. Use of hot compressed water (HCW) for starch hydrolysis

The batch reactor system for starch hydrolysis is shown in Figure 1, comprising a 250 mL reactor (Parr series 4570/80 HP/HT) made of alloy C-276 and equipped with a heat/agitation controller (model 4836) and a cooling system (Grant LTD6/20). Temperature and pressure were measured from inside the reactor to within 1 bar and 0.1 K.

For hydrolysis, starch (5 g from potato powder) was suspended in de-ionized water to a final reactant volume of 125 mL (40 g.L<sup>-1</sup>) or as otherwise stated and charged into the reactor for hydrolysis. This left a head space of about 120 mL. The reactor was sealed and purged with CO<sub>2</sub> (3 min) with agitation (850 rpm) before pressurising to 30 bar with CO<sub>2</sub> and heating to the set-point temperature. The reaction parameters are shown in Table 2. Reaction conditions were held for 15 min before cooling down to 100 °C by circulating water at 4 °C through the reactor internal cooling loop (ID 0.8 cm) at a flow rate of 900 cm<sup>3</sup>.min<sup>-1</sup>. Next, the reactor was removed from the heating surround and quenched in an ice-water bath. The reactor was depressurized and the products were recovered by washing out with 20-40 mL of de-ionized water. The hydrolysate was separated from solid residue by vacuum filtration through two layers of filter paper (Fisherbrand QL100); hydrolysates and samples were kept at -20 °C for analysis. The residue was dried at 60 °C and weighed. It is important to note that

after cooling some precipitate formed in some of the hydrolysates, this precipitate was removed by filtration and was not quantified.

Hydrolysate samples were analysed for organic acids (OA) by anion HPLC using a Dionex 600-series system [31] and sugars and 5-HMF by HPLC (Agilent 1100 series) equipped with on-line degasser, quaternary pump, auto-sampler and RI detector (1200 series). The column was a Resex-RCM (Phenomenex) equipped with a security column guard with the same stationary phase as the column. Sample injection was 20  $\mu\text{L}$ ; mobile phase: HPLC  $\text{H}_2\text{O}$  (Sigma); flow rate: 0.5  $\text{mL}\cdot\text{min}^{-1}$ ; 40 min experiment time. Column temperature was 75  $^\circ\text{C}$ . RI detector was at 40  $^\circ\text{C}$ . The total organic carbon (TOC) of hydrolysates was measured using a TOC analyser (Model TOC 5050A, Shimadzu Co., Japan).

### *Detoxification*

The hydrolysate was treated with 5% (w.v aq.<sup>-1</sup>) AC powder (except where otherwise stated) at 60  $^\circ\text{C}$  for 1 h with agitation at 180 rpm as described by Hodge *et al.* (2009) [21]. The treated hydrolysates were vacuum-filtered through filter paper (Fisherbrand QL100). Hydrolysates and samples were kept at -20  $^\circ\text{C}$  for tests and analysis.

### *2.4 Fermentation*

The effectiveness of the AC treatment and the efficacy of the hydrolysates as fermentation feedstocks was evaluated. Small fermentation tests were performed using 60 mL glass serum bottles leaving 75% of volume for gas space and 25% for culture media (15 mL). The bottles were sealed (10 mm butyl rubber stoppers). The initial pH was standardised to pH 6.5 ( $\pm 0.1$ ) with NaOH/ $\text{H}_2\text{SO}_4$ ; additions for pH adjustment were negligible. Stocks of *E. coli* HD701 were maintained at -80  $^\circ\text{C}$  in 75% (w.v aq.<sup>-1</sup> glycerol), and revived by plating on nutrient agar (Oxoid) and incubating overnight (30  $^\circ\text{C}$ ). Colonies were picked from the plates into 5 mL vials of nutrient broth solution (Fluka) with added sodium formate (0.5% w.v aq.<sup>-1</sup>) pH 7 (NBF8) and incubated for 6 h at 30  $^\circ\text{C}$ , 180 rpm for pre-culture. Cultures (inocula 10  $\mu\text{L}$  of sample equivalent to 0.001% inoculum) were grown in 2 L sterile Erlenmeyer flasks containing 1 L of the same medium; flasks were incubated at 30 $^\circ\text{C}$ , 180 rpm, 16 h. Cell pellets were obtained by centrifugation (Beckman J2-21M/E centrifuge at 7500 rpm, 10 min, 20  $^\circ\text{C}$ ), washed twice in 200 mL phosphate buffered saline (PBS: 1.43 g  $\text{Na}_2\text{HPO}_4$ , 0.2 g  $\text{KH}_2\text{PO}_4$ , 0.8 g NaCl, 0.2 g KCl.L<sup>-1</sup>, pH 7.0) and then re-suspended in 25 mL of PBS with their concentration measured using a UV/visible spectrophotometer Ultrospec 3300 pro. The cells' concentration was estimated by optical density using a previously-determined conversion factor;  $\text{OD}_{600} 1 = 0.482 \text{ g dry weight}\cdot\text{L}^{-1}$ .

Reaction bottles for fermentation tests contained 10 mL of sterile medium consisting of Bis-Tris buffer (0.1 M) and Na<sub>2</sub>SO<sub>4</sub> (0.0435 M; pH 6.5) and 5 mL of hydrolysate (filter sterilized) or glucose control (60 mM). Bottles were sealed using butyl rubber stoppers and made anaerobic by purging with N<sub>2</sub> for at least 30 min. 0.5-1 mL of the cell suspension was added to give a final cell concentration of 1 g dry weight.L<sup>-1</sup>, before purging for a further 3-5 min.

Reaction bottles were incubated at 30 °C (180 rpm for 20 h). The identity of H<sub>2</sub> as the sole combustible gas present was confirmed using a ThermoQuest gas chromatograph (TraceGC2000) with a Shimadzu shincarbon-ST column and thermal conductivity detector. Routine measurement of H<sub>2</sub> concentration was performed using a combustible gas meter (Gasurveyor2, GMI), intermittently cross-validated by GC. Averages of 3 samples were converted using a linear calibration ( $R^2 > 0.99$ ). The measured concentration of H<sub>2</sub> ( $y$ ) was used to determine the volume of H<sub>2</sub> produced ( $x$ ), using equation 1.

$$y = x/(ax + h) \therefore x = hy/(1 - ay) \text{ (equation 1)}$$

Where:

$y$ , [H<sub>2</sub>] in headspace (v.v<sup>-1</sup>);

$x$ , H<sub>2</sub> produced (mL);

$h$ , headspace volume (mL)

$a$ , the ratio of total gas produced to H<sub>2</sub> produced.

$a$  was close to 2 in these tests as confirmed by GC. This is as expected from the known pathways of mixed acid fermentation in which H<sub>2</sub> and CO<sub>2</sub> arise exclusively from the cleavage of formate : HCOOH → H<sub>2</sub> + CO<sub>2</sub> [32]. Therefore H<sub>2</sub>:CO<sub>2</sub> is initially 50:50;  $a=2$ . Two factors may influence  $a$  to be slightly different from 2. H<sub>2</sub> is oxidised by uptake hydrogenases but their influence is slight as shown by H<sub>2</sub> production tests of uptake hydrogenase-negative mutants [7] under conditions analogous to this study. There may also be a slight loss of CO<sub>2</sub> as part of the minor succinate formation pathway.

The variable addition of cell concentrate used in independent experiments and its minor effect on headspace volume was accounted for.

### 3. Results and Discussion

#### 3.1. Hot Compressed Water (HCW) hydrolysis

Experiments were repeated twice and average values are reported. The worse case error was within 10%. Table 2 shows that the pH of the post-reaction solution (pH<sub>f</sub>) decreased from the initial value of 7.0 (± 0.2) in most cases. The slight increase in pressure

after the reactions may be an indication that some gasification of the products occurred (Table 2). Conversions of starch into hydrolysis products ( $X_h$ ) were close to 100% in all cases, with a modest decrease with increasing temperature to a minimum value of 90% at 235 °C. Gas and residue were not analysed.

The incorporation of  $\text{CO}_2$  in the HCW reactions enhances the yield of monosaccharides [24]. Each type of polysaccharide requires different optimal reaction conditions. Miyazawa reported a 14-fold increase in the glucose yield when solid  $\text{CO}_2$  was included at a level of  $9 \text{ g CO}_{2(\text{s})} \cdot \text{g starch}^{-1}$  for starch hydrolysis at 200 °C and 15 min [24]. In order to better simulate the functioning of a large scale system, the present apparatus used gaseous  $\text{CO}_2$  and a maximum input of  $1.4 \text{ g CO}_{2(\text{g})} \cdot \text{g starch}^{-1}$ . In experiments carried out with cellulose (Orozco RL; unpublished) it was found that the addition of  $\text{CO}_2$  at this level enhanced the yield of glucose ~1.5-fold compared to a  $\text{N}_2$  control at 250 °C for 15 min (optimal parameters for hydrolysis of cellulose) and this level of  $\text{CO}_2$  incorporation was adopted in the current study.

The heating and cooling rates have a strong influence on decomposition and product distribution. Larger reactors, such as the one used in this work, cannot achieve instant temperature changes. It is important, therefore, to study the product distribution under different conditions and realistic profiles of heating and cooling. Other studies on the hydrothermal degradation of polysaccharides (Table 1) used small batch reactors (total volume ~ 3.3-3.6 mL) heated rapidly from room temperature up to 200 °C by immersion in a molten salt bath maintained at constant temperature giving a heat-up period of about 2 min included in the reaction time for reaction completion. The reactor was quenched in cold water [19,27,33,34].

The heating and cooling profiles of the HCW system in this study are shown in Figure 2 with different set maximum temperatures; note that the reaction times including the heat-up (from 50 °C) and cool-down (to 50 °C) periods are within the range of 37-60 min, with corresponding average heating and cooling rates between 7-9 °C.  $\text{min}^{-1}$ . A hold time of 15 min at the set-point temperature was selected based on previous studies made on HCW hydrolysis of starch [17,24] and parallel studies here on cellulose using the same reactor system (Orozco RL; unpublished).

Figure 3 shows the product yield distribution with temperature after hydrolysis but before AC treatment. Glucose was the main product identified by HPLC in the hydrolysate followed by 5-HMF. Maltose and lower concentrations of fructose, mannose, galactose were observed. The yield of glucose increased with temperature, reaching its highest value

(0.548 [g C. (g C in starting starch)<sup>-1</sup>]) at 200 °C and then decreased, reaching minimal levels at 235 °C. The other sugars exhibited similar behaviour but 5-HMF the main inhibitory product, which results from the thermal degradation of sugars, reached its maximum yield (~ 0.3 [g C. (g C in starting starch)<sup>-1</sup>] 30% carbon basis) at 220 °C.

Hydrolysates produced at 180 °C contained almost no sugars or 5-HMF but nevertheless had a TOC value similar to the maximum obtained, due to the presence of dextrans from partial starch hydrolysis, which was confirmed by Agilent HPLC (see Materials and Methods) with reference to a maltodextrins from potato starch standard (Sigma-Aldrich 419699; dextrose equivalent: 16.5-19.5). The relatively low fermentability observed for hydrolysates obtained at 180 °C (Figure 5) suggests that the majority of these short-chain polysaccharides were in branched forms, which (unlike linear maltodextrins) cannot be utilised by *E. coli* as it lacks a debranching enzyme [35].

The maximum sugar yield obtained (at 40 g starch.L<sup>-1</sup>, 200 °C) was very similar to yields reported previously using smaller reactors (Table 1). Therefore, the level of CO<sub>2</sub> used in the present work was effective in promoting hydrolysis but may have also enhanced the formation of 5-HMF as reported in previous studies [24-26]. Based on these results, HCW hydrolysis of starch at concentrations of 120 and 200 g.L<sup>-1</sup> were performed at an optimal temperature of 200 °C.

In addition to sugars, 5-HMF and minor products, organic acids (OA), which are decomposition products of glucose and fructose, were found in the hydrolysate in very small concentrations at starch concentration of 40 g.L<sup>-1</sup> and 200 °C. Butyric acid and acetic acid were the main OA produced (Table 3). OA yields at higher concentrations of starch were negligible which indicates insignificant degradation of 5-HMF and furfural at 200 °C.

The removal of toxic hydrolysis products by the treatment of hydrolysates with AC proved to be very effective. The concentrations of all sugars were relatively unaffected by AC treatment whereas significant removal of 5-HMF (Figure 4) and OA (Table 3) was observed.

It is noteworthy that the yield of hydrolysis products in HCW can be affected by leaching of the reactor material or nickel alloy [36,37] however these were not evaluated. TOC analysis before and after AC treatment (Table 4) indicated high extents of C removal, of which up to 85% was through the elimination of 5-HMF. This confirms that the pore structure of the AC used in this work was appropriate [12]. The 5-HMF retention capacity of the AC was in the range 0.033-0.096 g 5-HMF.[g AC]<sup>-1</sup>. For comparison, 0.06-0.12 g [g AC]<sup>-1</sup> was reported previously [21]. Furfural, was found in preliminary work,

to be at least 10-fold lower in concentration than 5-HMF, was removed by AC treatment and was not considered further.

### 3.2 Fermentation of starch hydrolysates and biohydrogen production

Figure 5 shows H<sub>2</sub> production and yields in fermentability tests using AC-treated and untreated hydrolysates from the HCW/CO<sub>2</sub> hydrolysis of starch (40 g.L<sup>-1</sup>). AC treated hydrolysates showed higher H<sub>2</sub> production than their untreated counterparts which demonstrated the effectiveness of the AC treatment in the removal of inhibitors for *E. coli* HD701. Hydrolysates made at (180, 220 or 235 °C; AC treated) contained 1.5, 53 and 6 mM glucose respectively (diluted 1/3 in fermentability tests to 0.5, 17.7 and 2 mM; initial glucose concentration) and glucose was completely consumed in the cases where H<sub>2</sub> was produced (Figure 5). Hence, H<sub>2</sub> production was limited by both substrate availability and by the influence of degradation products (DPs).

However, the hydrolysate made at 200 °C (AC treated), contained 106 mM glucose (35.3 mM in fermentability test; an excess of 15.3 mM compared to glucose control), leaving residual unused glucose after H<sub>2</sub> production. The initial substrate concentration is not critical in *E. coli* fermentations but due to the limited buffering capacity of the test medium, pH limitation occurred when the initial glucose was in excess of ~ 20 mM. This arose using hydrolysates made using higher starch loadings during hydrolysis (Table 5) and, in these cases, H<sub>2</sub> production was affected only by DPs.

The removal of 5-HMF was complete when starch was hydrolysed at a concentration of 40 g.L<sup>-1</sup> but at 120 g.L<sup>-1</sup> and 200 g.L<sup>-1</sup>, 5.2 mM and 15.9 mM 5-HMF persisted, respectively. As shown in Table 5, the hydrolysate glucose concentration increased with the initial starch loading but the H<sub>2</sub> yield decreased, suggesting inhibition by residual DPs. The hydrolysates were, therefore, diluted with deionised water to provide 20 mM glucose, leaving 0.33 mM 5-HMF and 0.6 mM 5-HMF, respectively. H<sub>2</sub> yields from diluted hydrolysates were indistinguishable from the glucose control and unrelated to the initial starch loading. Therefore, dilution minimised the impact of persistent inhibitory DPs in these hydrolysates and further AC treatment would be required at scale.

The maximum theoretical H<sub>2</sub> yield in *E. coli* is 2 mol H<sub>2</sub>.mol hexose<sup>-1</sup> [31]. Therefore, the observed yields represent about 19% (including the glucose control). The fermentability tests used here provided a rapid, high throughput screening of hydrolysates for the investigation of hydrolysis conditions, but provided sub-optimal fermentation conditions (inconstant pH, end product accumulation, fixed volume, poor mixing), to which the low conversions are attributed. The conversion of glucose to H<sub>2</sub> by *E. coli* in sophisticated

fermentation systems is well described and yields of close to 100% have been independently reported [38, 39] and also observed by the authors [40,41].

A detailed evaluation of the energy demand of HCW hydrolysis, within a waste-to-hydrogen process, indicated that the energy requirement of HCW would be ~10-20% of the electrical energy recoverable from bio-H<sub>2</sub> production (Redwood, Orozco and Macaskie, unpublished); this will be reported in full with reference to real wastes in a subsequent publication.

## 5. Conclusions

Hot compressed water (HCW) with CO<sub>2</sub> is an effective and potentially scalable method for starch hydrolysis. Detoxified hydrolysates from a 250 ml scale system here utilising scalable components (electric furnace and gaseous CO<sub>2</sub>) were equal in fermentability to pure glucose for *E. coli* HD701. Therefore, a production scale HCW/CO<sub>2</sub> system of similar design could be expected to support *E. coli* fermentations as a sustainable alternative to refined glucose.

The relatively large reactor used here (see Table 1) showed similar yields to smaller systems indicating that hydrolysis in HCW/CO<sub>2</sub> have the potential for large scale practical application. The optimum temperature for starch hydrolysis in HCW/CO<sub>2</sub> was 200 °C. Glucose was the main product with a yield of 548 g.kg<sup>-1</sup> starch which is very similar to the previous reports (Table 1). This shows that the relatively low CO<sub>2</sub> levels employed here using methods applicable at scale were sufficient and not limiting to starch hydrolysis. The generation of 5-HMF, however, was about 4-fold higher than in the previous reports, possibly due to the presence of CO<sub>2</sub> and the longer heating and cooling times associated with larger reaction volumes. AC treatment was effective in the selective removal of 5-HMF with an adsorption capacity in the range of 33-96 [mg 5-HMF (g AC)<sup>-1</sup>]. Under the selected conditions up to 86% of the carbon removed from the hydrolysate by AC was attributable to 5-HMF loss and typically furfural (representing up to 10%) was largely removed. As a consequence, fermentations of the treated hydrolysates produced more than 70% more H<sub>2</sub> than untreated controls at optimum HCW conditions. At temperatures above 200 °C, noteworthy H<sub>2</sub> production occurred only with AC treated hydrolysates (Figure 5) but further detoxification was required for hydrolysates after hydrolysis with more than 40 g.L<sup>-1</sup> starch (Table 5).

The fermentability of hydrolysates (obtained at 40 g.L<sup>-1</sup> starch, 200 °C) was the same as glucose controls. At higher initial starch concentrations it was possible to produce

hydrolysates with glucose concentration of up to 536 mM but additional detoxification was required to produce H<sub>2</sub> at the same level as pure glucose. This demonstrates that *E. coli* could adapt well to lower concentrations of other inhibitors and that dilutions improved the fermentability of the hydrolysate. This finding has a significant impact for reactor system utilisation efficiency and productivity. Future work will aim to further up-scale HCW while retaining optimum bio-conversion of starch to H<sub>2</sub>.

## 6. Acknowledgements

The financial support of the EPSRC (Grant Nos EP/D05768X/1 and EP/E034888/1), BBSRC (Grant Nos BB/C516195/2 and BB/E003788/1), the Royal Society (Industrial Fellowship to LEM), Advantage West Midlands (Grant ref. POC46) and the Government of Mexico (studentship no. 203186) to RLO is acknowledged, with thanks. We thank: for technical support, Combined Workshop, School of Biosciences, University of Birmingham, UK; For *E. coli* strains, Prof Frank Sargent, University of Dundee and for activated carbon, John Lever, JACOBI.

## References

- [1] Mandal TK, Gregory DH. Hydrogen: a future energy vector for sustainable development. *J Mech Eng Sci* 2009; 224:539-58.
- [2] Blanchette Jr S. A hydrogen economy and its impact on the world as we know it. *Energy Policy* 2008; 36: 522-30.
- [3] Lee D-H, Lee D-J. Biofuel economy and hydrogen competition. *Energy & Fuels* 2008; 22:177-81.
- [4] Tseng P, Lee J, Friley P. A hydrogen economy: opportunities and challenges. *J of Energy* 2005; 30:2703-20.
- [5] Tillmetz W and Bünger U. Development status of hydrogen and fuel cells-Europe. In: Stolten D and Grube T (Eds.): 18th World Hydrogen Energy Conference 2010 - WHEC 2010. Proceedings of the WHEC, May 16-21 2010, Essen. p.21-30
- [6] HyWays. European Hydrogen Energy Roadmap - Assumptions and final results. Posted 22 Feb 2008. Accessed 16 June 2011. At [http://www.hyways.de/docs/Brochures\\_and\\_Flyers/HyWays\\_Roadmap\\_FINAL\\_22Feb2008.pdf](http://www.hyways.de/docs/Brochures_and_Flyers/HyWays_Roadmap_FINAL_22Feb2008.pdf)
- [7] Redwood MD, Paterson-Beedle M, Macaskie LE. Integrating dark and light bio-hydrogen production strategies: towards the hydrogen economy. *Rev in Environ Science Biotechnol* 2009; 8:149-85.
- [8] Perlack RD, Wright LL, Turhollow AF, Graham RL, Stokes BJ, Erbach DC. Biomass as feedstock for a bioenergy and bioproduct industry: The technical feasibility of a billion-ton annual supply - Technical Report Number A357634; 2005.
- [9] Das D, Veziroglu TN. Hydrogen production by biological processes: a survey of Literature. *Int J Hydrogen Energy* 2001; 26:13-28.
- [10] Wang CC, Chang CW, Chu CP, Lee DJ, Chang BV, Liao CS. Producing hydrogen from wastewater sludge by *Clostridium bifermentans*. *J Biotechnol* 2003; 102:83-92.

- [11] Kapdan IK, Kargi F. Bio-hydrogen production from waste materials. *Enz Microb Technol* 2006; 38: 569-82.
- [12] Hawkes FR, Hussy I, Kyazze G, Dinsdale R, Hawkes DL. Continuous dark fermentative hydrogen production by mesophilic microflora: Principles and progress. *Int J Hydrogen Energy* 2007; 32:172-184.
- [13] Prakash O, Jaiswal N.  $\alpha$ -Amylase: An ideal representative of thermostable enzymes. *Appl Biochem Biotechnol* 2010; 160:2401-14.
- [14] Lee J-H, Choi H-W, Kim B-Y, Chung M-S, Kim D-S, Choi SW et al. Nonthermal hydrolysis using ultra high pressure: I. Effects of acids and starch concentrations. *Sci Technol* 2006; 39: 1125-32.
- [15] Tasic MB, Konstantinovic BV, Lazic ML, Veljkovic VB. The acid hydrolysis of potato tuber mash in bioethanol production. *Biochem Eng J* 2009; 43: 208-11.
- [16] Kamio E, Takahashi S, Noda H, Fukuhara C, Okamura T. Liquefaction of cellulose in hot compressed water under variable temperatures. *Ind Eng Chem Res* 2006; 45:4944-53.
- [17] Nagamori M, Funazukuri T. Glucose production by hydrolysis of starch under hydrothermal conditions. *J Chem Technol Biotechnol* 2004; 79:229-33.
- [18] Kruse A, Dinjus E. Hot compressed water as reaction medium and reactant: Properties and synthesis reactions. *J Supercrit Fluids* 2007; 39:362-80.
- [19] Miyazawa T, Ohtsu S, Funazukuri T. Hydrothermal degradation of polysaccharides in a semi-batch reactor: product distribution as a function of severity parameter. *J Mater Sci* 2008; 43:2447-51.
- [20] Mills TY, Sandoval NR, Gill RT. Cellulosic hydrolysate toxicity and tolerance mechanisms in *Escherichia coli*. *Biotechnol Biofuels* 2009; 2:26.
- [21] Hodge DB, Anderson Ch, Berglund KA, Rova U. Detoxification requirements for bioconversion of softwood dilute acid hydrolyzates to succinic acid. *Enzym Microb Technol* 2009; 44:309-16.
- [22] Palmqvist E, Hahn-Hägerdal B. Fermentation of lignocellulosic hydrolysates. I: inhibition and detoxification. *Bioresour Technol* 2000; 74:17-24.
- [23] Ezeji T, Qureshi N, Blaschek HP. Butanol production from agricultural residues: Impact of degradation products on *Clostridium beijerinckii* growth and butanol fermentation. *Biotechnol Bioeng* 2007; 97:1460-69.
- [24] Miyazawa T, Funazukuri T. Polysaccharide hydrolysis accelerated by adding carbon dioxide under hydrothermal conditions. *Biotechnol Prog* 2005; 21:1782-85.
- [25] Van Walsum GP, Garcia-Gil M, Chen SF, Chambliss K. Effect of dissolved carbon dioxide on accumulation of organic acids in liquid hot water pretreated biomass hydrolyzates. *Appl Biochem Biotechnol* 2007; 136-140: 301-11.
- [26] Hunter SE, Savage PE. Quantifying rate enhancements for acid catalysis in CO<sub>2</sub>-enriched high-temperature water. *AIChE* 2008; 54: 516-28.
- [27] Miyazawa T, Ohtsu S, Nakagawa Y, Funazukuri T. Solvothermal treatment of starch for the production of glucose and maltooligosaccharides. *J Mater Sci* 2006; 41:1489-94.
- [28] Rogalinski T, Liu K, Albrecht T, Brunner G. Hydrolysis kinetics of biopolymer in subcritical water. *J Supercrit Fluid* 2008; 46: 335-41.
- [29] Ajandouz EH, Desseaux V, Tazia S, Puigservera A. Effects of temperature and pH on the kinetics of caramelisation, protein cross-linking and Maillard reactions in aqueous model systems. *Food Chem* 2008; 107:1244-52.
- [30] Orozco RL, Redwood MD, Yong P, Caldelari I, Sargent F, Macaskie LE. Towards an integrated system for bio-energy: hydrogen production by *Escherichia coli* and use of palladium-coated waste cells for electricity generation in a fuel cell. *Biotechnol Lett* 2010.

- [31] Redwood MD, Macaskie LE. A two-stage, two-organism process for biohydrogen from glucose. *Int J Hydrogen Energy* 2006; 31:1514-21.
- [32] Clark DP. The fermentation pathways of *E. coli*. *FEMS Microbiol Rev* 1989; 63:223-4
- [33] Sakaki T, Shibata M, Miki T, Hirose H. Decomposition of cellulose in near-critical water and fermentability of the products. *Energy Fuels* 1996; 10:684-8.
- [34] Sina A, Kruse A, Rathert J. Influence of the heating rate and the type of catalyst on the formation of key intermediates and on the generation of gases during hydrolysis of glucose in supercritical water in a batch reactor. *Ind Eng Chem Res* 2004; 43:502-8.
- [35] Boos W, Shuman H. Maltose/maltodextrin system of *Escherichia coli*: transport, metabolism, and regulation. *Microbiol Mol Biol Rev* 1998; 62:204-29.
- [36] Antal MJ, Allen SG, Schulman D, Xu X. Biomass gasification in supercritical water. *Ind Eng Chem Res* 2000; 39:4040-53.
- [37] Yu Y, Lou X, Wu H. Some recent advances in hydrolysis of biomass in hot-compressed water and its comparisons with other hydrolysis methods. *Energy Fuels* 2007; 22:46-60.
- [38] Bisaillon A, Turcot J, Hallenbeck PC. The effect of nutrient limitation on hydrogen production by batch cultures of *Escherichia coli*. *Int J Hydrog Energ*, 2006; 31:1504-1508.
- [39] Turcot J, Bisaillon A, Hallenbeck PC. Hydrogen production by continuous cultures of *Escherichia coli* under different nutrient regimes. *Int J Hydrogen Energy* 2008; 33:1465-70.
- [40] Redwood MD, Bio-hydrogen and biomass supported palladium catalyst for energy production and waste minimisation. Ph.D. Thesis. 2007, University of Birmingham.
- [41] Redwood MD, Orozco RL, Majewski A and Macaskie LE. Biohydrogen production by extractive fermentation and photofermentation. Proceedings of the World Hydrogen Technologies Convention, Glasgow, 14<sup>th</sup>-16<sup>th</sup> Sept 2011 (in press).

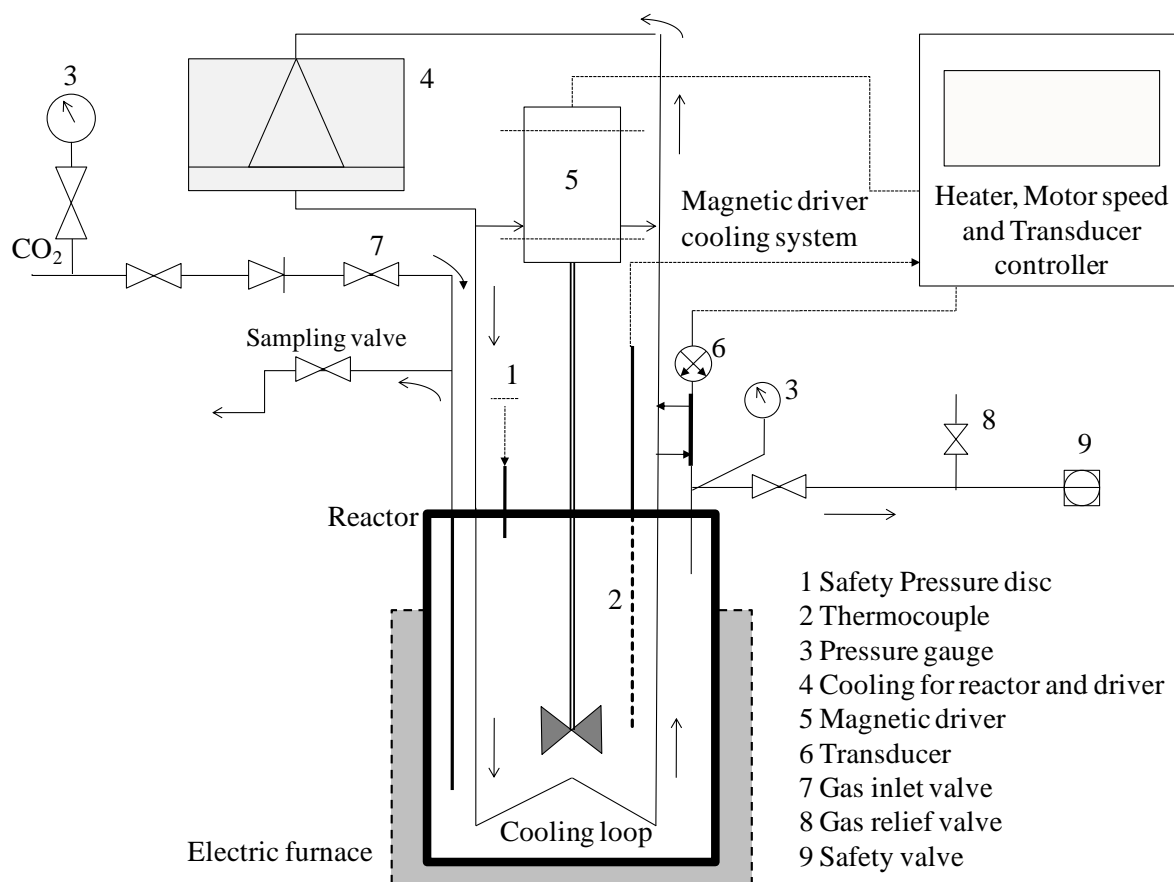


**Figure 1.** Batch reactor system for HCW hydrolysis. Arrows show direction of flow of CO<sub>2</sub>, coolant or sample.

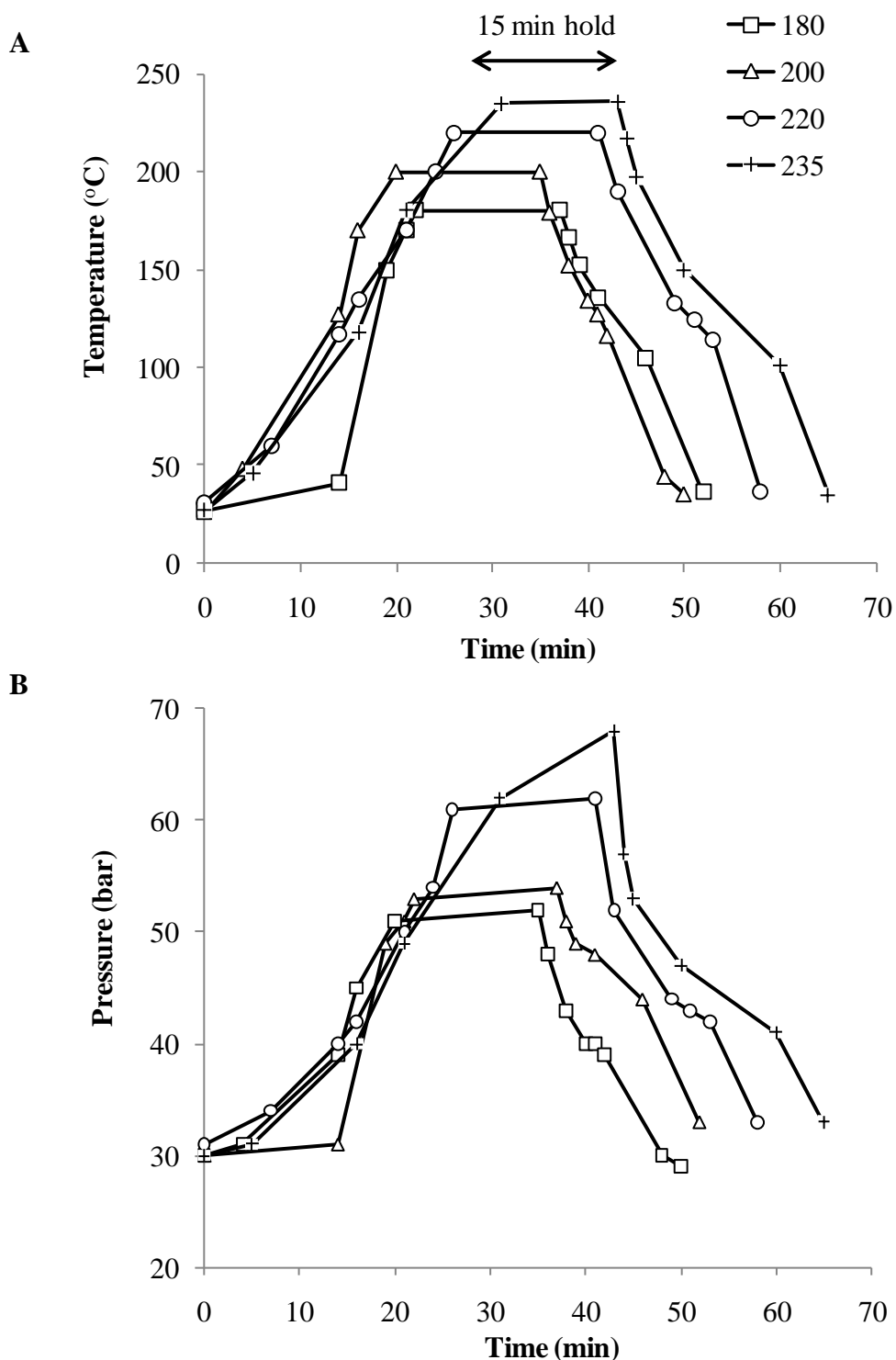


**Figure 2.** a) Reaction heating and cooling pathways; b) Pressure pathways at corresponding temperatures: (□) 180 °C, (△) 200 °C, (○) 220 °C and (+) 235 °C. 1 bar = 100 kPa. Reactions were performed in sequence from the lowest to the highest temperature. As a result, the temperature of the electric heating jacket was lower in the first reaction (180 °C) compared to the following reactions, resulting in ~5 min delay to reach 40 °C for the first reaction. Above 40 °C, the heating rate was consistent among experiments. Therefore, this delay was not considered to impact on the final products.

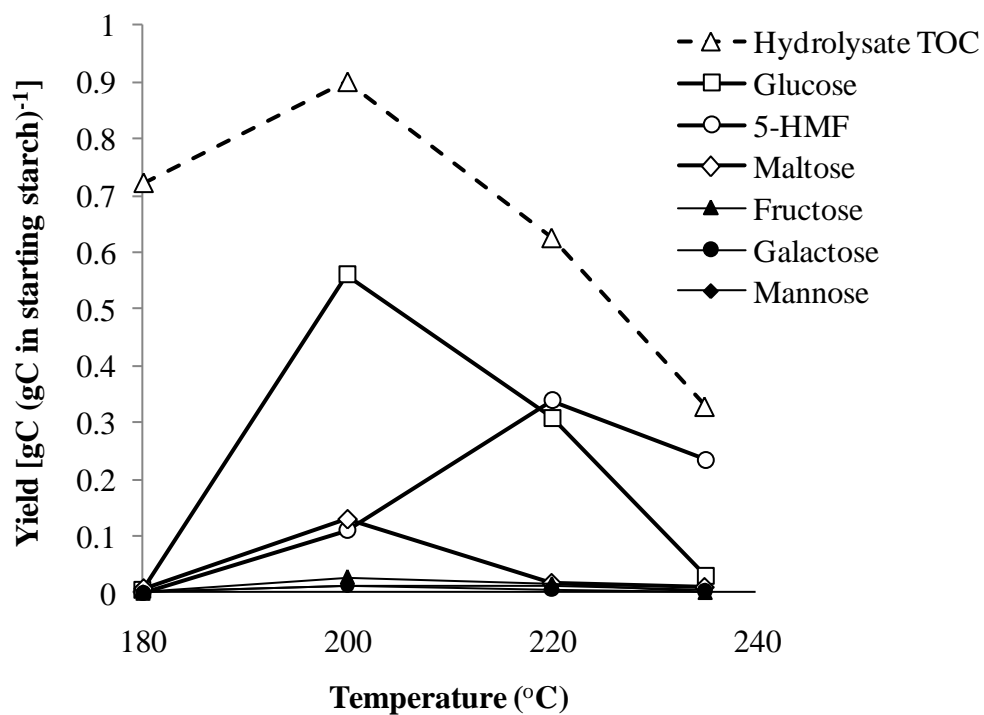


**Figure 3.** Product yield vs temperature before AC treatment. Hydrolysate values were calculated as a ratio of individual TOC in hydrolysate vs. TOC in starting starch. Symbols: ( -  $\Delta$  - ) hydrolysate TOC; ( -  $\square$  - ) glucose; ( -  $\diamond$  - ) maltose; ( -  $\circ$  - ) 5-HMF; ( -  $\blacktriangle$  - ) fructose; ( -  $\bullet$  - ) galactose; ( -  $\blacklozenge$  - ) mannose.

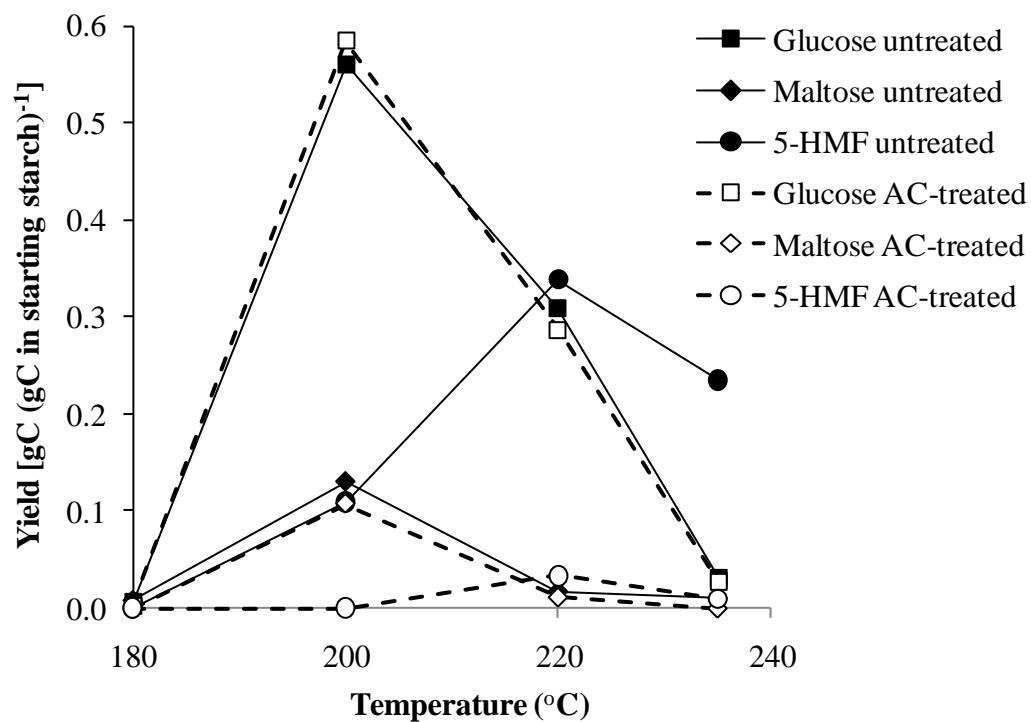


**Figure 4.** Product yield of main sugars in hydrolysates before (solid lines) and after (dashed lines) AC treatment. Values reported are mean of 2 experiments, variation was within 10%.

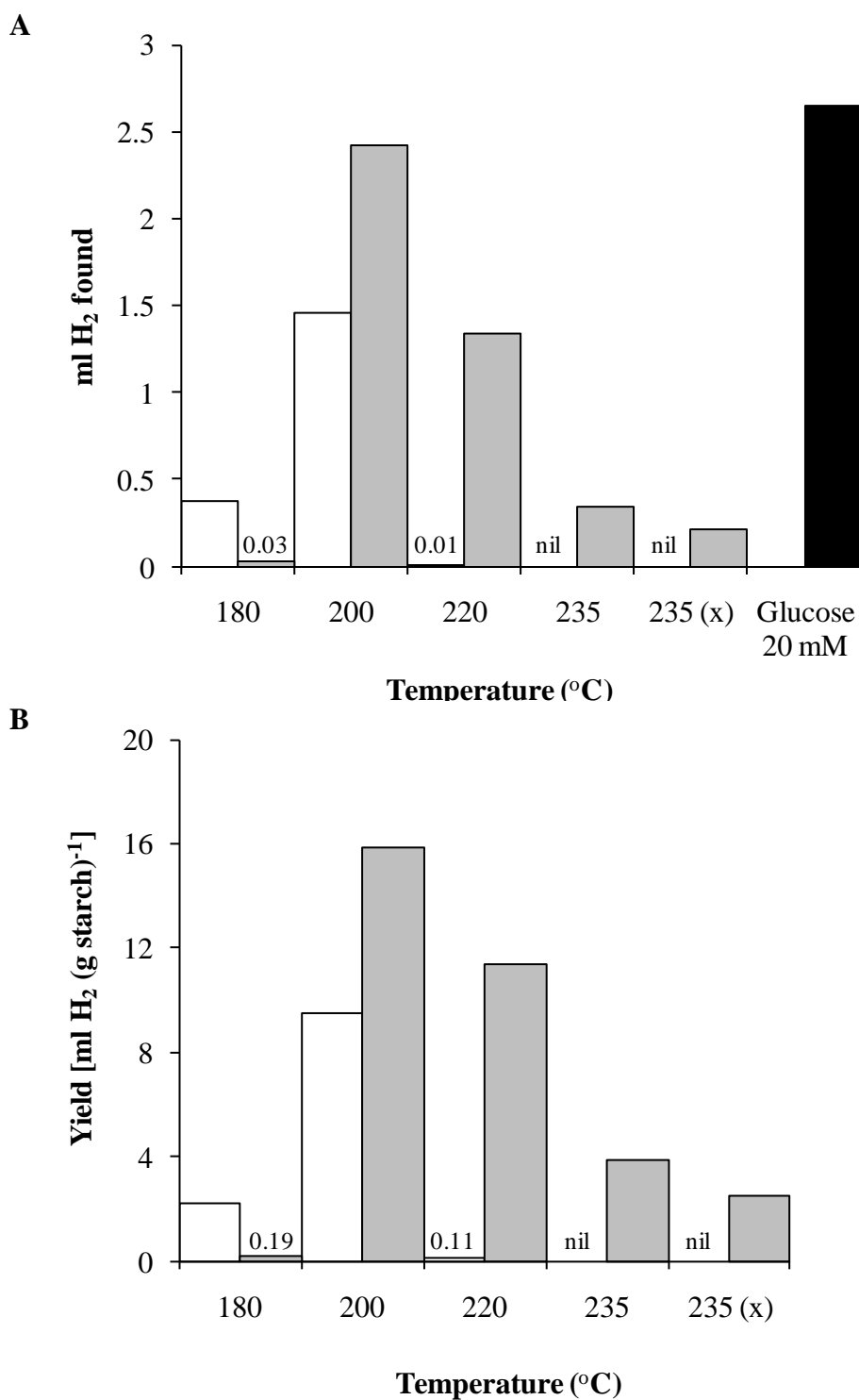


**Figure 5.** H<sub>2</sub> production from hydrolysate vs. hydrolysis temperature and AC treatment in small fermentability tests; a) mL H<sub>2</sub>; b) yield [mL H<sub>2</sub> (g starch)<sup>-1</sup>]. White bars represent hydrolysates before AC treatment; grey bars represent values after AC treatment (5% w.v aq<sup>-1</sup>) except 235 °C (x), where 7.5% AC was used instead of 5% in an attempt to remove more inhibitors and improve H<sub>2</sub> production. The black bar represents pure glucose (20 mM in fermentability test) as a positive control. . Data represent the mean of 2 experiments, variation was within 11%.

**Table 1.** Previous studies on starch hydrolysis in hot compressed water with carbon dioxide (HCW/CO<sub>2</sub>)

Reactor volume (type)	CO <sub>2</sub>	Heating method	Yield (% C to sugar)	Source
3.3 ml (batch)	No	Molten salt bath	~63 %	[17]
3.6 ml (batch)	Yes	Molten salt bath	~53 %	[24]
33.28 ml (batch)	No	Molten salt bath	~43.8 %	[27]
80 ml (batch)	Yes	Sand bath	NA	[25]
Pipe, 3 mm ID (continuous)	Yes	Water bath	NA	[28]
250 ml (batch)	Yes	Electrical furnace.	~55 %	This study

**Table 2.** Reaction parameters for hydrolysis of starch at various concentrations

Initial starch concentration	Temp (°C)	P <sub>f</sub> (bar)	pH <sub>f</sub>	X <sub>h</sub> %	Glucose yield g C (g C in starting starch) <sup>-1</sup>
40 g/L	180	34	3.7	99.9	0.002
	200	32	3.2	99.8	0.548
	220	33	2.8	97.8	0.287
	235	31	3.0	90.4	0.027
120 g/L	200	32	2.8	99.3	0.608
200 g/L	200	33	2.8	99.3	0.628

Initial pH was 7.0 (± 0.2) and initial pressure was 30 (± 1) bar for all experiments. P<sub>f</sub>: final pressure; pH<sub>f</sub>: final pH; X<sub>h</sub>: Starch conversion into soluble hydrolysis products. X<sub>h</sub> was calculated according to:  $X_h = (S - R)/S$  where S = Initial starch (g); R = Residue after the reaction (g).

**Table 3.** Yield of organic acids from starch hydrolysis

[Starch]	40 g.L <sup>-1</sup>	
Organic acid	BAC	AAC
Lactic	0.0013	0.0006
Acetic	0.0041	0.0021
Formic	0.0019	0.0007
Butyric	0.0063	0.0014

Organic acid (OA) yields in [g C. (g C in starting starch)<sup>-1</sup>] in starch hydrolysates obtained at 40 g starch.L<sup>-1</sup> at 200 °C before (BAC) and after (AAC) activated carbon (AC) treatment (5% w.v aq.<sup>-1</sup>). OA yields at starch concentrations of 120 and 200 g.L<sup>-1</sup> were negligible

**Table 4.** Removal of 5-HMF from hydrolysates by activated carbon.

Starch in hydrolysis g.L <sup>-1</sup>	Maximum AC Temp °C	AC loading g.L <sup>-1</sup>	Before AC		After AC		5-HMF removed	
			TOC g.L <sup>-1</sup>	5-HMF mM	TOC g.L <sup>-1</sup>	5-HMF mM	g (g AC) <sup>-1</sup>	% of removed C
40	180	50	8.9	0.0	3.2	0.0	0.000	0.0
	200	50	11.1	13.0	7.6	0.0	0.033	26.8
	220	50	7.7	40.5	4.6	4.0	0.092	84.7
	235	50	4.1	28.1	1.2	1.2	0.068	68.1
	235	100	4.1	28.1	0.5	0.0	0.035	56.8
120	200	50	34	42.3	30.9	5.2	0.093	86.1
200	200	75	55	73.0	43.4	15.9	0.096	35.4

Before AC, TOC values represent the carbon that remained soluble in the hydrolysate, which included 5-HMF; after AC, 5-HMF and other organic compounds such as organic acids and sugars (less than 5 %) were removed affecting the TOC content. The last two columns show the mass of 5-HMF removed mass of AC used in the treatment and as a % of the removed carbon from the hydrolysate.

**Table 5.** Effective HCW hydrolysis conditions, glucose yields and H<sub>2</sub> production.

Starch in hydrolysis (g.L <sup>-1</sup> )	Undiluted hydrolysates			Diluted hydrolysates		
	Glucose in fermentability test (mM)		Yield (mol H <sub>2</sub> /mol glucose consumed)	Glucose in fermentability test (mM)		Yield (mol H <sub>2</sub> /mol glucose consumed)
	Start	End		Start	End	
40	35.0	12.4	0.29	20	0	0.35
120	104.0	86.0	0.17	20	0	0.37
200	179.0	159.9	0.14	20	0	0.38
Glucose control <sup>a</sup>				20	0	0.35

Conditions producing glucose concentrations  $\geq 60$  mM after hydrolysis at 200 °C are shown. Other sugars were minor after treatment at 200 °C. Glucose concentrations in detoxified hydrolysates were 3-fold higher than initial glucose concentrations in fermentability tests (Start) as 5 mL hydrolysate was added to 10 mL medium. Fermentability tests were done in triplicate and yields varied within  $\pm 4\%$  (means are shown).

## VI.3 Hydrogen from cellulose

This section is divided into two parts:

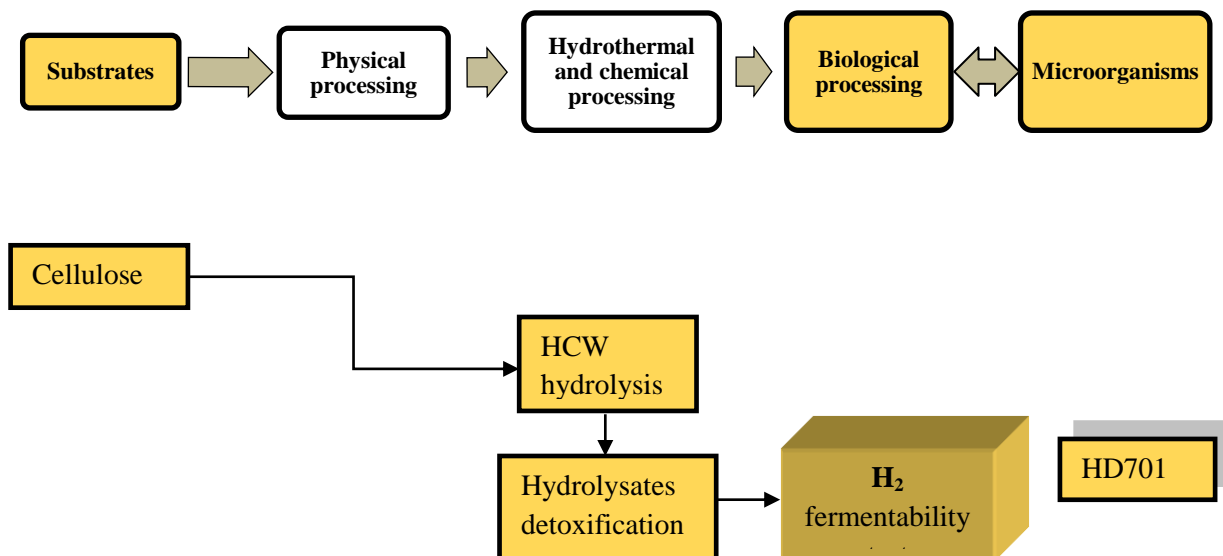
- Section VI.3.1 in form of a paper showing the effect of N<sub>2</sub> and CO<sub>2</sub> on cellulose hydrolysis and,
- Section VI.3.2 in a traditional part-chapter comparing two sets of experiments on cellulose hydrolysis under CO<sub>2</sub> and explaining the possible reasons why the results differ.

### VI.3.1 Paper on HCW hydrolysis of cellulose

“Bio-hydrogen production by *E. coli* HD701 following hot compressed water hydrolysis of cellulose under N<sub>2</sub> and CO<sub>2</sub>.”

Journal: Journal of Chemical Technology and Biotechnology, awaiting submission.

This paper was written by Rafael L. Orozco. All experiments and analysis were performed by Rafael L. Orozco.



Bio-hydrogen production by *E. coli* HD701 following hot compressed water hydrolysis of cellulose under N<sub>2</sub> and CO<sub>2</sub>.

Rafael L. Orozco,<sup>a</sup> Mark D. Redwood,<sup>a</sup> Gary A. Leeke,<sup>b</sup> Artur Majewski,<sup>b</sup> Regina C.D. Santos<sup>b</sup> and Lynne E. Macaskie<sup>a</sup>.

<sup>a</sup> Unit of Functional Bionanomaterials, School of Biosciences, University of Birmingham, Edgbaston, Birmingham B15 2TT, UK.

<sup>b</sup> School of Chemical Engineering, University of Birmingham, Edgbaston, Birmingham B15 2TT, UK.

## **Abstract**

Hydrogen provides a feasible alternative to fossil fuels as an energy vector for stationary and mobile applications. H<sub>2</sub> can be produced sustainably from cellulose, an abundant and renewable resource. However the hydrolysis of cellulose is a prerequisite for rapid microbial conversion to biohydrogen at mesophilic temperatures. Cellulose hydrolysis in hot compressed water (HCW) was enhanced by ~26 % by the addition of CO<sub>2</sub> at temperatures ranging from 220-260 °C and comparable hydrolysis products were obtained at a 10 °C lower temperature under CO<sub>2</sub> than under N<sub>2</sub>. Hydrolysates were detoxified with respect to 5-hydroxymethylfurfural (5-HMF) in order to better support growth and biohydrogen production by the model organism *Escherichia coli* HD701 via fermentation of the glucose and fructose hydrolysis products. Pre-treatment of cellulose under CO<sub>2</sub> offers 22 % more hydrogen production potential than that obtained under N<sub>2</sub>. Cellulose hydrolysis in HCW under CO<sub>2</sub> produced hydrolysates that, after AC treatment, were also promising for future integrated extractive bio-H<sub>2</sub> fermentations where the organic acids (OA) generated as a hydrolysis by-product can be used for a second, downstream H<sub>2</sub> fermentation.

Key words: activated carbon, cellulose, detoxification, hot compressed water hydrolysis, hydrolysate, hydrogen production

## INTRODUCTION

The depletion of fossil fuel deposits, along with the adverse effects on climate change due to atmospheric accumulation of CO<sub>2</sub>, are key drivers in the development of new energy technologies, with 90% of the current energy demand being met by burning fossil fuels [161].

Hydrogen is an environmentally benign energy carrier that can be effectively utilized for power generation which will play an important role in a new era of energy technologies [2, 4]. Strategic plans, enlargement of fiscal investment in H<sub>2</sub>, expansion of H<sub>2</sub> demonstration and deployment projects and international cooperation are actions adopted by developed countries to promote the transition from the fossil fuel to renewable and clean energy.

Hydrogen is a valuable commodity used in the chemical industry, petroleum refining, ammonia production and rocket fuel with an annual consumption of more than 50 million tonnes with a market value of £120 Billion in 2010 and 6 - 15% annual growth [38, 39]. The future use of hydrogen as a power source for stationary and mobile applications will considerably increase its demand. It is projected that by 2020 there will be ~ 800,000 cars powered by hydrogen and approximately 2500 fuelling stations in Germany alone [35]. Currently 96 % of the hydrogen produced comes from fossil fuel resources (natural gas, 48 %; liquid hydrocarbons, 30 % and coal, 18 %). Hence development of new H<sub>2</sub>-production technologies not based on fossil fuel are required.

Biomass is an abundant renewable resource to support the sustainability of the future hydrogen economy [39] but the hydrolysis of complex polysaccharides is fundamental for the biological utilization of biomass to provide an alternative source of biofuels (bioethanol, biobutanol or biohydrogen) via microbial metabolism. Cellulose, a major component of agri-food wastes, is a homopolymer comprising 100 to 3000 glucose units linked by  $\beta$  (1,4) glucosidic bonds, with a molecular weight within the range of 300,000 to 500,000 units depending of the length of the cellulose chain [53]. Due to intermolecular and intramolecular hydrogen linkages through the hydroxyl groups, cellulose molecules form crystalline structures that are insoluble in water under normal conditions; hence enzymatic hydrolysis of native cellulose is slow although many microorganisms have high cellulase activities [46, 53, 142].

Various approaches have been made to promote cellulose hydrolysis. The most common approach, acid hydrolysis, can be divided in dilute acid hydrolysis and concentrated acid hydrolysis. The former traditionally converts cellulose to glucose with yields of about 50-70 % using H<sub>2</sub>SO<sub>4</sub> (< 3 %) at high temperature (250-300 °C) and pressure (100 bar); however further degradation of glucose to other unwanted products such as furfurals also occurs. Other considerations regarding

this method include environmental and corrosion problems, high operating cost for acid consumption and high power demand and utility costs for operation at elevated temperatures [53, 135]. Concentrated  $H_2SO_4$  decrystallizes cellulose, forming homogeneous gelatine which is easily hydrolysed by diluting with water at lower temperatures (120 °C). This method gives low sugar degradation and yields in the order of 100% but with strong environmental and corrosion problems as well as high cost associated to the high consumption of  $H_2SO_4$  and product recovery [136].

An alternative approach, enzymatic hydrolysis, is achieved via three major classes of cellulase enzymes acting synergistically to decrystallise and then hydrolyse cellulose: *endoglucanases*, which act randomly on soluble and insoluble glucose chains; *exoglucanases*, which preferentially liberate glucose monomers from the end of the cellulose chain; and  *$\beta$ -glucosidases*, which release D-glucose from cellobiose dimers and soluble cellodextrins. Recently genetically modified organisms have been developed that produce large amounts of cellulases that digest cellulose efficiently [53] to yields of 75 to 95%. Traditionally, the enzymatic route was limited by the high cost but bespoke enzyme mixtures for lignocellulose breakdown (e.g. Novozyme CTec2) are now available at sufficiently low cost to enable some commercial processes [162].

An alternative approach, hydrolysis in hot compressed water (HCW), requires no addition of chemicals or enzymes. This uses water at temperatures ranging from 180 to 300 °C under pressure, under which water is a powerful solvent suitable for the solvolysis of cellulose and other complex polysaccharides (hemicelluloses, starch). Several groups have studied HCW hydrolysis and decomposition of cellulose under different conditions, reaction mechanisms and kinetics [78, 163-165]. Sasaki et al. [164, 166-168] investigated the hydrolysis of cellulose under critical ( $T_c = 374.15$  °C;  $P_c = 221.2$  bar) and subcritical water, obtaining cellulose hydrolysis yields of 75% at around the critical temperature, much higher than yields obtained at subcritical conditions. The reason is that at supercritical conditions the hydrolysis rate of cellulose is higher than that of glucose and oligomers, whereas at subcritical conditions the hydrolysis rate of glucose is higher than the cellulose. However this poses important operational challenges for process design at tonnage scale, e.g. high energy demands for the high heating rates needed to attain SCW conditions and low residence time and rapid quenching to low temperatures to minimize unwanted reactions. Therefore a more practical operational approach employing hot compressed water (HCW) treatment (below supercritical conditions) forms the focus of this investigation.

Minowa et al. used HCW to hydrolyse cellulose in a conventional autoclave (200 to 350 °C) at low pressure (30 bar) and short reaction times in the presence of sodium carbonate and reduced Ni

catalyst [77, 78, 169] confirming cellulose hydrolysis to glucose and fructose followed by further degradation to other non-sugar products. Maximum glucose yields were obtained at 260 °C.

The effect of heating rate on hydrolysis of cellulose in HCW has been investigated by several workers.[163, 168, 169] Kamio et al. found that the concentration of glucose increased when the heating rate was decreased from 10 to 2 °C.min<sup>-1</sup>, but the products from the degradation of glucose (glyceraldehyde, 5-hydroxymethyl furfural (5-HMF) were also favoured. These studies formed the starting point for the current work.

The first aim of this study was to apply HCW treatment of cellulose to obtain a hydrolysate suitable for downstream fermentation by a suitable model microorganism to produce H<sub>2</sub>. Two different sets of HCW reactions for the production of cellulose hydrolysates were employed, one under N<sub>2</sub> and the other under CO<sub>2</sub>. The model fermentative facultative anaerobe *E. coli* HD701 was derived from the parental strain *E. coli* MC4100 via derepression of formate hydrogenlyase in order to upregulate H<sub>2</sub> production [125, 170]. Other studies had confirmed that facultative anaerobes produce hydrogen from monomeric sugars hydrolysed from hemicelluloses such as mannose, galactose and xylose [56]. While strict anaerobes like the clostridia and thermatogales have the capacity to convert complex polysaccharides (e.g. cellulose, starch) these fermentations proceed slowly due to the demands on the cells to perform extracellular enzymatic hydrolysis and the crystalline nature of cellulose [134, 171, 172]. Therefore, a rapid physical hydrolysis followed by rapid fermentation by robust facultative bacteria may offer a significant advantage, particularly since the latter can be grown to high cell densities aerobically followed by use of 'resting' cells for hydrogen production anaerobically.

Fermentability of water soluble (WS) products obtained from the decomposition of cellulose in HCW at 330 °C and 10 s residence time in a tubular reactor was shown by Sakaki et al. [164], with ethanol production. Under these conditions 40% of the cellulose was converted to glucose; however the fermentation rate and yield was low compared to the control solution (formulated glucose 5%). These authors attributed these poor results to the presence of degradation products (DP) of glucose (eg. 5-HMF and organic acids) present in the hydrolysate [166, 167]. Some DP are potent inhibitors of growth and fermentation. Although each microorganism has different levels of tolerance to DP [173] these should be removed to improve fermentability. Activated carbon (AC) was found to be more effective than ionic exchange resins and overliming in the selective removal of DP [19, 174, 175] which was confirmed in fermentability tests of HCW hydrolysis biohydrogen production from starch [145]. The second aim of this study was to evaluate

the potential for microbial release of H<sub>2</sub> from the cellulose hydrolysates, evaluating the addition of an AC step to remove unwanted and toxic by-products.

The overall objective was to test the effectiveness and viability of this integrated approach for bio-hydrogen production from cellulose and determine strategies towards the creation of optimal process conditions anticipating further downstream conversion of organic acid (OA) end-products to additional H<sub>2</sub> via a photobioreactor within an integrated biorefinery approach [90]. Hence, the production of organic acids within the hydrolysate was also evaluated.

## **MATERIALS AND METHODS**

### *Chemical and bacteria used in this work*

Cellulose, D(-), fructose, D(+) and mannose were from Sigma. D(+) glucose (anhydrous) was from Fisher Scientific. 5-HMF, (99%) was from Aldrich and Furfural  $\geq 98\%$  was from FCC. Activated carbon colorsorb 5 (steam activated) was from JACOBI. *E. coli* HD701 was from laboratory stock.

### **Methods**

#### *Hot compressed water reaction*

The hot compressed water HCW reaction used a 250 cm<sup>3</sup> reactor (Parr series 4570/80 HP/HT) equipped with a heat/agitation controller (model 4836) and a cooling system (Grant LTD6/20) as described previously [145]. HCW hydrolysis reactions were repeated twice.

Cellulose (5 g) was suspended in de-ionised water (DW) to a final reactant volume of 125 cm<sup>3</sup> (40 g/L), leaving a headspace of 120 cm<sup>3</sup>. The reactor was sealed and purged with N<sub>2</sub> or CO<sub>2</sub> gases for 3 min with agitation (850 rpm) before pressurising to 30 bar with N<sub>2</sub> or CO<sub>2</sub> and heating to set-point temperature. Reaction conditions were held for 15 min before rapid cooling to 100 °C; the reactor was removed from the heating vessel and quenched in an ice-water bath. The reactor was depressurised and the hydrolysate was separated from the solid residue by vacuum filtration through two layers of filter paper (Fisherbrand QL100). The residue was washed with DW, dried at 60 °C and weighed. Total organic carbon (TOC) in hydrolysates after filtration was measured using a TOC analyser (TOC 5050A, Shimadzu Co., Japan) with autosampler (ASI-5000A, Shimadzu Co., Japan). Sugars and 5-HMF were quantified by HPLC using an Agilent 1100 system with RI detector (1200 series) and Resex-RCM (Phenomenex) column as described previously [145]. Gases during hydrolysis were neither collected nor analysed. For estimation of

residual polyglucose (unconverted cellulose, cellulodextrins and cellobiose) the residue was hydrolyzed as described elsewhere [176] and the glucose units quantified by the DNSA method [153]. Hydrolysates and samples taken were stored at -20 °C for tests and further processing. In some cases precipitate appeared in the hydrolysates upon thawing and was removed by filtration.

#### *Detoxification*

For removal of inhibitors the hydrolysate was treated with 5% (w.v<sup>-1</sup>) AC powder (60 °C, 1 h) with agitation at 180 rpm as described by Hodge et al. (2009) [175]. The treated hydrolysates were vacuum filtered through a layer of filter paper (Fisherbrand QL100). Hydrolysates and samples were kept at -20 °C before analysis and evaluation for fermentability.

#### *Toxicity of hydrolysates towards bacterial growth*

Colonies of *E. coli* were picked from nutrient agar plates maintained at 4 °C into 5 ml vials of nutrient broth solution with added sodium formate (0.5% w.v<sup>-1</sup>) pH 7 and incubated for 6 h at 30 °C, 180 rpm before use. The concentration of cells (OD<sub>600</sub>) was measured using a UV/visible spectrophotometer (Ultrospec 3300 pro) and the suspension was used as inoculum for fermentation tests in minimal medium.

Minimal medium comprised: citric acid (1.05 g.L<sup>-1</sup>); formic acid (0.978 mL.L<sup>-1</sup>); (NH<sub>4</sub>)<sub>2</sub>HPO<sub>4</sub> (0.264 g.L<sup>-1</sup>); (NH<sub>4</sub>)<sub>2</sub>SO<sub>4</sub> (0.462 g.L<sup>-1</sup>); NH<sub>4</sub>OH 15.325 M (2.871 mL.L<sup>-1</sup>); BIS-TRIS base (12.55 g.L<sup>-1</sup>). The pH was adjusted to 6.5. After autoclaving the following additives were added aseptically: glucose 2 M (30 mL.L<sup>-1</sup>); MgSO<sub>4</sub> 1 M (2 mL.L<sup>-1</sup>); thiamine 1 mg.mL<sup>-1</sup> (10 mL.L<sup>-1</sup>) filter sterilized; trace elements solution (TE) was according to Hewitt et al. (2006) [152] (2 mL.L<sup>-1</sup>).

The glucose was added to the media to ensure the presence of a sugar that is appropriate for growth, allowing observation of variation in growth attributable to the inhibitors contained in the samples rather than to the possibility of substrate limitation.

The inoculum (10 mL.L<sup>-1</sup>) was introduced and mixed. Aliquots (90 mL) of inoculated media were placed in 250 mL Erlenmeyer flasks previously autoclaved and mixed with 10 mL of the hydrolysate stock (filter sterilized). Aliquots (5 mL) were taken into universal bottles and incubated (30 °C; 180 rpm). The OD<sub>600</sub> was measured after 18 h.

#### *Fermentative biohydrogen production*

To evaluate firstly, the effectiveness of the AC treatment and secondly, the viability of the hydrolysates as potential feedstocks for larger scale fermentation, small fermentation tests using

*E.coli* HD701 were performed and H<sub>2</sub> production calculated as described by Orozco et al. (2011) [145].

## RESULTS AND DISCUSSION

The hydrolysates produced at different temperatures had a brown colour, the intensity of which increased from pale to dark with the hydrolysis temperature. The final pH of the hydrolysates was between 2.6 and 3.6 falling from an initial pH of 6.3.

Thermal pathways of the experiments between 220-260 °C are illustrated in Figure 1. The heating rate achieved was  $\sim 7 \text{ }^\circ\text{C}\cdot\text{min}^{-1}$  which is higher than the minimum  $2 \text{ }^\circ\text{C}\cdot\text{min}^{-1}$  needed for maximum sugar yields [163]. The total reaction times were from 50 to 90 min according to:  $R = t_1 + 15 + t_2$ , where R is total reaction time,  $t_1$  is time to heat from 50 °C to set point (min) and  $t_2$  is time to cool from set point to 100 °C (min).

### *Conversion of cellulose to products using HCW hydrolysis under N<sub>2</sub> and the effect of CO<sub>2</sub>*

The cellulose conversion ( $X_c$ ) to products is shown in Figure 2 for two independent experiments that gave similar results under N<sub>2</sub>.  $X_c$  increased exponentially with respect to temperature (Fig. 2b).

Initial tests showed that the effect of substituting N<sub>2</sub> for CO<sub>2</sub> was to increase  $X_c$  largely independently of the temperature at 230 to 250 °C. The conversion ( $X_c$ ) (at 250 °C) under N<sub>2</sub> was  $59.2 \pm 12.8$  (n=3) and under CO<sub>2</sub> (figure 3) was  $73.3 \pm 8.1$  (n=3) and it was concluded that, overall, CO<sub>2</sub> promotes cellulose hydrolysis by  $\sim 26 \%$  at 250 °C in accordance with similar conclusions reported in the literature [144].

Throughout, the effect of CO<sub>2</sub> was to shift down by 10 °C the TOC and products profiles, which were otherwise comparable in the case of N<sub>2</sub> and CO<sub>2</sub> supplemented hydrolysis (Figure 4 a). Hence, it was concluded that although the level of CO<sub>2</sub> used in these experiments is beneficial in terms of a lower reaction temperature for the same degree of conversion and hydrolysis there is no overall benefit in terms of TOC in the hydrolysate, production of sugar (glucose and fructose) or in decreased production of 5-HMF. Some product decomposition was observed above 250 °C under CO<sub>2</sub> and 260 °C under N<sub>2</sub> (Figure 4 b). This behaviour was observed consistently in all similar experiments with cellulose.

The maximum yield of glucose under CO<sub>2</sub> was  $0.225 \text{ [g C (g C initial cellulose)}^{-1}]$  obtained at 250 °C and that under N<sub>2</sub> was  $0.198 \text{ [g C (g C ini. cellulose)}^{-1}]$  at 260 °C (i.e. approx 20 % yield of glucose). However this represents 59 and 64 % respectively less than the yields obtained at

200 °C in similar experiments under CO<sub>2</sub> using starch as a starting material showing that hydrolysis of cellulose is less efficient than that of starch, probably attributable to its crystalline structure.

Acetate and formate were the main organic acids (OAs) found in the hydrolysate at 250 °C under CO<sub>2</sub> at low yields of 0.03 and 0.01 [g (g of starting material)<sup>-1</sup>] respectively (Table 1) and they were not removed significantly by treatment with activated carbon (Table 1; see below). The production of OAs was ~ 2-fold greater under CO<sub>2</sub> than under N<sub>2</sub> (Table 1; mean data from three temperatures). Formate arises from the degradation of 5-HMF whereas acetate is a decomposition product from sugars (glucose, fructose); at the same time acids and aldehydes are precursors of gaseous compounds which usually occur above 260 °C [53]. The hydrolysates obtained at 220, 230, 240 and 260 °C were not analysed for OA before AC treatment.

The results shown in Figure 4 suggest that glucose contained in the hydrolysate would be suitable for fermentation, but the presence of toxic 5-HMF may affect significantly both microbial growth and fermentation yields.

#### *Formation of 5-HMF and OA during HCW hydrolysis and their removal using AC.*

The concentration of sugars was unaffected by the AC treatment removing no more than 10 % of the glucose and fructose. The residual OA after AC treatment is shown in Table 1. The concentration of acetate and formate was largely unchanged by AC treatment and increased with temperature reaching maximum yields in both cases at 260 °C with 0.017 and 0.008 [g (g starting material)<sup>-1</sup>] respectively under N<sub>2</sub>; 0.030 and 0.017 [g (g starting material)<sup>-1</sup>] under CO<sub>2</sub> which yielded more OAs than under N<sub>2</sub>. At 250 °C yields were 3.7 and 2.8 fold higher respectively with CO<sub>2</sub>; in addition it was observed that ~15% of both OA were removed by AC treatment in this case.

In contrast to sugars and OAs, AC produced a high degree of removal of 5-HMF as shown in Figure 5. The highest concentration of 5-HMF occurred at 250 °C (37.3 mM) and 260 °C (35 mM) under CO<sub>2</sub> and N<sub>2</sub> respectively, AC was able to remove more than 71 % of the 5-HMF produced under CO<sub>2</sub> and N<sub>2</sub>. This result is consistent with HCW experiments using starch where AC also showed preference towards 5-HMF [145].

#### *Growth and H<sub>2</sub> production from cellulose hydrolysates with and without removal of 5-HMF using AC.*

The effect of hydrolysis degradation products on the growth of *E. coli* HD701 was determined by performing a toxicity test using hydrolysates prepared at temperatures between 220 and 250 °C under CO<sub>2</sub> before and after AC treatment. Figure 6 shows that growth of *E. coli* was inhibited in all untreated hydrolysates prepared at 230- 250 °C. However, from preparation

temperatures of 220 and 230 °C both untreated and treated hydrolysates supported more *E. coli* growth than the control (by 29% and 100 % respectively), suggesting that the sugar contained in the hydrolysate at those temperatures has a synergistic effect towards *E. coli* growth. Using hydrolysates obtained at 240 °C only the AC treated hydrolysate supported *E. coli* growth at the same level as the control and from those obtained at 250 °C both untreated and treated samples gave less growth than the control (74 and 33 % respectively) indicating that at this temperature the DP persist in the hydrolysates in quantities and have a detrimental effect despite AC treatment. The conclusion from Figure 6 is that growth was approximately doubled by the application of HCW hydrolysis of cellulose at 230 °C under CO<sub>2</sub> with AC treatment.

Hydrogen yields obtained from fermentation before and after AC treatment are shown in Figure 7. Before AC no H<sub>2</sub> was produced from samples prepared at temperatures above 220 °C in the case of CO<sub>2</sub> and 230 °C with N<sub>2</sub>. However after AC all hydrolysates permitted H<sub>2</sub> production showing that AC considerably improved their fermentability. The yields increased with the hydrolysis reaction temperature reaching maximum values between 10-11 mL H<sub>2</sub> (g of cellulose)<sup>-1</sup> from samples prepared at 250-260 °C in both cases due to their higher glucose concentration. However, this represents ~31 to 37 % less yields than those obtained from starch from samples hydrolyzed under CO<sub>2</sub> at 200 °C.[145] No H<sub>2</sub> was produced from hydrolysates obtained at 270 °C (not shown) due to high sugar degradation to 5-HMF and OA.

Based on these findings the utilisation of CO<sub>2</sub> would confer only the advantage of higher conversions and shifting down the cellulose hydrolysis temperature by 10 °C. However, according to Table 2, the utilisation of CO<sub>2</sub> offers 53 % more hydrogen production potential (HPP unit as defined by Eroğlu et al. 2004) [97] compared to 25 % for N<sub>2</sub> when both are compared to the glucose control (20 mM in the fermenter) due to the richer content in sugars (Figure 4) and higher content of OA (Table 1) in the hydrolysates. This would make the hydrolysates under CO<sub>2</sub> more suitable for integrated extractive bio-H<sub>2</sub> fermentations where the OA are used for a second, downstream H<sub>2</sub> fermentation [90, 100].

The maximum theoretical H<sub>2</sub> yield in *E. coli* is 2 mol H<sub>2</sub>.mol hexose<sup>-1</sup> and therefore 20 mM glucose in the control would yield a maximum of 14.4 mL. The volumes of H<sub>2</sub> produced shown in Table 2 represent about 18 % of the expected yield from glucose. These low conversions are attributed to sub-optimal fermentation parameters in the small tests, particularly with respect to pH, end product accumulation and agitation. In previous work around 80 % conversion was typically achieved from glucose using a commercial fermentation system with agitation and automatic pH

regulation [100] and future studies will focus on the use of cellulose in this biohydrogen system with the upstream processing reported here. However the yield was low as compared to starch hydrolysis reported previously [145]; hence the fermentative hydrogen yield from cellulose hydrolysate and the overall utility of this rapid method for cellulosic waste breakdown would require a detailed comparison with (e.g.) thermophilic cellulolytic fermentation.

## CONCLUSIONS

Supplementing the reaction mixture with CO<sub>2</sub> gives an increase of between 25 to 40 % in cellulose conversion compared to N<sub>2</sub>. CO<sub>2</sub> permits a downshift in temperature by 10 °C to obtain similar conversion to hydrolysate products than under N<sub>2</sub>, however the generation of OA was 2-fold higher with CO<sub>2</sub> which would represent an advantage in integrated extractive bio-H<sub>2</sub> fermentations. AC treatment removed inhibitory degradation products, particularly 5-HMF, without affecting sugar yields and improved the quality of the hydrolysates as substrates for growth and bio-H<sub>2</sub> production; negligible H<sub>2</sub> was produced from untreated solutions. The yields of H<sub>2</sub>, ~ 11 mL.(g of cellulose)<sup>-1</sup> were very similar in the hydrolysates prepared under CO<sub>2</sub> and N<sub>2</sub> at 250 and 260 °C. Future studies will focus on a scale up of the method to produce feedstocks from wastes for bioconversion in larger scale fermentations and comparisons with thermophilic cellulosic waste fermentations.

## ACKNOWLEDGEMENTS

The financial support of the EPSRC (Grant Nos EP/D05768X/1 and EP/E034888/1), BBSRC (Grant Nos BB/C516195/2 and BB/E003788/1), the Royal Society (Industrial Fellowship to LEM), Advantage West Midlands (Grant ref. POC46) and the Government of Mexico (studentship no. 203186) to RLO is acknowledged, with thanks. For technical support we thank the Combined Workshop, School of Biosciences, University of Birmingham, UK and for *E. coli* strain HD701, Prof Frank Sargent, University of Dundee, UK.

**Table 1.** Organic acid yields [g (g starting material)<sup>-1</sup>] before and after AC treatment; ND (not done).

		Acetate				Formate			
		Before AC		After AC		Before AC		After AC	
	Temp	N <sub>2</sub>	CO <sub>2</sub>						
Cellulose 40 g.L <sup>-1</sup>	240		ND	0.005	0.014		ND	0.004	0.008
	250	ND	0.031	0.007	0.026	ND	0.013	0.004	0.011
	260		ND	0.017	0.030		ND	0.008	0.017

**Table 2.** Volumes of H<sub>2</sub> produced by *E. coli* during the fermentation of the hydrolysates obtained at different reaction temperatures under CO<sub>2</sub> and N<sub>2</sub> and volumes of HPP\* from glucose and OA contained in the hydrolysates after AC treatment. HPP volumes for OA calculated from mol H<sub>2</sub>.mol OA<sup>-1</sup> which are Acetate 4; Formate 2; Sasikala et al. (1995). [177]

Condition	Reaction temperature (°C)	H <sub>2</sub> produced (mL)	HPP* in hydrolysates fermentation test		
			From glucose	From OA	Total
CO <sub>2</sub>	220	0.4	3.5	ND	ND
	230	1.1	5.7		
	240	1.2	10.4	5.7	16.1
	250	1.5	11.7	10.3	22.0
	260	1.6	10.0	12.6	22.6
	220	0.3	0.7		ND
N <sub>2</sub>	230	0.4	1.5		
	240	0.9	2.7	2.2	5.0
	250	1.6	7.8	2.9	10.6
	260	1.6	10.5	7.6	18.0
Glucose		2.6	14.4	0	14.4

\*Hydrogen production potential [97] assuming that HPP is proportional to H<sub>2</sub> yield and that OAs from the hydrolysate pass to a secondary stage photobioreactor for additional hydrogen production. [97, 100].

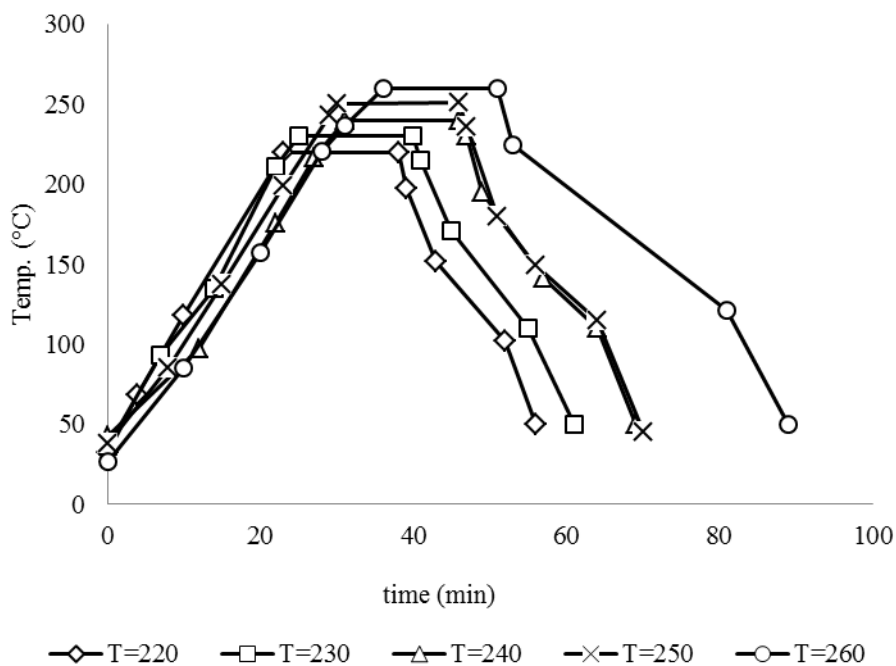


**Figure 1.** Reaction heating and cooling pathways delivered by the reactor at different temperatures. There was no difference between tests using CO<sub>2</sub> and N<sub>2</sub>. Set temperatures (°C) were: ◇, 220; □, 230; △, 240; X, 250; ○, 260.

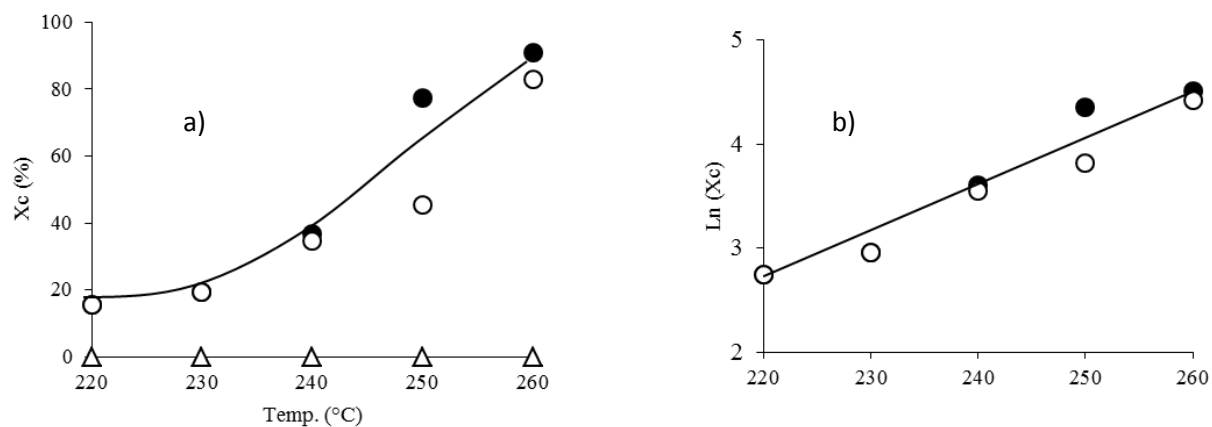


**Figure 2. a)** Cellulose conversion ( $X_c$ ) to products with reaction temperature. Two independent experiments under  $N_2$  shown ((●), (○)) are for a starting cellulose concentration of  $40 \text{ g.L}^{-1}$ ; (—) represents average  $X_c$  under  $N_2$ ; (Δ) is the control experiment with no heat; **b)** Shows natural logarithm of  $X_c$  under  $N_2$  with temperature.

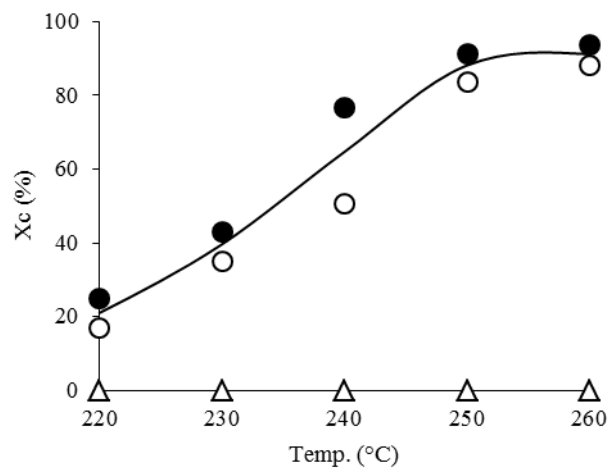


**Figure 3.** Cellulose conversion ( $X_c$ ) to products with reaction temperature under  $CO_2$ ; (●), (○) denote two independent experiments under  $CO_2$ ; (—) represents average  $X_c$  under  $CO_2$ ; (Δ) is the control experiment with no heat.

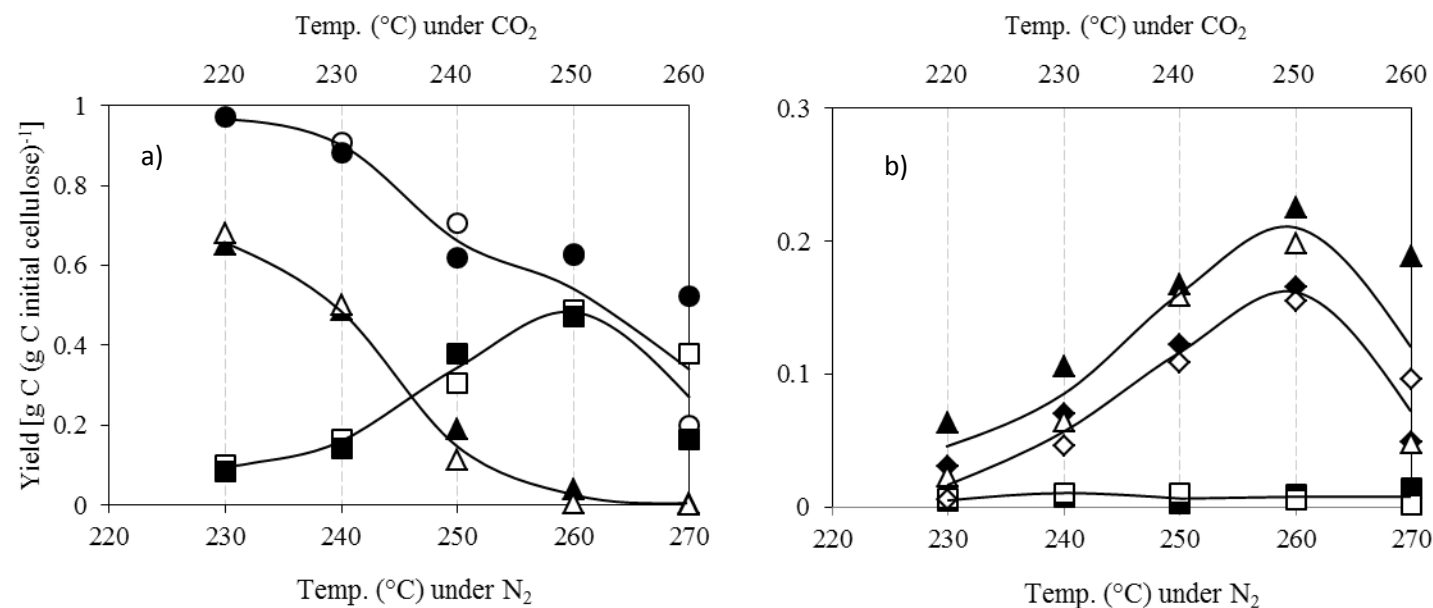


**Figure 4.** Total organic carbon (a) and product yield (b) in hydrolysates before AC under CO<sub>2</sub> (filled symbols) and N<sub>2</sub> (open symbols). **a):** (●,○), TOC total (hydrolysate + residue); (▲,△), TOC residue; (■,□), TOC hydrolysate. **b):** (▲,△), glucose; (■,□), fructose; (◆,◇), 5-HMF in hydrolysates. The TOC total does not include material lost in some samples due to precipitation, char in residue and gas composition.

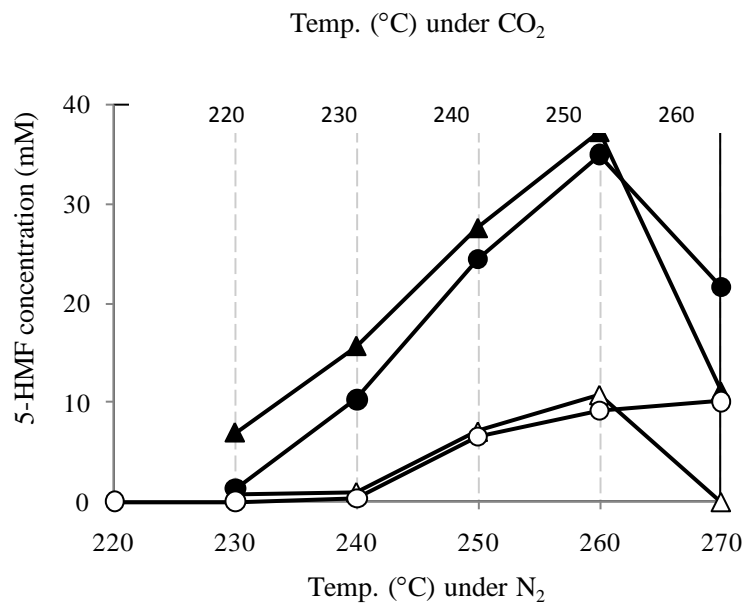


**Figure 5.** Concentrations (mM) of 5-HMF before (filled symbols) and after (open symbols) AC treatment for experiments prepared under CO<sub>2</sub> (▲, Δ) and N<sub>2</sub> (●, ○) at different reaction temperatures. Results shown are average values of two experiments with variation within ± 5 %.

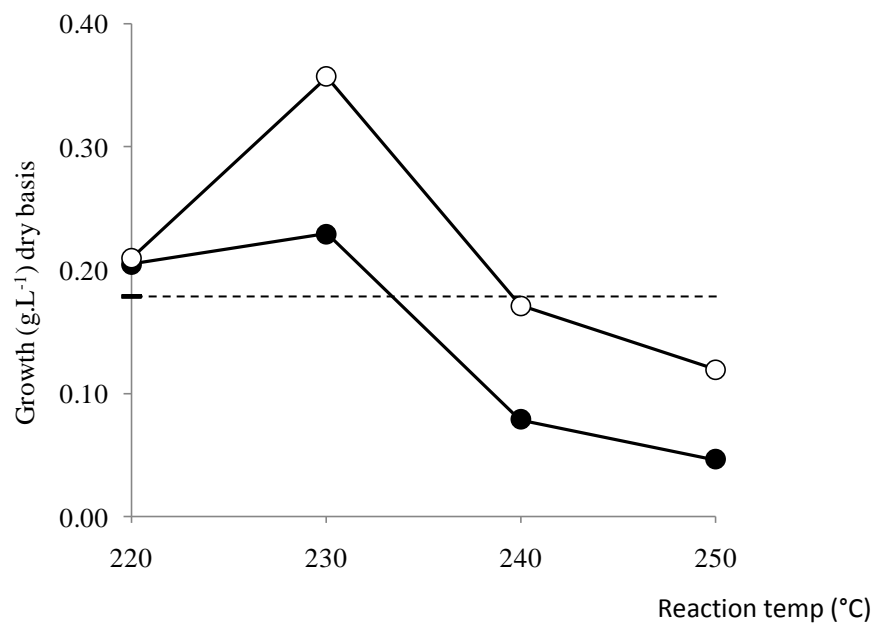


**Figure 6.** Growth of *E.coli* HD701 in hydrolysates prepared under CO<sub>2</sub> at different reaction temperatures (●) before and (○) after AC treatment. The dotted line represents the biomass yield from the glucose control (20 mM).

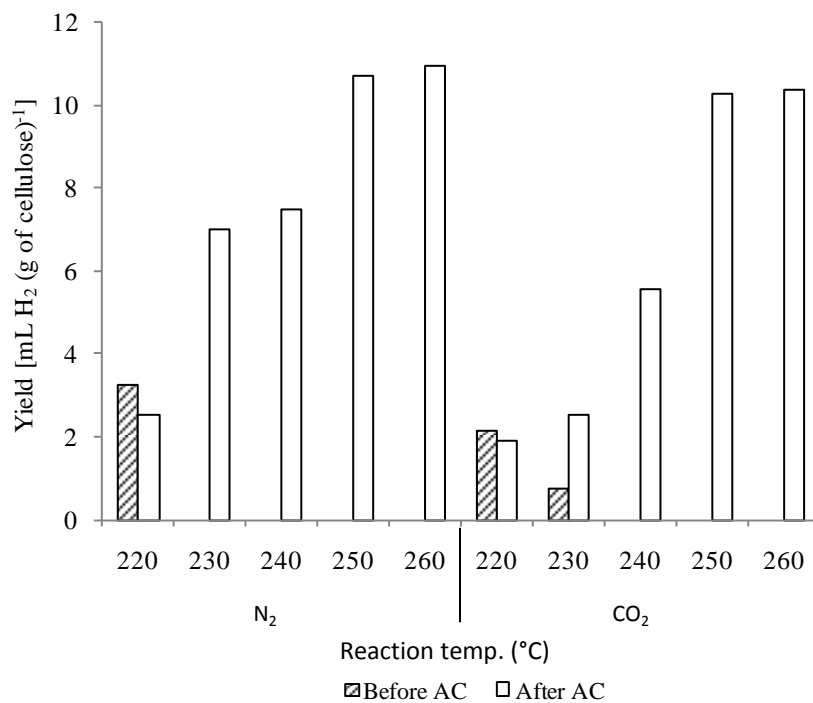


**Figure 7.** Hydrogen yields obtained after fermentation of the hydrolysates produced at various temperatures. Under CO<sub>2</sub> no H<sub>2</sub> was produced before AC from samples prepared at temperatures higher than 230 °C; under N<sub>2</sub> no H<sub>2</sub> was produced from samples prepared at above 240 °C before AC.

### VI.3.2 Comparison between HCW cellulose hydrolysis set 1 and set 2 experiments

#### Introduction

In the previous section the results obtained from the HCW/CO<sub>2</sub> and HCW/N<sub>2</sub> hydrolysis on cellulose (set 1) were presented and discussed with inclusion of some data from the previous section. Repetitions of both HCW hydrolysis experiments under the same conditions of temperature and pressure (set 2) were made approximately 5 months after set 1. Materials, methods and analysis were performed exactly as described in the previous section with set 1. The results obtained in set 2 were inconsistent with those found in set 1. The main differences between both sets of experiments are shown and the possible reasons of these variations discussed in this section. In addition to set 1, higher concentrations of cellulose in the reactor (100 and 167 g.L<sup>-1</sup>) were also hydrolysed under HCW/CO<sub>2</sub> at 250 °C. Tests were carried out as described in section VI.3.1.

#### Results and discussion

Reaction parameters of both sets of experiments are shown in Table 15. After the reaction the final pressure (P<sub>f</sub>) remained fairly constant at lower temperatures in all cases but began to increase at T ≥ 250 °C indicating that gasification of products initiated at higher temperatures [144]. Under CO<sub>2</sub> final pressures (P<sub>f</sub>) were about 10 bars lower in 1<sup>st</sup> set experiments compared to 2<sup>nd</sup> set, which can be attributed to CO<sub>2</sub> dissolution in the aqueous media to form H<sub>2</sub>CO<sub>3</sub> during set 1 [144]; this did not occur in set 2 where P<sub>f</sub> remained the same as initial pressure (P<sub>i</sub>) for all conditions except at 260 °C where P<sub>f</sub> was ~10 % higher than P<sub>i</sub>. Under N<sub>2</sub> P<sub>f</sub> was similar to P<sub>i</sub> in all cases. In both sets the final pH (pH<sub>f</sub>) decreased with temperature but pH<sub>f</sub> values were generally higher in set 2 under both conditions especially under N<sub>2</sub>, this is consistent with the lower X<sub>c</sub> in set 2 which translates in less hydrolysis products including OA. Cellulose conversion to products (X<sub>c</sub>) were calculated according to Equation 5 and are shown in Table 15.

#### Equation 5

$$X_c = \frac{C - R}{C} \times 100$$

Where,

*X<sub>c</sub>* = cellulose conversion to products (%)

*C* = Initial cellulose (g dw.L<sup>-1</sup>)

*R* = Residue (g dw.L<sup>-1</sup>)

Under CO<sub>2</sub> Xc increased with temperature in both sets but Xc in set 2 were much lower compared to set 1. Under N<sub>2</sub> Xc also increased with temperature and was very similar in both sets except at temperatures  $\geq 250$  °C where Xc became much lower in set 2. Cellulose conversions under CO<sub>2</sub> were higher than N<sub>2</sub> in both sets indicating catalytic activity of CO<sub>2</sub> during the decomposition of cellulose to products as discussed in the previous section.

**Table 15** A comparative of reaction parameters between 1<sup>st</sup> and 2<sup>nd</sup> set; starting material is cellulose; initial pressure (P<sub>i</sub>) and pH<sub>i</sub> is 30 bars and 6.3 respectively, cellulose conversion to products (Xc).

Condition	[Starting material] (g.L <sup>-1</sup> )	1 <sup>st</sup> set				2 <sup>nd</sup> set		
		Temp (°C)	P <sub>f</sub>	pH <sub>f</sub>	Xc (%)	P <sub>f</sub>	pH <sub>f</sub>	Xc (%)
CO <sub>2</sub>	40	220	20	3.13	25.1	30	4.9	15.1
		230	20	2.92	42.8	30	4.0	25.1
		240	20	2.74	76.7	30	3.3	40.6
		250	21	2.60	91.4	30	3.0	78.5
		260	24	2.44	93.8	33	2.6	83.2
	100	250	Not done			34	2.5	67.0
	167	250				34	2.4	62.7
N <sub>2</sub>	40	220	31	3.63	15.6	32	6.4	15.6
		230	32	3.45	19.2	32	6.3	19.2
		240	32	3.22	36.7	31	4.9	34.7
		250	32	2.82	77.5	33	4.6	45.5
		260	33	2.61	90.9	33	2.7	83.0

Hence it is concluded that, apart from the conversion obtained at 250 °C, the advantage of using CO<sub>2</sub> is not seen in set 2 i.e. the catalysis offered by CO<sub>2</sub> had failed.

Product distribution in the hydrolysates after AC treatment for both sets is shown in table 16. Unexpectedly, 5-HMF was the main product identified in set 2 followed by glucose and fructose. Optimum yields to glucose occurred at 250 °C under CO<sub>2</sub> and N<sub>2</sub> (0.057 and 0.014 [gC (gC initial cellulose)<sup>-1</sup>] respectively), this also differs from set 1 where optimum glucose yields under N<sub>2</sub> were at 260 °C. Important variations in yields were noticed between both sets; the yield of glucose was ~ 4 fold higher in set 1 at 250 °C under CO<sub>2</sub> and ~ 20 fold higher in set 1 at 260 °C under N<sub>2</sub>. The yields of 5-HMF were also higher in set 1. Yields of glucose and 5-HMF were ~ 4 and ~ 3 fold higher respectively under CO<sub>2</sub> than with N<sub>2</sub> at 250 °C in set 2.

**Table 16** A comparative in product yield [ $\text{g C (g C initial cellulose)}^{-1}$ ] between both sets of experiments. AAC (after activated carbon); BAC (before activated carbon). AC utilized for treatment was  $50 \text{ g.L}^{-1}$  in all cases. Last column shows 5-HMF removed by AC in the 2<sup>nd</sup> set.

Sample	Temp (°C)	Yield of products 1 <sup>st</sup> set				Yield of products 2 <sup>nd</sup> set				
		Glucose	Fructose	5-HMF		Glucose	Fructose	5-HMF		5-HMF removed
		AAC	AAC	BAC	AAC	AAC	AAC	BAC	AAC	[ $\text{mg (g of AC)}^{-1}$ ]
CO <sub>2</sub>	220	0.065	0.004	0.031	0.003	0.002	0.000	0.003	0.000	1.70
	230	0.105	0.007	0.070	0.004	0.005	0.003	0.023	0.000	13.02
	240	0.192	0.003	0.123	0.032	0.024	0.007	0.073	0.000	41.69
	250	0.216	0.008	0.166	0.048	0.057	0.008	0.158	0.008	85.27
	260	0.184	0.006	0.049	0.000	0.025	0.006	0.031	0.004	15.75
N <sub>2</sub>	220	0.013	0.000	0.000	0.000	0.000	0.000	0.000	0.000	0.00
	230	0.028	0.000	0.006	0.000	0.002	0.000	0.006	0.000	3.24
	240	0.051	0.001	0.046	0.002	0.006	0.001	0.050	0.000	28.42
	250	0.143	0.002	0.109	0.029	0.014	0.002	0.058	0.002	11.60
	260	0.193	0.005	0.155	0.041	0.010	0.006	0.069	0.004	36.93
	270	0.045	0.002	0.096	0.033	not done				

In summary, in both the conversion and the products obtained, the results obtained in set 2 were inconsistent with the results obtained in set 1 under both CO<sub>2</sub> and N<sub>2</sub> and stronger differences between the utilization of CO<sub>2</sub> and N<sub>2</sub> were observed in set 2. The only difference between set 1 and set 2 was that the reactor ‘had aged’ (probably via other use) in the 5 months between the two sets.

Minowa et al., 1998 [77] studied the decomposition of cellulose in HCW with alkali or nickel catalysts; in a more detailed analysis of his findings, the influence of these catalysts on the cellulose degradation pathway to products is significant compared to catalyst free conditions. Under alkali catalysts cellulose decomposition began at 180 °C and increased gradually with temperature. Between 180-260 °C only aqueous products were obtained which quickly decomposed to gases at  $T > 260$  °C, total conversion of cellulose was achieved at 300 °C. In the case of nickel catalyst cellulose decomposition occurred between 260 and 320 °C, below 260 °C; almost 100 % of the cellulose remained unreacted with no product formation. After 260 °C only aqueous products and gases were obtained with little glucose formed. At  $T > 320$  °C the formation of gases continued despite no cellulose remaining. This indicates a quick transition from cellulose to aqueous products and from aqueous products to gases.

The reactor vessel used in this work is made of Hastelloy C-276 (a Nickel (~ 55 %)-Molybdenum-Chromium alloy); this material, when corroded, leaches nickel to the reaction medium thereby possibly affecting cellulose decomposition [178, 179] to many different water soluble organic products before being finally converted to gaseous products. When the 1<sup>st</sup> set of experiments was done the reactor was new, five to six months later the 2<sup>nd</sup> set was performed, in between several reactions involving food waste were conducted. It is thought that the salts present in the waste attacked the wall of the reaction vessel causing corrosion [178]. This led us to conclude that it was highly likely that the presence of nickel in the reaction medium was what caused the discrepancies in results between set 1 and set 2; in set 2 under N<sub>2</sub> the high pH<sub>f</sub> (Table 15) along with low conversions of cellulose to products achieved (Table 16) at lower temperatures support the argument. Under CO<sub>2</sub> it can be postulated that a combinatory effect took place in which CO<sub>2</sub> acted as a catalyst towards the conversion of cellulose to hydrolysis products and at the same time nickel catalysed the conversion of these hydrolysis products to gases. This would explain the difference in P<sub>f</sub> (Table 15) and the yield of products between both sets and also the difference between CO<sub>2</sub> and N<sub>2</sub> reactions in set 2.

The fermentability of the hydrolysates from set 2 after AC treatment was performed, as expected H<sub>2</sub> produced was ~ 70 % lower at 250 and 260 °C compared to set 1 due to the lower sugar content on hydrolysates from set 2.

It is important to mention that experiments in set 2 were only done once but in all of the 10 reactions performed the alteration in product distribution possibly attributable to the corrosion of the reaction vessel, was evident.

## **Conclusions**

Two sets of experiments involving HCW hydrolysis of cellulose at various temperatures were performed under CO<sub>2</sub> and N<sub>2</sub>. The strong variations in results between both sets are probably attributable to corrosion of the reactor wall material (Hastelloy C-276; ~ 55 % nickel) which was likely to have occurred after several reactions involving food waste before set 2 experiments. Results obtained from set 1 were more consistent with literature reports [144, 169].

## **VI.4 Hydrogen from biowastes**

This section is presented in form of a paper that is in preparation for journal submission. It describes the hydrolysis of representative agricultural and kitchen wastes in HCW and the fermentability of the products.

“Hydrothermal Bio-H<sub>2</sub> production from agricultural and kitchen wastes: impact of degradation products on *E. coli* HD701 growth and H<sub>2</sub> fermentation”.

Journal: still to be selected.

This proposed paper was written by Rafael L. Orozco. All experiments and analysis were performed by Rafael L. Orozco. The lignin determination was performed jointly with R.M.N. Roque.

Hydrothermal Bio-H<sub>2</sub> production from agricultural and kitchen wastes: impact of degradation products on *E. coli* HD701 growth and H<sub>2</sub> fermentation.

R.L. Orozco<sup>1</sup>, M.D. Redwood<sup>1</sup>, G.A. Leeke<sup>2</sup>, R.M.N. Roque<sup>2</sup>, A. Majewski<sup>2</sup>, R.C.D. Santos<sup>2</sup> and L.E. Macaskie<sup>1</sup>.

<sup>1</sup> Unit of Functional Bionanomaterials, School of Biosciences, University of Birmingham, Edgbaston, Birmingham B15 2TT, UK.

<sup>2</sup> School of Chemical Engineering, University of Birmingham, Edgbaston, Birmingham B15 2TT, UK.

## Abstract

Biowastes are continuously generated worldwide in quantities of billions of tonnes per year causing substantial environmental damage. Among these lignocellulosic and food wastes are among the most abundant. Disposal is not only an environmental problem but an opportunity since these materials constitute a valuable renewable resource for the sustainable production of fuels and chemicals.

Hot compressed water (HCW) is a promising method of biowaste pretreatment, providing hydrolysis of polysaccharides as renewable bioprocess feedstocks. But hydrolysis also produces degradation products (DP) which can affect bacterial action. We investigated the effects of key DPs on growth and fermentative H<sub>2</sub> production by *E. coli* HD701. Both stimulatory and inhibitory properties we identified, highly specific to the culture condition.

Three important biowastes (brewery grain, food waste and wheat straw) were hydrolysed in HCW at temperatures from 200 to 250 °C in the presence of CO<sub>2</sub> for bio-H<sub>2</sub> fermentation with *E. coli* HD701. The obtained hydrolysates from each waste were evaluated for growth and bio-H<sub>2</sub> before and after their detoxification with activated carbon (AC). Food waste was the most promising biowaste hydrolysate and it was tested for bio-H<sub>2</sub> production in a 3 L fermentation.

## Introduction

Climate change due to increased concentration of CO<sub>2</sub> in atmosphere, rapid exhaustion of fossil fuel reserves in association with increases in oil prices, and bio-waste disposal to landfill (and associated costs) are key drivers for the search of new and renewable energy sources from biomass. Policies around the world include targets of at least 20% reductions in CO<sub>2</sub> emissions by 2020 and 50% by 2050 (section I.4), increases in landfill tax for waste disposal (e.g. in UK from current £56 to £72 per tonne by April 2013) [34] were established in recognition of the need to promote environmental quality and energy security which involves the transition from the fossil fuel to the renewable and clean energy age.

In opposition to these goals, energy demand increasing rapidly in parallel to the world population which is estimated to grow from 6 to 9 billion by 2050 (chapter I), the number of light-duty vehicles expected to grow from 1 to 2.8 billion by 2050 and by the fact that highly populated and rapidly developing nations will become more energy intensive as they expand their economies [3, 4]. Currently, ~ 85 - 90% of energy production comes from fossil fuel resources [161] (section I.3).

Biomass resources are abundant, renewable and varied; they include agricultural crops and wastes, food and drink waste, sewage sludge, manure and forestry waste among others. Biomass availability in the USA is between 512 million to 1.3 billion of dry tons per year [45] (section II.3). Energy and chemicals can be obtained from biomass, it has been estimated that the available biomass in the USA has the potential to supply over 33 % of the current demand for transportation fuels [45]. Renewable energy should account for at least 20 % of EU's final energy consumption by 2020 [35].

As a result, technologies to convert biomass efficiently to alternative fuels and chemicals are under development and it is estimated that the full resource potential from biomass will be available by 2050 when large scale bioenergy and biorefinery industries are expected to be commonplace [45].

Hydrogen has been recognized as a viable alternative for energy production for stationary and mobile applications. It has an energy content of 122 MJ.kg<sup>-1</sup> which is 2.75 fold than hydrocarbon (HC) fuels and will reduce dependence on oil while substantially and efficiently reducing emissions of air pollutants and greenhouse gases (CO<sub>2</sub>). Projections in oil savings could be of 5.3 M barrels.day<sup>-1</sup> assuming a 37 % market penetration of light duty fuel cell vehicles with H<sub>2</sub>, in the EU according to the H<sub>2</sub> road map, by 2020 sales of 0.4 to 1.8 M of hydrogen powered vehicles

per year are considered a realistic goal and by 2050 approximately 80 % of light-duty vehicles and city buses will be fuelled with CO<sub>2</sub>-free H<sub>2</sub> [35, 180] (sections I.4 and I.5). In countries like USA, UK, Germany, Japan, France, Italy and Sweden which are leading car manufacturers a strong H<sub>2</sub> infrastructure is being built consisting of production, delivery, storage, conversion and end use energy applications along with a strategic network of stationary and mobile refuelling stations (section I.5)

Biomass is, and will be, an important source for H<sub>2</sub> production, it has been projected that 64 M tonnes of H<sub>2</sub> per year will be needed for 300 M fuel cell vehicles and that the biomass required to produce 20 % of this demand will be 140 – 280 M MT.y<sup>-1</sup> [181]. In the EU between 15-30 % of H<sub>2</sub> production will come from biomass [35].

Current technologies for H<sub>2</sub> production depend on fossil sources which account for about 95 % of the H<sub>2</sub> produced [43, 95] (section I.3). Other technologies that are non-fossil fuel dependent and are under active research and development utilize renewable biomass (biomass gasification and biological hydrogen) and water (electrolysis, thermochemical splitting and solar photovoltaics) [43, 58, 141] (chapter II).

Due to increased attention to sustainable development based on clean and renewable energy sources and waste minimization, this study focuses our attention on biological hydrogen (bio-H<sub>2</sub>) technologies, in particular dark and photo fermentative processes which use the capabilities of different micro-organisms to convert sugars and organic acids (OA) derived from biomass to hydrogen [90] (sections II.4.2II.4.3). Hence, biomass hydrolysates rich in sugars and other useful derivatives (e.g. OA) are necessary for further conversion to produce bio-H<sub>2</sub>.

‘Biomass’ consists of 25 – 50 % cellulose, 20 – 40 % hemicellulose, 15 – 35 % lignin (section II.3). Food and lignocellulosic wastes are two of the most abundant and important sources of biomass.

#### *Food waste*

Food waste (FW) includes food materials discarded before or during food preparation. It includes a proportion of lignocellulosic material (peelings, husks, etc) as well as easily-degraded materials. The largest producers of FW are domestic and commercial kitchens. FW has an important social, economic and environmental impact especially in countries such as US and UK [25, 26]. It is estimated that ~ 16 M tonnes of food and drink waste is generated in the UK every year [182]. In 2002, Americans threw away ~ 43.6 M tonnes of food (leftovers from residences, commercial establishments and factory lunch rooms). Dumping food waste in landfill causes severe

environmental damage; it is an important contributor to anthropogenic release of methane gas, which is a greenhouse gas 25 times more potent than CO<sub>2</sub> [12], just the food and drink waste produced in the UK is equivalent to ~ 20 M tonnes of CO<sub>2</sub> emissions which constitutes ~ 3 % of the total UK annual GHG emissions [182]. The total “digestable” (able to be anaerobically digested) waste generated in the UK is ~ 110 M tonnes per year, including manure and agricultural wastes.

Food waste was shown previously to be digested microbially to make H<sub>2</sub> but previous studies did not include the recalcitrant lignocellulosic components. Furthermore other studies involving the conversion of food waste to H<sub>2</sub> by thermophilic acidogenesis long acclimation period (~ 3 months) of the seed sludge to the food waste was necessary to avoid methanogenesis during the thermophilic and acidogenic operational conditions [183].

#### *Lignocellulosic waste*

Lignocellulosic materials (wood, agricultural residues, grass, etc) are amongst the most abundant organic compounds representing a resource of hundreds of billions of tons per year [136, 142].

Agricultural residues (wheat, rice and corn straw, corn stover, grass, etc) are the biomass materials remaining after harvesting agricultural crops. These constitute an important biomass resource. Due to its abundance and availability, wheat straw (WS) provides an opportunity to provide feedstock for biotechnology plants for energy production. In 2000 the availability of WS in the EU was ~44 M tonnes.yr<sup>-1</sup> [17], an increase of up 7-fold on 2007 [182].

Spent grains (SG) are the by-products of the mashing process in brewing and, depending on the separation process, the amount of brewers’ SG would be 85 % of the total by products [21, 22]. About 3.4 M tonnes of brewery SG are produced in the EU every year and the UK contributes with 0.5 M tonnes annually. Brazil, the 4<sup>th</sup> largest beer producer, generated 1.7 M tonnes of SG in 2002 [23]. Brewery SG is a high volume low cost by-product valuable for bio-processing.

#### *Bioprocessability of biowaste*

Biowastes are not readily fermented by microorganisms due to their complex structure which also makes them resistant to enzymatic attack. Main factors that affect bio-processing are the porosity and crystallinity of lignocellulosic biomass and the lignin content; typically cellulosic materials are combined with lignin (section II.3). Biomass requires pretreatment for its utilization in bioprocesses such as biofuel production.

Pretreatment methods depend on biomass composition and are generally serve to remove lignin, hydrolyse hemicellulose, reduce cellulose crystallinity, and increase the porosity of materials;

the final goal is to improve the generation of sugars through the effective cleavage of the  $\beta$ -1,4-glycosidic linkage of the carbohydrate polymers (hydrolysis step), avoid the formation of inhibitory products for fermentation processes and be cost effective [46, 142] (see chapter III).

Common pre-treatment technologies for biomass include: physical (ball milling, grinding, etc), physico-chemical (hot compressed water), chemical (acid or alkaline), biological (fungi) and enzyme saccharification (cellulases and hemicellulases) (see chapter III) [141].

Hot compressed water (HCW) treatment is a suitable process to treat biomass; it can be defined as water at temperatures above 180 °C and various pressures (see chapter III). For lignocellulosic biomass, for example, HCW can be used firstly, as a pre-treatment step necessary to remove the lignin and hydrolyse the hemicellulose fraction which occurs at lower temperatures (200 °C) than cellulose hydrolysis. The cellulose part will become more accessible to either further HCW hydrolysis or enzymatic saccharification which will be the preferred step since it has been shown that glucose yields can be considerably improved by this process after HCW pre-treatment [46, 141, 142]. Many agricultural and food wastes contain starch, for those HCW treatment becomes an excellent alternative to hydrolyse the starch portion. Starch hydrolysis reactions in HCW proceed faster than cellulose due to the amorphous semi-crystalline structure with less hydrogen bonding and higher yields of sugars along with 5-hydroxymethylfurfural (5-HMF), a degradation product (DP) of sugars [145].

HCW hydrolysis of lignocellulosic materials produces hydrolysates containing not only sugars but a wide variety of compounds formed or released that could be toxic to microbial growth and fermentation. These can be divided in three main categories: furans, phenolics and aliphatic acids [174, 184]. Fig. 30 illustrates the main degradation pathways of the hydrolysis of lignocellulose. Further reactions between compounds will form different polymers that will be also present in the hydrolysates.

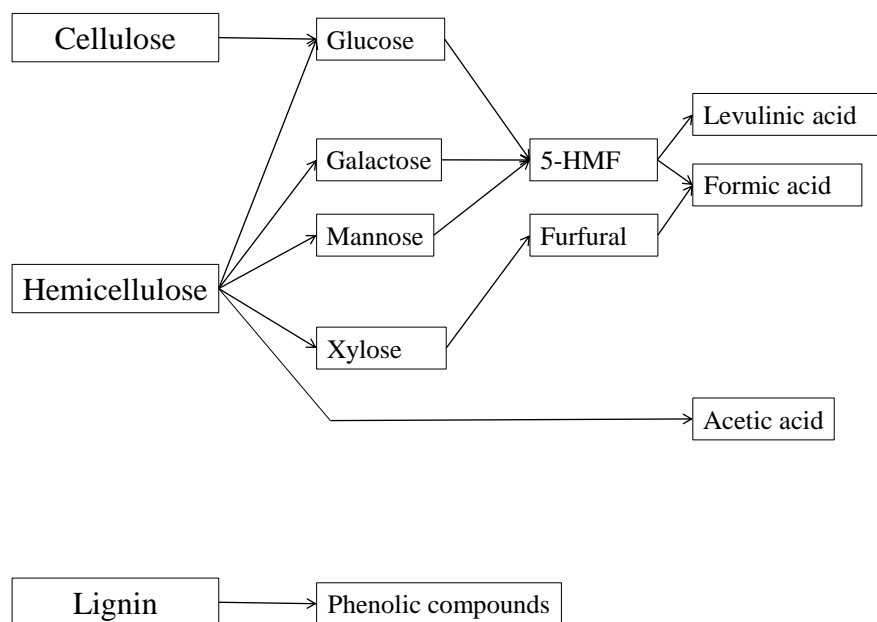


**Fig. 30** Degradation pathway of lignocellulosic compounds, adapted from Palmqvist (2000) [184].

Phenolic compounds are generally found to be more toxic than aliphatics or furans [173, 185], however different lignocellulosic hydrolysates produce a varied DP profile which is also influenced by treatment conditions (temperature, time). Some of these interact with each other positively or negatively for biological treatment; microorganisms exhibit different tolerance mechanisms towards DP and can tolerate them to varying degrees [174, 175]. Several authors have tried to elucidate the steps of inhibition of individual compounds and their interaction effects, which are important to optimize conditions during fermentation [141, 173, 174]. For example, Ezeji et al., 2007 investigated the impact of DP from agricultural residues on *Clostridium beijerinckii* and acetone-butanol-ethanol (ABE) fermentation, finding that furfural and 5-HMF in concentrations as high as 3 g.L<sup>-1</sup> are not inhibitory to *C. beijerinckii* BA101, yet a mixture of the two affected the culture negatively. Syringaldehyde, ferulic and p-coumaric acids which are DP derived from lignocellulosic materials however, were potent inhibitors of ABE production by this strain [19].

A detoxification step is necessary to increase the quality of the hydrolysate as fermentation feedstock through the removal of inhibitors without the loss of fermentable sugars. For this purpose enzymatic, physical and chemical methods can be employed. Biological methods are based on treatments with enzymes such as peroxidase and laccase which leads to selective and virtually

complete removal of phenolic monomers and phenolic acids; Physical methods are based on phase equilibria separations such as liquid-liquid extractions or physical adsorption onto a solid substrate as for example activated carbon (AC); Chemical methods such as ‘overliming’ consist on chemical modification of the inhibitor to a less toxic or non-toxic compound [19, 141, 175]. Comparisons between these methods, however, are difficult when different lignocellulosic hydrolysates and different microorganisms have been used.

In this work we studied the impact of some of the lignocellulosic waste and food waste hydrolysates inhibitors on growth and hydrogen fermentation by *E. coli* strain HD701. Hydrolysates obtained from HCW + CO<sub>2</sub> treatment at 200-240 °C of wheat straw (WS), brewery grain (BG) from a brewery and food waste (FW) from a central kitchen were detoxified with AC and evaluated for hydrogen production using *E. coli* strain HD701, the best hydrolysate was selected for a larger scale (5 L) fermentation using the same *E. coli* strain.

## Materials and Methods

Unless otherwise stated chemicals and laboratory media components were obtained from Sigma-Aldrich or Fisher Scientific and were of analytical grade. Activated carbon (AC) COLORSorb G5 was provided by John Lever, Jacobi, UK. *E. coli* HD701 ( $\Delta hycA$ ; upregulated for production of H<sub>2</sub>) derived from parental strain MC4100 was provided by Professor Frank Sargent (University of Dundee, Dundee, UK). Wheat straw was provided by Professor Guy Barker, University of Warwick, UK; spent brewery grain was provided by Heineken UK Ltd and food waste was supplied by Mark Houghton, Central Kitchens, University of Birmingham, UK.

### *Effect of degradation products (DP) on growth*

For growth and fermentation inhibition of DP, different concentrations of some aldehydes or phenolic compounds usually found in lignocellulosic hydrolysates were introduced into Erlenmeyer flasks containing 10.8 g.L<sup>-1</sup> (60 mM) glucose. This mixture (MX) was sterilised by autoclaving just before use.

For combinatory tests to determine the effect of the interaction of DP on growth and H<sub>2</sub> production, a mixture (Mix1) containing (in g.L<sup>-1</sup>): 1.5 of 5-HMF, 0.9 of furfural and 3.6 of glucose; and a mixture (Mix2) containing (in g.L<sup>-1</sup>): 0.3 Furfural, 0.6 SA, 0.6 FA, 0.3 CA, 0.6 5-HMF and 3.5 of glucose were prepared, phenol was not included.

Colonies were picked from nutrient agar plates maintained at 4 °C into two 5 ml vials of nutrient broth solution with added sodium formate (0.5% w.v<sup>-1</sup>) pH 7 and shaken (180 rpm) for 6 h at 30 °C, 180 rpm before use. The contents of each vial were mixed together and the concentration of cells (OD<sub>600</sub>) was measured.

The media formulation used in this test was prepared according to appendix section VIII.1.5.

After inoculation (1 % v.v<sup>-1</sup>) aliquots (10 mL) of the inoculated media were transferred into sterile 50 mL Erlenmeyer flasks and mixed with 5 mL of the MX stock. Aliquots (5 mL) were incubated in universal flasks (30 °C; 180 rpm). The OD600 was measured after 18 h.

#### *Toxicity of hydrolysates on growth*

Media formulation and inocula were prepared as described above. Hydrolysate stocks were obtained by HCW treatment (see below). Aliquots (45 mL) of the inoculated media were poured into 100 mL Erlenmeyer flasks previously autoclaved and mixed with 5 mL of the hydrolysate stock (filter sterilized). Aliquots (5 mL) were taken into universal bottles and incubated (30 °C; 180 rpm). OD600 was measured after 18 h.

#### *Effect of DP on Hydrogen production*

To evaluate the impact of the DP contained in MX, Mix1, Mix2 and hydrolysates on *E. coli* HD701 and hydrogen fermentation, small fermentation tests were performed using 60 ml glass serum bottles as described in appendix VIII.1.4. For the DP the pH was not adjusted.

Stocks of *E. coli* HD701 were maintained and aerobically pre-grown as described in appendix section VIII.1.1. [100].

Reactors contained 10 ml of sterile medium consisting of Bis-Tris buffer (0.1 M) and Na<sub>2</sub>SO<sub>4</sub> (0.0435 M) (pH 6.5) and 5 ml of each mixture MX or hydrolysate (filtered sterilized) stock solution, made anaerobic by purging with N<sub>2</sub> for at least 30 minutes. To this was added 0.5-1 ml of the cell suspension to a final cell concentration of 1 g dry weight.L<sup>-1</sup>, before purging for a further 3-5 min.

Reactors were incubated at 30 °C (180 rpm, 20 h). After incubation H<sub>2</sub> produced was calculated as described by Orozco et al., 2011 [145].

#### *Bio-waste pretreatment*

Wastes (Table 17) were blended using a standard kitchen blender and except for the kitchen food waste, they were dried at 60 °C to determine the moisture content and passed through a 420 µm mesh (mesh 36) before samples were treated by hot compressed water (HCW).

### *HCW reaction*

The reaction was performed in a 250 cm<sup>3</sup> reactor (Parr series 4570/80 HP/HT) made of alloy C-276, equipped with a heat/agitation controller (model 4836) and a cooling system (Grant LTD6/20) as described in [145].

Concentrations of each bio-waste ranging from 30 - 40 g (dry basis).L<sup>-1</sup> were suspended in de-ionized water (DW) to a final volume of 150 cm<sup>3</sup> leaving a headspace in the reactor of about 100 cm<sup>3</sup>. The reactions were performed at temperatures within 200-250 °C; 15 min holding time with the addition of CO<sub>2</sub> as described by Orozco et al. 2011 [145].

Reaction conversions ( $X_p$ ) will be calculated according to the formula: [(Initial sample concentration (ISC)-residue after the reaction)/ISC]\*100; ISC and residues are expressed in g (dry basis).L<sup>-1</sup>

### *Detoxification*

After cooling, the hydrolyzates were treated with AC powder as described in appendix section 0 [175]. The treated hydrolyzates were vacuum filtered through a layer of filter paper (Fisherbrand QL100). Hydrolyzates and samples were kept at -20 °C for tests and analysis.

### *Fermentation and H<sub>2</sub> production*

Cells of *E. coli* were aerobically pre-growth for high density culture (EF media) in fermenter as described in appendix section VIII.1.2. The pH control was not required during aerobic growth for the initial 40 - 44 h, after which the transition to anaerobic fermentation was made by purging with oxygen-free N<sub>2</sub> (30 min, 1 L.min<sup>-1</sup>) and after the addition of 20 mL of 2 M glucose the pH was allowed to fall to 6 and thereafter was maintained automatically by the addition of 2 M NaOH for the 2<sup>nd</sup> phase of hydrogen production. Once H<sub>2</sub> production had ceased and glucose was totally consumed (verified by DNSA reducing sugars assay) (see appendix section VIII.4.1) approximately 700 mL of the produced hydrolysate was added to the fermenter (filter sterilized) while purging with N<sub>2</sub> to maintain anaerobiosis; after hydrolysate addition N<sub>2</sub> was stopped and a 3<sup>rd</sup> phase of H<sub>2</sub> production that depended on the sugar content of the hydrolysate was allowed to proceed. H<sub>2</sub> and CO<sub>2</sub> production were measured using low-flow gasmeters, as described previously [186]. Meters were placed upstream and downstream of a 'scrubber' solution containing 2 M NaOH and universal indicator, so that the CO<sub>2</sub> could be calculated by subtraction. Saturation of the scrubber solution is revealed by a colour change. This method was shown by gas chromatography (GC) to remove CO<sub>2</sub> to below 0.05% (v.v<sup>-1</sup>) from the H<sub>2</sub> stream.

### *Analysis*

Organic acids (OA) in hydrolysates and fermentation samples were analysed by anion HPLC using a Dionex 600-series system [107]; sugars and 5-HMF by HPLC (Agilent 1100 series) as described in [145]. Preliminary work showed that H<sub>2</sub> and CO<sub>2</sub> are produced in 1:1 ratio for most *E. coli* fermentations (section 0). Furfural and phenolics were analysed by reverse phase HPLC using an Agilent 1100 with a DAD-UV detector/analyser (270nm, 320nm) fitted with a Phenomenex Synergi 4u Fusion-RP 80A, 250 x 4.6 mm column coupled with a guard cartridge.

The column temperature was set to 40°C with a flow rate of 1.0 mL.min<sup>-1</sup>. The mobile phase was water/methanol both modified with 0.1% formic acid. The HPLC method starts with 100% water for 5min and then changes to water/methanol 50:50 for 30 min. Finally the mobile phase returns to 100% water for 5min.

Cellulose was quantified as described in appendix section 0.

Lignin in WS and BG was analysed using the Klason assay as described in the appendix section 0.

The concentration of cells for the fermentations was measured using a UV/visible spectrophotometer (Ultrospec 3300 pro) and H<sub>2</sub> produced was measured using a combustible gas meter (Gasurveyor2, GMI) as described in appendix section VIII.2.1.

FW and BG were analysed after drying to constant mass at 60 °C and grinding to pass through a 420 µm mesh. Starch and total sugars were estimated as described in [132] (see section VIII.4.1).

## **Results and discussion**

### *Effect on growth and fermentation by DP*

Hot compressed water hydrolysis (HCW) of a food waste (FW) rich in starch and lignocellulosic biomasses such as wheat straw (WS) and spent brewery grain (BG) was examined in this work. These hydrolysates contain a variety of DP that may have a negative impact on growth of the model organism *E. coli* HD701 and fermentation. These products include furfural, 5-HMF, syringaldehyde (SA), *p*-coumaric acid (CA), ferulic acid (FA), phenol and other phenolic compounds. A preliminary test was done involving various concentrations of these chemicals (0.75, 1.5 and 3 g.L<sup>-1</sup>) that were used in the preparation of MX and their effects on growth and H<sub>2</sub> production were investigated. Experiments were repeated twice and variations between them were

within 7 %. It is important to note that during the preparation of MX, some of the chemicals (SA, CA, FA and furfural) were insoluble or partially soluble in water but (at the concentrations tested) became soluble after autoclaving. As shown in Fig. 31, all of these compounds had a negative impact on cell growth which increased with concentration of the DP when compared to the glucose control. SA was found to be the least toxic compound, reducing growth by 16 % when media contained 0.75 g.L<sup>-1</sup> reaching maximum inhibition (66 %) at a concentration of 3 g.L<sup>-1</sup>. 5-HMF at 0.75 g.L<sup>-1</sup> reduced growth by 43 % and by 61% at concentrations of 1.5 g.L<sup>-1</sup> and 3 g.L<sup>-1</sup>. Furfural, CA, phenol and FA were the most toxic as they completely inhibited growth at concentrations above 1.5 g.L<sup>-1</sup> and furfural reduced growth by 77 % when present at 0.75 g.L<sup>-1</sup>. Conversely, furfural and 5-HMF were suggested to stimulate the growth of *C. beijerinckii* BA101 (a butanol producing strictly anaerobic bacterium); furfural (2 g.L<sup>-1</sup>) increased cell growth by 7 % compared to the maximum achieved in the control and 5-HMF (2 g.L<sup>-1</sup>) by 14 % [19].

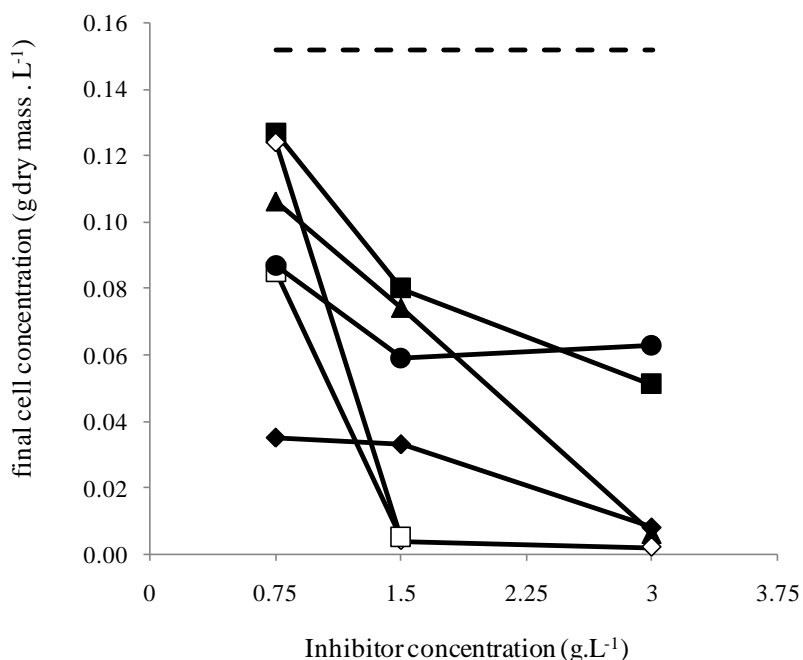


**Fig. 31** *E.coli* HD701 growth after 18 h vs. inhibitor concentration. (◆) Furfural; (■) SA;( ▲) FA; (◇) Phenol;( □) CA;(●) 5-HMF; (---) Control (glucose alone, no additives).

In contrast to their effects on growth, DPs had the opposite effects on *E. coli* anaerobic fermentation, and were stimulatory to varying degrees. H<sub>2</sub> production was stimulated by SA reaching a maximum at 0.75 g.L<sup>-1</sup> with a yield 37% higher than the glucose control (C) (Fig. 32).

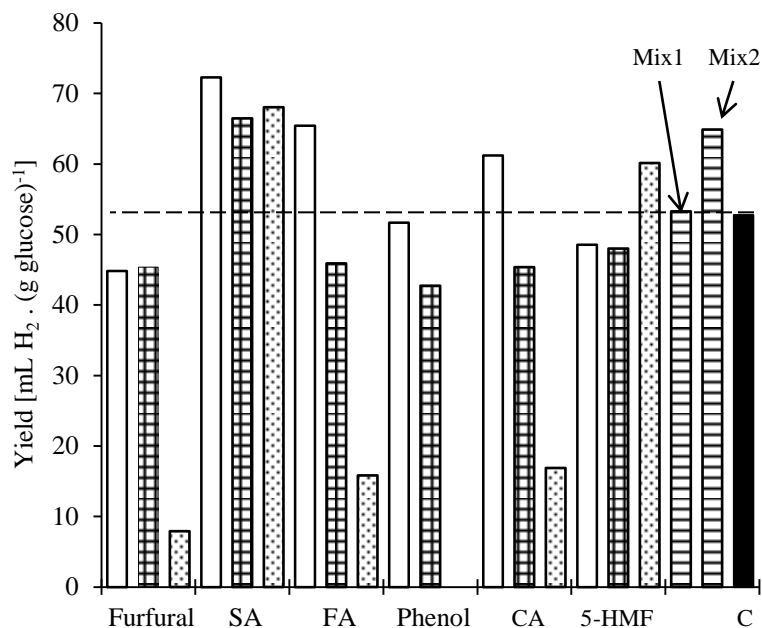


**Fig. 32** Yields of *E. coli* HD701 H<sub>2</sub> fermentation at different DP concentrations. (White bars) 0.75 g.L<sup>-1</sup>; (square filled bars) 1.5 g.L<sup>-1</sup>; (dotted bars) 3 g.L<sup>-1</sup>; (black bar/dotted line) glucose control (20 mM).; SA, syringaldehyde; FA, ferulic acid; CA, *p*-coumaric acid; Mix1, mixture 1; Mix2, mixture 2. Phenol H<sub>2</sub> yield at 3 g.L<sup>-1</sup> was zero.

At higher concentrations (1.5 and 3 g.L<sup>-1</sup>) its effect was still stimulatory (~ 27 %), which is interesting considering that SA was the least inhibitory DP during aerobic growth. FA, CA and 5-HMF also had stimulatory effects on H<sub>2</sub> production at concentrations of 0.75, 0.75 and 3 g.L<sup>-1</sup> with H<sub>2</sub> yields of 24, 16 and 14 % respectively, higher than the control. FA and CA began to inhibit H<sub>2</sub> production as their concentration increased reaching a minimum yield which was 70 % less than the control at 3 g.L<sup>-1</sup> in both cases. Furfural and phenol were completely or almost completely inhibitory to H<sub>2</sub> production when present at 3 g.L<sup>-1</sup>; at lower concentrations they reduced H<sub>2</sub> production in the order of ~15 % than that achieved in the control. FA, CA and phenol are phenolic compounds which, at lethal concentrations, have been found to cause inhibition by affecting membrane permeability [173]. However *E. coli* HD701 exhibited good tolerance of these compounds at concentrations of 0.75 g.L<sup>-1</sup>. At these sub-lethal concentrations of FA and CA, bacterial cells have been shown to modify the fatty acid composition of their lipids; as a consequence there is an increase in the degree of saturation of lipids which probably compensates for the increase in fluidity of the membrane induced by the phenols [187]. Furfural and 5-HMF are the main furan derivatives found in lignocellulosic hydrolysate. Intracellular sites seem to be the primary inhibition targets of these compounds which cause DNA mutation and probably have a direct effect on glycolytic and fermentative enzymes since furfural and 5-HMF can react with many

types of biological molecules such as proteins, nucleic acids and lipids [185]. Furfural is more toxic than 5-HMF and has been found to be a strong inhibitor that also interacts synergistically with other inhibitors [185]. As indicated by H<sub>2</sub> production, furfural had an inhibitory effect on the cell metabolism even at the lowest concentration tested (0.75 g.L<sup>-1</sup>) (Fig. 32).

Conversely, *E. coli* HD701 exhibited good tolerance and even stimulation via SA as shown by its H<sub>2</sub> yields which are > 27 % compared to the glucose control (Fig. 32). SA, an aromatic aldehyde, has been proved to have strong detrimental effects on fermentation of *Clostridium beijerinckii* BA101 and to reduce growth and ethanol production by *E. coli* LY01 [185]. The hydrophobicities of furfural, 5-HMF and SA correlates with their toxicities, which implies that their toxicity involves a hydrophobic target such as cell membrane or other hydrophobic sites within the cell [174, 185]. Miller et al., 2009 found that in long adaptation experiments with ethanologenic *E. coli* furfural tolerance was achieved by silencing several NADPH-dependent oxidoreductases [188]. The enzymes, genes involved and the metabolic mechanism that allowed the assimilation of SA and other compounds by *E. coli* HD701 and enhanced H<sub>2</sub> production have not yet been determined.

In the combinatory tests utilizing Mix1 and Mix2 to determine the effect of the interaction of furfural and 5-HMF on growth and H<sub>2</sub> production, the concentrations of these DP was chosen to be higher than the expected to be found in the hydrolysates after detoxification with AC (see later in this section). Mix2 reduced growth by 91 % compared to the glucose control showing that there is a synergistic effect by all the DP present in the mixture in growth inhibition. Growth test on Mix1 was not done, however in previous work (data not shown) a 3<sup>rd</sup> mixture (not previously introduced) containing 0.24 g.L<sup>-1</sup> 5-HMF, 0.14 g.L<sup>-1</sup> furfural and 3.6 g.L<sup>-1</sup> of glucose (concentrations still higher than in detoxified hydrolysates) reduced growth by 26 % compared to the control confirming a synergistic inhibition on growth of *E. coli* HD701 by this binary combination. H<sub>2</sub> production by *E. coli* in the presence of Mix1 and Mix2 is shown in Fig. 32. Mix1 generated a similar H<sub>2</sub> yield to the control, however in Mix2 the combinatory effect of the DP used was additive yielding 23 % more H<sub>2</sub> than the control.

#### *Bio-wastes*

Bio-wastes were sourced from a catering kitchen, University of Warwick and a brewery (see Materials and Methods). Their composition is shown in Table 17, Lignocellulosic wastes were BG and WS. FW contained significant starch (21 % wet weight).

**Table 17** Characterization of food waste, brewery grain and wheat straw.

Waste	Description	Moisture content (% w/w)	Cellulose (% w/w dry matter)	Hemicellulose <sup>b</sup> (% w/w dry matter)	Lignin <sup>c</sup> (% w/w dry matter)	Starch (% w/w wet matter)
Food waste (FW) <sup>d</sup>	Rice, pasta (cooked). Blended	72.6	ND	ND	ND	21.1
Brewery grain (BG) <sup>a</sup>	Spent grain from brewery process. Dried and ground to pass through a mesh 36	75.5	16-25 <sup>a</sup>	28-35 <sup>a</sup>	7-27 <sup>a</sup>	1.22
Wheat straw (WS)	Agriculture residue Grinded to pass through a mesh 36	1.5	39.5 <sup>b</sup>	21.2 <sup>b</sup>	20.2 <sup>c</sup>	ND

<sup>a</sup> Also contains 15-23 % dry weight proteins; from Aliyu et al. (2010) [22].

<sup>b</sup> From Wiseloge et al. (1996) [189].

<sup>c</sup> Determined by Klason assay following the ASTM Standard method E 1721 – 01 (appendix section 0).

<sup>d</sup> Same sample as ‘catering waste X’ described in BITE IBR paper, nearly in submission

ND = Not Determined.

### *HCW reaction parameters*

Table 18 shows HCW reaction parameters for the selected wastes. HCW hydrolysates were obtained at different temperatures ranging from 200 to 250 °C for BG; 200 to 230 °C for FW and; 200, 240 °C for WS. The variety of product conversions ( $X_p$ ) observed may be associated to waste composition. For BG small variations in final pH ( $pH_f$ ) were noticed compared to initial pHs ( $pH_i$ ), at temperatures of 200 and 220 °C  $pH_f$  was lower and  $X_p$  related to those temperatures were between 53 and 58 %; at 240 and 250 °C  $pH_f$  were higher with also higher  $X_p$  (63-64 %). At the lower temperatures (200-220 °C) it is likely that the lignin and hemicellulosic fraction of the BG hydrolysate is hydrolysed (see Chapter III), and most cellulose expected to remain unreacted. At higher temperatures cellulose begins to hydrolyse, which explains the higher  $X_p$ , but degradation of the lignin and hemicellulose products may also have occurred, and probably some reactions between DP that would explain the increase in  $pH_f$ .

FW HCW hydrolysis yielded higher  $X_p$  at the temperatures tested (83-93 %) suggesting almost complete hydrolysis of the starch and other constituents of the waste. Variations in pH were small but always lower than the  $pH_i$  probably due to the generation of OA.

WS HCW reactions showed not only the lowest  $X_p$  at the corresponding temperatures but also the most change in pH (Table 18). As with BG, it is expected that the lignin and hemicellulose

fraction were hydrolysed at 220 °C with most cellulose remaining unreacted. At 240 °C the ~ 58 % increase in  $X_p$  suggests that some of the cellulose present in the reaction has hydrolysed. The pH decrease could also be attributed to the production of OA.

**Table 18** Reaction parameters for the tested wastes at different temperatures.  $X_p$  is calculated according to the formula:  $[(\text{Initial sample concentration (ISC)} - \text{residue}) / \text{ISC}] * 100$

Sample	Temp	pH <sub>i</sub>	pH <sub>f</sub>	$X_p$
g.L <sup>-1</sup>	(°C)			(%)
BG	33.4	200		57.5
	33.6	220	4.2 ± 0.1	53.0
	40.1	240		63.2
	40.1	250		64.2
FW	32.5	200		83.4
	37.8	220	4.5 ± 0.1	93.3
	36.9	230		93.3
WS	38.5	220	7.2	34.5
	38.5	240		54.3

#### *Hydrolysate products*

Hydrolysate product distribution before AC treatment for BG is illustrated in Fig. 33. The maximum yields [mg (g starting material (SM))<sup>-1</sup>] of sugars were obtained at a reaction temperature of 200 °C, attributable to the hydrolysis of the hemicellulose fraction. Galactose was the main sugar produced with a yield of 32.4 mg.g SM<sup>-1</sup> followed by fructose (resulting from the keto-enol tautomerization of glucose) [54] (16.6), glucose (10.4), sucrose (10.4), maltose (7.6). At 220 °C furfural, a DP from hemicellulose, was the main inhibitor and product produced with a maximum yield of 52.7 mg.g SM<sup>-1</sup> along with lower amounts of 5-HMF (6.7), a DP from glucose and fructose. At temperatures of 240 and 250 °C the yields of sugars strongly decreased with fructose predominating as the main identified sugar and also with lower yields of furfural and 5-HMF.

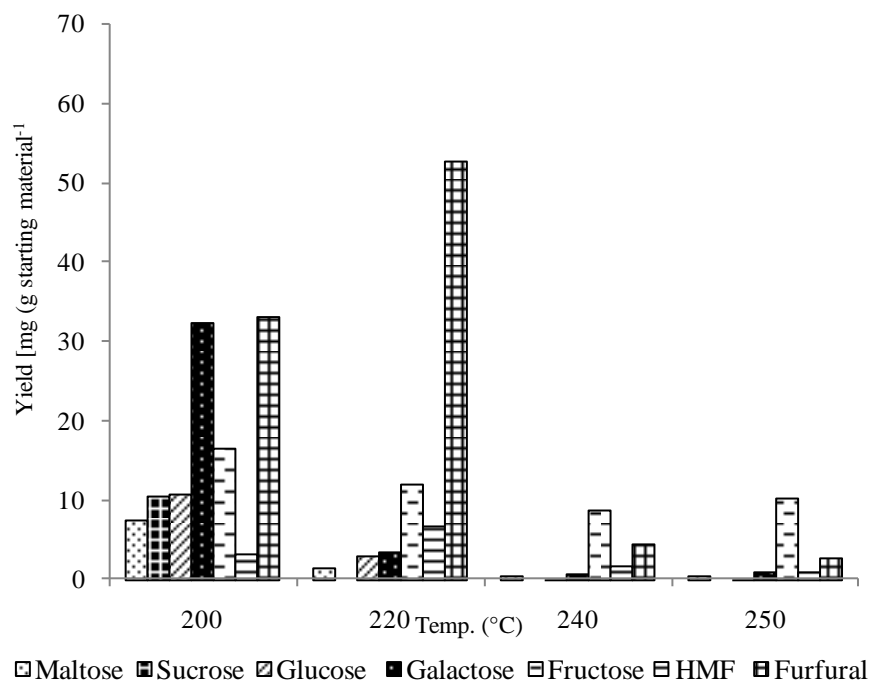


**Fig. 33** Shows yields of products in BG hydrolysates before AC at different reaction temperatures.

For example, Fig. 34 shows an HPLC chromatogram of the BG hydrolysate at 220 °C which has the highest content in furfural and 5-HMF. The peaks of these compounds are shown along with other various unidentified compounds before treatment with AC.

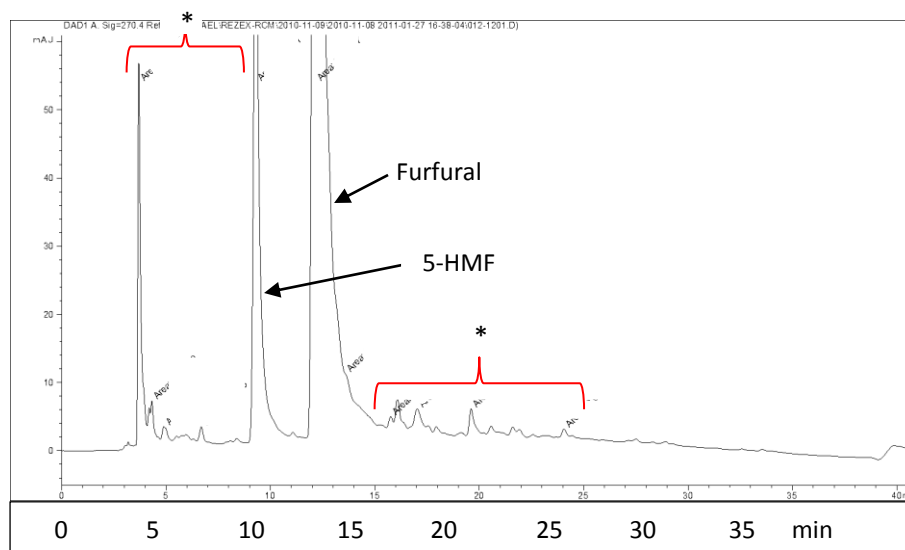


**Fig. 34** HPLC chromatograph for BG hydrolysate at 220 °C before AC. The horizontal axis represents retention time (min); the vertical axis represents the refractive infrared units (RIU). (\*) shows unidentified peaks.

BG contains proteins in significant amounts [22]. Proteins hydrolyse to amino-acids (AA) which under HCW conditions at temperatures within 225-300 °C (depending on the AA) decompose following two main degradation pathways: de-amination to produce ammonia and OA, and decarboxylation to produce carbonic acid and amines [23, 190]. The presence of ammonia would explain the higher  $\text{pH}_f$  at temperatures of 240 and 250 °C but was not tested. The addition of protein hydrolysis products (PHP) and in some cases AA to the reaction will increase the complexity and variety of hydrolysis products which would also influence, in turn, the growth and fermentation of *E. coli*. In the presence of heat, amines and aldose sugars react *via* the Maillard reaction [191]; the carbonyl group of the sugar reacts with the nucleophilic amino group of the AA forming a complex mixture of molecules that are responsible for a range of odors and flavours. At high temperatures, acrylamide can be formed. The reduction in sugars found at 220 °C (Fig. 33) suggests such reactions may have taken place under these conditions.

The products resulting from FW hydrolysis are shown in Fig. 35. FW yielded sugars at optimum yield at 200 °C; the main sugar produced was glucose with a yield of 35.9 mg.g  $\text{SM}^{-1}$  followed by maltose (27.3) and fructose (8.5). Galactose (not shown) was also present in smaller amount. 5-HMF was the main DP (8.5) and traces of furfural (0.93). At 220 °C the yields of glucose and fructose remained fairly constant whereas the yield of maltose decreased to 5.3 in combination with a strong increase in 5-HMF and furfural yields to 34.9 and

4.9 [mg (g starting material)<sup>-1</sup>] respectively. Furfural would come from further degradation of hemicellulose derived sugars whereas the increase of 5-HMF without a decrease in glucose can be explained by the combinatory hydrolysis of maltose (a disaccharide) to form more glucose with the degradation of glucose to form more 5-HMF. At 230 °C however glucose and fructose remained in very small amounts, furfural probably degraded to formic acid and 5-HMF remained as the main compound with its yield down to 24.9 [mg (g SM)<sup>-1</sup>].

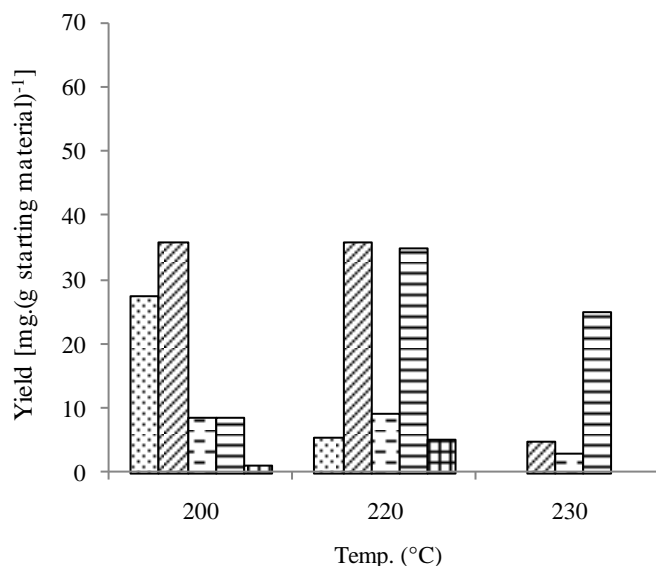


**Fig. 35** Shows yields of products in FW hydrolysate before AC at different reaction temperatures. Symbols are the same as in Fig. 33.

Fig. 36 shows the product distributions after HCW treatment of WS at 220 and 240 °C. In contrast to BG and FW little sugar was obtained from WS. Furfural was the main product yielding 68.4 [mg (g SM)<sup>-1</sup>] followed by 5-HMF, which is indicative of sugar degradation.

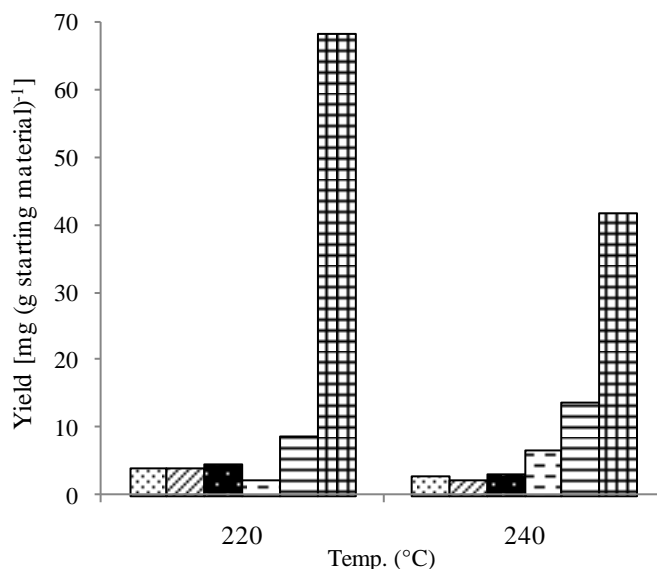


**Fig. 36** Show yields of products of WS hydrolysate before AC at 220 and 240 °C. Symbols are the same as in Fig. 33.

It is important to take in consideration that product distribution could be also affected by leaching of the reactor wall materials (see section VI.3.2) [178].

OA were analysed only after hydrolysates underwent detoxification with AC and the OA found in each hydrolysate are shown in Table 19. AC treatment was applied for the removal of toxic compounds (below) and AC was shown previously not to remove significant amounts of OAs.

In BG lactic acid was the main OA found at 220 °C with a yield of 24.3 [mg (g SM)<sup>-1</sup>] followed by acetic and formic acid (yields of 23.9 and 5.9 respectively); lactic acid would come from the dehydration, decarboxilation and deamination of several AA such as Serine and Alanine [190] which are very likely to be present in these hydrolysates.

For FW acetic and formic acids were present in the hydrolysate with yields of 8.9 and 4.5 respectively along with smaller amounts of lactic acid which will probably come from some protein content in the FW (Table 17). Acetic acid was the main OA generated by WS (Table 19).

**Table 19** Shows hexoses (glucose, galactose and fructose) concentration (mM) and yields [mg (g starting material)<sup>-1</sup>] in the hydrolysates after AC; Cell concentration on growth test for the selected hydrolysates before and after AC (BAC, AAC); H<sub>2</sub> and OA yields AAC at indicated reaction temperatures. FW, food waste; BG, brewery grain and WS, wheat straw.

Waste	Reaction temp. (°C)	Hexose (mM)	Hexose yield mg.(g waste) <sup>-1</sup>	Organic acids			Cell concentration		H <sub>2</sub> yield mL H <sub>2</sub> (g waste) <sup>-1</sup>
				Lac	Ac	Form	g dry mass.L <sup>-1</sup>		
				mg (g waste) <sup>-1</sup>			BAC	AAC	AAC
BG	200	10.85	55.3	ND	ND	ND	ND	ND	5.4
	220	3.157	13.3	24.2	23.9	5.9	0.05	0.20	2.5
	250	1.8	9.2	ND	ND	ND	ND	ND	0
	240	2	8	ND	ND	ND	ND	ND	0
FW	200	11.5	45.5	1.5	8.9	4.5	0.21	0.78	11.1
	220	9.1	43.5	ND	ND	ND	ND	ND	10.5
	230	1.2	5.9	ND	ND	ND	ND	ND	0.5
WS	220	1.32	5.8	3.7	32.7	6.7	ND	0.32	1.6
	240	0.9	5.6	ND	ND	ND	ND	ND	1.7
Control		20					0.151		47.7

#### *Application of AC to remove inhibitory compounds.*

Physical detoxification methods based on adsorption onto AC have proved to be effective at removing furans and phenolics while retaining the sugars in the hydrolysate [145, 175]. The critical phase of adsorption involves an attraction similar to Van der Waals forces (London forces). It is the intensity of these forces along with the potential of the adsorbate (AC) to remain in contact with the wall of the pores of AC for a sufficient time to effect the electrical attraction and for adsorption to take place. The potential of the adsorbate is a result of the combination of its micropore ( $r \leq 1$  nm) and mesopore ( $r = 1-25$  nm) structure which in this case is  $0.19$  and  $0.37$  cm<sup>3</sup>.g<sup>-1</sup>, respectively (supplier data).

For BG, 5-HMF was practically removed from all hydrolysates. Furfural gave a 5 and 36-fold decrease in concentration at 200 and 220 °C, respectively (not shown) and was completely adsorbed from the hydrolysates obtained at higher temperatures. HPLC analysis showed that AC also removed most of the minor components as shown in Fig. 37 corresponding to BG's 220 °C hydrolysate before and after AC. In regards to sugars, 83 to 96 % of all sugars present remained in the hydrolysate obtained at 200 °C, which had the highest sugar concentration.

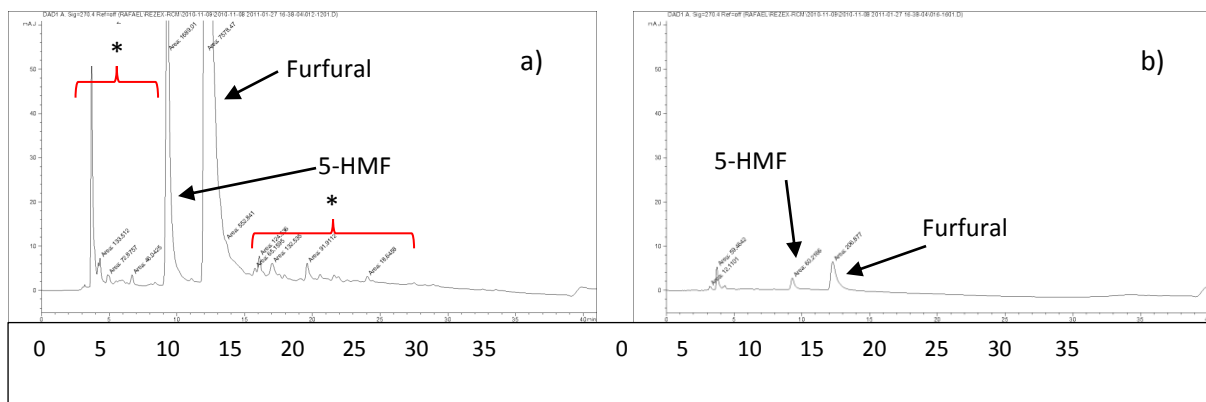


**Fig. 37** Shows HPLC chromatographs for BG hydrolysate at 220 °C a) before and b) after AC. Note that most of the peaks have diminished or disappeared after the AC treatment. (\*) unidentified peaks; vertical axis represents the refractive infrared units (RIU)

In the case of FW, 5-HMF and furfural were completely removed by AC (not shown) while 85 to 92 % of the sugars generated remained in the hydrolysates at temperatures of 200 and 220 °C.

In WS, all 5-HMF was removed by AC along with 98 % of the furfural at 220 and 240 °C (not shown).

These results show that the hydrolysates obtained from the different wastes were highly detoxified by AC treatment without substantial losses in sugar content demonstrating that AC had more affinity towards furans, phenolic, OA and amine compounds. The removal of sugars by the AC treatment was not bigger than 10 % (data not shown).

Table 19 summarizes the concentrations and yields of hexose sugars (glucose, galactose and fructose) in detoxified hydrolysates. BG hydrolysate at 200 °C had the highest yield with 55.3 mg hexose.(g starting material)<sup>-1</sup> followed by FW hydrolysates at 200 and 220 °C yielding 17 and 21 % less. The rest of the hydrolysates (T ≥ 220 °C) only reached yields within the range of 5.6 –13.3 mg hexose.(g starting material)<sup>-1</sup> which is evidence of sugar degradation and/or possible reactions between hydrolysis and degradation products catalyzed by temperature or by other substance leached from the reactor wall materials (Ni) into the reaction media [178].

Even though BG and FW hydrolysates rendered the highest hexose yields, they were far below compared to those obtained at optimum conditions under the same reaction system from starch [145] and cellulose [192] (see sections 0 and VI.3 respectively), 587 and 228 mg hexose (g SM)<sup>-1</sup> respectively.

### *Growth tests on hydrolysates before and after AC treatment*

For growth tests a hydrolysate from each waste was selected based on its sugar and DP yields. Table 19 shows the growth observed for FW, BG and WS hydrolysates at 200, 220 and 220 °C, respectively, before and after AC treatment (except for WS which was only examined after AC treatment); in all cases the detoxified hydrolysates supported substantially more growth than the un-treated hydrolysates and with the exception of the BG hydrolysate BAC, which was evidently toxic, the cell yields all exceeded the glucose test. This suggests that the unidentified DP present in these hydrolysates were assimilated by *E. coli* HD701 and had an additive effect that promoted growth. FW hydrolysate AAC yielded the most growth with a yield 5-fold bigger than the control. BG and WS also supported more growth than the glucose test but not as much as FW.

### *Fermentability of the waste hydrolysates AAC*

Table 19 shows the hydrogen yields resulting from the fermentation test of the hydrolysates AAC with *E. coli* HD701. Hydrolysates of FW at 200 and 220 °C produced the highest yield of H<sub>2</sub> with 11.1 and 10.5 [mL H<sub>2</sub>.(g SM)<sup>-1</sup>], respectively. These yields are, however, ~ 4 times lower than the H<sub>2</sub> yield of the glucose test; yet the glucose concentration in the C test was 20 mM which is ~5 times higher than the hexose concentration, therefore, an unidentified component of the FW hydrolysate enabled the production of more H<sub>2</sub> per mol hexose. As discussed above, *E. coli* showed, with the exemption of furfural and phenol, excellent tolerance to individual DP tested when present at concentrations of 0.75 g.L<sup>-1</sup> (4-6 mM), in addition they were found to have a stimulatory effect on H<sub>2</sub> production even in the combinatory tests (Mix1 and Mix2), after detoxification of the hydrolysates the DP concentrations were highly diminished or eliminated by the treatment as previously demonstrated.

Despite its higher hexose concentration, the H<sub>2</sub> yield from BG (200 °C) was 49 % lower than from FW (220 °C) indicating additional H<sub>2</sub> inhibitory compounds in the BG hydrolysate.

BG H<sub>2</sub> yield at 220 °C was 54 % lower than the BG at 200 °C attributed to its lower sugar content (see Table 19). BG hydrolysates at 240 and 250 °C did not produce any H<sub>2</sub>.

The H<sub>2</sub> low productivity of 1.6-1.7 [mL H<sub>2</sub>.(g SM)<sup>-1</sup>] from WS hydrolysate could also be due to the low sugar content of the hydrolysates at 220 and 240 °C but it should be noted that *E. coli* is not the best microorganism to be employed in these experiments due to its limited substrate utilization.

With the exception of BG hydrolysates, from these results we can summarise that: 1) Low H<sub>2</sub> yields are attributed to the low sugar content of the hydrolysates rather than the presence of inhibitors and 2) with the exception of phenol and furfural, the inhibitors included in this study if present in amounts ~ 0.75 g.L<sup>-1</sup> (4-8 mM) could have a synergistic additive effect on H<sub>2</sub> yields by *E. coli* HD701, also assuming that their extra yield is not due to an unidentified additional fermentation substrate.

#### *Fermentation of wastes*

FW was selected for 3 L fermentations due to its high sugar content and the H<sub>2</sub> yields supported. It was necessary to repeat the HCW reaction 3 times at 220 °C using 200 g.L<sup>-1</sup> dry basis of FW to obtain ~700 mL of hydrolysate (enough only for one experiment) with hexose content of 46.2 mmol distributed as follows: Glucose 33.04 mmol, Galactose 4.8 mmol and fructose 8.4 mmol as the main sugars. The hydrolysates were de-toxified using 7.5 % (w.v<sup>-1</sup>) AC instead of the usual 5 % since increased amounts of DP were expected due to the higher concentration of FW (~200 g.L<sup>-1</sup>) in reactions, after detoxification a concentration less than 0.31 mmol of furfural and 5-HMF remained in the combined hydrolysate. Fermentation was performed with aerobic pre-growth in fermenter as described in appendix section VIII.1.2. Fig. 38 illustrates the fermentation pathway and product distribution which proceeded in 3 stages. During the 1<sup>st</sup> stage (0 - 43.5 h) aerobic growth took place. Formate and glucose were totally consumed during this stage while low levels of acetate and butyrate appeared transiently (after 24 h) and were consumed by end of the growth phase (43.5 h), when the concentration of cells reached 1.9 g dry mass.L<sup>-1</sup>.

To initiate the fermentative 2<sup>nd</sup> stage, the system was made anaerobic by purging with N<sub>2</sub> (60 min; 43.5 h – 44.5 h) and 20 mL of 2 M glucose was added to obtain a final glucose concentration of ~39 mmol with the purpose of adjusting the system to begin H<sub>2</sub> production while bringing the pH down from 7.76 to 6 through the simultaneous generation of OA. The low sugar content of the hydrolysate would probably have been quickly consumed in the pH adjustment before any H<sub>2</sub>. The 2<sup>nd</sup> stage proceeded from 44.5 to 66.5 h and consumed all glucose. At the end the cell concentration increased to 2.1 g dry cells.L<sup>-1</sup> and the amount of H<sub>2</sub> produced was 934 mL with a yield of 53 %. Acetate (47.1 mmol), formate (5.7 mmol) and lactate (3.6 mmol) were present, but no butyrate was found.

For the 3<sup>rd</sup> and final stage (67 h onwards) ~690 mL hydrolysate was added while keeping the system anaerobic as described in Materials and Methods. After adding hydrolysate the culture

volume was 3.65 L, cell concentration was 1.8 g dry cells.L<sup>-1</sup> (due to dilution) and the sugars amount were glucose 27.74 mmol, galactose 4 mmol and fructose 6.0 mmol, making a total of 38.7 mmol. The amount of OA in the fermenter changed due to the addition of the hydrolysate, acetate increased to 84.7, formate to 29.6, lactate to 19.7 and butyrate to 2.2 mmol whereas ethanol content was 111 mmol.

After 46 h of fermentation, cell concentration remained fairly constant at 1.7 g dry cells.L<sup>-1</sup>, H<sub>2</sub> produced was 470 mL; all glucose was consumed however only 27 % of the galactose and 26 % of the fructose were consumed delivering a total of 29.93 mmol of sugars consumed, this represents a potential H<sub>2</sub> of 1440 mL, therefore the H<sub>2</sub> yield obtained during the 3<sup>rd</sup> stage was 32.6 %.. Lactate was totally eliminated and at the same time butyrate reached an amount of 25.2 mmol replicating the apparent lactate-butyrate conversion observed in previous work [100] (see section VI.1) took place during this stage. Acetate remained fairly constant (93 mmol) and formate and ethanol decreased to 19.3 and 76.4 mmol, respectively.

H<sub>2</sub> productivity during the 2<sup>nd</sup> stage was 23,409 mL H<sub>2</sub>.mol of hexose<sup>-1</sup> which represents ~49 % of the theoretical maximum [123] whereas for the 3<sup>rd</sup> stage was 15,703 mL H<sub>2</sub>.mol of hexose<sup>-1</sup>, only ~32 % of the maximum achievable based on consumed sugars. The average H<sub>2</sub> production rates were 42.5 and 10.2 mL H<sub>2</sub>.h<sup>-1</sup> for the 2<sup>nd</sup> and 3<sup>rd</sup> stages, respectively. These differences in productivities and rates probably originate from the substantial increase in OA and ethanol that accumulated during the 2<sup>nd</sup> stage and increased during the addition of the hydrolysate in preparation for the 3<sup>rd</sup> stage. It is unlikely that the presence of inhibitors at the given concentrations affected H<sub>2</sub> production negatively since it was demonstrated that instead, when present at low concentrations a stimulatory effect on H<sub>2</sub> production would be expected. However the high content of OA provides the potential for downstream use of OA in other processes including photofermentation for further H<sub>2</sub> production or methanogenesis [90, 126] thereby increasing the productivity of this fermentative process (~80 %) [100].

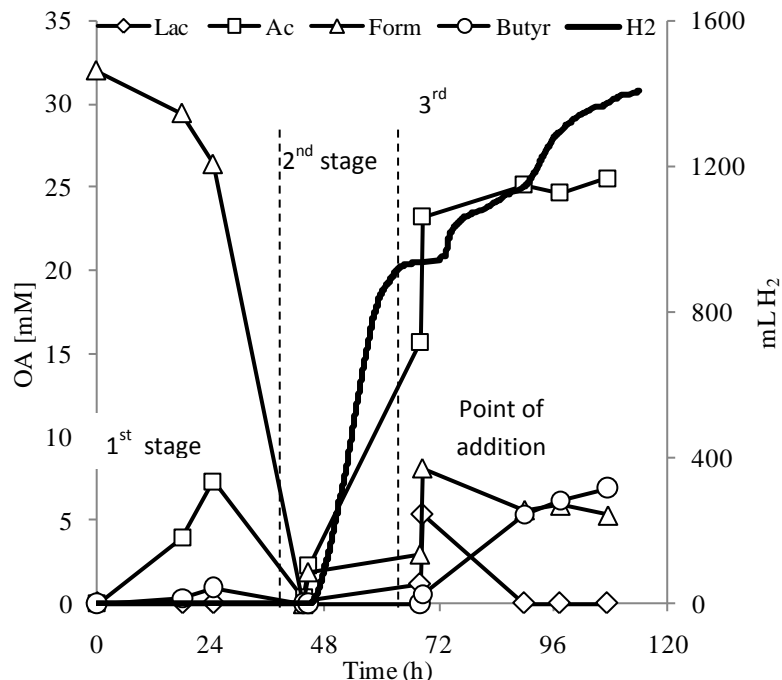


**Fig. 38** Shows the three stages of the fermentation with *E. coli* HD701 and product distribution of FW hydrolysates obtained at 220 °C after AC. Experiment was only done once.

## Conclusions

At the concentrations tested ( $0.75 - 3 \text{ g.L}^{-1}$ ) furfural, phenol, CA, SA, FA and 5-HMF all affected the growth of *E. coli* HD701 negatively, and increasingly with concentration. SA and 5-HMF were the least toxic whereas furfural, phenol and CA were the most toxic. The combinatory effect of the mixture (Mix2) strongly affected growth negatively. Alternatively, in  $\text{H}_2$  production SA had a stimulatory effect and 5-HMF showed little or no inhibition, whereas FA, phenol and CA began to inhibit  $\text{H}_2$  production at concentrations of  $0.75 \text{ g.L}^{-1}$ . Furfural was the most potent inhibitor at all concentrations tested. In general *E. coli* HD701 showed the capacity to adapt and successfully metabolize several of the DP tested and the stimulatory effect of some of them on  $\text{H}_2$  production is of great interest. The mechanisms underlying these phenomena, however, need further investigation.

The products and product distribution of the different waste hydrolysates was dependant on waste composition and HCW conditions, however it is highly possible that reactor wall-catalysed reactions have also occurred. AC exhibited strong removal of a wide variety of DP without severely affecting the sugar content of the hydrolysates. The best hydrolysate in terms of sugar content, growth and  $\text{H}_2$  production by *E. coli* HD701 was FW at 200–220 °C after AC. A larger fermentation (3 L) of these hydrolysates delivered low yields of  $\text{H}_2$  production (attributed to the accumulation of OA and ethanol), however HCW treatment of starch rich wastes, integrated with

fermentation-photofermentation processes may constitute a viable potential alternative for H<sub>2</sub> production in terms of HPP. In regards to lignocellulosic biowastes, HCW could be used as a pre-treatment to hydrolyse the lignin and hemicellulose portion leaving the cellulosic residue for further enzymatic or HCW hydrolysis. The lignin fraction can be utilized for the production of H<sub>2</sub> or bio-fuels through gasification or pyrolysis (section II.3.1)

## **VI.5 Hydrogen from biomass by HCW and extractive fermentation**

This section is presented in two parts:

- Section VI.5.1 is in a form of a paper describing the extractive fermentation of food wastes and,
- Section 0 also in a form of paper including an energy balance for an integrated bio-refinery.

### **VI.5.1 Electroextractive fermentation for efficient biohydrogen production.**

Journal: Bioresource Technology, in submission.

The experiment design and the writing of this paper were done by Dr. Mark D. Redwood. My contribution to this paper was in assisting Mark D. Redwood in the equipment set-up, operation and control of the experiments during the fermentation time, performing analysis of samples and collection of data.

## Electro-extractive fermentation for efficient biohydrogen production

Mark D. Redwood\*<sup>a</sup>, Rafael L. Orozco<sup>a</sup>, Artur J. Majewski<sup>a</sup> and Lynne E. Macaskie<sup>a</sup>

<sup>a</sup>School of Biosciences, University of Birmingham, Edgbaston, Birmingham UK B15 2TT

*Corresponding author:*\*

Tel: +44 121414 5434

Fax: +44 121414 5889

Email: m.d.redwood@bham.ac.uk

### **Abstract**

Electrodialysis, an electrochemical membrane technique, was found to prolong and enhance the production of biohydrogen and purified organic acids via the anaerobic fermentation of glucose by *Escherichia coli*. Through the design of a model electrodialysis medium using cationic buffer, pH was precisely controlled electrokinetically, i.e. by the regulated extraction of acidic products with coulombic efficiencies of organic acid recovery in the range 50-70% maintained over continuous 30-day experiments. Contrary to previous reports, *E. coli* produced H<sub>2</sub> after aerobic growth in minimal medium without inducers and with a mixture of organic acids dominated by butyrate. The selective separation of organic acids from fermentation provides a potential nitrogen-free carbon source for further biohydrogen production in a parallel photofermentation. A parallel study incorporated this fermentation system into an integrated biohydrogen refinery (IBR) for the conversion of organic waste to hydrogen and energy.

### **Keywords (5 keywords)**

Fermentation; biohydrogen; electrodialysis; *Escherichia coli*; organic acid

### **1. INTRODUCTION**

Biohydrogen technology offers practical options for clean, fuel gas production relying on only sustainable resources: organic material and sunlight [193]. Hydrogen gas can provide electricity via combustion in a traditional generator or, with higher efficiency, in a fuel cell. BioH<sub>2</sub> from a fermentative culture has been shown to power proton exchange membrane fuel cells directly [194].

Dark hydrogen fermentations typically provide 2-3 mol H<sub>2</sub>/mol hexose sugar, with maximal production rates in the range 10-50 mmol H<sub>2</sub>/h/L culture [108, 193, 195-197]. *E. coli* is a useful

model organism for the study of bioH<sub>2</sub> fermentation because it is oxygen tolerant, mesophilic, non-sporulating, unaffected by the partial pressure of H<sub>2</sub> and highly amenable to metabolic engineering [198; and references therein, 199]. Furthermore, as a facultative anaerobe, *E. coli* presents the opportunity for fast aerobic growth to high density followed by a longer period of anaerobic H<sub>2</sub> production with little additional growth, an approach which is reported here for the first time.

Sustained operation is a challenge for biohydrogen fermentations. In an excess of substrate, the first obstacle is acidification of the medium by newly formed organic acids (OA), which is normally overcome by adding caustic pH titrants. However, the fermentation is ultimately limited by the toxicity of accumulated end products [200]. Chemostat operation (with suspended cells) is non-ideal for biohydrogen fermentation because of the continual discard of cells and unmetabolised nutrients in the outflow [e.g. 201]. Immobilisation of cells (particularly through granule formation) has been successful in retaining fermenting cells with improved substrate loading rates and H<sub>2</sub> production rates but the production rate is limited by diffusion into the immobilisation matrix or granule [202].

We identified electrodialysis (ED) as a possible means of sustaining indefinitely a free-cell biohydrogen fermentation with a high H<sub>2</sub> production rate, substrate loading rate and cell density, without the use of pH titrant or immobilisation. The key function of ED is the selective transport and removal of acidic fermentation products, thereby simultaneously controlling fermentation pH and forestalling the accumulation of OAs to limiting concentrations. Extractive fermentation (using ED) shares some common features with microbial fuel cells (MFC) in which the definitive feature is the exchange of current between living cells and a chemical electrode. This may involve a direct exchange between an electrode and a biofilm of exoelectrogenic bacteria or a mobile electrochemical mediator to pass current between the electrode and free cells [203]. When a voltage is applied across a microbial fuel cell, the result is microbial electrolysis (or electrohydrogenesis) in which the external voltage augments the microbially-generated voltage to enable water electrolysis coupled to organic compound oxidation. Microbial electrolysis has been found to enhance dark H<sub>2</sub> production from a range of organic substrates [204]. Extractive fermentation (EF) differs in that the electrical terminals of the ED cell are shielded by flanking ion selective membranes and a large culture circulates through a small ED cell chamber so that a small fraction of the culture is subject to separation at any one moment. Unlike in MFC, the bacteria 'store' electrochemical potential in charged organic molecules which are then removed in combination with pH regulation.

Products including benzoic acid, lactic acid, acetic acid, propionic acid and pyruvic acid have been actively extracted from fermentations [205, 206, 207; and references therein, 208-210] but to the authors' knowledge, this study represents the first application of electro-separation to the production of bioH<sub>2</sub>. In this context ED is doubly effective as it also generates a purified stream of separated OAs suitable for conversion to an additional bioH<sub>2</sub> stream by purple non-sulphur (PNS) bacteria (to be reported in a subsequent paper).

ED techniques employ cation-selective (CSM), anion-selective (ASM) and bi-polar (BP) membranes, to achieve the charge-selective separation of valuable products or unwanted contaminants and the generation of acid and alkali, applicable in processes such as seawater desalination [211] and OA production (see above). Ion-selective membranes consist of a co-polymer matrix (e.g. vinyl compounds), which support charged functional groups conferring selectivity [positive in the case of CSM or negative in the case of ASM; 212].

In this study the ED cell functioned as shown in Figure 1. It was composed of four chambers (named C, M, MA and A, from - to +). The two outer compartments were named C and A, being in contact with the cathode and anode, respectively. The two inner compartments were named M and MA, M representing the 'main' compartment (source of anions for recovery) and MA representing the space separating compartments M and A into which anions were recovered. These four compartments were divided by three membranes (BP, ASM and CSM). In the ED cell, CSM and BP membranes prevent direct contact between bacterial cells and the electrodes, as the extremes of pH at the electrode surfaces would result in unwanted reactions [205, 213]. The BP membrane also splits water, generating H<sup>+</sup> on the cathode side and OH<sup>-</sup> on the anode side, a function exploited to provide pH control simultaneously during extractive fermentations [213, 214]. The CSM also functions to transport Na<sup>+</sup> from the C chamber, resulting in the formation of sodium salts in the MA chamber.

We describe the adaptation of fermentation techniques to incorporate electroseparation and the performance of long-term glucose-fed extractive fermentations.

## **2. MATERIALS AND METHODS**

All media and solutions were prepared using deionised water and analytical grade reagents.

### 2.1 Extractive fermentation apparatus and operation

Thin-cell electrodialysis (ED) apparatus (C-Tech Innovation Ltd, Capenhurst, UK) was configured as shown in Figure 1, comprising stainless steel electrodes of which the anode was Pt-coated. The cell was divided into four chambers (named C, M, MA, and A from cathode to anode) separated by 3 membranes; bi-polar (BP: Fumasep FBM), anion-selective (ASM: Fumasep FAB) and cation-selective (CSM: Fumasep FKB), respectively (Figure 1). Fresh membranes were used in each experiment. Silicone rubber gaskets (1 mm thickness) were cut to expose membrane areas of 200 cm<sup>2</sup> (128x157 mm). A 4-channel peristaltic pump was used to circulate solutions and medium at 300 mL/min through all four chambers. Chambers A and C (flanked by the anode and cathode, respectively) were in contact with a single solution of 0.5 M Na<sub>2</sub>SO<sub>4</sub> (1 L), the M chamber was in contact with the *E. coli* culture (initially 3 L) and MA was in contact with the permeate vessel containing initially 2 L of stirred phosphate buffer (0.366 g K<sub>2</sub>HPO<sub>4</sub>, 0.443 g KH<sub>2</sub>PO<sub>4</sub>/L; pH 6.8).

The configuration of extractive fermentation (EF) is shown in Figure 1. Fermentations used a modular fermentation system (Electrolab, UK; 300-series). In accordance with Table 1, macronutrients and buffers were sterilised by autoclaving in a volume of 2.7 L inside the fermentation vessel ('M') before sterile MgSO<sub>4</sub>, thiamine, antifoam, microelements and water were added aseptically to make a final volume of 3 L at pH 6.5±0.1. The medium was heated to 30 °C and aerated (1 L/min) with turbine agitation (600 rpm) before adding 1% (v/v) inoculum from a pre-culture. Pre-cultures were incubated for 16-18 h (30 °C, 180 rpm) using 100 mL of nutrient broth (no. 8; Oxoid UK) with 5 g/L added sodium formate.

pH control was not required during aerobic growth for the initial 24 h, after which the transition to anaerobic fermentation was made by purging with oxygen-free N<sub>2</sub> (30 min, 1 L/min) and the culture was also connected to the M chamber of the ED cell (Figure 1), which had been cleaned by circulating 75% ethanol (15 min) and washing three times with sterilised water. The pH was allowed to fall to 6.0, where it was maintained automatically by the removal of acidic products across the ASM in a pH-sensing feedback loop (C-Tech Innovation, Capenhurst, UK). Glucose was fed starting from the end of the N<sub>2</sub> purge at a constant rate of 0.15 mol/day (1.5 M solution, 0.1 L/day, sterile and under air).

In electroseparation of any type, current efficiency (or Faraday efficiency) represents the fraction of charge passed in a time period, which can be attributed to the detected transfer of target anion [215].

$$\text{Current Efficiency (\%)} = \frac{100NF}{i} \quad (\text{equation 1})$$

where  $N$  is the charge flux as target anion (here, organic acid) in mol/s/m<sup>2</sup>,  $F$  is the Faraday constant (96485.38) and  $i$  is the current density in A/m<sup>2</sup>.

## 2.2 Bacterial strains and maintenance

*Escherichia coli* strain FTD67 (provided by Dr F. Sargent, University of Dundee) was selected as previous studies showed its lack of uptake hydrogenase to be conducive to H<sub>2</sub> production [199].

## 2.3 Analysis

H<sub>2</sub> and CO<sub>2</sub> production were measured using low-flow gasimeters as described by [186]. Meters were placed upstream and downstream of a 'scrubber' solution containing 2 M NaOH so that the CO<sub>2</sub> fraction could be calculated by subtraction. The scrubber solution also contained universal indicator so that its depletion would be apparent by colour change. This method was shown by GC to remove CO<sub>2</sub> to below 0.05% (v/v). Anions were analysed by HPLC and glucose was measured colorimetrically as described previously [107].

# 3. RESULTS AND DISCUSSION

## 3.1 Preliminary extractive fermentation method development

Preliminary work showed that electrodialysis (ED) can recover organic acids (OA) from *E. coli* fermentations without causing significant inhibition but that automatic, demand-based regulation is necessary. The preliminary tests showed that intermittent high intensity separation (9.6 A, 1 h per day) caused temporary inhibition of H<sub>2</sub> production, whereas a slow constant-current (400 mA) was not inhibitory. Glucose was fed continuously from 24 h onwards and pH was controlled by the automatic addition small amounts of titrants. Cells were grown aerobically then resuspended in a fermentation medium (containing Na<sub>2</sub>SO<sub>4</sub> and (NH<sub>4</sub>)<sub>2</sub>SO<sub>4</sub> as the main salts) and made anaerobic by N<sub>2</sub> purging. H<sub>2</sub> production (0.7 L/L culture/day) and glucose utilisation (20 mmol/L/day) continued for ~10-15 days, as compared to 7 days in controls without ED but the coulombic efficiency of OA separation was poor; initially 5%, rising steadily to 12% over 14 days. This poor current efficiency was attributed to competitive ion transfer, i.e. the movement of inorganic anions (particularly SO<sub>4</sub><sup>2-</sup>) and the increasing trend in current efficiency with respect to

the separation of OAs was attributed to their increasing concentration in the fermentation medium, which reached 90 mM and ultimately limited fermentation despite an excess of glucose and favourable pH (pH 5.5).

Therefore, to improve the current efficiency and maintain non-limiting OA concentrations the fermentation medium was redesigned (Table 1) and the ED was put under pH-linked automatic feedback control. This provided electrokinetic pH control in place of pH titrant additions (Figure 2).

An 'ED' medium was designed (Table 1) and tested in a new protocol for aerobic growth and subsequent H<sub>2</sub> production in a single vessel. Growth took place over 23 h in 3 L reactors (aerated at 1 L/min; pH 7.0). Using ED media with either formic acid or lactic acid (23 mM) the cultures reached the same density of 4.15 g DW/L in 23 h aerobic cultivation, followed by H<sub>2</sub> production after transition to the anaerobic fermentation mode (see further discussion below).

### *3.2 Electrokinetic pH control in biohydrogen fermentations*

As shown in Figure 2, pH was controlled within 0.01 pH units using custom software provided by C-Tech Innovation (Capenhurst, UK). A baseline current of 10 mA was maintained in order to prevent back-diffusion of separated anion but when the fermentation pH decreased as a result of acid production, the applied current was increased until the pH increased (due to the removal of OA across the ED membrane with simultaneous OH<sup>-</sup> generation by the BP membrane; Figure 1) prompting a return to the baseline current. At steady state the pH typically oscillated by ~0.0005 units with a period of ~5 min, while the current remained predominantly at the baseline (10 mA) rising briefly up to 20-fold several times per min (Figure 2). No attempt was made to optimise the frequency or responsiveness of current variation.

Figure 3 shows the effectiveness of electrokinetic pH control in two independent experiments ('EF1, EF2'). From a neutral starting point, the pH fell towards the end of the aerobic growth phase (<1 days) and was subsequently maintained at pH 6.0 by the action of ED. H<sub>2</sub> production started on the third day and 40 L H<sub>2</sub> was produced over 20 days at maximally ~4.7 L/day/L culture. Initially a voltage limit of 4 V was sufficient to achieve pH control but as growth continued into the anaerobic phase the rate of acid formation increased and the limit was increased to 10 V after 6 days.

The permeate solutions (MA chamber) remained clear (as shown in Figure 1B) during 30 days of uninterrupted activity in which the ASM was the only barrier separating the permeates from dense (~5 g DW/L) *E. coli* cultures. The current efficiencies representing the main part of the

fermentations (days 2-20) were 57% and 55% for EF1 and EF2, respectively. It is noteworthy that the current efficiency increased after 22 days in EF1, which was 'rescued' from ethanol toxicity (see below) but declined slightly in EF2, in which ethanol was not removed (see below). Hence, there was no indication of a progressive change in membrane function over 30 days of constant activity. i.e. lack of inhibition by biofouling was implied but this was not specifically quantified. At the end of the experiments, solid material was found on the M-side of the membranes but this was, evidently, not problematic. Previously, for pyruvate production in a glucose-fed *E. coli* fermentation, Zelic et al. [216] incorporated microfiltration and ultrafiltration (10 kDa cut-off) upstream of ED to remove, cells, cell debris and proteins which might foul ED membranes. However, such pre-separation was unnecessary in this study and is disadvantageous due to the additional complexity and cost.

Therefore, ASM are capable of simultaneous cell retention and charge-selective ion separation in glucose-fed *E. coli* fermentations and, furthermore, this was confirmed in extractive fermentations producing H<sub>2</sub> from food wastes (M. D. Redwood et al.; unpublished; Environ. Sci. Technol. in submission).

### 3.3 Comparison with non-extractive fermentation

Figure 4 shows that standard fermentations could consume up to 1 mol glucose, whereas extractive fermentations consumed 2.5 mol. Furthermore, standard (non-extractive) fermentations tolerated ~1 mol of accumulated OA (190 mM in 5.5 L final volume) within the culture, whereas 2.5-5 mol was extracted from fermentations with ED (Figure 4A). The extracted liquors contained 39.5% butyrate, 26.3% acetate, 23.8% formate, 7.9% lactate, 2.2% succinate and 0.4% propionate (averaged molar fractions; 70 analyses). The dominance of butyrate, rather than acetate and lactate, is a further unusual feature [217] apparently enhanced by this culture technique. Short (24-48 h) *E. coli* fermentations in batch mode followed the well-described fermentation balance of *E. coli* [e.g. 199], whereas when fermentation was prolonged by traditional pH control a switch to butyrate production (with lactate uptake) occurred 1-2 days into the anaerobic stage. The identity of butyrate was cross-validated by HPLC and mass spectrometry. Lugg et al. [217] discussed the sparse previous reports of butyrate production and molecular support for a putative metabolic pathway in *E. coli*.

While the non-extractive fermentations (fed-batch) gained fluid volume as additional substrate was added, the volume of extractive fermentations varied very little due to the movement of water into MA across the anion-selective membrane. Show et al. [202] stated, "*The key to*

successful application of anaerobic fermentation is to uncouple the liquid retention time and the biomass retention time in the reactor system" and they discussed granules, biofilms and flocs as potential solutions. Using extractive fermentation the two retention times were uncoupled but with suspended cells, thereby avoiding the diffusion limitations of immobilised or granular fermentations. Due to the absence of outflow, feed rates need not be carefully controlled to minimise outflow of excess substrate and the longer adaptation times (typically 48h) required for adaptation to new substrates would not cause washout, as is problematic in chemostat cultures [218].

As shown in Figure 4B experiments EF1 and EF2 produced 2.3 and 2.8 mol H<sub>2</sub> from 1.6 and 1.9 mol glucose, respectively. Therefore, fermentative H<sub>2</sub> yield was low at 0.7 mol H<sub>2</sub>/mol glucose in both cases, as yields close to the theoretical maximum (2 mol/mol) have been reported previously [201]. The low yield is attributed in part to the extraction of formate, the sole precursor of H<sub>2</sub> in *E. coli* [219]. The extracted formate amounted to 1.1 mol in EF1 and 0.9 mol in EF2 (as measured in MA solutions). Adding this potential H<sub>2</sub> to the actual H<sub>2</sub> (i.e. if extracted formate had been converted to H<sub>2</sub>) would increase the yield to 1.0-1.2 mol/mol. Therefore extraction of formate cannot account for the whole yield deficit. Although similar in reactor volume, the earlier experiments [201] operated as chemostats from which ethanol would be diluted continuously. We propose (see below) that the accumulation of ethanol (not actively removed by ED) is the most likely cause of the lower yield in the current work.

### 3.4 'Rescue' experiments: indication of ethanol limitation

After 22 days EF1 and EF2 (Figure 3) had ceased H<sub>2</sub> production despite continuing favourable conditions (excess glucose, optimal pH and very little OA accumulation). Hence the cessation may be attributed either to the depletion of another nutrient (e.g. N or P) or to the accumulation of an inhibitory end-product, not removed by ED, such as ethanol. To preclude the former, EF2 was re-dosed with the initial provisions of vitamins, trace elements and ammonium citrate (Table 1). This had no effect on the production of H<sub>2</sub> or OA (Figures 3D and 4), indicating that nutrient limitation was not responsible.

Zaldivar et al. [220] reported growth inhibition by ethanol at 20 g/L for the *E. coli* strain LY01 having enhanced ethanol tolerance. Therefore, it is reasonable to suggest that *E. coli* FTD67 (derived from MC4100), could be inhibited in H<sub>2</sub> production by ethanol at 14-17 g/L (peak values, Figure 3). In further support of this hypothesis EF1 was 'rescued' by harvesting cells from 50% of the culture, and resuspending in an equal volume of a solution containing concentrations of OAs

matched precisely to those measured in the culture at 20 days. The solution contained (mM) lactic acid, 0.85; acetic acid, 8.37; formic acid, 4.57; butyric acid, 29.23; succinic acid, 0.23 and bis-tris base to pH 6.0 (~50 mM). Upon returning the resuspended cells into EF1, the result would be a ~50% dilution of all other soluble products. The ethanol concentration fell from 12.3 g/L (267 mM) to 5.2 g/L (Figure 3B) and this was followed by resurgence in H<sub>2</sub> production (Figures 3B and 4B) and current efficiency (Figure 3B) and OA production (Figure 4A). Unknown end-products cannot be excluded but ethanol is the only known major uncharged product [221] and was detected in potentially inhibitory concentrations (see above). Therefore it is most likely that ethanol was the cause of limitation. In this work EF prolonged fermentation time from ~3 days to 3 weeks and increased H<sub>2</sub> production per culture by 3-fold.

Losses in H<sub>2</sub> yield due to formate extraction would not be significant in a larger integrated system because the extractive fermentation would function primarily as an OA generator, rather than as the primary H<sub>2</sub> producing reactor (see later).

### *3.5 Aerobic growth and H<sub>2</sub> production in a single reactor*

It has been accepted that “[*E. coli*] cells cultivated aerobically ... lack the ability to produce hydrogen” [222]. Furthermore, it was reported that amino acids are necessary as anaerobic growth on defined media, with NH<sub>4</sub><sup>+</sup> as the sole nitrogen source resulted in the absence of H<sub>2</sub> production activity unless amino acids (particularly glutamate) were added [223]. This was confirmed more recently as *E. coli* cultivated aerobically on nutrient broth (growing up to ~0.8 g DW/L), would produce H<sub>2</sub> when mixed directly with phosphate buffer but not when harvested, washed and resuspended in phosphate buffer [224]. Later, this was overcome by adding formate (100 mM) to the aerobic pre-growth medium, which enabled H<sub>2</sub> production by washed cells in a range of nutrient-poor buffers [199, 225]. Similarly, Yoshida et al. [222] designed a 3-step process in which cells were first grown aerobically, and required activation with formate before entering the anaerobic H<sub>2</sub> production phase. Therefore, it would appear that either amino acids or formate are necessary as inducers of H<sub>2</sub> production for aerobically grown *E. coli*. Hence, the results of the present study are surprising as high H<sub>2</sub> production rates (maximally 8 mmol/h/L culture) were observed after aerobic growth in minimal media. The phenomenon was not strain specific as the parent strain MC4100 and its derivatives HD701 and FTD67 [125, 199], were all capable of H<sub>2</sub> production after aerobic growth in a single vessel using ED medium.

Furthermore, when formic acid in the ED medium (Table 1) was replaced with lactic acid  $H_2$  production took place normally in the anaerobic phase, whereas formate was previously found to be a necessary inducer of  $H_2$  production after aerobic growth.

The capability for  $H_2$  production without induction by formate or amino acids may result from the properties of the single-reactor technique, in which there is a gradual progression from oxygen saturation at pH 7, into oxygen limitation with growth and concomitant OA formation and resultant fall to pH 6 (before a 30 min purge with  $N_2$  to ensure anaerobiosis). Hewitt et al. [226] reported progressive changes in cell physiology throughout aerated *E. coli* fermentations. Hence, this transition is a natural property of the culture and appears to promote metabolic reconfiguration (for  $H_2$  production) whereas sudden artificial transitions were unsuccessful.

The facility to produce a dense culture and then produce  $H_2$  in a single reactor represents a significant advance with several advantages over methods reported to date. Firstly, it does not require cell harvest so it is more suitable for large scale implementation. Secondly, it achieves a higher culture density. Cultures grew to maximum densities of 2-4 g DW/L (as compared to 0.8 g/L using nutrient broth in shake flasks). Much higher densities could be reached by established techniques, i.e. monitoring the respiratory quotient of the culture (RQ) while limiting the glucose supply to restrict 'overflow metabolism' (the aerobic formation of inhibitory OAs) [226]. The single-reactor method described here uses the onset of overflow metabolism (and resultant fall in pH to 6.0) as a trigger for the switch to anaerobic fermentation. Therefore overflow metabolism is inherently limited, without the need for careful RQ and feed-rate monitoring.

### *3.6 An indefinite extractive fermentation?*

According to an *ideal model*, an extractive fermentation (EF) could be sustained indefinitely. This would require the removal of charged products in balance with pH, while maintaining a constant ionic composition in the culture medium. In the ideal model the concentration of OA in the fermentation medium remains constant because each unit of organic acid generated by fermentation results in a detectable fall in pH, which triggers the exchange of 1 unit of anion for 1 unit of  $OH^-$  (with the corresponding rise in pH). This chemical balance is illustrated in Figure 1.

This situation was created in the glucose-fed extractive fermentations (EF1, EF2), where the duration of  $H_2$  production was significantly extended from ~3 days to 3 weeks but was not indefinite. EF1 and EF2 were limited by the formation of non-ionic end products, which cannot be actively separated by the same method as charged products. 'Rescue' experiments (see above) confirmed

that OA concentrations remained non-limiting, indicating that an unidentified fermentation product, and not the depletion of any key nutrient, was the cause. The most likely non-ionic end product is ethanol, given the well-described mixed acid fermentation in *E. coli* [221]. Ethanol formation plays an important redox balancing role in *E. coli* and mutants defective in alcohol dehydrogenase cannot ferment glucose anaerobically [221]. For lactic acid production, homofermentative lactic acid bacteria have been applied successfully in long-term EF [208], whereas for bioH<sub>2</sub> production non-solventogenic alternative species are elusive. *Enterobacter* spp. function similarly to *E. coli* (producing ethanol) while clostridia can produce mainly acetic and butyric acids but are prone to switching to acetone-butanol metabolism (and sporulation) in response to a variety of stresses, including OA toxicity [227]. The threshold for OA-induced solventogenesis in clostridial-type fermentation is reportedly 19 mM free acid (at pH 5.5, glucose substrate) [227] which could be achieved by precisely controlled electroseparation, whereas *E. coli* tolerated up to 90 mM OAs in this work (while continuing to produce H<sub>2</sub>). Certain thermophilic and hyperthermophilic bacteria (including some *Clostridium* spp.) and archaea are promising candidates for biohydrogen production [see 193] but the upper temperature limit for bipolar membranes is currently ~60°C, which precludes their use.

Finally, water balance also presents a practical challenge for the indefinite fermentation. Ion separation is accompanied by a degree of water transport from the fermentation chamber so that the permeate chamber slowly gains volume via transport from the fermentation while water is constantly lost from the electrode wash solution by electrolysis. In this study, non-extractive fermentations gained 100 mL/day from glucose additions and typically ~110 mL/day from titrant additions, reaching the capacity of the fermentation vessel in 12 days. Conversely in EFs the rates of feed addition and water transport from the fermentation chamber ('M') were relatively in balance as the fermentation volumes (M chamber) changed by only ±30 mL/day while over 100 mL was fed. Therefore, the retention times of fluid and biomass were uncoupled using suspended cells, aiding mixing and mass transfer. EF can be described neither as 'fed-batch' nor 'continuous' culture. Unlike 'fed-batch' there was a (reasonably) constant culture volume despite feeding and unlike 'continuous' culture there was very little dilution of biomass and no outflow of unused substrate or soluble products.

A precise water balance may be addressed by controlling the water-separation capacity of the ED cell using a moderate pressure gradient, preferably a small negative pressure to either A/C or MA, although this would dilute the contents of these vessels. This hypothesis could not be tested

using the current apparatus due to the use of peristaltic pumps, which are sensitive to fluid pressures. However, water movement into MA was observed consistently. Alternative pump mechanisms (e.g. positive displacement or centrifugal) may enable such control but these are usually too large for bench-scale experiments. Since, in this study, ~30% of fed water was retained in the fermentation vessel, in practice an outflow would be required and the resultant dilution may be sufficient to control ethanol accumulation and achieve a continuous fermentation. Since ethanol accumulated to much higher concentrations than OAs only a small fraction of OAs would be lost in the outflow.

Hence, the technique described in this study offers practical advantages over traditional approaches (i.e. fed-batch, chemostat or cell immobilisation) but an indefinite extractive biohydrogen fermentation remains elusive mainly due to the solventogenic properties of suitable organisms.

### *3.7 Extractive fermentation as a bioresource technology*

This study demonstrated the effectiveness of extractive bioH<sub>2</sub> fermentation using glucose substrate. However, the capacity to utilise bioresources is important for the technique to be useful in sustainable fuel production. Complex substrates would be more challenging for EF due to the presence of insoluble components and inorganic salts. The presence of inorganic salts could reduce the OA separation efficiency and also potentially distort the balance of pH regulation and OA removal, while the sugars of key bioresources exist primarily as polysaccharides (e.g. starch, cellulose and lignocellulose) requiring hydrolysis to enable rapid fermentation and also to prevent fouling of the narrow channels of the ED cell with solid particles. Such upstream hydrolysis of starch was achieved (R. Orozco, unpublished) and EF took place with high separation efficiency and H<sub>2</sub> production using sugars derived from a range of real biowastes. This work will be reported in a subsequent publications.

Finally, and moving towards a zero waste high output process, the extracted OAs were coupled to a second phase of photofermentative bioH<sub>2</sub> production (M. D. Redwood et al., unpublished; Environ. Sci. Technol. in submission), while growth of *Spirulina*, a high value foodstuff, on fermentation waste CO<sub>2</sub> was achieved in a parallel study (X. Zhang & L. E. Macaskie, unpublished).

#### 4. CONCLUSIONS

- Aerobic cultivation and subsequent fermentation by *E. coli* to produce H<sub>2</sub> can occur in one vessel using a minimal medium without added inducers (formate or amino acids).
- Electrodialysis provides simultaneously the electrokinetic control fermentation pH while preventing the accumulation of organic acids (OA), thereby enhancing and prolonging H<sub>2</sub> fermentation.
- Electroseparation of OA from an active fermentation can be maintained over long periods (30 days) with cell retention while maintaining high OA separation efficiency.
- Extractive fermentation with suspended cells uncouples the retention times of fluid and biomass.
- The main limitation for extractive biohydrogen fermentation is solventogenesis.

#### 5. ACKNOWLEDGEMENTS

We acknowledge with thanks the financial support of the EPSRC (refs EP/D05768X/1, EP/E034888/1), BBSRC (refs BB/C516195/2, BB/E003788/1), Royal Society (Industrial Fellowship to LEM), Advantage West Midlands (ref. POC46) and Gov. Mexico (studentship 203186 to RLO). We thank, for technical support, Combined Workshop (University of Birmingham, UK) and for *E. coli* strains, F. Sargent (University of Dundee, UK).

#### FIGURE CAPTIONS

**Figure 1.** Application of ‘BAC’ electrodialysis to fermentative and photofermentative biohydrogen production.

BP, bi-polar membrane; ASM, anion-selective membrane; CSM, cation-selective membrane; C, cathode chamber; M, main chamber; MA, permeate chamber; A, anode chamber; -, cathode; +, anode.

**Figure 2.** Automatic control of fermentation pH by extractive fermentation.

pH was regulated automatically using a program provided by C-Tech Innovation (Capenhurst, UK) which varied the applied current within set limits (10-3000 mA). pH and I were recorded at 1 s intervals and was not smoothed.

**Figure 3.** Electrokinetic pH control in extractive fermentation (EF1 and EF2).

*E. coli* fermentations were sustained for 1 month by the removal of organic acid products by an electro dialysis (ED) cell controlled by pH. The voltage applied over the ED cell (thin solid lines in A and C) varied up to the set limit (thin broken lines in A and C). Arrows indicate the time of 'rescue' experiments (see text). The bracket in C indicates a temporary pump malfunction. Glucose was in excess throughout. Despite continuous substrate addition, culture volume remained relatively constant due to water loss via ED (see text). pH and V were recorded at 2 min intervals and data smoothing was applied (100 points; 200 min) because V fluctuated rapidly with I (see Figure 2). Current efficiency (equation 1) was derived from 2-3 daily recordings of the fluid volume in MA, the accumulated charge passed over the ED cell and analyses of the OA concentration in MA. Current efficiencies shown in B and D represent time-weighted averages smoothed by 5 points (i.e.  $\pm 1$  day) as individual outputs varied widely attributed to the combined error on several measured inputs.

**Figure 4.** Comparison of standard and extractive fermentations: Maintenance of low organic acid concentrations in extractive fermentations (A) and extension of fermentation (B).

EF1 and EF2: extractive fermentations using electro dialysis for simultaneous pH control and organic acid separation. SF1 and SF2: Standard fermentations took place under the same conditions as extractive fermentations apart from the presence of the electro dialysis system. SF1 and SF2 were stopped at 14 days as H<sub>2</sub> production ceased at 7 days and organic acid formation ceased at 12 days. A shows the organic acids present in and extracted from fermentations. Standard fermentations could accumulate ~1 mol organic acids whereas 2.5-5 mol was extracted from fermentations with electro dialysis. Arrows indicate 'rescue' experiments showing that the cessation in H<sub>2</sub> production can be attributed to the accumulation of a secondary metabolite such as ethanol and not to cell age, nutrient depletion or organic acid toxicity. B shows the yield of H<sub>2</sub> from glucose in each experiment. All fermentations were fed glucose constantly (150 mmol/day) but standard fermentations could not consume >1 mol glucose, whereas extractive fermentations consumed 2.5 mol before requiring a 'media refresh' (see text).

## TABLES AND FIGURES

**Table 1.** Development of ‘ED’ medium for extractive fermentation of *E. coli*.

Component class	Chemical	Final concentration (mM)	
		SM <sup>a</sup>	ED (this work)
Macronutrients and buffers	Glucose	27.75	as SM
	(NH <sub>4</sub> ) <sub>2</sub> SO <sub>4</sub>	20.43	3.5
	Na <sub>2</sub> SO <sub>4</sub>	14.08	-
	NH <sub>4</sub> Cl	9.348	-
	K <sub>2</sub> HPO <sub>4</sub>	83.82	-
	NaH <sub>2</sub> PO <sub>4</sub>	28.99	-
	(NH <sub>4</sub> ) <sub>2</sub> -H-citrate	4.782	-
	(NH <sub>4</sub> ) <sub>2</sub> HPO <sub>4</sub>	-	2
	Citric acid	-	5
	BIS-TRIS base	-	50
	Formic acid	-	23
NH <sub>4</sub> OH	-	44	
Additions	MgSO <sub>4</sub>	2	as SM
	Thiamine (vitamin B1)	0.030	as SM
Micronutrients (Used as 3 mL/L)	Na <sub>2</sub> -EDTA	0.1702	as SM
	ZnSO <sub>4</sub>	0.001878	as SM
	MnSO <sub>4</sub>	0.001775	as SM
	CuSO <sub>4</sub>	0.001201	as SM
	CoSO <sub>4</sub>	0.002241	as SM
	FeCl <sub>3</sub>	0.1743	-
	CaCl <sub>2</sub>	0.01721	-
	FeSO <sub>4</sub>	-	0.1743
CaSO <sub>4</sub>	-	0.01721	
Final inorganic anion charge (equivalents)		323.2	15.7

‘ED (electrodialysis)’ medium was formulated to minimise the influence of competing inorganic anion. The nutrient content of SM<sup>a</sup> medium [226] which was optimised for aerobic growth to high density, was mimicked while minimising inorganic ion. Phosphate buffer was replaced with the cationic buffer, bis-tris base ( $pK_a$  6.15). 50 mM was found to be a suitable bis-tris concentration in short aerobic growth tests. Inorganic salts were replaced with formic acid, as an ‘inducer’ of H<sub>2</sub>-producing metabolism [199]. The level of inorganic anion equivalent was reduced from 323 mM to 16 mM but could not be reduced to zero because of the minimum requirements for S and P, which are preferably supplied as phosphate and sulphate ion. *E. coli* K12 strains required only 0.1 mol P and 0.04 mol S per mol N [201], which were matched. All media also contained 0.5 mL/L polyethylene glycol (antifoam). Citrate is an organic acid which does not serve as a carbon source for *E. coli*. It functions (along with EDTA) as a chelating agent and was monitored among organic acids for its contribution to current efficiency.

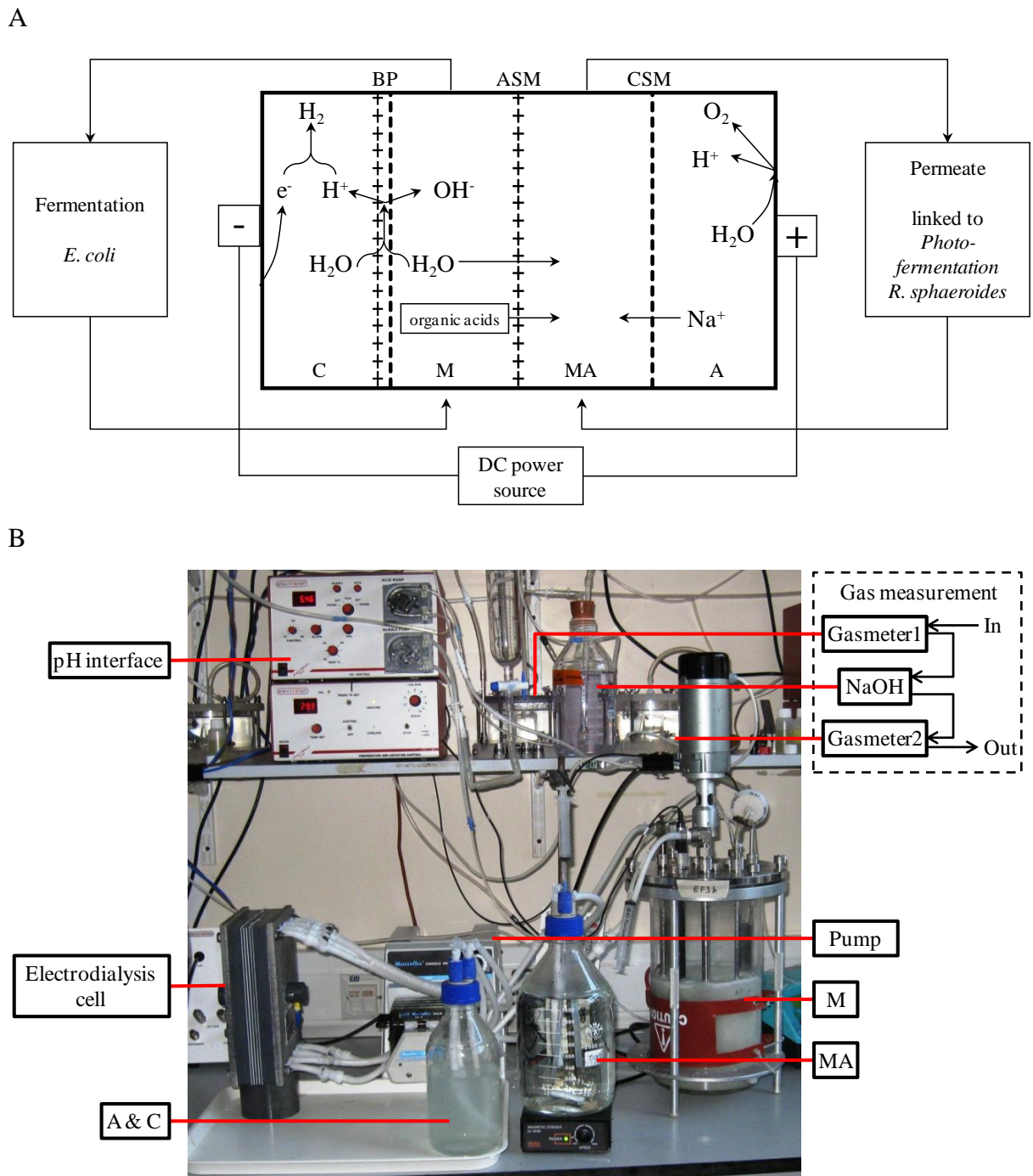


Figure 1

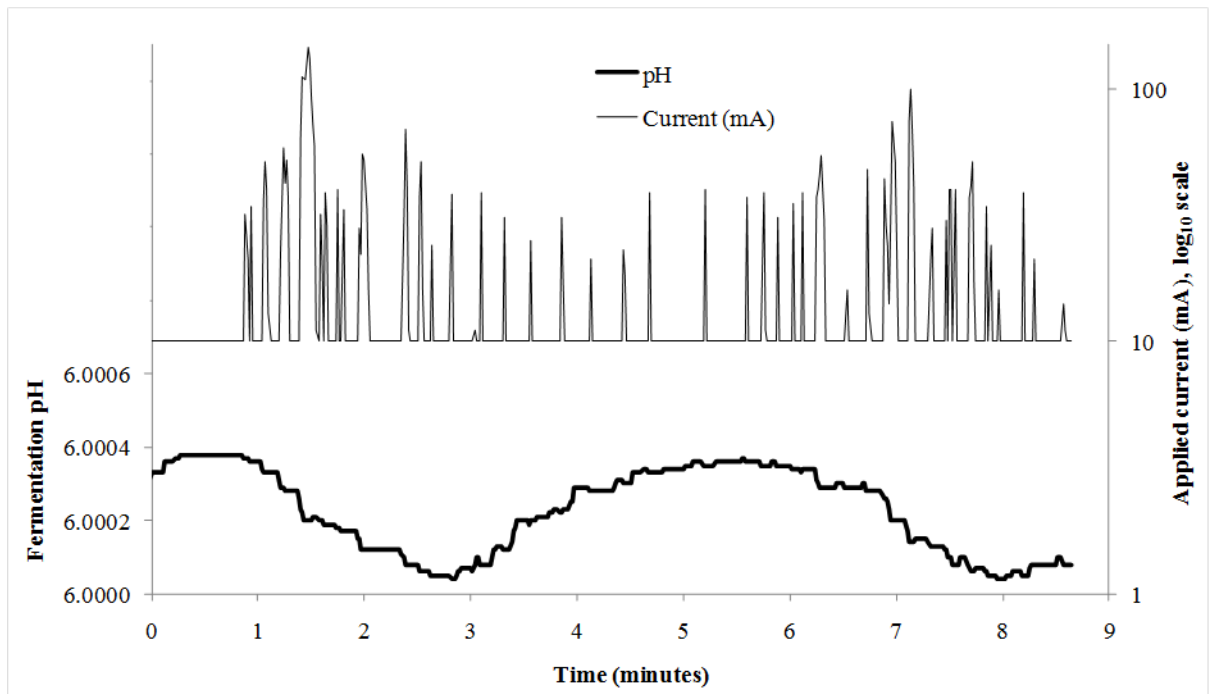


Figure 2

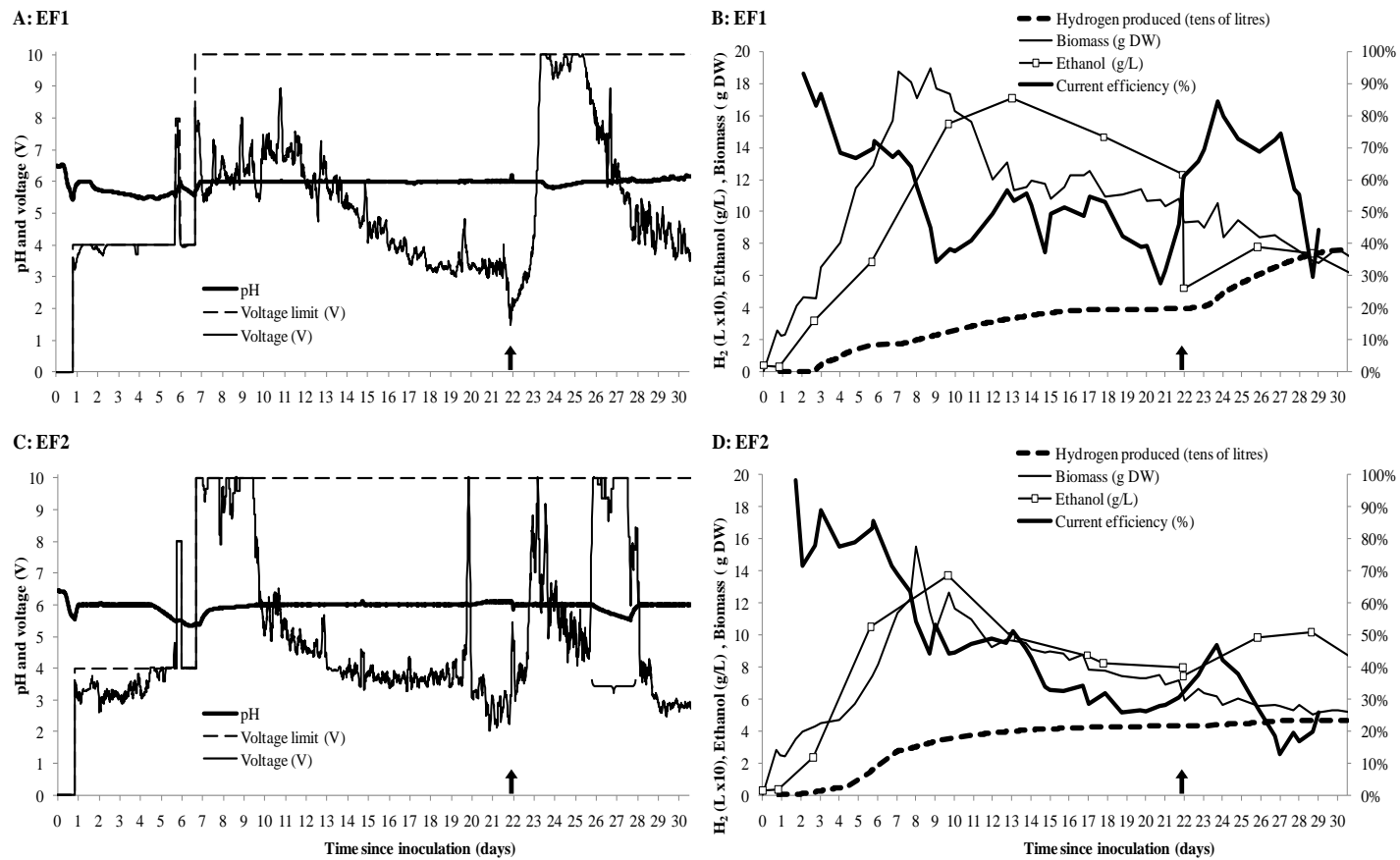
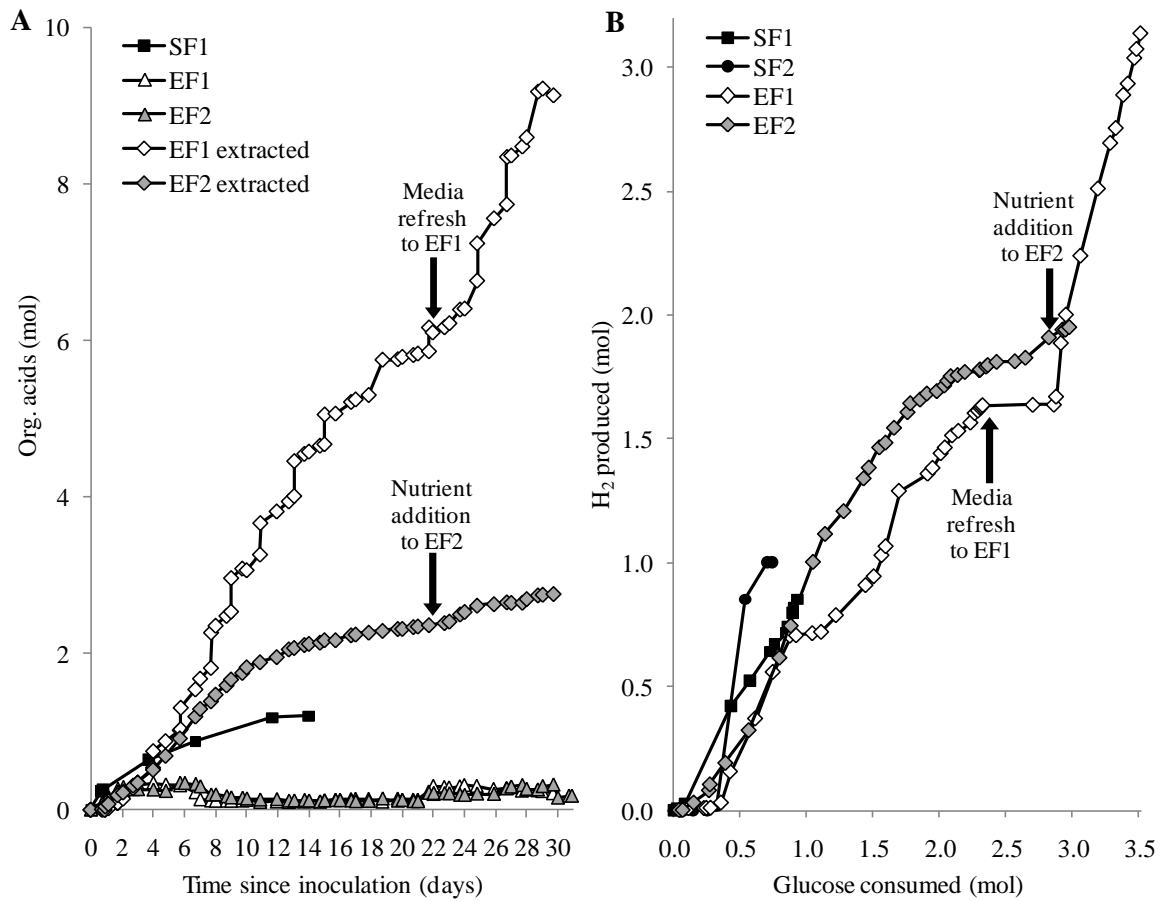


Figure 3



**Figure 4**

**VI.5.2 An integrated biohydrogen refinery: Synergy of photofermentation, extractive fermentation and hydrothermal hydrolysis of food wastes.**

Journal: Environmental, Science & Technology, in submission.

The experiment design and the writing of this paper were done by Dr. Mark D. Redwood. My contribution was in performing the hydrothermal hydrolysis (HCW) of the solid biomasses residues, in assisting Dr. Redwood in the equipment set-up, operation and control of the extractive fermentation process, in providing data for the energy calculation of the HCW process, sample analysis and data collection.

The first two pages of the paper are presented below, the whole paper can be found in appendix section VIII.5.1.

**An integrated biohydrogen refinery: Synergy of photofermentation, extractive fermentation and hydrothermal hydrolysis of food wastes.**

*AUTHOR NAMES: Mark D. Redwood,\* Rafael L. Orozco, Artur J. Majewski and Lynne E. Macaskie*

**AUTHOR ADDRESS:** School of Biosciences, University of Birmingham, Edgbaston, Birmingham UK B15 2TT

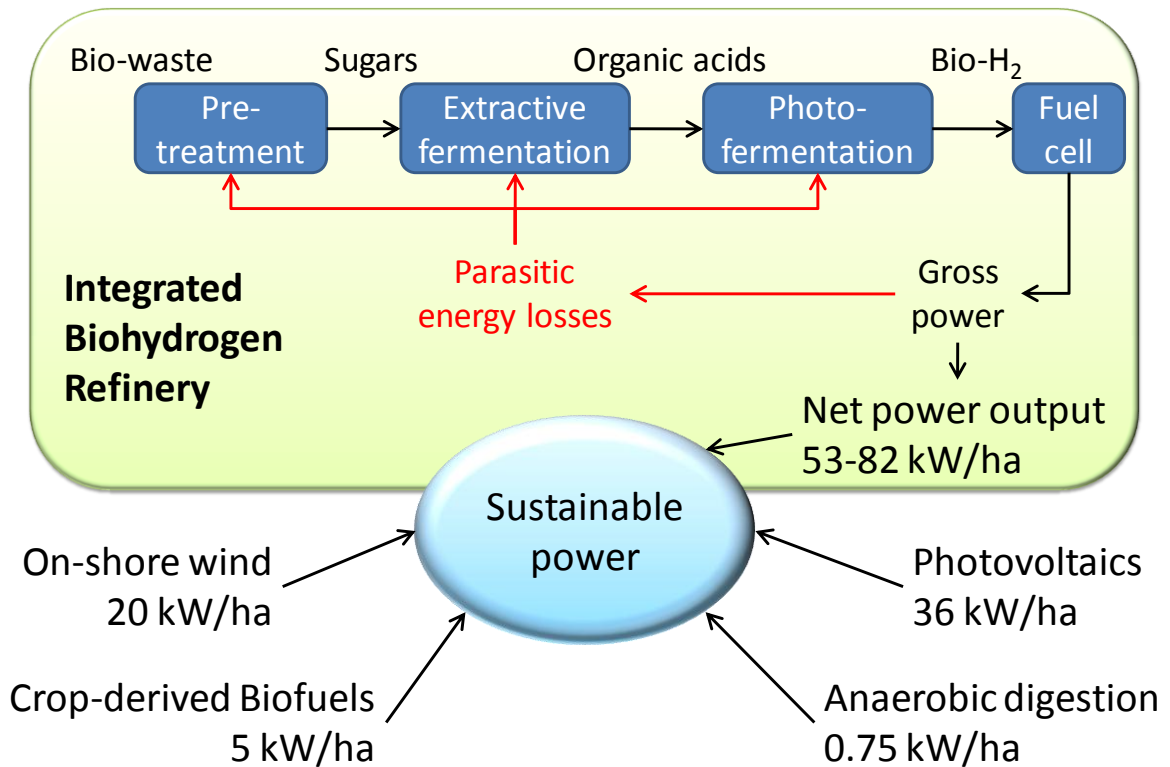
**AUTHOR EMAIL ADDRESS:** m.d.redwood@bham.ac.uk

**RECEIVED DATE**

**TITLE RUNNING HEAD:** Integrated Biohydrogen Refinery

**CORRESPONDING AUTHOR FOOTNOTE** \*Phone: +44-121414-5434; fax: +44-121414-5889; e-mail: m.d.redwood@bham.ac.uk

**ABSTRACT**



We report an *Integrated Biohydrogen Refinery* (IBR) with experimental net energy analysis. The IBR converts biomass to electricity using hydrothermal hydrolysis, extractive biohydrogen fermentation and photobiological hydrogen fermentation for electricity generation in a fuel cell. An extractive fermentation, developed previously is, here, applied to waste-derived substrates, following hydrothermal pre-treatment, achieving 83-99% biowaste destruction. The selective separation of organic acids from waste-fed fermentations provided suitable substrate for photofermentative hydrogen production, which enhanced the gross energy generation up to 11-fold. Therefore, electrodialysis provides the key link in an IBR for 'waste to energy'. The IBR could be more productive than 'renewables' (photovoltaics, on-shore wind, crop-derived biofuels) and also emerging biotechnological options (microbial electrolysis, anaerobic digestion).

**KEYWORDS:** fermentation, photofermentation, biohydrogen, waste, electrodialysis

## VI.6 Pilot plant

### Abstract

Information available on pilot plant (PP) studies for biological H<sub>2</sub> production is very limited. *E. coli* fermentations for H<sub>2</sub> production using glucose and food wastes have been optimized at bench scale experiments performed in 0.005 m<sup>3</sup> fermentation vessels (bioreactors). H<sub>2</sub> production yields of about 80 % of the theoretical maximum were achieved during several days in fed batch and fed continuous fermentations using glucose as substrate [100, 132]. Optimum parameters and process conditions learned were now tested at pilot plant scale (PPS) of 0.120 m<sup>3</sup> total capacity to perform *E. coli* fermentations using glucose and pear waste juice as substrate. The results obtained were far from optimum, the process conditions were analysed and are discussed in this chapter for future improvement and optimization of fermentative H<sub>2</sub> production at pilot plant scale (PPS).

### Introduction

Escalation of the fermentation process from 0.005 m<sup>3</sup> bench lab scale to PP volumes (> 0.1 m<sup>3</sup>) is not a straight forward task. Equipment and operating conditions that enable cells in a given formulation of medium to be made at scale, protected from contamination and with retention of biological activity, along with the design, implementation and operation of the bioreactors in which the cells perform and generate product (H<sub>2</sub>) constitute a major challenge and focus of attention. Fig. 39 depicts an integral fermentation process; the successful operation of this system relies on the ability to solve the problems involved in achieving the desired final product (H<sub>2</sub>) in a novel or particular approach in the most cost effective way and with production and separation of OA for the downstream PBR. Fig. 40 shows the PP fermentation unit at the University of Birmingham that was employed in this work.

The purpose of these final experiments is to transfer initial experience into the main aspects of the model described, and methods and operation to get initial knowledge from the PP equipment. Examples of PP that have been operated successfully with rates of H<sub>2</sub> comparable with that of the bench scale data can be found in Debabrata et al., 2008 [111]. The current system is made more complex, but potentially of much higher H<sub>2</sub> production overall, by the future incorporation of an electro dialysis (ED) unit and downstream photobioreactor, integrated at bench-scale as described elsewhere [100].

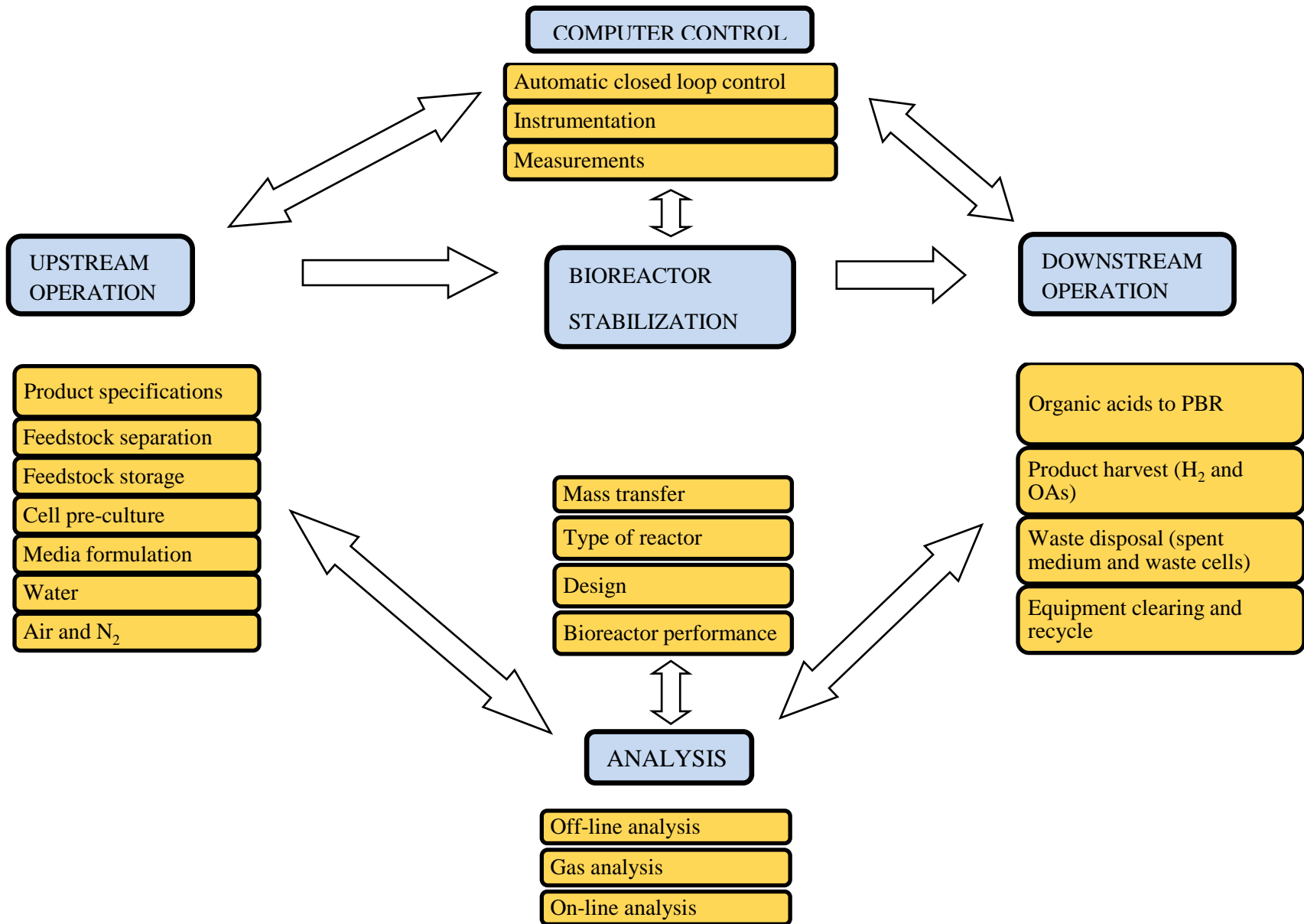


**Fig. 39** Shows a model of a fermentation system, the blocks in light blue represent main unit operations, the blocks in pale orange show important components of each unit operation. The whole system is interconnected as shown by the arrows.

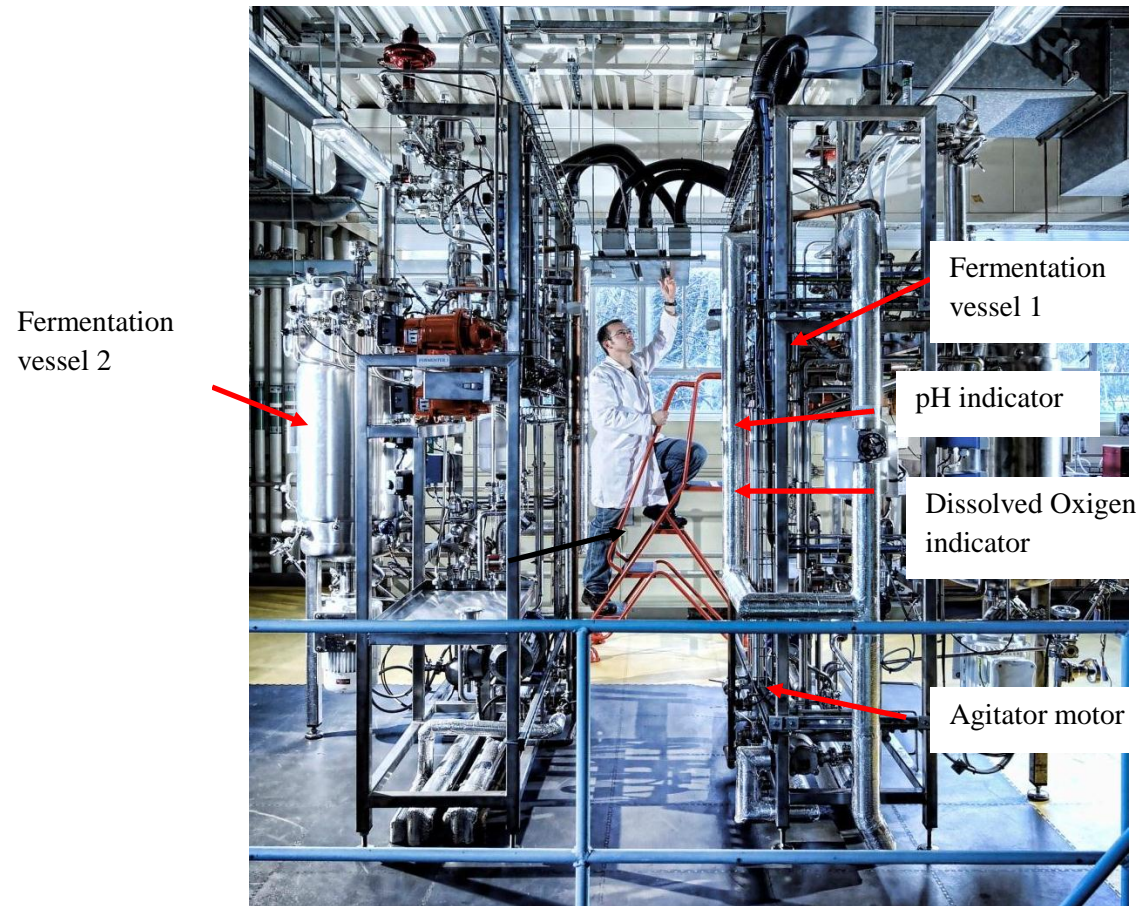


**Fig. 40** Twin fermentation system at the University of Birmingham.

### *Upstream operation*

Upstream operation involves cells development, feedstock preparation, media formulation, quality of water utilized and air and N<sub>2</sub> sources to maintain aerobic/anaerobic conditions that are appropriate for cell growth and performance. Whenever possible the presterilization of the equipment, media, water and additives must be done to avoid the presence of contaminating microorganisms. An exception to this is the use of a rapidly growing organism in a sparse or toxic medium to which it has been pre-adapted, although quality control checks need to establish the failure of contaminants to become established in the culture. Cell culture deals with the appropriate selection of efficient high yielding strains of microorganisms. The advantages of *E. coli* as a model microorganism for fermentative H<sub>2</sub> production from sugars were discussed in section II.4.3 and VI.1. From the *E. coli* strains available (Table 6) strain HD701 proved to be a robust strain with excellent growth, good productivity (Table 7) and adaptability suitable for this production-scale operation. For example strain MC4100 and strain FTD67 failed to produce H<sub>2</sub> in small 15 mL fermentation tests possibly due to media nutrient limitations and pressure conditions inside the sealed serum bottle, however strain HD701 performed well and was a reliable strain for these purposes despite the non-optimum conditions. Certainly the utilization of other strains for PP experiments should not be disregarded since each strain offer different capabilities and valuable advantages such as strain RL009; despite its more difficulty to grow it generates less ethanol (Table 7) an accumulating inhibitory product) than the other strains which might be an important advantage in long term batch or continuous fermentations.

Media formulations provide the nutrients and substrates (sugars) at the correct levels required by *E. coli* (discussed in section II.4.3) and certainly this quality should be maintained during the fermentation process; however the economics of the raw materials and their pre-treatment is an important parameter to manage. The introduction or accumulation of inhibitory by-products (such as 5-HMF, OA and ethanol) should be avoided or controlled to maintain high productivity.

Water utilized for PP experiments was tap water as de-ionized water (DW) is costly; experiments at bench scale fermentations using tap water revealed no significant difference in comparison with DW in terms of H<sub>2</sub> production and growth by *E. coli* HD701.

### *Bioreactor*

The bioreactor is the heart of the fermentation system, it provides the appropriate biological environment to favour a desired biological process, in this case the production of bio-H<sub>2</sub>. Bioreactors are usually operated as batch, fed-batch and continuous operation processes.

Our system is complicated since upstream dark fermentation is operated as fed-batch while the ED extraction of OAs is intermittent (controlled by feedback loop from the pH of the upstream vessel) while Rhodobacter feed from the permeate chamber is/can be operated on a continuous basis. The integrated system, overall, is projected as a continuous process once the problem of ethanol accumulation in the dark fermentation is overcome, as it was described in section 0. by using strain RL009.

Batch operation is one of the most common modes of process operation since it provides several advantages such as lower risk of contamination as fresh inoculum and media can be introduced safely, it allows successive biomass growth stages followed by a product formation stage under different operating conditions to run in the same vessel and batch operation gives greater operational flexibility and production planning [228]. However one of the main disadvantages of the batch mode is the accumulation of inhibitory products (OAs, ethanol), while fermenter down-time between batches is an economic consideration.

Fed-batch operations permit the operation of batch modes for extended periods as this allows the replenishment of consumed nutrients and substrates into the bioreactor providing control over the specific growth rate of the microorganism while maintaining maximum H<sub>2</sub> production rates. Room has to be made in the bioreactor for the fresh ingredients and one of the best ways is to remove part of the suspension before each addition (fill and draw), however the accumulation of inhibitory products is still an issue that eventually will affect H<sub>2</sub> productivity. In the present process, operated as an electrofermentation (see section VI.5) a part of the dark fermenter volume is lost via electrolysis of water in the electrochemical cell. This offset, in part, the volume increase in the dark fermenter vessel.

Continuous operation mode has strong advantages compared to batch and fed-batch operations since this operates in long production runs resulting in high productivity and steady state conditions that favour easier process control and even demand on utilities which translates in being more cost efficient while achieving consistency of product quality [228]. As this mode of operation operates an extended period, it requires the utilization of organisms with high genetic stability, operation under low risk of contamination and the continuous removal of inhibitory products [100].

With respect to the design of the bioreactor, aerated (gas sparged) stirred cylindrical vessels with the agitator shaft placed along the vertical axis of the cylinder are commonly used for fermentations and the most common impeller type is the bladed turbine operated at variable speed, which produces radial flow and high shear rates near the impeller which are very important for air dispersion in aerobic growth and to achieve homogeneity, mass and heat transfer in the fermentation media. A key feature is the double mechanical seal between the impeller shaft and the vessel top plate. This allows free rotation of the impeller shaft while precluding entry of contaminant microorganisms into the fermentation.

Special consideration should be given to increasing agitation speed (mixing condition) since higher agitation will improve the performance of the bioreactor in this respect but also will bring an increase in shear stress which could reach levels that damage the bacteria; dissolved oxygen tension (DOT) has a strong effect on cell physiology and biomass yield therefore a poor mixing condition would lead to low biomass yield but high cell viability (a measure of healthy cells), while on the contrary high mixing conditions give higher biomass yield but low cell viability. Therefore it is important to avoid environmental stress associated with appropriate levels of dissolved oxygen through mixing [229]. On the other hand, at high cell densities and 'aerobic culture' contains areas of transient anaerobiosis therefore these cells are continually switching rapidly between aerobic and anaerobic metabolism [229].

Air flow should also be controlled to meet the oxygen demand of an aerobic growth process. The sparged gas also dissipates energy into the culture medium and contributes to agitation. Bubble dispersion may be employed, or the vessel may be baffled to assist mixing.

The volume of the vessel should be between 30-50 % larger than the fermentation culture volume to allow a head-space necessary for the separation of liquid from the gas phase. The vessel should also be designed to withstand the internal sterilization pressures and temperatures.

The performance of the scale-up system will be evaluated in terms of achieving the same *E. coli* growth, H<sub>2</sub> yields and production rates as in the 3 L scale fermentations at minimum unit cost. This task implies the use of rational optimization procedures, especially those based in statistical methods as a valuable tool to determine the combination of controllable process operating conditions that will yield the desired values.

#### *Computer control*

Computers and software (fermentation control algorithm) strategies provide an indispensable control function in fermentation processes and are extremely helpful in monitoring, data logging and

control, and in computer simulations for optimization as models on fermentation kinetics are developed. Important fermentation parameters such as temperature, pressure, pH, airflow, COD and agitation speed can be monitored and controlled. Correlation of these parameters with other “off-line” variables such as biomass concentration, sample quantitative analysis and product evolution are facilitated and processes can be optimized at lower costs [228].

Automatic controllers require accurate measurements to achieve good closed-loop control therefore the incorporation of appropriate instrumentation (for example probes resistant to steam sterilization or fouling) and instrument calibration methods are important factors to consider in having a true and an accurate measurement of the processes parameters.

#### *Analysis*

As some biological variables are still difficult to be measured on-line, off-line analysis is widely used and their incorporation to the control loop requires the intervention of an interactive operator; in addition the obtained data may be several hours delayed.

Vent gases such as H<sub>2</sub>, N<sub>2</sub>, CO<sub>2</sub> and O<sub>2</sub> can be effectively measured on-line using mass spectrometers.

#### *Downstream operation*

It is said that the downstream operation could capture 60-90 % of the total processing costs of the fermentation system as described in Fig. 39. It embraces the cost of separation of biomass (disc centrifuges are commonly used at large scale) and also the finishing operations that deal with product purification, product concentration, product packing and storage (among others) and that are subject to the composition of the process stream (which is subject to variations) and to the specifications of regulatory agencies or product requirements. Limited information is available, therefore downstream processing is a very active research area, and good examples of relevance to this study are H<sub>2</sub> storage systems and carbon capture and storage (CCS) in steam methane reforming (SMR) for H<sub>2</sub> production plants (section II.1).

### **Materials and methods**

All chemicals were analytical grade. *E. coli* HD701 was provided by Dr. F. Sargent (University of Dundee). Pear waste was provided by Minor, Weir & Willis (MWW).

Fermentations were carried out utilizing a twin system of two 0.100 m<sup>3</sup> parallel steam pilot plant (PP) (Pierre Guerin Ltd) automated bioreactors with an effective volume of 0.07 m<sup>3</sup> as illustrated in fig XX. A mass spec model Prima dB (Thermo Scientific) was connected on-line to

provide immediate gas analysis. Air was supplied using a conventional air compressor and N<sub>2</sub> was supplied through an Atlas Copco N<sub>2</sub> generator both filtered sterilized. A fed batch fermentation mode will be described. The purpose of twin reactors is to provide control data (e.g. from glucose) and experimental data (e.g. from pear juice) in a single experiment using a divided inoculum. Unfortunately, in the 'glucose control' reactor the shaft impeller motor overheated and the experiment in that fermenter had to be stopped. By the way the fermenters are fixed; the company admitted the impeller shaft should not have failed on the small hours of usage logged and they are investigating the cause of the problem.

Due to limitations such as manpower needed to process the input feed (in this case ~ 30 Kg of pear per load) only a single 40 L twin fermentation experiment was made, with the aforementioned problem in the glucose control reactor. The fermentation volume established implies that more than 65 % head space in contrast to 40 % head space in 0.005 m<sup>3</sup> (5 L) bench scale fermenters. Glucose was used as a substrate for the aerobic growth phase whereas pear juice obtained from pear wastes was used as a substrate for the anaerobic phase. The juice from pear waste was extracted using a Ferrari 5 L hand-cranked fruit press. No infusion was used.

Bioreactors were washed and temperature, pH and OD electrodes were calibrated previously, solutions of 2 M NaOH and 2 M H<sub>2</sub>SO<sub>4</sub> (5 L each) were prepared for pH control.

Fermentation media (40 L) was prepared according to *aerobic pre-growth in fermenter media formula* described in the appendix section VIII.1.2. Tap water was utilized for media preparation. Fermentation media was autoclaved (120 °C; 30 min; cooling to 30 °C) in the fermenter followed by the aseptic addition of pre-sterilized media additives. Media additives (as described in the same appendix section) were trace elements (0.12 L), Glucose (500 g.L<sup>-1</sup>)(1.6 L), MgSO<sub>4</sub> (0.080 L) prepared using DW and autoclaved separately; Thiamine (0.050 L) was filter sterilized. All additives were mixed before added to the fermenter through special ports using autoclaved connectors.

For inoculum, cells of *E. coli* HD701 were pre-growth overnight as described in appendix section VIII.1.1 but utilizing 0.4 L (1 % v.v<sup>-1</sup>) of NBF8. Cells were introduced into the bioreactor through an inoculation port using autoclaved connectors.

With the aim to achieve high cell concentration (2-4 g dw.L<sup>-1</sup>), the system was programmed for a first aerobic growth phase followed by a manual switch to a second anaerobic fermentation phase. Conditions for the aerobic growth phase were as follows:

- pH acid set point 7.5
- pH base set point 5.75
- Air flow rate 13 L.min<sup>-1</sup>.
- Agitation speed 100 rpm
- Temperature 30 °C
- Head pressure 0.2 bar

At pH ~ 6.0 the fermentation will be switched to the anaerobic phase with the pH controlling both the switch and the automated control of titrants to maintain pH at 5.75. Conditions for the anaerobic phase were as follows:

- pH acid set point 7.5
- pH base set point 5.75
- N<sub>2</sub> flow rate 6 L.min<sup>-1</sup> continuously
- Agitation speed 200 rpm
- Temperature 30 °C
- Head pressure 0 bar

### **Analysis**

*E. coli* growth was followed by measuring OD<sub>600</sub>, OA were analysed by HPLC (as described in [107] , glucose was analysed by DNSA assay (appendix section VIII.4.1) and biogas was analysed using an on-line mass spectrophotometer.

### **Results and discussion**

*E. coli* HD701 growth and pH profile are shown in Fig. 41; glucose and OA generation are shown in Fig. 42. The maximum aerobic growth was ~ 0.45 g dw.L<sup>-1</sup> achieved after 72 h, the pH was 6 and ~ 40 % of the initial glucose was consumed. This growth was only ~ 20 % higher than the traditional *E. coli* aerobic pre-growth using erlenmeyer flasks containing ‘NBF8’ media (appendix section VIII.1.1) after fermentation inoculation [100] and ~ 6 times lower than the aimed 2-4 g dw.L<sup>-1</sup> achieved in similar fermentations at 5 L scale after the initial 24 h [132].

In an attempt to re-stimulate growth, the pH was adjusted to 7, and agitation speed and air flow were increased to 250 rpm and 30 L.min<sup>-1</sup> respectively. However, after 16 h (88 h since t=0) only 15 % more growth was obtained, the pH decreased to 6.6 and an additional 10 % of glucose

was consumed (total of 50 % consumed). Afterwards the system was switched to anaerobic mode (after 88 h from  $t=0$ ).

Substrate (glucose) concentration and DOT [132, 229] are important factors to consider in the utilization of this method in order to achieve maximum growth yields.

Glucose concentration helps to restrict the aerobic formation of inhibitory OA (overflow metabolism, which produces primarily acetate) which is utilized to signal the transition (at pH 6.0) to the anaerobic phase; an excess of glucose has an immediate effect of decreasing the growth rate and increasing the generation of OA [229]. However the transition to anaerobic phase helps to mitigate overflow metabolism due to any excess in glucose concentration (Fig. 42) [132]. The concentration of acetate reached  $\sim 55$  mM which is  $\sim 7$  fold higher than that obtained in the smaller fermentations (section VI.1.1). Also, acetate was produced throughout aerobic growth.

DOT has a strong effect on cell physiology and biomass yield, as explained earlier in this chapter a poor mixing condition usually leads to low biomass yield but high cell viability and high mixing conditions give higher biomass yield but low cell viability. Therefore it is important to avoid environmental stress associated with glucose limitation and to maintain appropriate levels of dissolved oxygen through mixing. The glucose concentration utilized was equivalent to the glucose concentration in previous successful experiments, consequently the low growth obtained in our experiment could be attributed to an initial poor mixing and possibly a limiting DO concentration but this was not monitored, which will be very important in future experiments.

After 24 h of the growth phase formate decreased from initial 22 mM to 13.5 mM and set between 11.6-12.8 mM for the rest of the fermentation but in the small batches there was almost no formate. This shows that conversion to  $H_2$  was not happening effectively. Acetate began to accumulate in significant amounts; in contrast with previous fermentations where formate levels rapidly declined from initial 23 mM to 4-8 mM and lactate (up to  $\sim 8$  mM) was mainly produced instead (sections VI.1.1 and VI.5). During the next 64 h formate remained steady and pyruvate began to accumulate; before switching to anaerobic phase acetate and pyruvate levels reached a maximum of 56 and 28 mM respectively (2.24 and 1.12 mol). Once in anaerobic phase, pyruvate gradually decreased to 0 after 185 h of fermentation, acetate decreased to 44 mM during the initial 24 h of the anaerobic phase and remained at 34-38 mM for the rest of the fermentation period. Lactate increasingly accumulated finally  $\sim 43$  mM. The lactate-butyrate transition did not occur in this experiment as it was observed throughout *E. coli* fermentations (section VI.1.1). No changes in trend were observed after the addition of 3.25 L of pear juice after 114 H of fermentation (24 h after

anaerobic phase) which resulted in accumulation of glucose (from 37 to 75 mM) without significant consumption during the rest of the fermentation (60 mM).

During the metabolism of glucose by *E. coli* whether in aerobic or anaerobic conditions, glucose is transported into the cell by the phosphotransferase system and catabolised to pyruvate in a process that liberates energy as ATP [230]. Pyruvate is metabolised to acetyl CoA by the pyruvate dehydrogenase (PDH) complex, at the same time the FHL complex is activated through the addition of formate. In subsequent anaerobiosis the synthesis of the PDH complex is mostly repressed and totally inhibited possibly by NADH being replaced by pyruvate formate lyase (PFL) [123]. Acetyl-CoA is still produced but the activated FHL complex shift pyruvate metabolism to formate and H<sub>2</sub> along with competing pathways to lactate, acetate and ethanol (section VI.1) [123]. H<sub>2</sub> was not detectable against the large excess of N<sub>2</sub> but the persistence of high levels of formate in the aerobic phase would suggest poor conversion of HCOOH to H<sub>2</sub> + CO<sub>2</sub> via FHL (Fig. 42). It is evident from the accumulation of pyruvate and acetate during the aerobic growth that the FHL complex was not adequately expressed during the aerobic growth phase and as a consequence the FHL metabolic pathway to formate and H<sub>2</sub> was ineffective. This could be attributed to low mixing/aeration conditions during the growth phase employed in this experiment. A positive response in growth was found when air flow and agitation speed were increased (Fig. 41) and the rate of glucose consumption increased ~ 2 fold (Fig. 42). However in order to avoid further accumulation of inhibitory OAs the system was switched to anaerobic mode.

The big head space left inside the fermenter (due to low culture volume) and the minimal N<sub>2</sub> flow required by the mass spec (6 L.min<sup>-1</sup>) diluted any H<sub>2</sub> produced to very low levels making analysis very difficult. In future fermentations it will be important to increase the volume of fermentation to ~ 100 % of the effective volume (75-80 L) to improve the concentration of H<sub>2</sub> produced.

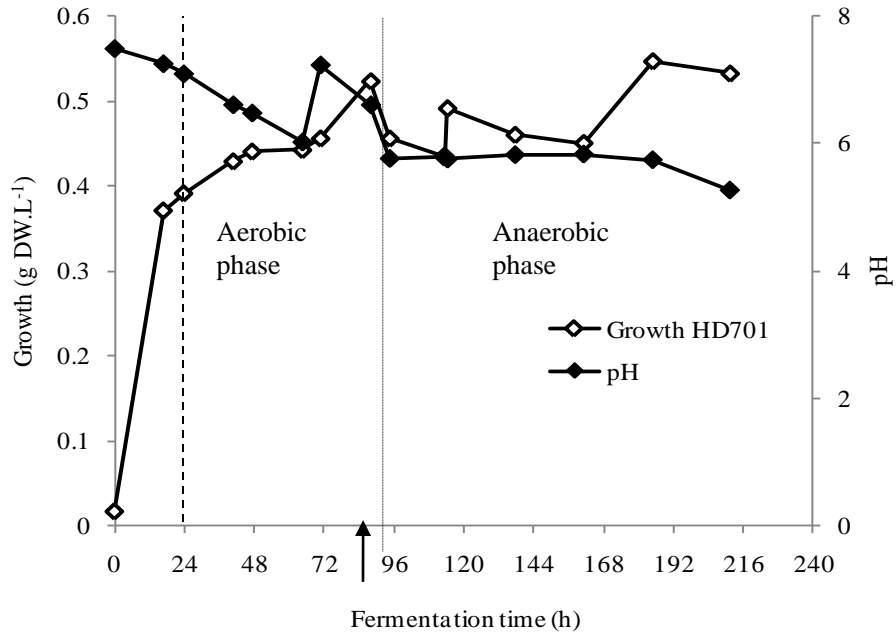


**Fig. 41** HD701 growth and pH during fermentation time. The arrow indicates the time where pH was adjusted to 7 and agitation and air flow increased in an attempt to stimulate growth. The dotted line indicates the point where the fermentation was switched to anaerobic phase; (- - -) indicates the onset of the stationary growth phase. Glucose control experiment is not represented in the graph due to a reactor failure.

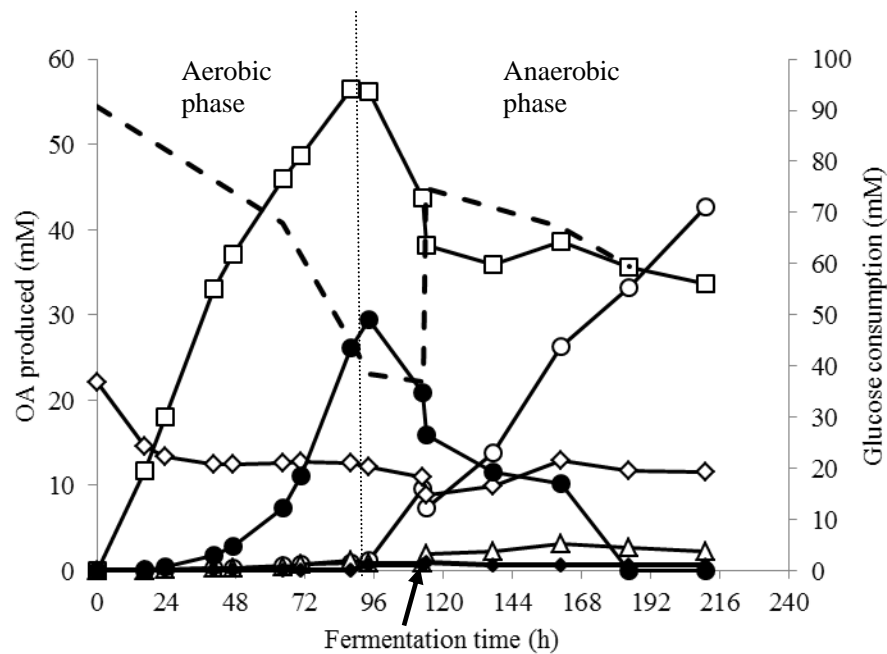


**Fig. 42** OA produced and glucose consumption by HD701 with fermentation time. (○) lactate; (□) acetate; (◇) formate; (△) succinate; (●) pyruvate; (◆) H<sub>2</sub> production; (- - -) glucose consumption. Aerobic and anaerobic phase are divided by the dotted line. The arrow indicates the time of addition of pear juice. Glucose control experiment is not represented in the graph due to a reactor failure.

In other parallel studies, a pilot plant of 1.48 m<sup>3</sup> (effective volume capacity) was operated to produce H<sub>2</sub> from molasses using seed sludge from local municipal wastewater continuously for 200 days. The H<sub>2</sub> production rate obtained was compared with previous bench-scale studies. In these experiments H<sub>2</sub> yield (m<sup>3</sup>.d<sup>-1</sup>) and specific H<sub>2</sub> production rate (m<sup>3</sup>.Kg MLSS.d<sup>-1</sup>) increased when the organic load rate (OLR) ranged from 6.32 kg COD.m<sup>-3</sup>.d<sup>-1</sup> to 68.21 kg COD.m<sup>-3</sup>.d<sup>-1</sup>; H<sub>2</sub> yield: 8.25 m<sup>3</sup>.d<sup>-1</sup> (0.75 m<sup>3</sup>.Kg MLSS.d<sup>-1</sup>), however H<sub>2</sub> decreased when OLR was > 68.21 kg COD.m<sup>-3</sup>.d<sup>-1</sup>. It was also observed that a high concentration of biomass in PP bioreactor improved H<sub>2</sub> yield [96].

### **Conclusion**

The results obtained show that poor agitation had a negative impact on aerobic growth. Nevertheless this preliminary experiment enabled the first steps towards scale up and future studies would:

- Use two fermenters in parallel; one control and one altered by just one parameter.
- Analyse DO during the growth phase.
- Larger culture volume to minimise head gas and hence diluent N<sub>2</sub>.
- Careful study of agitation and air supply.
- Strict control over the other parameters such as temperature and pH.

Minimizing the amount of experimentation at PP scale is essential for economic reasons, therefore the utilization statistical experimental design becomes a valuable tool to make the experimental procedure cost effective.

## VII. GENERAL DISCUSSION: OUTCOMES WITH RESPECT TO OBJECTIVES

The subprojects and activities part of this research project were completed and all its primary objectives were achieved.

Results on *E. coli* bench scale fermentations revealed different capabilities and advantages of these microorganisms for the downstream processing as discussed in section VI.1. Mutants that provided low ethanol concentration gave promising results.

Results indicated that the hydrolysates produced from HCW hydrolysis of starch, cellulose and food wastes with high starch content are suitable for bio-H<sub>2</sub> production after their detoxification with AC; however an important factor that should be taken in consideration is the reactor wall material which in this case is Hastelloy C-276, an alloy rich in Ni that, when corroded, (usually after reactions with materials containing salt) may provoke wall-catalysed reactions affecting sugar yields negatively while increasing the formation of DP as discussed in section VI.3.2. An alternative reactor material may include stainless steel (SS-316L).

Extractive fermentation of different food wastes utilizing a novel electro dialysis technique (developed by Dr. M. D. Redwood) for the separation and transport of the OA generated during the dark fermentation was also successful and proved to be a promising technology for a synergistic integration of both fermentation processes for H<sub>2</sub> production. This part of the project was a team project lead by Dr. M. D. Redwood and my contribution was in assisting Dr. Redwood during the equipment installation and start-up procedures, operation and process control throughout the experiments, sample processing and analysis.

Fermentations at pilot plant scale provided an invaluable contribution to the escalation of the dark fermentation process for bio-H<sub>2</sub> production as it enabled the first steps towards scale-up and the design of future pilot plant experiments.

A larger fermentation (3 L) of food waste hydrolysates revealed a low rates and yield of H<sub>2</sub> production that can be attributed to the accumulation of OA and ethanol. Additional experiments are necessary for a more definite conclusion.

As an additional outcome from this project very interesting lines of research were identified and remained to be explored in the near future.

Although results were already discussed for each subproject in chapter VI, this section summarises the main project outcomes and outlines the most important challenges to pursue.

## VII.1 Final discussion and conclusions

Improvement in H<sub>2</sub> yield from all the strains tested (Table 6) most within the range of 22-35 % were achieved in 3 L scale fermentations compared to small 0.1 L scale (section VI.1) as a consequence of improvements in growth methods [100], advances in media formulations [152, 231] and the utilization of more sophisticated fermentation equipment.

*E. coli* strains showed different capabilities associated to their particular genetic modifications. Strain HD701 (lacking the FHL repressor), FTD67 (devoid of up-take hydrogenases Hyd-2) and FTD89 (devoid of Hyd-1 and 2) performed better than the parent strain MC4100 in evolving better H<sub>2</sub> yields and rates, demonstrating that those deletions effectively enhanced H<sub>2</sub> production. All these strains produced similar amounts of ethanol compared to the parent strain MC4100.

Among the OA generated by the strains, butyrate is the best OA for the downstream process in terms of HPP (10 mol H<sub>2</sub>.mol OA<sup>-1</sup>) and current efficiency whereas acetate and succinate are the worst options as there are likely to yield no energy profit. Considering this criterion, strain FTD67 offers more viability in terms of HPP and net energy profit above the other three strains.

The presence of butyrate is an interesting, little-reported and un-expecting phenomenon discovered during these *E. coli* fermentations, having major implications for integration with a downstream PBR and as such needs further investigation to elucidate its metabolic pathway. In the case of strains MC4100, HD701, FTD67 and FTD89 butyrate is generated at the expense of lactate under glucose depletion.

Mutant strain RL007 (devoid of *ldhA*) compensated the effect of lacking the lactate dehydrogenase by making more succinate and consequently less ethanol. The H<sub>2</sub> produced by this strain was less compared to the parent strain, however, and despite having the highest HPP of all strains, ~ 85 % of this comes from succinate and acetate implying that the utilization of this strain is likely to result in no energy profit after the utilization of its OA in the photofermentation process. In addition this strain and the parent strain were the only strains tested for their ability to make Bio-Pd/Pt catalyst from the waste biomass for use in a hydrogen fuel cell to produce electricity and the results showed that palladized cells from strain RL007 produced ~ 3 fold more electricity as compared to Bio-Pd<sub>MC4100</sub>.

In mutant strain RL009 (devoid of *ldhA* and *ackA*) the additional deletion of the *ackA* enzyme blocked the route to acetate provoking an accumulation of pyruvate. This resulted in an

activation of the POX complex which not only opened another route to acetate synthesis which did not generate ATP, resulting in poor growth but also enhanced H<sub>2</sub> production reaching the highest yield of all strains (~ 1.7 mol H<sub>2</sub>.mol glucose<sup>-1</sup>) and decreased the generation of ethanol by half compared to strain RL007. In terms of HPP this strain could be interesting as it has the second highest HPP (10.3 mol H<sub>2</sub>.mol OA<sup>-1</sup>) of which ~ 50 % comes from butyrate (the best OA) and ~ 50 % from acetate (one of the worst).

These two mutant strains showed a different route to butyrate in which butyrate was generated at the expense of pyruvate (as these strains do not make lactate). This is also unexpected and deserves further study as butyrate is a desirable product for the photofermentation process. Evaluation of palladized and platinized cells from RL009 to produce electricity also needs examination. This is important as re-use of the used bacteria 'in process' is important towards the concept of zero waste; palladized cells from H<sub>2</sub>-fermentation have been shown to be effective catalysts. Towards 'in process' recovery of CO<sub>2</sub>; initial studies have shown promise on the production of a value algal product on fermentation waste CO<sub>2</sub> (See appendix VIII.6.2).

Overall, and based on the information collected so far, strains FTD67 and RL009 seem to be the most suitable *E. coli* strains to be used in the dark fermentation process for the downstream processing, even though more study is necessary to understand and improve the performance of *E. coli* strains according to the criteria established as biological hybrid systems for bio-H<sub>2</sub> production have to be envisioned as one single integrated process where the potential and performance of each microorganism has to be evaluated in terms of its contribution to an overall objective.

Hydrolysis of biomass to fermentable sugars is essential for its utilization for downstream bio-H<sub>2</sub> production. In addition to biomass composition, costs and effectiveness, environmental factors are also important in the selection of the hydrolysis method (chapter III).

HCW in the presence of CO<sub>2</sub> is an environmental friendly method of biomass hydrolysis as it utilizes water at high temperatures and pressure. The addition of CO<sub>2</sub> forms H<sub>2</sub>CO<sub>3</sub> which is a weak acid that catalysed the reaction, improving yields of hydrolysis products, mainly sugars, but also 5-HMF, furfurals, phenolics, amines and OA depending on biomass composition. While at the same time reducing the optimum hydrolysis temperature by 10 °C compared to the use of N<sub>2</sub>.

Model compounds (starch and cellulose) and wastes (food waste, spent grain and wheat straw) were hydrolysed in HCW/CO<sub>2</sub>. Starch produced hydrolysates with highest glucose content (548 g.kg starch<sup>-1</sup> carbon at 200 °C) due to its weaker semi-crystalline structure which was easier to

hydrolyse. From the wastes food waste produced the hydrolysate with more sugar content ( $45.5 \text{ mg.g waste}^{-1}$ ).

For lignocellulosic wastes the conversion to sugars was very low, therefore a combination of HCW and enzymatic methods may offer a feasible alternative for the optimum hydrolysis to sugars of these complex wastes that are also not enzymatically biodegradable due to the complex structure of lignin (chapter IIIVI.4). In this HCW pretreatment lignin and hemicellulose will be separated first and the residue (rich in cellulose) is more susceptible to enzymatic attack or for further HCW hydrolysis (chapter III). The lignin fraction can be utilized as a source of chemicals, particularly phenolic compounds [232] and for the production of  $\text{H}_2$  and bio-fuels through the utilization of gasification and pyrolysis technologies (section II.3.1). This would add value and importance to HCW hydrolysis technology and constitute another very interesting line of research to follow.

It was demonstrated that the hydrolysates produced from the hydrolysis of the model compounds and bio-wastes using HCW/ $\text{CO}_2$  were suitable for fermentation by *E. coli* after their detoxification with AC; before AC treatment the fermentability of the hydrolysates to produce  $\text{H}_2$  was nil whereas after AC treatment in most cases  $\text{H}_2$  production was comparable or equivalent to glucose control (chapters 0VI.3 and VI.4).

The AC treatment removed most of the degradation products identified as potential inhibitors for fermentation without severely affecting sugars, thereby considerably improving the fermentability of the hydrolysates. An alternative to AC that is interesting to evaluate is the utilization of ionic exchange resins such as Ambertlite XAD1180N, XAD761 or XAD4 resin utilized with satisfactory results (but inferior to AC) in the removal of 5-HMF, furfural and other DP for the production of butanol from agricultural residues by fermentation after hydrolysis. These polymeric resins offer the advantage of an easier regeneration on-site which translates in smaller costs. But nevertheless ion exchange resins are expensive, whereas AC is the bulk method of choice in, for example, the water industry where it is used to remove chlorination by products at scale.

In the case of starch and cellulose, the main degradation product was 5-HMF and its removal by AC was very selective and effective (Chapter 0 and VI.3). 5-HMF can be converted to 2,5-furandicarboxylic acid by aerobic oxidation involving titania-supported gold catalyst (99 mol % yield achieved under optimal conditions) [233]. This organic compound (2,5-furandicarboxylic acid) was identified by the US department of energy as one of 12 priority chemicals for a future “green” chemistry industry [234], this chemical may replace terephthalic acid as a monomer in the production of plastics [235]. This process may offer another opportunity that is worth to explore as it

could be integrated to the HCW hydrolysis technology for value product co-production. In this context *E. coli* bacteria have been shown to recover gold from wastes [236] and bio recovered nano Au(0) is highly active as an oxidation catalyst. The use of ‘aurized’ waste *E. coli* to develop a value product from waste 5-HMF is a clear future opportunity to value-add to the ‘waste into energy’ process described in this thesis.

Another interesting use of 5-HMF that needs investigation is for the synthesis of 2,5-dimethylfuran (DMF) which is a powerful fuel that contains as much energy as petrol and ~ 40 % more than ethanol. The usual synthesis path includes sugar transformation to 5-HMF (in this case 5-HMF is obtained by HCW hydrolysis) and then to DMF through the utilization of acid, copper catalysts, salt and butanol as solvent [237]. DMF can be utilized in enormous quantities as bio-fuel for the transportation industry. However the “value” of the synthesized fuel needs to be balanced against the butanol consumed. In this context the butyrate production pathway is very relevant; others have reported the use of *E. coli* to produce butanol after substantial modifications [238] and the discovery of a ‘natural’ pathway of 4-carbon fatty acid metabolism as reported here may be of relevance in this context if conversion of butyrate to butanol (as a simple metabolic pathway diversion) can be achieved. However this would detract from the use of butyrate in the downstream PBR and here of HPP from the process.

Furfural was the main DP product from the hydrolysis of lignocellulosic wastes (spent grain and wheat straw) (chapter VI.4) and it was also efficiently removed by AC. The recovery of furfural by utilizing ionic exchange resins like the ones mentioned above might be easy after resin regeneration and offers another area of investigation that may be easily integrated to the HCW hydrolysis. Furfural is a very important industrial chemical intermediate for the synthesis of a wide range of high value chemicals with several uses and applications within the chemical industry; furfural is first converted into furfuryl alcohol via hydrogenation, for which palladized waste *E. coli* cells have been found to be an effective hydrogenation catalyst (see appendix VIII.5.2), and further processed into furan resins used mainly for foundry sand binders in the metal casting industry [239, 240].

The utilization of FW hydrolysates obtained from HCW/CO<sub>2</sub> treatment, in 3 LF scale fermentation delivered low yields of H<sub>2</sub> production (attributed to the accumulation of OA and ethanol), however HCW treatment of starch rich wastes integrated with fermentation-photofermentation processes should not be disregarded as it may be possible to increase sugar extraction from these wastes by: processing wastes with a higher starch content; ensuring that

reactor wall material is not leaching and catalysing sugar degradation (see section VI.3.2) and finding optimum concentration of starting material for the HCW reactions. It may constitute a viable potential alternative for H<sub>2</sub> production and bio-waste utilization.

It is vital for the future of all these technologies to achieve scale-up operation to pilot plant scale. University of Birmingham modern pilot plant facility provides an excellent opportunity to conduct research towards finding the optimum conditions, best microorganisms at scale and best substrates for the reproducibility of results already obtained at bench scale experiments before the pre-industrial application of the technologies reported here. In the first experiment conducted in the pilot plant a number of incidents occurred that resulted in undetectable yields of H<sub>2</sub> from the fermentation sugar rich substrates by *E. coli* HD701. Among these were: insufficient aeration, pH control failures, low volume of media (~ 40 % relative to the effective volume utilization of the fermenters), low culture density (inoculum), H<sub>2</sub> on-line analysis, among others. Such scale-up of the biological processes is a very important task to pursue in the near future.

Finally, based on results, learning and experiences from this research work the concept of an integrated bio-refinery process is broadly schematized in Fig. 43. This conceptual model contemplates a versatile process considering the integration of the most important technologies (to my judgement and knowledge) for the processing of biomass into high value chemicals and fuels for energy. Product yields, mass and energy balances and economic evaluation will have to be integrated to the scheme as we progress through the development of these technologies; some of them already are in the commercialization stage such as anaerobic digestion, gasification and pyrolysis.

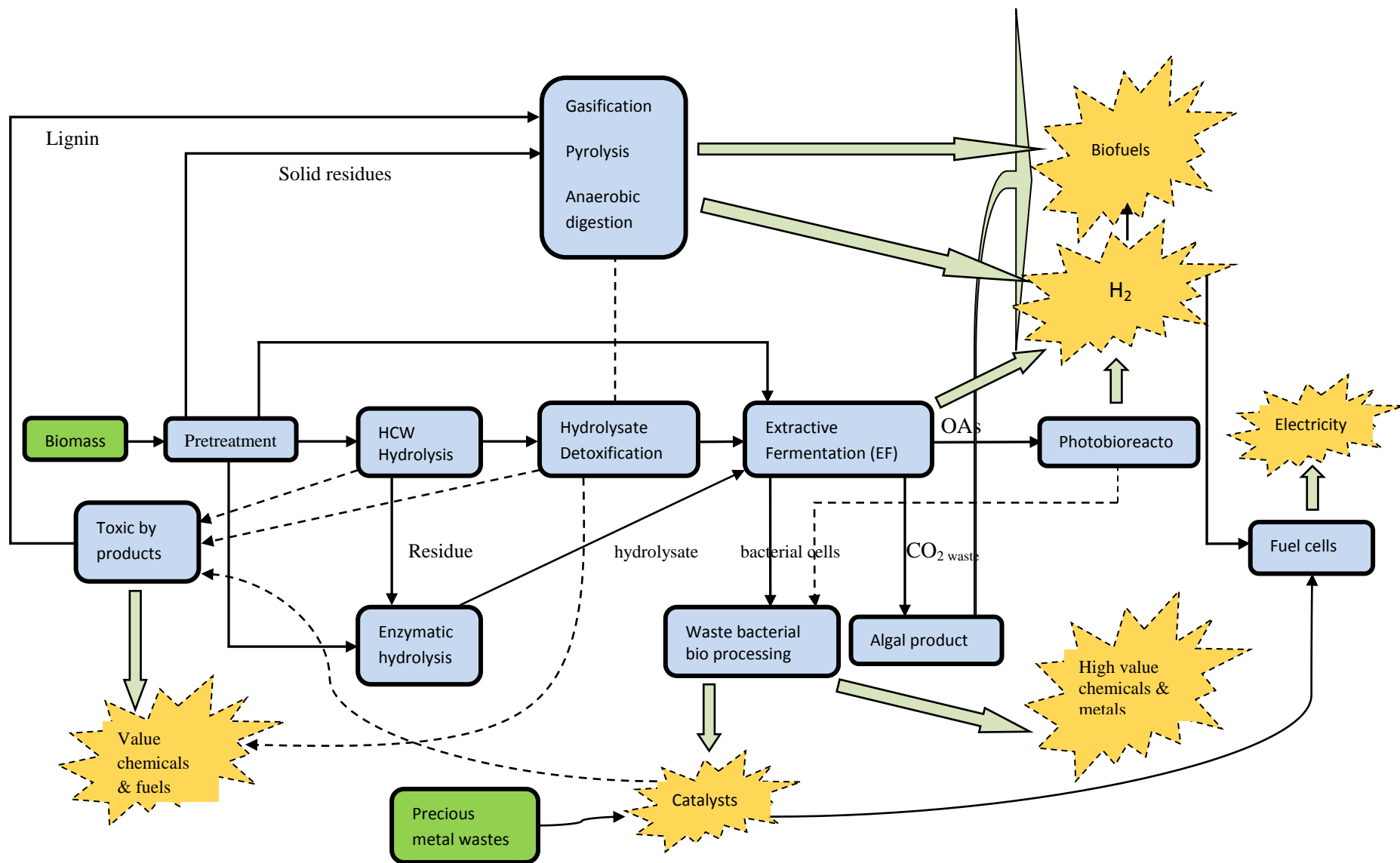


**Fig. 43** Schematization of a bio refinery process. Green boxes represent starting raw materials, blue boxes represent processes, blue stars are products and green arrows yield of main products. Solid and broken arrows represent process inputs.

## VIII. APPENDICES

### VIII.1 APENDIX I. Methods of cell growth and testing

#### VIII.1.1 Aerobic pre-growth in flask and harvesting of cells (for chapter VI.1)

Stock maintenance: Stocks of *E. coli* strains were maintained at -80 °C in 75% glycerol, plated on nutrient agar (Oxoid) and incubated overnight at 30°C.

Pre-culture preparation: For the experiments, colonies were picked up for pre-culture into 5 ml vials of nutrient broth solution with added sodium formate (0.5% w.v<sup>-1</sup>) (“NBF8”) pH 7, and incubated for 6h at 30°C, 170 rpm before use.

Harvesting: After preculture, cells were harvested in two 2 L Erlenmeyer flasks containing 1 L of the same NBF8 with added sodium formate (0.5% w/v) previously autoclaved, flasks were inoculated with 10 µL of sample equivalent to 0.001% inoculum and incubated at 30°C, 150 rpm, 16 h. Cell pellets were then obtained by centrifugation using a Beckman J2-21M/E centrifuge at 7500 rpm, 10 min, 20°C then washed twice in 100 ml phosphate buffer saline (PBS: 1.43 g Na<sub>2</sub>HPO<sub>4</sub>, 0.2 g KH<sub>2</sub>PO<sub>4</sub>, 0.8 g NaCl, 0.2 g KCl / L<sup>-1</sup>, pH 7.0) before resuspending in 20 ml PBS to produce a concentrate containing ~ 35—50 mg dry weight/mL.

Biomass concentration was estimated by using a conversion factor; an OD<sub>600nm</sub> of 1 corresponds to a concentration of 0.480 mg dry weight/mL (determined previously by D.W. Penfold and V. Marcadet, UoB). The cell concentrate was kept in a 20 ml sterile syringe before it was transferred into the fermenter.

#### VIII.1.2 Aerobic pre-growth in fermenter (EF media) (for chapter VI.4)

Aerobic pre-growth in fermenter was performed using a modular system (Electrolab, UK; 300-series). Media was prepared as follows: citric acid (1.05 g.L<sup>-1</sup>); formic acid (0.98 mL.L<sup>-1</sup>); (NH<sub>4</sub>)<sub>2</sub>HPO<sub>4</sub> (0.264 g.L<sup>-1</sup>); (NH<sub>4</sub>)<sub>2</sub>SO<sub>4</sub> (0.462 g.L<sup>-1</sup>); NH<sub>4</sub>OH (2.44 mL.L<sup>-1</sup>); BIS-TRIS base (10.462 g.L<sup>-1</sup>) in a volume of 2.7 L inside the fermentation vessel, pH was adjusted at 6.5±0.1 with H<sub>2</sub>SO<sub>4</sub> (2M). After autoclaving medium additions were added aseptically to a final volume of 3 L: glucose 2.78 M (20 mL.L<sup>-1</sup>); PEG (0.5 mL.L<sup>-1</sup>); MgSO<sub>4</sub> 2 M (2 mL.L<sup>-1</sup>); Thiamine 10 mg.L<sup>-1</sup> (10 mL.L<sup>-1</sup>); Trace elements (2 mL.L<sup>-1</sup>): Na<sub>2</sub>-EDTA 0.1702 mM; ZnSO<sub>4</sub> 0.00188 mM; MnSO<sub>4</sub> 0.00178 mM; CuSO<sub>4</sub> 0.0012 mM; CoSO<sub>4</sub> 0.00224 mM; FeCl<sub>3</sub> 0.1743 mM; CaCl<sub>2</sub> 0.01721 mM;

FeSO<sub>4</sub> 0.1743 mM; CaSO<sub>4</sub> 0.01721 mM (Hewitt et al. (2006)) [152]. De-ionized water (as needed). For a 1<sup>st</sup> aerobic growth phase the medium was heated to 30 °C and aerated at 1 L.min<sup>-1</sup> (sterile compressed air pre-filtered with through glass wool and activated carbon filter) turbine agitation (300 rpm) before adding 0.17% (v.v<sup>-1</sup>) inoculum from a pre-culture. Pre-cultures were prepared as described in VIII.1.1.

### **VIII.1.3 Fermentation media formula (for chapter VI.1)**

The fermentation vessels contained 3 L of fermentation medium (de-ionized water, 42.6 g Na<sub>2</sub>SO<sub>4</sub>, 10.456 g K<sub>2</sub>HPO<sub>4</sub>, 0.204 g KH<sub>2</sub>PO<sub>4</sub>, 0.1982 g (NH<sub>4</sub>)<sub>2</sub>SO<sub>4</sub>, pH 5.8). All eluents and solutions were prepared using de-ionized water (DW). The following supplements previously autoclaved were aseptically added to the fermenter just before inoculation: 6 ml of 1 M MgSO<sub>4</sub>, 30 ml of 2 M glucose, 9 ml of trace elements solution (quantities in g/L): CaCl<sub>2</sub>.H<sub>2</sub>O (0.74); ZnSO<sub>4</sub>.7H<sub>2</sub>O (0.18); MnSO<sub>4</sub>.H<sub>2</sub>O (0.10); Na<sub>2</sub>-EDTA (20.1); FeCl<sub>3</sub>.6H<sub>2</sub>O (16.7); CuSO<sub>4</sub>.5H<sub>2</sub>O (0.10); CoSO<sub>4</sub>.7H<sub>2</sub>O (0.21) solution and 0.5 ml of poly ethylene glycol (PEG).

The system was purged with oxygen free nitrogen (OFN), (through a 2 µm filter) for at least 30 minutes before inoculation, conditions for the fermenter were set up and automatically pH control maintained at pH 5.5 - 5.7 using 2M NaOH and 2M H<sub>2</sub>SO<sub>4</sub> solutions, temperature at 30°C and stirring at 300 rpm.

### **VIII.1.4 15 mL H<sub>2</sub> fermentation tests (for chapters 0, VI.3 and VI.4).**

Small fermentation tests were performed using 60 mL glass serum bottles leaving 75% of volume for gas space and 25% for culture media (15 mL). The bottles were sealed (10 mm butyl rubber stoppers). The initial pH was standardised to pH 6.5 (± 0.1) with NaOH/H<sub>2</sub>SO<sub>4</sub>; additions for pH adjustment were negligible.

Fermenters for fermentation tests (60 mL glass serum bottles) contained 10 mL of sterile medium consisting of Bis-Tris buffer (0.1 M) and Na<sub>2</sub>SO<sub>4</sub> (0.0435 M; pH 6.5) and 5 mL of hydrolysate or sample (filter sterilized) or glucose control (60 mM) leaving 75 % of volume for gas space and 25 % for culture media (15 mL). Fermenters were sealed using butyl rubber stoppers and made anaerobic by purging with N<sub>2</sub> for at least 30 min. 0.5-1 mL of the cell suspension was added to give a final cell concentration of 1 g dry weight.L<sup>-1</sup>, before purging for a further 3-5 min. Fermenters were incubated at 30 °C (180 rpm for 20 h).

### **VIII.1.5 Media for growth tests (for chapters VI.3 and VI.4).**

Media formulation used in growth tests consists of the following ingredients: citric acid ( $1.05 \text{ g.L}^{-1}$ ); formic acid (90 %) ( $0.978 \text{ mL.L}^{-1}$ );  $(\text{NH}_4)_2\text{HPO}_4$  ( $0.264 \text{ g.L}^{-1}$ );  $(\text{NH}_4)_2\text{SO}_4$  ( $0.462 \text{ g.L}^{-1}$ );  $\text{NH}_4\text{OH}$  ( $2.871 \text{ mL.L}^{-1}$ ); BIS-TRIS base ( $12.55 \text{ g.L}^{-1}$ ). pH was adjusted to 6.5; after sterilising by autoclave the following were added aseptically: glucose 2 M ( $10 \text{ mL.L}^{-1}$ );  $\text{MgSO}_4$  1 M ( $2 \text{ mL.L}^{-1}$ ); thiamine  $1 \text{ mg.mL}^{-1}$  ( $10 \text{ mL.L}^{-1}$ ; filter sterilized); trace elements (TE) as in Hewitt et al. (2006) [152].

For this test, the glucose that was added to the media is to ensure the presence of a sugar that is appropriate for growth; this allows us to attribute any observed variation in growth to the inhibitors contained in the samples rather than to the possibility of substrate limitation.

## VIII.2 APENDIX II. Gas analysis and measurements

### VIII.2.1 Combustible gas meter (CGM)

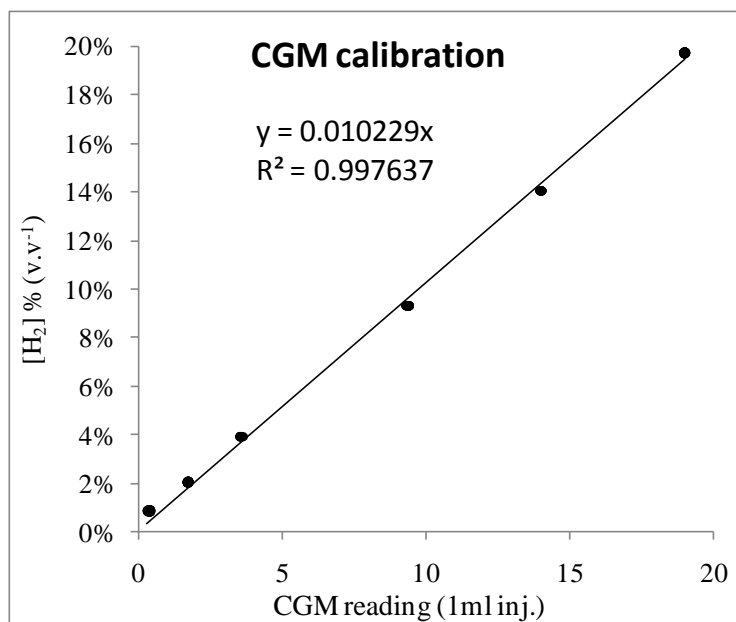
The concentration of H<sub>2</sub> in the headspace after incubation was measured by withdrawing a gas sample (1 mL) using a gas-tight syringe (Hamilton) immediately after shaking to ensure gases were evenly dispersed and injecting the sample into a combustible gas meter (Gasurveyor2, GMI). The system produced a numerical result that was related to the concentration of combustible gas in the injected sample.

For this, a calibration method was developed to correlate the output obtained from the CGM to a quantitative amount of hydrogen expressed as (v.v<sup>-1</sup>); the averages of 3 samples withdrawn from bottles with known H<sub>2</sub> concentration were converted using a linear calibration ( $R^2 > 0.99$ ). The measured concentration of % H<sub>2</sub> was used to determine the volume of H<sub>2</sub> produced (y).

The variable addition of cell concentrate used in independent experiments and its minor effect on headspace volume was accounted for.

This calibration method has to be performed each time in parallel with the experiment and preferentially each experiment should have its own calibration curve. Below is an example of a calibration curve obtained for a particular experiment.

Bottle	Space (mL0)	vol H <sub>2</sub> added (mL)	% H <sub>2</sub>	CGM outputs (1ml inj) at V=6.00 and unlimiting current			
A	245	0.5	0.20%	0.0			
B	244	2	0.81%	0.3	0.4	0.3	0.4
C	244	5	2.01%	1.7	1.7	1.7	
D	247	10	3.89%	3.5	3.6	3.5	
E	244	25	9.29%	9.3	9.4	9.3	9.4
F	245	40	14.04%	14	14	14	
F	244	60	19.74%	19	19	19	



To convert from % H<sub>2</sub> concentration to mL H<sub>2</sub> produced:

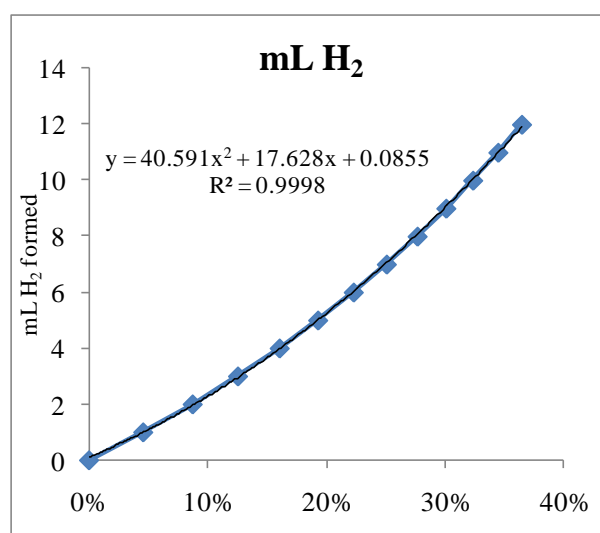
Average bottle volume: 57.75 mL

Headspace bottle volume after inoculum: 41.85 mL

HD701 usually makes 50:50 (H<sub>2</sub>:CO<sub>2</sub>) (from preliminary work)

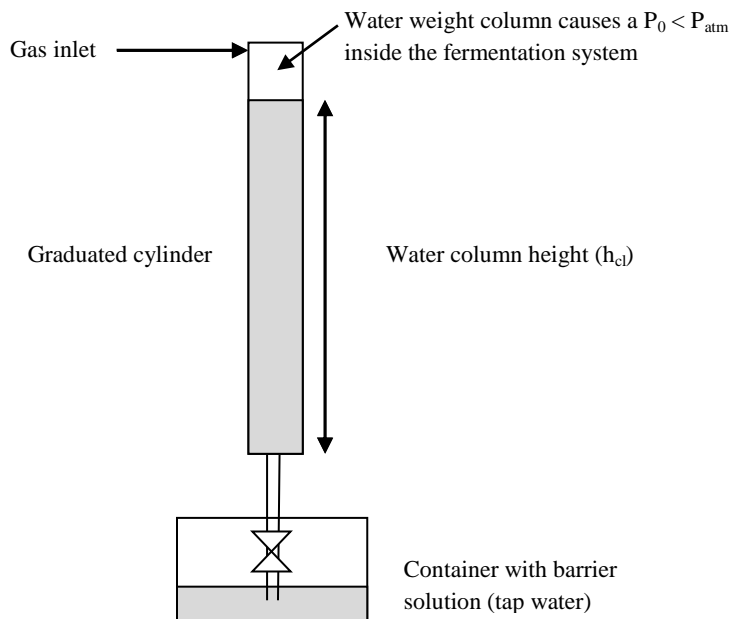
$$\% [H_2] = y = x \cdot (ax+h)^{-1}$$

Gases formed (ml)		[H <sub>2</sub> ] %
H <sub>2</sub>	CO <sub>2</sub>	
0	0	0.0%
1	1	4.6%
2	2	8.7%
3	3	12.5%
4	4	16.0%
5	5	19.3%
6	6	22.3%
7	7	25.1%
8	8	27.7%
9	9	30.1%
10	10	32.3%
11	11	34.5%
12	12	36.4%



### VIII.2.2 Water height displacement column (WHDC)

In this method, a closed water filled graduated cylinder partially submerged in an open container of a barrier solution (tap water) was used. The system is allowed to equilibrate until the water stops draining from the cylinder; this generates an internal pressure ( $P_0$ ) inside the fermentation vessel that is less than the external atmospheric pressure ( $P_{atm}$ ) hereby generating a partial vacuum. The gas produced after trapping the  $CO_2$  generated in a 2M NaOH solution entered the top of the cylinder displacing the water into the container. The volume of water displaced corresponds to the volume of  $H_2$  produced. By the use of time lapse photography it was possible to calculate the  $H_2$  production rates.



### VIII.2.3 Low flow gasmeters (LFG)

In some experiments,  $H_2$  and  $CO_2$  production were also measured using low-flow gasmeters. Meters were placed upstream and downstream of a 'scrubber' solution containing 2 M NaOH and universal indicator, so that the  $CO_2$  could be calculated by subtraction. Saturation of the scrubber

solution will be revealed by a colour change. This method was shown by gas chromatography (GC) to remove CO<sub>2</sub> to below 0.05% (v.v<sup>-1</sup>).

Low flow gasmeters operate based on an inverted “tripping bucket” submerged in liquid (usually water), the water is displaced by the gas produced in a bucket of known volume. The gas produced in the fermenters generates a positive partial pressure that drives the gas into the bucket. Once the gas bubbles fill the bucket it trips and by means of a magnet a signal is activated and registered through a connected counting device. By multiplying the number of trips by the bucket volume is possible to quantify the volume of gas and the flow rate. Fig. 44 illustrates this method.

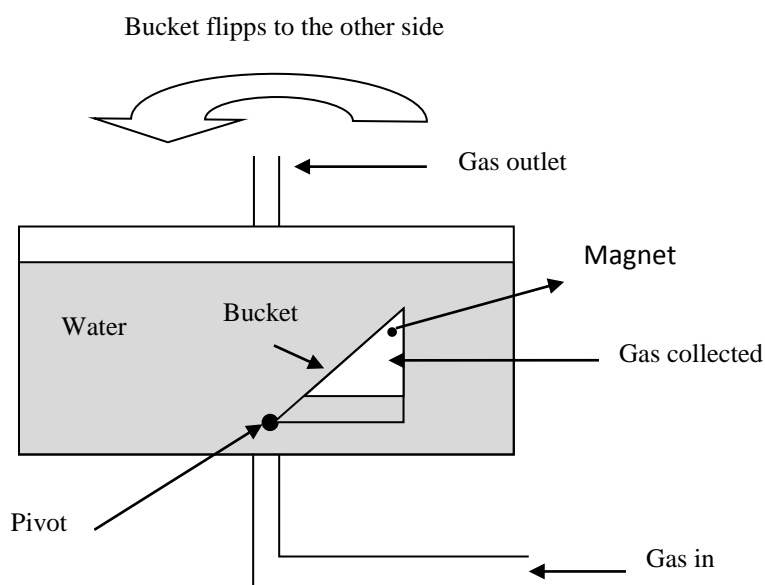
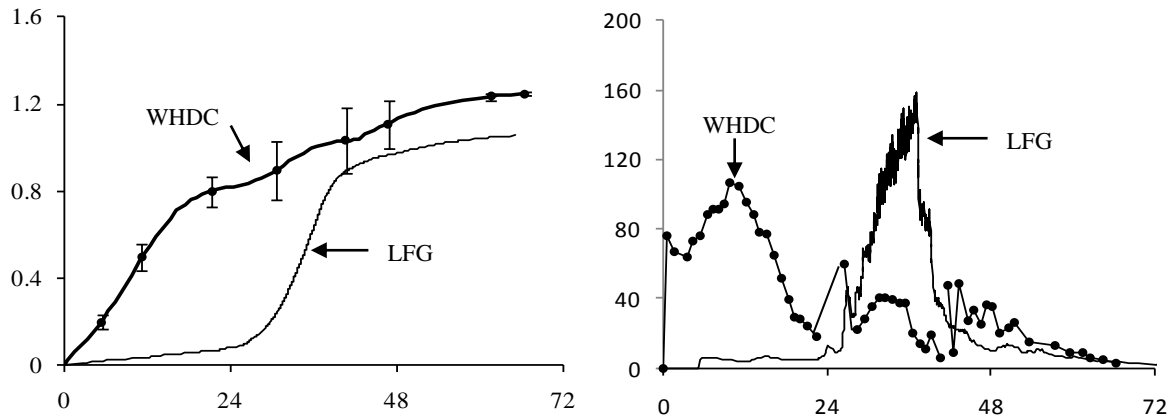


Fig. 44 Low flow gasmeter.

LFG has several advantages vs. WHDC, among them a continuous monitoring of the volume and rates of H<sub>2</sub> produced and the possibility to quantify the CO<sub>2</sub> generated by difference between the upstream and downstream gasmeter readings. However it was observed that there was a lag period in the beginning of H<sub>2</sub> production when the LFG method was used compared to the WHDC. This was attributed to the difference in fermentation vessel internal pressure due to the vacuum exerted by the weight of the water column in the WHDC, whereas with the LFG the internal pressure in the fermentation vessel was in equilibrium with the P<sub>atm</sub>. Based on these examples, there is no reason to conclude that this difference in internal pressures affects H<sub>2</sub> production and rates; *E. coli* is less sensitive to H<sub>2</sub> back pressure than other species (section II.4.3); hence care should be taken if comparison between species as these can be influenced by the gas measurement method. However as can be noticed from these two figures the H<sub>2</sub> production retardation time is much less for HD701

than for strain MC4100 suggesting that different *E. coli* strains respond differently to internal pressure. This phenomena should also be taken in consideration in future experiments especially those that incorporate a H<sub>2</sub> storage systems that requires some pressure build up in the fermentation system to function.



**Fig. 45** Shows the difference in (A) H<sub>2</sub> production (vertical axis: mol H<sub>2</sub> . mol glucose<sup>-1</sup>) and (B) H<sub>2</sub> rates (vertical axis: mL H<sub>2</sub>.h<sup>-1</sup>) pathways by strain MC4100 when LFG and WHDC were employed. Horizontal axis represents fermentation time (h).

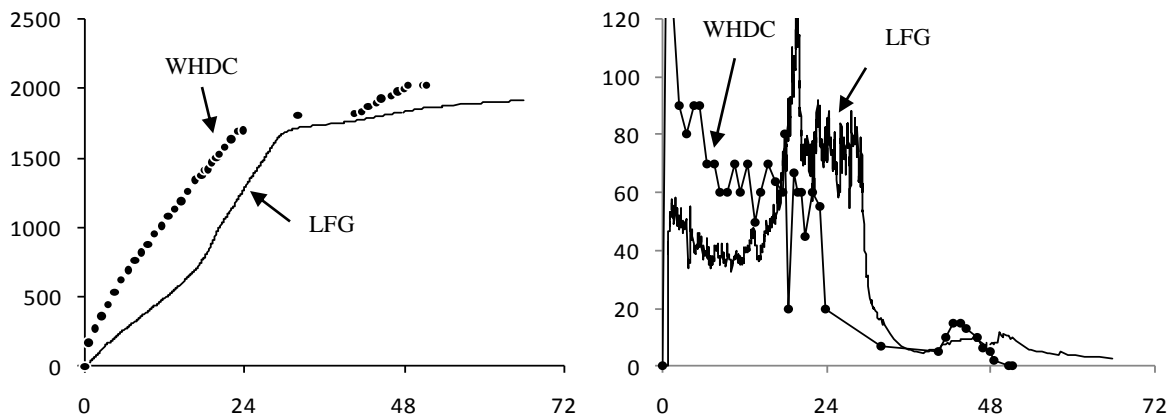


**Fig. 46** Shows the difference in (A) H<sub>2</sub> production (vertical axis: mL H<sub>2</sub>) and (B) H<sub>2</sub> rates (vertical axis: mL H<sub>2</sub>.h<sup>-1</sup>) pathways by strain HD701 when LFG and WHDC were employed. Horizontal axis represents fermentation time (h). As can be noticed the H<sub>2</sub> production retardation time is much less than for strain MC4100

### **VIII.3 Appendix III. Detoxification method**

The hydrolysates were treated with 5% (w.v aq.<sup>-1</sup>) (except where otherwise stated) wood derived steam activated carbon (AC) powder (ColorSorb G5, Jacobi, UK) at 60 °C for 1 h with agitation at 180 rpm as described by Hodge *et al.* (2009) [21], pH was not adjusted. The treated hydrolysates were vacuum-filtered through filter paper (Fisherbrand QL100). Hydrolysates and samples were kept at -20 °C for tests and analysis.

## VIII.4 Appendix IV. Quantitative chemical analysis

### VIII.4.1 DNSA assay for glucose quantification

Mixed samples were mixed with DNSA reagent in varying proportions Table 20, boiled for 10 min, cooled on ice and the  $A_{570}$  was recorded [100]. For the preparation of DNSA reagent, 0.25 g of 3,5-dinitrosalicylic acid (DNSA) and 75 g sodium potassium tartarate were dissolved in 50 ml of 2 M NaOH overnight in a brown glass bottle (reagent is light sensitive) after which the volume was made up to 250 ml with de-ionized water . The reagent was stored in darkness at 4 °C [153].

**Table 20** Samples and reagent proportions according to assay range.

Sample vol ( $\mu$ l).	Reagent vol ( $\mu$ l)	Assay range (mM glucose)
20	800	25-250
50	800	10-100
100	800	5-50
300	700	0.5-5

Aqueous solution from experiments exhibit different colours (light orange), since DNSA is a colorimetric method a blank should be run mixing the sample with reagent in the proper proportions and then put in spectrophotometer. Final  $OD_{570}$  reading will be the difference between blank and sample. Dilutions of samples may also be needed when sample is too dark.

As the method is sensitive to all reducing sugars, the accurate quantitative analysis of glucose is dependent upon glucose being the only reducing sugar (or agent) present.

#### **VIII.4.2 Total Organic Carbon (TOC)**

Total Carbon (TC) is composed of total organic carbon (TOC) and Inorganic Carbon (IC); TOC results from the difference between TC and IC. All samples were run through a total organic carbon analyser (Model TOC 5050A, Shimadzu Co., Japan) equipped with an autosampler (ASI-5000A, Shimadzu Co., Japan) with no prior pre-treatment. The operation of the analyser is based on the combustion/non-dispersive infrared gas method that is widely employed for TOC measurements (Shimadzu Instruction Manual, 2001).

The preparation of the samples was done based on the results obtained from the analysis of the hydrolysates by the DNSA method; samples were diluted with de-ionized water estimating a carbon content not larger than 1000 ppm. Vials of 6 ml were prepared and placed in the auto-sampler. The measuring principle for TC is as follows: High purity air (carrier gas) is supplied into a TC combustion tube, which is filled with oxidation catalyst and heated to 680 °C. When the sample has been introduced into the TC combustion tube, the TC component in the sample is decomposed into CO<sub>2</sub>. The carrier gas, containing the combustion gas from the TC tube flows through an IC reaction vessel, is cooled and dried. It is then sent through a halogen scrubber into a sample cell set in a non-dispersive infrared gas analyser (NIDR) where CO<sub>2</sub> is detected. The NDIR outputs a detection signal, generating a peak whose area is calculated by a data processor. The peak area is proportional to the TC concentration of the sample. For IC measurement, the sample is introduced into the IC reactor vessel, where carrier gas is flowing in the form of tiny bubbles in the solution acidified by IC reagent. Only the IC component in the sample is decomposed to CO<sub>2</sub>, which is detected by the NDIR. The IC concentration is determined in the same manner as the TC concentration. TOC is thus obtained by difference of TC and IC.

### VIII.4.3 Lignin determination

Lignin in WS and BG was analysed using the Klason assay following the ASTM Standard method E 1721 – 01 (Determination of Acid-Insoluble Residue in Biomass)

Labelled crucibles were ignited at  $575 \pm 25^\circ\text{C}$  to achieve constant weight ( $\pm 0.3$  mg). After that,  $0.3 \pm 0.01$  g of sample were weighed, W1, to the nearest 0.1 mg, and placed in a test tube. Then  $3.00 \pm 0.01$  mL ( $4.92 \pm 0.01$  g) of 72 %  $\text{H}_2\text{SO}_4$  was added, and the mixture stirred for 1 min or until mixed thoroughly. The test tubes were placed in a water bath at  $30 \pm 1^\circ\text{C}$ , and hydrolyzed for 2 h. Samples were stirred every 15 min to ensure complete mixing and wetting. Then, the hydrolysate was transferred to a glass bottle, and diluted to a 4 % acid concentration by adding  $84 \pm 0.04$  mL of DW or by bringing the combined weight of sample, acid, and water up to  $89.22 \pm 0.04$  g. Bottles were closed and the aluminium seals crimped into place. Afterwards, the samples were put in the autoclave in their sealed bottles for 1 h at  $121 \pm 3^\circ\text{C}$ . After completion of the autoclave cycle, the samples were cooled for approximately 20 min at room temperature before removing the seals and stoppers. After hydrolysis in the autoclave, the hydrolysis solution was vacuum filtered through a previously ignited filtering crucible. With hot water, any particles clinging to the glass bottle should be washed into the crucible allowing the filtered residue free of acid, as well. Next, crucibles and their contents were dried at  $105 \pm 3^\circ\text{C}$  for 2 h or until a constant weight of  $\pm 0.3$  mg was achieved upon reheating. The crucibles were then cooled in the desiccator and the weight recorded to the nearest 0.1 mg, W2, this weight will be the weight of the crucible plus acid insoluble residue, and acid-insoluble ash. The crucible and its contents were placed in the muffle furnace, and ignited at  $575 \pm 25^\circ\text{C}$  for a minimum of 3h, or until all the carbon was eliminated. Heating rate was  $10^\circ\text{C}\cdot\text{min}^{-1}$  to prevent flaming. The container was partially covered during this step if the sample tends to flame. Heating above the maximum stated temperature should be avoided. The weigh of the crucible with acid-insoluble ash was recorded to the nearest 0.1 mg after being cooled in a desiccator (W3). Finally, the percentage of acid-insoluble residue (Klason lignin) on a  $105^\circ\text{C}$  dry-weight basis was calculated as follows:

$$\% \text{ acid insoluble residue} = \frac{W2 - W3}{W1 \times \frac{T_{105}}{100}} \times 100$$

Where:

$W1$  = initial sample weight

$W2$  = weight of the crucible, acid-insoluble residue, and acid-insoluble ash

$W3$  = weight of the crucible and acid-insoluble ash

$T_{105}$  = % of total solids determined at 105 °C in accordance with Test Method E 1756.

One limitation of this method is that it can not be utilized with samples containing protein.

#### VIII.4.4 Saccharification of cellulose

This method was developed by Seaman et al., 2002 [176] for the hydrolysis of cellulosic materials to reducing sugars. It consists of a primary hydrolysis of the cellulosic material with 72% of sulphuric acid and 45 minutes at 30 °C followed by a secondary hydrolysis for 1 h in a 15 psi autoclave as described below:

Grind sample to pass a 30-mesh screen

Air dry and determine moisture

Weight 0.35 g of cellulose sample into a 30 ml shell vial

Add 1 ml of 72% sulfuric acid (cooled at 15 °C). Mix with a stirring rod.

Add 4 ml more of 72% H<sub>2</sub>SO<sub>4</sub>

Put in water bath at 30 °C for 45'. Stir at 5 – 10 minutes interval

Wash mixture from vial into an Erlenmeyer flask with 140 ml of DW

Autoclave at 15 psi steam pressure for 1 h

Cool sample and dilute exactly to 250 ml

Neutralize w/excess chalk (CaCO<sub>3</sub>). (Note: once pH starts to rise by itself stop adding the chalk).

Vacuum-filter through filter paper (Fisherbrand QL100)

Analyze for sugar using DNSA method (appendix section VIII.4.1).

The accuracy of this method is better compared with other methods such as Kiesel and Semiganovski method. However not any method gives truly quantitative yields of reducing sugar. However for these purposes (cellulose decomposition) it provides good reference data.

## VIII.5 Appendix V. Conferences and additional publications

### VIII.5.1 An Integrated biohydrogen refinery: Synergy of photofermentation, extractive fermentation and hydrothermal hydrolysis of food wastes.

*AUTHOR NAMES: Mark D. Redwood,\* Rafael L. Orozco, Artur J. Majewski and Lynne E. Macaskie*

*AUTHOR ADDRESS: School of Biosciences, University of Birmingham, Edgbaston, Birmingham UK B15 2TT*

*AUTHOR EMAIL ADDRESS: m.d.redwood@bham.ac.uk*

#### **RECEIVED DATE**

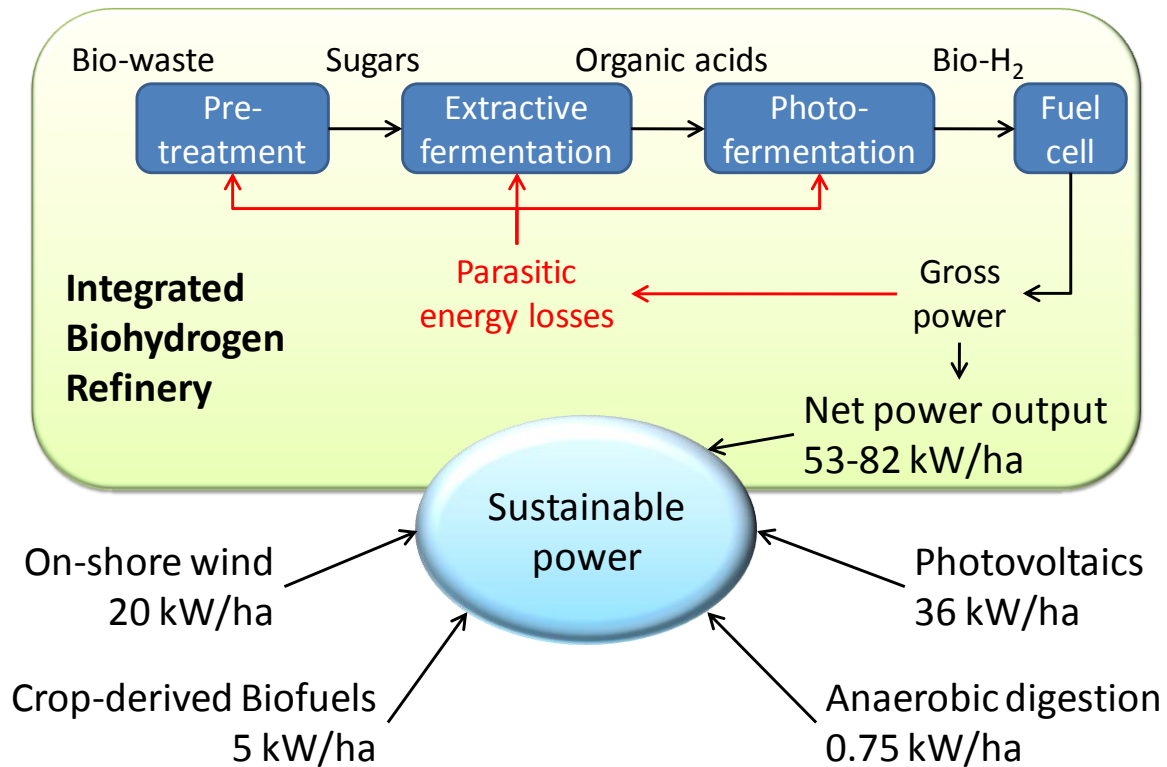
*TITLE RUNNING HEAD: Integrated Biohydrogen Refinery*

*CORRESPONDING AUTHOR FOOTNOTE \*Phone: +44-121414-5434; fax: +44-121414-5889; e-mail: [m.d.redwood@bham.ac.uk](mailto:m.d.redwood@bham.ac.uk)*

*Journal: Environmental, Science & Technology, in submission.*

The experiment design and the writing of this paper were done by Dr. Mark D. Redwood. My contribution was in performing the hydrothermal hydrolysis (HCW) of the solid biomasses residues, in assisting Dr. Redwood in the equipment set-up, operation and control of the extractive fermentation process, in providing data for the energy calculation of the HCW process, sample analysis and data collection.

**ABSTRACT**



We report an *Integrated Biohydrogen Refinery (IBR)* with experimental net energy analysis. The IBR converts biomass to electricity using hydrothermal hydrolysis, extractive biohydrogen fermentation and photobiological hydrogen fermentation for electricity generation in a fuel cell. An extractive fermentation, developed previously is, here, applied to waste-derived substrates, following hydrothermal pre-treatment, achieving 83-99% biowaste destruction. The selective separation of organic acids from waste-fed fermentations provided suitable substrate for photofermentative hydrogen production, which enhanced the gross energy generation up to 11-fold. Therefore, electro dialysis provides the key link in an IBR for 'waste to energy'. The IBR could be more productive than 'renewables' (photovoltaics, on-shore wind, crop-derived biofuels) and also emerging biotechnological options (microbial electrolysis, anaerobic digestion).

**KEYWORDS:** fermentation, photofermentation, biohydrogen, waste, electro dialysis

## INTRODUCTION

Biohydrogen provides opportunities for sustainable energy from biowastes using fermentative and photosynthetic microorganisms. We focus on a dual bioreactor system combining dark fermentation (DF) and photofermentation (PF), which offers a theoretical maximum yield of 12 mol H<sub>2</sub>/mol hexose equivalent. The concept has been advocated by many authors [193] and research continues to progress rapidly.[241-247]

It is well known that organic acids (OAs) from DF can be valorised by re-use as substrates to produce methane,[248, 249] electricity [250] or H<sub>2</sub> via PF. Guwy et al. [251] highlighted the challenge of recovering OA from DF for use in downstream processes including PF, which is inhibited by excess nitrogen sources (especially NH<sub>4</sub><sup>+</sup>) via the inhibition of nitrogenase.[252] Usually, OA are co-transferred with other solutes from DF to PF, hence the input feedstock must be low in N-sources to permit nitrogenase-mediated H<sub>2</sub> production. Biowaste feedstocks usually contain bioavailable N allowing microbial NH<sub>4</sub><sup>+</sup> release. In several studies, DF extracts rich in OA contain excess N.[107, 247, 253]

The application of electrodialysis in extractive fermentation (EF)[254] involves separating a fermenting culture from a permeate chamber with an anion selective membrane (ASM) to transfer anions specifically, rapidly and unidirectionally under DC. As the ASM is impermeable to cations including NH<sub>4</sub><sup>+</sup>, electrodialysis renders the process robust and versatile, immune to the feedstock nitrogen/NH<sub>4</sub><sup>+</sup> content.

Biomass is an abundant renewable source of fermentable sugars to support the future hydrogen economy.[2, 255, 256] However, the application of electrodialysis as a bioprocess adjunct to the fermentation of real wastes requires investigation. Firstly, the energetic input for OA separation could exceed the potential energy output from bioH<sub>2</sub> production. Secondly, inorganic anion present in real wastes could detract excessively from efficient target anion separation or upset the balance of retained anion with pH.[254] Thirdly, liquefaction of feedstock could be restrictively complex or energetically costly. These factors would vary according to the waste stream. Therefore, a range of example wastes were processed to generate clarified solutions of soluble fermentable sugars.

Food and agricultural wastes normally contain complex polysaccharides requiring hydrolysis for their utilisation as fermentation substrates. Hydrolysed can be achieved by chemical, enzymatic and hydrothermal methods. Enzymatic hydrolysis is slowrequires optimisation to obtain the best combination of enzymes for each feedstock and cannot quickly adapt to variable feedstock composition, while chemical hydrolysis consumes chemicals and produces chemically aggressive

effluents, whereas hydrothermal hydrolysis is an environmentally benign, rapid method requiring only water, relatively moderate temperatures (200-260 °C) and pressure.

Here, we describe an experimentally based model of a complete *integrated biohydrogen refinery* (IBR). We test two hypotheses; firstly that EF can function efficiently using real wastes, and secondly that the IBR can function as a net energy producing system, accounting for the parasitic energy requirements and can, therefore, provide sustainable energy from biowaste.

## EXPERIMENTAL SECTION

### Extractive fermentation

Fermentations were connected to an electrodialysis cell, composed of four chambers (named C, M, MA and A, from - to +), separated by bipolar membrane (BP), anion selective membrane (ASM) and cation selective membrane (CSM), respectively.[254] Anions were actively transported across the ASM from the M chamber (connected to the fermenter) into the MA chamber (connected to a permeate vessel), in response to an externally applied current, regulated automatically in response to the fermentation pH using custom software (C-Tech Innovation Ltd, Capenhurst, UK).

In EFs (3 L), glucose (initially 28 mM) was completely consumed during an initial aerobic growth phase, before rendering anaerobic by nitrogen purge (30 min). At this point, waste-derived sugars (non-sterile) were added in pulses of 0.1 mol reducing sugars at intervals (Figure 2).

In electroseparations, current efficiency represents the fraction of passed charge attributed to target anion transfer.[215]

$$\text{Current Efficiency (\%)} = \frac{100NF}{i} \quad (\text{equation 1})$$

where N is the charge flux as OA (mol/s/m<sup>2</sup>), F is the Faraday constant (96485.38) and *i* is the current density (A/m<sup>2</sup>).

### Hot compressed water treatment

The HCW/CO<sub>2</sub> reactor contained 5 g (dry basis) homogenised waste in de-ionized water to a volume of 160 mL (±5 mL). The reactor was operated (peak conditions: 200 °C, 50 bar, 15 min) and hydrolysates were detoxified (activated carbon, 5% w/v) as described previously.[225]

### Fermentability tests

*Escherichia coli* strains HD701 and FTD67[199] (provided by F. Sargent, Dundee) were used in fermentability tests as previously[225] except using 10 mL of ‘ED’ medium[254] (pH 6.5, sterile) and 5 mL of test solutions (non-sterile), which were diluted to ensure substrate limitation if >60 mM hexose equivalent was present. Reactors were incubated (30 °C, 180 rpm, 16 h) before estimation of  $[H_2]^{19}$  and conversion to  $H_2$  volume (equation 2).

$$y \approx \frac{x}{ax+h} \quad \therefore \quad x \approx \frac{hy}{1-ay} \quad (\text{equation 2})$$

Where  $y$  is  $[H_2]$  in headspace (v/v),  $x$  is volume of  $H_2$  produced (mL),  $h$  is headspace volume (mL) and  $a$  is the ratio of total gas produced to  $H_2$  produced;  $a=2$ . [199, 221]

### Photofermentability tests

*Rhodobacter sphaeroides* ZX5 (provided by Z. Zhou, Shanghai) was selected for its substrate range[257] and maintained as described previously.[107] Permeates from the end of EFs were tested as carbon sources for PF. Cultures were grown using yeast extract (YE, 1 g/L) as the sole nitrogen source and then harvested, washed and transferred into media without YE for  $H_2$  production. To ensure cells were prepared for each OA mixture, the same batch of permeate provided the OA for growth and for  $H_2$  production.

‘Growth buffer’ was based on ‘SyA’[258] omitting carbon sources and adding permeate samples (adjusted to pH 6.8 with 3 M NaOH) to provide 60 mM total OA carbon. For growth, preparations were incubated in fully-filled flat glass flasks (30 °C, static, 75 W/m<sup>2</sup>; tungsten-halogen lamp, 48 h). Light intensity was measured with a 400-1000 nm thermopile-type sensor (Skye, UK). After growth, cells were harvested (4000 g, 15 min) and washed twice in ‘HP buffer’; as growth buffer omitting YE and including permeate samples (pH 6.8) diluted to 30-60 mM hydrogen production potential (HPP[259]).

For  $H_2$  production tests, washed cells were resuspended to 1 g DW/L ( $OD_{660nm}$ : 3.307) and dispensed in 5 mL aliquots into 15 ml glass reactors. Controls used cells washed in HP buffer omitting carbon sources. Reactors were purged with Ar (30 min) before incubation (30 °C, static, 75 W/m<sup>2</sup> tungsten lamp, 48 h).  $H_2$  was estimated as above using equation 2 with an  $a$  value of 1 since PNS bacteria produce ~100%  $H_2$  (v/v), due to the internal recycling of  $CO_2$ . [260]

## **Analysis**

Inorganic anions and OAs were analysed by ‘anion-HPLC’[107] while sugars, HMF and ethanol were analysed by ‘Refractive Index (RI) HPLC’.[261] Total reducing sugars were analysed using the dinitrosalicylic acid (DNSA) method.[262]

Total sugars and starch in solid wastes were measured after drying (60 °C) and grinding to pass through a 420 µm mesh. Starch was estimated by digestion in KOH (2 M, 4 °C, 2 h), then colorimetric analysis ( $A_{570}$ ) of dextrans by the reaction with  $I_2/KI$  (0.0044%/2% w/v, respectively) with reference to an analytical grade starch standard.[263] Total sugars were estimated by digestion[264] then reducing sugars analysis.

## **RESULTS AND DISCUSSION**

### **Food wastes: Description and processing details**

Commercial food wastes were sourced from a fruit wholesaler, catering kitchen and brewery. The wastes were diverse (Table 1), containing 57-90 % water and 7-28% sugars by mass. Only catering waste 3 contained significant starch (21 % wet weight). Solids were processed to generate fermentable solutions (Figure 1).

### **Fermentability tests**

Waste treatments yielded 13 types of clarified liquid preparations (3 juices, 3 infusions and 7 hydrolysates; Figure 1), all of which were screened for fermentability (Table 1). Analysis of hydrolysates showed that treatment with activated carbon removed inhibitory 5-hydroxymethylfurfural (5-HMF).[225] Relatively low  $H_2$  yields (below 1 L/kg raw waste) were obtained from Av waste and CW2, whereas Ap waste supported a high yield of 5.7 L  $H_2$ /kg raw waste, as the sum of juice, infusion and hydrolysate. The highest yield was obtained from CW3 despite the fact that it yielded no juice or infusion but was characterised by low moisture content and high total sugars, most of which was starch (Table 1), which is highly susceptible to HCW hydrolysis[265] to generate fermentable substrate.[225]

$H_2$  production in fermentability tests was limited by substrate availability as pH remained  $>5.5$ . Further fermentability tests used *E. coli* strain HD701/pUR400 (sucrose-capable[266]) but no additional  $H_2$  was produced, confirming the absence of sucrose shown by RI-HPLC.

### **Waste-fed extractive fermentations: Three case histories**

The small scale tests (Table 1) indicated that food waste-derived solutions were suitable substrates for DF. The juices of waste mango (Ma), waste asian pear (Ap) and catering waste 1 (CW1) were selected for sustained H<sub>2</sub> production and product separation in 3 L EFs.

The only significant substrates for H<sub>2</sub> production were waste-derived, since all initial glucose was consumed during the aerobic growth of *E. coli* before initiating anaerobic fermentation. Without additional feeding no H<sub>2</sub> production occurred. Residual formate from the growth medium (initially 23 mM) was depleted within 36 h and before the onset of H<sub>2</sub> production and, therefore, this exogenous formate did not contribute to H<sub>2</sub> yields. Only permeates from the end of the EFs were tested in PF. Figure 2 shows the progress of three sustained dark EFs dosed 3 or 4 times each with waste-derived juices.

Figure 2A shows EF using Ma juice. The current efficiency (equation 1) on organic anion (CE<sub>OA</sub>) was 86% and based on total anion (CE<sub>TA</sub>) was 92%. The remainder is attributed to a combination of measurement error (e.g. fluid volumes) and current leakage, chemical reactions (e.g. water electrolysis) and the movement of non-measured anion. Anion analysis of extracts is shown in Table 2A. The OA concentration in the reactor (M chamber, not shown) was stable at ~80 mM total charge equivalents during H<sub>2</sub> production.

Conversely, using Ap juice (Figure 2B), the OA concentration (M chamber) fell progressively from ~100 mM to ~50 mM total charge equivalents during H<sub>2</sub> production. The H<sub>2</sub> production rate was initially slow, increasing after 96 h. The delay may be due to acclimatisation to unidentified inhibitors from the Ap juice; nitrates (which could inhibit H<sub>2</sub> production) were not detected by anion-HPLC. CE<sub>OA</sub> was 86% and CE<sub>TA</sub> was 91%.

Using CW1 juice (Figure 2C), H<sub>2</sub> production commenced 20 h after feed 1 and progressed rapidly to an apparent yield of 2.5-3.0 mol H<sub>2</sub>/mol hexose, which exceeds the maximum yield (2 mol H<sub>2</sub>/mol hexose[221]) predicted from the concentration of sugars in waste juice, measured by RI-HPLC. This is attributed to linear maltodextrins which are fermentable to *E. coli*[267] and were detected by RI-HPLC, whereas galactose, sucrose, maltose, mannitol, mannose, xylose and citrate were not detected. Here, CE<sub>OA</sub> was 85% and CE<sub>TA</sub> was 95%.

It was concluded from three case histories that waste-fed EF is an efficient method for generating bioH<sub>2</sub> purified OA (Table 2A) from liquefied biowastes. Hence, the challenges posed to EF by solids and inorganic salts in wastes were addressed.

### **Photofermentability of permeates from waste-fed extractive fermentations**

OA derived entirely from the EF of food wastes supported H<sub>2</sub> production in photofermentability tests. However, the simple reactors (5 mL static vials) resulted in sub-optimal conditions and low substrate conversion efficiency (16-49%; Table 2B), whereas typical values in the range of 70-90% were obtained previously[268] and are widely reported.[269-271] Therefore, extrapolation was applied using an efficiency of 80% (representing optimised full-scale PF; Tables 3B, 4C). Therefore, PF would increase the H<sub>2</sub> yield but also the parasitic energy.

### **Net energy analysis of the IBR**

Our experimental data informed a model of an *Integrated Biohydrogen Refinery* (IBR). Although only juices were available in sufficient volumes for EFs, fermentability was confirmed for all infusions and hydrolysates and we extrapolate on the basis of experimental OA yields from juice fractions (via EF) and experimentally measured energy requirements of OA separation. OAs in HCW hydrolysates were found at ~0.01% of sugar levels and hence disregarded.

In the UK the gross power generation of biogas plants is currently rewarded via the feed-in tariff (fIT) at a rate of GBP 0.14/kWh[272] indicating fIT revenues of GBP 32/tonne plus standard export revenues of ~GBP 13/tonne and gate fees of 50-90 GBP/tonne, and in contrast to landfill costs of GBP 76/tonne (inc tax).[273] The UK produces 16M tonnes of waste food per year, plus a further 90M tonnes of farm manures and slurries.[274] Assuming the food wastes are as productive as those assessed here (average gross output: 170 kWh/tonne; Table 3C) and that manures are ~half as productive (~100 kWh/tonne), applying the IBR could generate potentially ~12 terawatt-hours pa with fIT revenues of GBP ~1.6 billion, plus export revenues, gate fees, and avoided landfill costs.

However, to offer a solution for sustainable energy production the IBR must perform independently of present subsidies. Therefore, for each case history was estimated the net energy ratio (NER) of a dark EF (Table 3A-B) and the complete IBR (Table 3C-D). NER is defined as total process energy output over parasitic energy requirements (energy out / energy in). If a process generates a net energy output, then NER>1.

Parasitic energy was based on four factors (Table 3); HCW hydrolysis (0.022-0.032 kWh/kg raw waste), electroseparation of OA (0.021-0.091 kWh/kg), DF mixing energy (0.0008-0.0027 kWh/kg) and PF mixing energy (0.0008-0.0029 kWh/kg raw waste) as these are the core scalable elements, whereas other costs would be case-specific, e.g., an IBR co-located with a dairy farm (manure and

milk processing residues) would have near-zero transport and communiton costs, in contrast to an IBR utilising organic fractions of municipal wastes located on a city outskirts.

The energy demands of HCW treatment and mixing were estimated, while that of OA separation was determined experimentally from the three waste-fed EFs (Figure 2). The presented parasitic energy demands are applicable to production scale HCW treatment and electroseparation of OA.

The estimated energy demand of the experimental HCW reactor was  $\sim 100$  kWh/kg dry matter, leading to parasitic costs of 3-11 kWh/kg raw waste, which would exceed the IBR energy output. However, this would misrepresent a production-scale HCW system because the experimental HCW reactor and contents were heated and cooled in sequential batches without heat recovery, whereas a production scale system would incorporate an effluent-to-feed heat exchanger to obtain much of the heating and cooling. Around 95% of the heat can be obtained in this way[275, 276] making a heat demand of 0.0102 kWh/kg HCW reactant (97% H<sub>2</sub>O, approximated to 100%). The case-specific HCW energy demands (Table 3B) vary due to the different yields of washed pressings from raw wastes (Figure 1). The sensitivity of the NER to the fraction of heat recovered varied with the energy yield in each case. For example, CW1 yielded the lowest gross energy output (0.10 kWh/kg raw waste; Table 3A) requiring at least 83% heat recovery to break even (NER=1), whereas an Ap waste-fed IBR (0.25 kWh/kg) would break even with only 64% heat recovery (WEO3).

Unlike the experimental HCW reactor, the experimental electroseparation cell was essentially representative of production scale. Nevertheless we overestimated the parasitic cost because the experimental cell contained a stack of 3 membranes (BP,A,C) (see Materials and Methods), whereas production systems employ stacks of many layers (BP,[A,BP]<sub>n</sub>,A,C), thereby reducing the relative contribution of flanking membranes, which are non-separating, to the stack resistance. The observed variation in separation cost relates to differences in the separated OA profiles (Table 2A), which is important due to differences in the HPP/charge ratio. For example, succinate (divalent) provides only 3.5 mol HPP/mol ionic charge, whereas butyrate (monovalent) provides 10 mol HPP/mol. The dominant OAs were acetate and butyrate in all cases except CW1 juice where there was also propionate. Note also that EF produces a third stream of H<sub>2</sub> via water electrolysis, which in operation would be pooled with the bioH<sub>2</sub> streams (Figure 3) and is not included in NER calculations.

The mixing requirement is lower in anaerobic culture (un-gassed), than in aerobic culture because, here, the mixing functions primarily to maintain homogeneity (rapid) rather than to promote oxygen transfer into the aqueous phase (slow). Hence, adequate mechanical mixing

requires only 40-90 Wh/m<sup>3</sup>/day.[277] Mixing energy has been optimised in anaerobic digestion, where headspace re-circulation (or ‘gas mixing’) is a common method, requiring only 1-2 W/m<sup>3</sup>. [277, 278] For example, Utile Engineering (UK) manufacture digesters with a gas-based mixing system requiring 3 W/m<sup>3</sup>. Fully passive mixing uses the movement of biogas bubbles (e.g. BIMA system, Entec Biogas GmbH) or the accumulated pressure of formed gas.[279] AgroEnergien (Germany) have applied this principle in a ‘Self Mixing Digester’. For EF, culture circulation by an external pump would make double use of the circulation to the electro dialysis cell, requiring 4 W/m<sup>3</sup> for a turnover time of ~5 h,[280] on which DF mixing energy was estimated (Table 3B).

PF mixing energy is reportedly 1.0 kWh/m<sup>2</sup>/year[281] for a tubular photobioreactor (PBR;  $d=90$  mm). The space-time requirement was estimated using 5% light conversion efficiency and 80% substrate conversion efficiency with a horizontal irradiance of 2.12 MWh/m<sup>2</sup>/year[282] for Kampala, an equatorial region rich in biowaste. Hence, the PBR would process 1667 mol HPP/m<sup>2</sup>/year, from which land use rates were determined (Table 3D).

For the single-stage EF,  $NER < 1$ , so this system would consume energy. Conversely, the IBR’s average NER was 2.4, with the PBR requiring only 2-3% of the total parasitic energy to produce 63-91% of the total bioH<sub>2</sub>. Therefore, we conclude that (i) EF functions mainly to convert biowaste into purified OA and (ii) that IBR is a viable route to energy from waste, independent of subsidies and credit systems.

A model of an IBR utilising waste mango (Figure 3) shows a net output of 102 kWh/tonne raw waste, which could power a typical home for around 1 week[283] with estimated revenues of ~GBP100/tonne under current UK market conditions[284] and the economics would be further enhanced by incentives for landfill and carbon avoidance, by-products, and electrolytic H<sub>2</sub> (Figure 3).

### **Hydrolysis and electro dialysis in the IBR**

Wastes were first pressed and infused with water to release soluble sugars (where possible; Figure 1). Finishing the process without treatment of the solid pressings by HCW would result in higher NERs of up to 6.6 (average: 4.7) but would also yield solid residues at 0.5-0.9 kg/kg waste (WEO10), requiring further disposal. HCW hydrolysis reduced the NERs to an average of 2.4 but eliminated 90% of the solid remnants. It is, therefore, effective for the conversion of biowaste to energy.

The integration of DF and PF is technically challenging (see above). Here, the challenge is addressed through the anion-selective property of EF, particularly against the cation NH<sub>4</sub><sup>+</sup>. In this

study, fermentations contained initially 55 mM  $\text{NH}_4^+$  from the starting ('ED') medium, whereas permeates contained  $\ll 0.1$  mM  $\text{NH}_4^+$  and supported  $\text{H}_2$  production by *Rhodobacter sphaeroides* OU001 and ZX5, accordingly (Table 2). Other noteworthy features of EF are discussed separately.[254]

Hence electro dialysis is key to the integration of dark and light biohydrogen fermentations. Other approaches include co-culture, cell separation and immobilisation, all of which are sensitive to the nitrogen influx which may vary in a waste-fed IBR. Due to the difficulty of balancing the growth rates of dark fermentative and photofermentative bacteria, co-culture requires precise control[285] and has not been applied to wastes. Cell separation from DF effluent is the most common laboratory approach but has limited scalability due to its reliance on slow and energy-intensive centrifugation or ultrafiltration, whereas EF does not rely on solvent flow through a membrane and hence requires no pressure gradient and is relatively immune to fouling. Immobilisation of the dark phase (e.g. granulation) has proven effective, although immobilisation limits diffusion and mixing.

An average of 95% of the IBRs parasitic energy was distributed equally between OA separation and HCW treatment. Therefore, eliminating these energy requirements would enhance the NER 20-fold. However, HCW treatment was highly effective in hydrolysing and liquefying the solid biomass residues. Without it, the process would achieve only 26% biowaste destruction. Electro dialysis is also important, as it enables the IBR to accept diverse feedstocks regardless of nitrogenous components which may inhibit PF. Therefore, HCW and electro dialysis offer 'good value' for their parasitic costs.

### **Comparison with leading waste to bioenergy technologies**

An alternative biowaste to  $\text{H}_2$  method is the microbial electrolysis cell (MEC) in which occurs biocatalysed electrolysis.[204, 286-291] An MEC using a fuel cell to meet its power demand would have an NER of 2.0 (excluding other energy requirements; WEO11). Therefore, the IBR (NER: 2.4) compares favourably with the MEC.

Anaerobic digestion (AD) is a ubiquitous process, applied worldwide domestically to produce biogas for cooking[292] and at scale for biowaste treatment. A renewed interest in AD bioenergy has prompted incentives and regulatory frameworks to valorise digestate sustainably as fertilizer.[274] AD requires little parasitic energy; 4-8 kWh/tonne feedstock[293], hence its NER is high although the parasitic energy of feedstock and digestate transport, dewatering and comminution were omitted. As with any solar process, the IBR has a significant land requirement. Land use rates

for PF were 0.8-2.8 m<sup>2</sup>·years/tonne, varying with the feedstock (Table 3D). For example, to match the capacity of a typical AD plant (5000 tonnes/year), an IBR in Kampala would require 1.4 hectares processing Ap waste or 0.4 ha for CW1. An equivalent AD process would require ≥120 ha of agricultural land for spreading digestate within nitrate release regulations.[293] Therefore, the IBR has 0.3-1.2% of AD's land requirement and, furthermore, the IBR's land need not be arable, including industrial areas, rooftops, contaminated land and slopes. Due to a ~2-fold lower solar irradiance the IBR's space requirement would be ~2-fold higher in locations 50° from the equator (e.g. Northern Europe, Northern USA or Australia) but due to the minor contribution of PF energy requirements, the effect on NER would be negligible.

To compare the IBR with other solar processes, the power/land ratios in the range 53-82 kW/ha (equator) or 27-41 kW/ha (~50° N or S) were calculated (WEO6). For comparison, the Sarnia photovoltaic (PV) power plant, currently the world's largest (380 ha), outputs 36 kW/ha. Meanwhile onshore wind (UK) and crop-biofuels (UK) produce ~20 and ~5 kW/ha, respectively.[294] Therefore, in locations ~50° from the equator (e.g. UK, Germany) the IBR could easily out-produce wind and crop-derived biofuels, with a similar output to PV, while providing sustainable biowaste disposal and earning associated revenues.

## CONCLUSIONS

- This study supports the two hypotheses; biowastes are suitable for extractive fermentation (EF) and the IBR is a practical approach for biowaste-to-energy.
- Extracts from waste-fed EF were suitable for photofermentation.
- Dark EF has a negative energy balance, whereas the IBR has a positive energy balance whereby PF requires 2.5% of the parasitic energy and provides ~80% of the output.
- Hydrothermal hydrolysis and electro dialysis represent 95% of the parasitic energy but enable ≤99% destruction of biowaste and NH<sub>4</sub><sup>+</sup>-immune solar bioenergy production at 67 kW/ha, with a net energy ratio of 2.4.
- The IBR compares favourably with leading waste to bioenergy processes, microbial electrolysis and anaerobic digestion and also to core renewable (wind, crop-biofuels and photovoltaics).

## ACKNOWLEDGMENT

We acknowledge with thanks the financial support of the EPSRC (EP/D05768X/1, EP/E034888/1), BBSRC (BB/C516195/2, BB/E003788/1), Royal Society (Industrial Fellowship to LEM), Advantage West Midlands (POC46) and Gov. Mexico (studentship 203186 to RLO). We thank, for helpful discussions, guidance and technical support G. Leeke, R. Santos, B. Al-Duri and the Combined Workshop (University of Birmingham, UK), for *E. coli* strains, F. Sargent (University of Dundee, UK), for *R. sphaeroides* ZX5, Z. Zhou (Shanghai Institute for Biological Sciences, Chinese Academy of Sciences, China) and for waste samples Minor Weir & Willis Ltd, Heineken UK Ltd and Central Kitchens (University of Birmingham).

### SUPPORTING INFORMATION PARAGRAPH

Mathematical derivations for Table 3 and values given in text (spreadsheet).

## FIGURE CAPTIONS

**Figure 1.** Food waste processing scheme and mass flows.

Values represent masses (kg/kg raw waste). Av, CW2, CW3 and BG were unsuitable for pressing and were treated only by blending and hot compressed water (HCW), which took place at 200 °C except for grain which was at 220 °C. Raw wholesalers waste avocado contained 0.16 g stones which were removed before blending (not shown). Detoxification (Detox.) used activated carbon (5% w/v; see text).

**Figure 2.** Waste-fed extractive fermentations (dark fermentations).

Fermentations were fed with the juices of A: wholesalers mango waste; B: wholesalers asian pear waste; C: catering waste 1. Arrows indicate time of substrate dosings. Volumes added were A, 238mL; B, 255mL; C, 245mL, designed to provide ~0.1 mol reducing sugars content per dose. However, due to the variable nature of waste feedstocks variation in substrate dosing was unavoidable in practice. Major sugars (glucose, fructose) are shown although maltose, mannose, xylose and mannitol were detected in low concentrations. Sucrose was not detected. Note that volume increase was partially compensated by water transport into the permeate chamber. The total volume increase was A: 0.20 L B: 0.36 L; C: 0.62 L. Total organic anion represents the summed charges of lactate, acetate, propionate, formate, butyrate and succinate. All except succinate have

single  $pK_a$  values in the range 3.8-4.9 and were treated as fully dissociated at pH 6.0. Succinate ( $pK_a$  4.2, 5.6) has theoretically 1.59 charge equivalents/mol at pH 6.0.

**Figure 3.** Techno-economic analysis of an integrated biohydrogen refinery (IBR) using pre-treatment by HCW and extractive fermentation.

Annotations in bold italics indicate the features of a process using wholesalers mango waste, where values are derived from the experimental data of this study. <sup>a</sup>Incentive revenues were based on current UK feed-in tariff for anaerobic digestion: GBP 0.14/kWh up to 250 kW[272]; <sup>b</sup>Fuel cell efficiency: 75%; <sup>c</sup>Approx. price of exported power: GBP 0.06/kWh; <sup>d</sup>In addition to bioH<sub>2</sub>, the IBR also produces H<sub>2</sub> via electrolysis however the yield of electrolytic H<sub>2</sub> in a full scale IBR is unclear hence only bioH<sub>2</sub> was included in this analysis. HCW: hot compressed water. <sup>e</sup>Excess *E. coli* and *R. sphaeroides* cells can be valorised via metal recovery for fuel cell manufacture.[261, 295]

## TABLES

**Table 1.** Food wastes characterisation and fermentability

Waste <sup>a</sup>	Description	Moisture content (% w/w)	Total sugars (% w/w wet matter)	Starch content (% w/w wet matter)	H <sub>2</sub> yield (L/kg raw waste)			
					Juice	Infusion	Hydrolysate <sup>f</sup>	Total
Ma <sup>d</sup>	Variety: 'keit' Stones removed.	84.9	10.6	0.23	0.85	0.47	1.33	2.65
Ap <sup>d</sup>	Variety: <i>Purus x bretschnideri</i> Whole fruit used.	87.2	7.25	0.18	1.08	1.60	0.64	3.32
Av <sup>e</sup>	Varety: 'Avo Hass' Stones removed.	70.6	8.83 <sup>b</sup>	ND <sup>c</sup>	e	e	0.52	0.52
CW1 <sup>d</sup>	Red onion, tomato, lettuce, spring onion, pepper, pasta, lemon peel.	89.7	7.02	1.35	0.77	0.44	0.66	1.87
CW2 <sup>e</sup>	Onion, pea, potato, carrot, courgette.	87.3	4.08	1.51	e	e	0.93	0.93
CW3 <sup>e</sup>	Rice, pasta (cooked).	57.4	28.5	21.1	e	e	5.99	5.99
BG <sup>e</sup>	Malted barley from beer process.	75.5	16.4	1.22	e	e	1.07	1.07

<sup>a</sup>For waste abbreviations see Figure 1; <sup>b</sup>The oil fraction was omitted from acid digestion; <sup>c</sup>Avocado was too oily for starch analysis; <sup>d</sup>pressed to extract juice and solids were infused, see Figure 1; <sup>e</sup>No juice or infusion could be produced due to the physical nature of the waste; <sup>f</sup>HCW hydrolysis took place at 200 °C except for grain which was at 220 °C and hydrolysates were detoxified with activated carbon as reported previously.[225]

**Table 2.****A:** Anion analysis of extracts from waste-fed extractive fermentations

Fermentation substrate <sup>a</sup>	Inorganic anion (mM)					Organic anion (mM)							
	Chloride	Nitrite	Nitrate	Sulphate	Phosphate	Lactate	Acetate	Propionate	Formate	Butyrate	Succinate	Citrate	Total HPP <sup>b</sup>
Ma juice	2.7	0.0	0.0	5.6	2.4	54.6	90.4	0.0	34.5	98.8	8.1	0.6	1777
Ap juice	2.7	0.3	0.0	5.5	2.6	8.0	75.5	0.0	47.0	84.0	25.9	0.3	1422
CW1 juice	6.9	0.0	0.04	12.7	4.5	10.2	98.1	58.4	17.4	39.5	3.2	0.0	1297

<sup>a</sup>source of OA via extractive fermentation; <sup>b</sup>HPP values (mol H<sub>2</sub>/mol OA) are: Lactate 6; Acetate 4; Propionate 7; Butyrate 10; Succinate 7; Citrate 14.[296]

**B:** Experimental and potential H<sub>2</sub> yields by photofermentation of waste juices

Original waste (source of OA via EF)	Initial substrate concentration mM HPP <sup>c</sup>	Substrate conversion efficiency % <sup>d</sup>	Yield of OA from EF mol HPP/kg juice	Extrapolated photo-fermentative H <sub>2</sub> yield from waste juices. L H <sub>2</sub> /kg juice <sup>f</sup>
Ma juice	34.64	17.7%	5.748 <sup>e1</sup>	110.6
Ap juice	39.60	48.9%	5.257 <sup>e2</sup>	101.2
CW1 juice	61.46	15.6%	0.956 <sup>e3</sup>	18.4

<sup>c</sup>HPP, hydrogen production potential as proposed by[259] is a convenient unit for the potential H<sub>2</sub> production from any mixture of substrates, e.g. a solution of 1 mM acetate and 1 mM butyrate contains 14 mM HPP, because acetate can yield a theoretical maximum of 4 H<sub>2</sub>/mol while butyrate can yield 10 H<sub>2</sub>/mol[296]; <sup>d</sup>Substrate conversion efficiency[297]; <sup>e</sup>Extractive fermentations fed with the juices of waste mango, asian pear and catering waste 1, yielded respectively 4.02 mol HPP from 0.70 kg juice, 4.02 mol HPP from 0.77 kg juice and 0.80 mol HPP from 0.84 kg juice; <sup>f</sup>To extrapolate the productivity at full scale, a substrate conversion efficiency of 80% was used, typical for optimised photobioreactors as opposed to static vial tests, used here as a high throughput method to confirm the suitability of electroseparated organic acids (OA) (see text). EF: extractive fermentation.

**Table 3****A: Gross energy production by a single-stage extractive fermentation.**

Waste	H <sub>2</sub> yield in juice-fed EF	H <sub>2</sub> yield (Juice fraction)	Fraction of total H <sub>2</sub> from juice <sup>b</sup>	H <sub>2</sub> yield from juice, infusion & hydrolysate	Gross electricity production potential <sup>c</sup>
Unit	mol H <sub>2</sub> / kg juice	mol H <sub>2</sub> from the juice of 1 kg raw waste <sup>a</sup>	%	mol H <sub>2</sub> / kg raw waste	kWh/kg raw waste
Ma	0.631	0.102	31.9%	0.319	0.019
Ap	0.433	0.127	32.6%	0.391	0.023
CW1	0.457	0.262	41.1%	0.638	0.038

**B: Parasitic costs and net energy production of a single-stage extractive fermentation.**

Waste	Hot Compressed Water (HCW) treatment			Electroseparation of organic acids			Mixing energy for dark fermentation <sup>f</sup>			Total parasitic energy	Net Energy Ratio <sup>h</sup>
Unit	Moisture of washed pressings	kg HCW reactant / kg raw waste <sup>a</sup>	kWh / kg raw waste <sup>d</sup>	kWh / mol HPP <sup>e</sup>	kWh / kg juice	kWh / kg raw waste <sup>f</sup>	Days of mixing	kWh / kg juice <sup>g</sup>	kWh / kg raw waste <sup>f</sup>	kWh / kg raw waste	Out / In
Ma	84.9%	3.126	0.0318	0.0073	0.0422	0.021	3.863	0.0016	0.00080	0.0539	0.35
Ap	87.2%	2.116	0.0216	0.0192	0.1011	0.091	4.042	0.0015	0.00137	0.1142	0.20
CW1	84.7%	2.349	0.0239	0.0128	0.0123	0.017	5.617	0.0019	0.00269	0.0438	0.87

**C: Gross energy production by an integrated biohydrogen refinery (IBR).**

Waste	H <sub>2</sub> yield in juice-fed fermentations			Total H <sub>2</sub> yield from juice, infusion and hydrolysate <sup>b</sup>	Gross electricity production potential <sup>c</sup>
	Dark fermentation	Photo-fermentation	Total		
Unit	mol H <sub>2</sub> / kg juice <sup>a</sup>	mol H <sub>2</sub> / kg juice	mol H <sub>2</sub> from the juice of 1 kg raw waste <sup>b</sup>	mol H <sub>2</sub> / kg raw waste	kWh / kg raw waste
Ma	0.631	4.598	0.842	2.642	0.157
Ap	0.433	4.206	1.364	4.187	0.249
CW1	0.457	0.769	0.703	1.711	0.102

**D: Parasitic costs and net energy production of an integrated biohydrogen refinery (IBR).**

Waste	Yield of organic acids (HPP) via extractive fermentation of wastes		Land use rate	Mixing energy for photofermentation	Total parasitic energy <sup>k</sup>	Net Energy Ratio <sup>h</sup>
Unit	mol HPP from the juice of 1 kg raw waste <sup>i</sup>	mol HPP / kg raw waste <sup>j</sup>	m <sup>2</sup> ·years / kg raw waste	kWh / kg raw waste	kWh / kg raw waste	Out / In
Ma	0.925	2.905	0.00174	0.0059	0.093	1.70
Ap	1.546	4.746	0.00285	0.0096	0.118	2.11
CW1	0.549	1.334	0.00080	0.0027	0.075	1.36

<sup>a</sup>Calculated using the mass yields shown in Figure 1;<sup>b</sup>Calculated in Table 1;<sup>c</sup>with a power conversion efficiency of 75% via a fuel cell, 285.9 kJ/mol H<sub>2</sub>.<sup>d</sup>Author's estimation for the power demand for heating in a continuous flow HCW system (see text);<sup>e</sup>Extractive fermentations fed with the juices of waste mango, asian pear and catering waste 1 required for electroseparation 29.5 Wh, 77.3 Wh and 10.3 Wh, respectively;<sup>f</sup>for juice, infusion and hydrolysate.<sup>g</sup>Estimated using 4 W/m<sup>3</sup> mixing power[280] using the fed juice volumes (Table 2B, legend);<sup>h</sup>Net Energy Ratio (NER) includes the necessary and scalable process energy requirements and excludes variable requirements such as feedstock transport, and communitation.<sup>i</sup>Calculated using the yields of juice from raw waste (Figure 1) and yields of HPP from juice (Table 2B);

<sup>j</sup>Estimated HPP yield via extractive fermentation of all waste fractions (juice, infusion and hydrolysate), assuming that HPP yield is proportional to H<sub>2</sub> yield (Table 2);

<sup>k</sup>Sum of PF mixing energy and single-stage parasitic energy (B).

For further detail see WEO2-5.

## REFERENCES

- (1) Redwood, M. D.; Paterson-Beedle, M.; Macaskie, L. E., Integrating dark and light biohydrogen production strategies: towards the hydrogen economy. *Rev. Environ. Sci. Bio/Technol.* **2009**, 8, (2), 149-185.
- (2) Abo-Hashesh, M.; Ghosh, D.; Tourigny, A.; Taous, A.; Hallenbeck, P. C., Single stage photofermentative hydrogen production from glucose: An attractive alternative to two stage photofermentation or co-culture approaches. *Int. J. Hydrog. Energy* **2011**, *In press*.
- (3) Afsar, N.; Özgür, E.; Gürkan, M.; Akköse, S.; Yücel, M.; Gündüz, U.; Eroğlu, I., Hydrogen productivity of photosynthetic bacteria on dark fermenter effluent of potato steam peels hydrolysate. *Int. J. Hydrog. Energy* **2011**, 36, (1), 432-438.
- (4) Argun, H.; Kargi, F., Bio-hydrogen production by different operational modes of dark and photo-fermentation: An overview. *Int. J. Hydrog. Energy* **2011**, 36, (13), 7443-7459.
- (5) Avcioglu, S. G.; Özgür, E.; Eroğlu, I.; Yücel, M.; Gündüz, U., Biohydrogen production in an outdoor panel photobioreactor on dark fermentation effluent of molasses. *Int. J. Hydrog. Energy* **2011**, *In press*.
- (6) Chu, C.-Y.; Wu, S.-Y.; Hsieh, P.-C.; Lin, C.-Y., Biohydrogen production from immobilized cells and suspended sludge systems with condensed molasses fermentation solubles. *Int. J. Hydrog. Energy* **2011**, *In press*.
- (7) Lo, Y.-C.; Chen, C.-Y.; Lee, C.-M.; Chang, J.-S., Photo fermentative hydrogen production using dominant components (acetate, lactate, and butyrate) in dark fermentation effluents. *Int. J. Hydrog. Energy* **2011**, *In press*.
- (8) Özgür, E.; Mars, A. E.; Peksel, B.; Louwerse, A.; Yücel, M.; Gündüz, U.; Claassen, P. A. M.; Eroğlu, I., Biohydrogen production from beet molasses by sequential dark and photofermentation. *Int. J. Hydrog. Energy* **2011**, 35, (2), 511-517.
- (9) Kyazze, G.; Dinsdale, R.; Guwy, A. J.; Hawkes, F. R.; Premier, G. C.; Hawkes, D. L., Performance characteristics of a two-stage dark fermentative system producing hydrogen and methane continuously. *Biotechnol. Bioeng.* **2007**, 97, (4), 759-770.
- (10) Martínez-Pérez, N.; Cherryman, S. J.; Premier, G. C.; Dinsdale, R. M.; Hawkes, D. L.; Hawkes, F. R.; Kyazze, G.; Guwy, A. J., The potential for hydrogen-enriched biogas production from crops: Scenarios in the UK. *Biomass Bioenerg* **2007**, 31, (2-3), 95-104.
- (11) Kyazze, G.; Popov, A.; Dinsdale, R.; Esteves, S.; Hawkes, F.; Premier, G.; Guwy, A., Influence of catholyte pH and temperature on hydrogen production from acetate using a two chamber concentric tubular microbial electrolysis cell. *Int. J. Hydrog. Energy* **2010**, 35, (15), 7716-7722.
- (12) Guwy, A. J.; Dinsdale, R. M.; Kim, J. R.; Massanet-Nicolau, J.; Premier, G., Fermentative biohydrogen production systems integration. *Bioresour. Technol.* **2011**, *In press*.
- (13) Redwood, M. D.; Orozco, R.; Majewski, A. J.; Macaskie, L. E., An integrated biohydrogen refinery: Synergy of photofermentation, extractive fermentation and hydrothermal hydrolysis of food wastes. *Environ. Sci. Technol.* **2011**, *in submission (Aug 2011)*.

- (14) Chen, C. Y.; Yang, M. H.; Yeh, K. L.; Liu, C. H.; Chang, J. S., Biohydrogen production using sequential two-stage dark and photo fermentation processes. *Int. J. Hydrog. Energy* **2008**, *33*, (18), 4755-4762.
- (15) Redwood, M. D.; Macaskie, L. E., A two-stage, two-organism process for biohydrogen from glucose. *Int. J. Hydrog. Energy* **2006**, *31*, (11), 1514-1521.
- (16) Redwood, M. D.; Orozco, R.; Majewski, A. J.; Macaskie, L. E., Electro-extractive fermentation for efficient biohydrogen production. *Bioresour. Technol.* **2011**, *in submission*.
- (17) Blanchette Jr, S., A hydrogen economy and its impact on the world as we know it. *Energ. Policy* **2008**, *36*, (2), 522-530.
- (18) Tseng, P.; Lee, J.; Friley, P., A hydrogen economy: opportunities and challenges. *Energy* **2005**, *30*, (14), 2703-2720.
- (19) Claassen, P. A. M.; van Lier, J. B.; Lopez-Contreras, A. M.; van Niel, E. W. J.; Sijtsma, L.; Stams, A. J. M.; de Vries, S. S.; Weusthuis, R. A., Utilisation of biomass for the supply of energy carriers. *Appl. Microbiol. Biotechnol.* **1999**, *52*, 741-755.
- (20) Madzingaidzo, L.; Danner, H.; Braun, R., Process development and optimisation of lactic acid purification using electrodialysis. *J. Biotechnol.* **2002**, *96*, (3), 223-239.
- (21) Orozco, R. L.; Redwood, M. D.; Reza, A.; Leeke, G.; Santos, R.; Macaskie, L. E., Hydrothermal hydrolysis of starch with CO<sub>2</sub> and detoxification of the hydrolysates with activated carbon for bio-hydrogen fermentation. *Int. J. Hydrog. Energy* **2011**, *in submission*.
- (22) Redwood, M. D.; Mikheenko, I. P.; Sargent, F.; Macaskie, L. E., Dissecting the roles of *E. coli* hydrogenases in biohydrogen production. *FEMS Microbiol. Lett.* **2008**, *278*, 48-55.
- (23) Clark, D. P., The fermentation pathways of *Escherichia coli*. *FEMS Microbiol. Rev.* **1989**, *5*, (3), 223-234.
- (24) Tao, Y.; He, Y.; Wu, Y.; Liu, F.; Li, X.; Zong, W.; Zhou, Z., Characteristics of a new photosynthetic bacterial strain for hydrogen production and its application in wastewater treatment. *Int. J. Hydrog. Energy* **2008**, *33*, (3), 963-973.
- (25) Hoekema, S.; Bijmans, M.; Janssen, M.; Tramper, J.; Wijffels, R. H., A pneumatically agitated flat-panel photobioreactor with gas re-circulation: anaerobic photoheterotrophic cultivation of a purple non-sulfur bacterium. *Int. J. Hydrog. Energy* **2002**, *27*, (11-12), 1331-1338.
- (26) Eroğlu, E.; Gündüz, U.; Yücel, M.; Türker, L.; Eroğlu, I., Photobiological hydrogen production by using olive mill wastewater as a sole substrate source. *Int. J. Hydrog. Energy* **2004**, *29*, 163-171.
- (27) Ormerod, J. G.; Gest, H., Hydrogen photosynthesis and alternative metabolic pathways in photosynthetic bacteria. *Bacteriol. Rev.* **1962**, *26*, 51-66.
- (28) Orozco, R. L.; Redwood, M. D.; Yong, P.; Caldelari, I.; Sargent, F.; Macaskie, L. E., Towards an integrated system for bio-energy: Hydrogen production by *Escherichia coli* and use of palladium-coated waste cells for electricity generation in a fuel cell. *Biotechnol. Lett.* **2010**, *32*, 1837-1845.
- (29) Chaplin, M. F., Monosaccharides. In *Carbohydrate analysis: a practical approach*, Chaplin, M. F.; Kennedy, J. F., Eds. IRL Press at Oxford University press, UK: 1986; p 324.
- (30) Birch, G. G.; Priestley, R. J., Degree of gelatinisation of cooked rice. *Starch - Stärke* **1973**, *25*, (3), 98-100.
- (31) Saeman, J. F.; Bubl, J. L.; Harris, E. E., Quantitative saccharification of wood and cellulose. *Ind. & Eng. Chem. Anal. Ed.* **1945**, *17*, (1), 35-37.
- (32) Miyazawa, T.; Funazukuri, T., Polysaccharide hydrolysis accelerated by adding carbon dioxide under hydrothermal conditions. *Biotechnol. Prog.* **2005**, *21*, (6), 1782-1785.

- (33) Penfold, D. W.; Macaskie, L. E., Production of H<sub>2</sub> from sucrose by *Escherichia coli* strains carrying the pUR400 plasmid, which encodes invertase activity. *Biotechnol. Lett.* **2004**, *26*, 1879-1883.
- (34) Boos, W.; Shuman, H., Maltose/maltodextrin system of *Escherichia coli*: transport, metabolism and regulation. *Microbiol Mol Biol Rev* **1998**, *62*, (1), 204-29.
- (35) Redwood, M. D. Bio-hydrogen and biomass supported palladium catalyst for energy production and waste minimisation. Ph.D. Thesis. University of Birmingham, 2007.
- (36) Akkerman, I.; Janssen, M.; Rocha, J.; Wijffels, R. H., Photobiological hydrogen production: photochemical efficiency and bioreactor design. *Int. J. Hydrog. Energy* **2002**, *27*, (11-12), 1195-1208.
- (37) Rocha, J. S.; Barbosa, M. J.; Wijffels, R. H., Hydrogen production by photoheterotrophic bacteria: Culture media, yields and efficiencies. In *Biohydrogen II : An Approach to Environmentally Acceptable Technology*, Miyake, J.; Matsunaga, T.; San Pietro, A., Eds. Pergamon: 2001; pp 3-32.
- (38) Sasikala, C. H.; Ramana, C. V.; Rao, P. R., Regulation of simultaneous hydrogen photoproduction during growth by pH and glutamate in *Rhodobacter sphaeroides* O.U. 001. *Int. J. Hydrog. Energy* **1995**, *20*, (2), 123-126.
- (39) Anon, Department of Energy & Climate Change (DECC). Feed-in tariffs scheme: Summary of responses to the fast-track consultation and Government response, 9 June 2011.
- (40) Anon, Waste & Resources Action Programme (WRAP). Gate Fees Report. Comparing the cost of alternative waste treatment options, July 2010.
- (41) Anon, Department of Energy and Climate Change (DECC) and Department for Environment Food and Rural Affairs (Defra). Anaerobic digestion strategy and action plan. Report number PB 13541, June 2011.
- (42) Jogwar, S. S.; Baldea, M.; Daoutidis, P. In *Dynamics and control of reactor - Feed effluent heat exchanger networks. Paper reference WeC08.2 in Proceedings of the American Control Conference. Westin Seattle Hotel, Seattle, Washington, USA*, 11-13 June 2008, 2008; 2008; pp 1481-1486.
- (43) Chen, Y.-H.; Yu, C.-C., Design and control of heat-integrated reactors. *Ind. Eng. Chem. Res.* **2003**, *42*, (12), 2791-2808.
- (44) Cumiskey, A.; Dawson, M.; Tillotson, M., Thick sludge digestion - Research, design and validation of key process unit operations. In *Residuals and Biosolids*, Baltimore, Maryland USA, 2002.
- (45) Karim, K.; Hoffmann, R.; Klasson, T.; Al-Dahhan, M. H., Anaerobic digestion of animal waste: Waste strength versus impact of mixing. *Bioresour. Technol.* **2005**, *96*, (16), 1771-1781.
- (46) Lee, S. R.; Cho, N. M.; Maeng, W. J., Using the pressure of biogas created during anaerobic digestion as the source of mixing power. *J. Ferment. Bioeng.* **1995**, *80*, (4), 415-417.
- (47) Mills, P. J., Minimisation of energy input requirements of an anaerobic digester. *Bioresour. Technol.* **1979**, *1*, (1), 57-66.
- (48) Burgess, G.; Fernandez-Velasco, J. G., Materials, operational energy inputs, and net energy ratio for photobiological hydrogen production. *Int. J. Hydrog. Energy* **2007**, *32*, 1255-1234.
- (49) Šúri, M.; Huld, T. A.; Dunlop, E. D.; Ossenbrink, H. A., Potential of solar electricity generation in the European Union member states and candidate countries. *Solar Energy* **2007**, *81*, (10), 1295-1305.
- (50) Levin, D. B.; Pitt, L.; Love, M., Biohydrogen production: prospects and limitations to practical application. *Int. J. Hydrog. Energy* **2004**, *29*, 173-185.

- (51) Anon, Waste & Resources Action Programme (WRAP). Gate Fees Report. Comparing the cost of alternative waste treatment options. Available from [www.wrap.org.uk](http://www.wrap.org.uk). **July 2010**.
- (52) Sun, Q.; Xiao, W.; Xi, D.; Shi, J. P.; Yan, X.; Zhou, Z. H., Statistical optimization of biohydrogen production from sucrose by a co-culture of *Clostridium acidisoli* and *Rhodobacter sphaeroides*. *Int. J. Hydrog. Energy* **2010**, *35*, (9), 4076-4084.
- (53) Lui, H.; Grot, S.; Logan, B. E., Electrochemically assisted microbial production of hydrogen from acetate. *Environ Sci Technol* **2005**, *39*, 4317-4320.
- (54) Logan, B. E.; Call, D.; Cheng, S.; Hamelers, H. V. M.; Sleutels, T.; Jeremiasse, A. W.; Rozendal, R. A., Microbial electrolysis cells for high yield hydrogen gas production from organic matter. *Environ. Sci. Technol.* **2008**, *42*, (23), 8630-8640.
- (55) Cheng, S.; Logan, B. E., Sustainable and efficient biohydrogen production via electrohydrogenesis. *PNAS USA* **2007**, *104*, (47), 18871-18873.
- (56) Sun, M.; Sheng, G. P.; Zhang, L.; Xia, C. R.; Mu, Z. X.; Liu, X. W.; Wang, H. L.; Yu, H. Q.; Qi, R.; Yu, T.; Yang, M., An MEC-MR-coupled system for biohydrogen production from acetate. *Environ. Sci. Technol.* **2008**, *42*, (21), 8095-8100.
- (57) Uwe, S., From wastewater to hydrogen: Biorefineries based on microbial fuel-cell technology. *ChemSusChem* **2008**, *1*, (4), 281-282.
- (58) Call, D.; Logan, B. E., Hydrogen production in a single chamber microbial electrolysis cell lacking a membrane. *Environ. Sci. Technol.* **2008**, *42*, (9), 3401-3406.
- (59) Clauwaert, P.; Toledo, R.; Van der Ha, D.; Crab, R.; Verstraete, W.; Hu, H.; Udert, K. M.; Rabaey, K., Combining biocatalyzed electrolysis with anaerobic digestion. *Water Sci. Technol.* **2008**, *57*, (4), 575-579.
- (60) Limmeechokchai, B.; Chawana, S., Sustainable energy development strategies in the rural Thailand: The case of the improved cooking stove and the small biogas digester. *Renew. Sust. Energ. Rev.* **2007**, *11*, (5), 818-837.
- (61) Redman, G., National Non-Food Crops Centre (NNFCC) and The Anderson Centre. Economic assessment of anaerobic digestion technology and its suitability to UK farming and waste systems: AD cost calculator (Tool). Report number 10-010, 30 Jun 2011.
- (62) MacKay, D. J. C., *Sustainable Energy - without the hot air*. UIT Cambridge: 2008; Vol. ISBN 978-0-9544529-3-3. Available free online from [www.withouthotair.com](http://www.withouthotair.com).
- (63) Yong, P.; Mikheenko, I.; Deplanche, D.; Redwood, M. D.; Sargent, F.; Macaskie, L. E., Biorefining of precious metals from wastes: An answer to manufacturing of cheap nanocatalysts for fuel cells and power generation via an integrated biorefinery? *Biotechnol. Lett.* **2010**, *32*, 1821-1828.
- (64) Sasikala, K.; Ramana, C. V.; Rao, P. R.; Kovacs, K. L., Anoxygenic phototrophic bacteria : Physiology and advances in hydrogen production technology. *Adv. Appl. Microbiol.* **1995**, *38*, 211-295.
- (65) Koku, H.; Eroğlu, I.; Gündüz, U.; Yücel, M.; Türker, L., Kinetics of biological hydrogen production by the photosynthetic bacterium *Rhodobacter sphaeroides* O.U. 001. *Int. J. Hydrog. Energy* **2003**, *28*, 381-388.

FIGURES

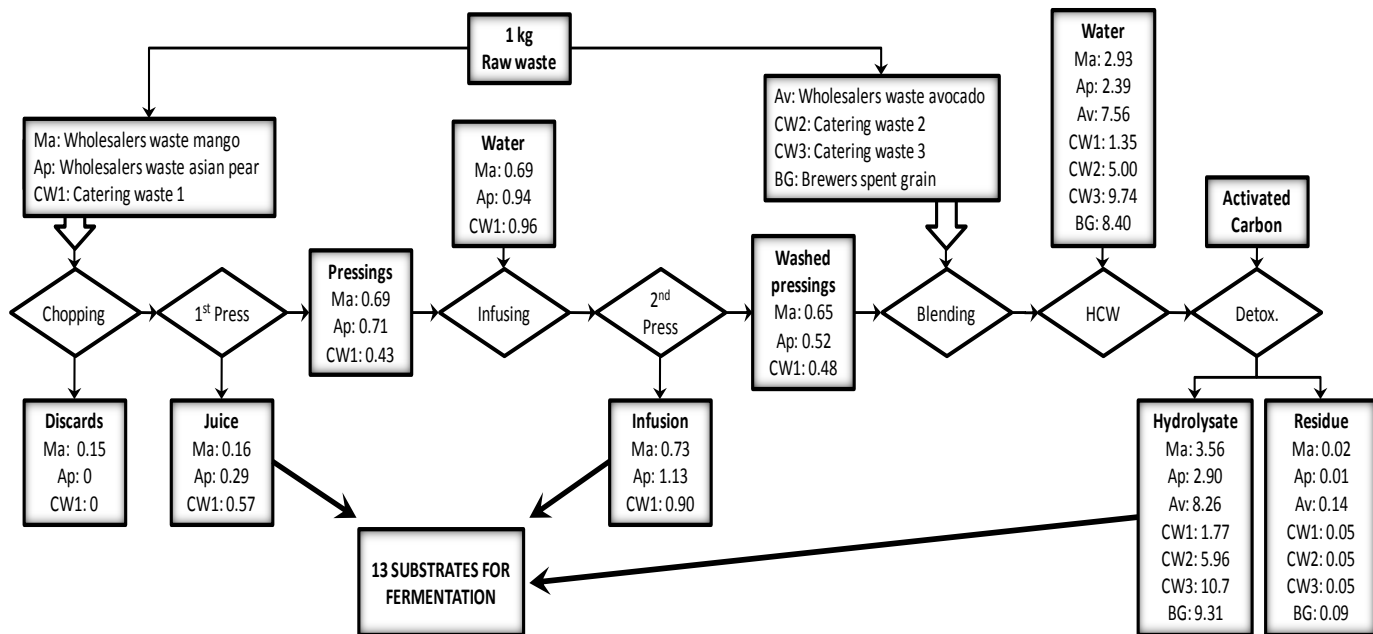


**Figure 1.** Food waste processing scheme and mass flows.

Values represent masses (kg/kg raw waste). Wastes comprised 3 samples of spoiled fruits, 2 samples of catering wastes and brewers malted grain. Solids were pressed using a Ferrari 5 L hand-cranked fruit press. Solid residues were homogenised (except for grain) using a standard kitchen blender and then dried at 60 °C, to determine the moisture content before wet samples were treated with hot compressed water (HCW). Av, CW2, CW3 and BG were unsuitable for pressing and were treated only by blending and hot compressed water (HCW), which took place at 200 °C except for grain which was at 220 °C. Raw wholesalers waste avocado contained 0.16 g stones which were removed before blending (not shown). Detoxification (Detox.) used activated carbon (5% w/v; see text).

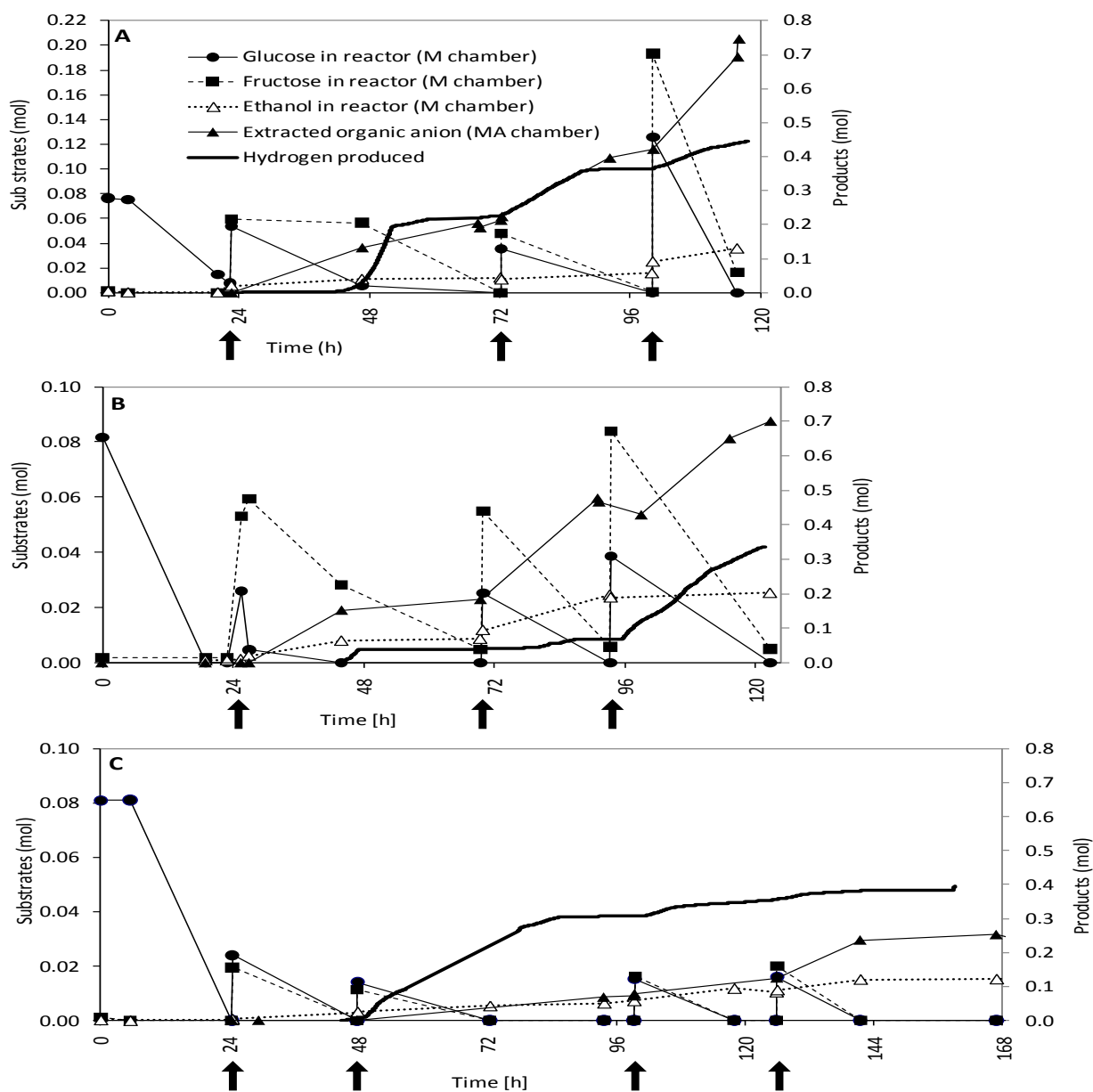


**Figure 2.** Waste-fed extractive fermentations.

Fermentations were fed with A: Wholesalers mango juice; B: Wholesalers asian pear juice; C: Catering waste 1 juice. Arrows indicate repeated substrate dosings into the dark fermenter. Volumes added were A, 238mL; B, 255mL; C, 245mL, designed to provide ~0.1 mol of reducing sugars content per dose. However, due to the variable nature of waste feedstocks variation in substrate dosing was unavoidable in practice. Major sugars (glucose, fructose) are shown although maltose, mannose, xylose and mannitol were detected in low concentrations. Sucrose was not detected. Total organic anion represents the summed charges of lactate, acetate, propionate, formate, butyrate and succinate. All except succinate have single  $pK_a$  values in the range 3.8-4.9 and were treated as fully dissociated at pH 6.0. Succinate ( $pK_a$  4.2, 5.6) has theoretically 1.59 charge equivalents/mol at pH 6.0.

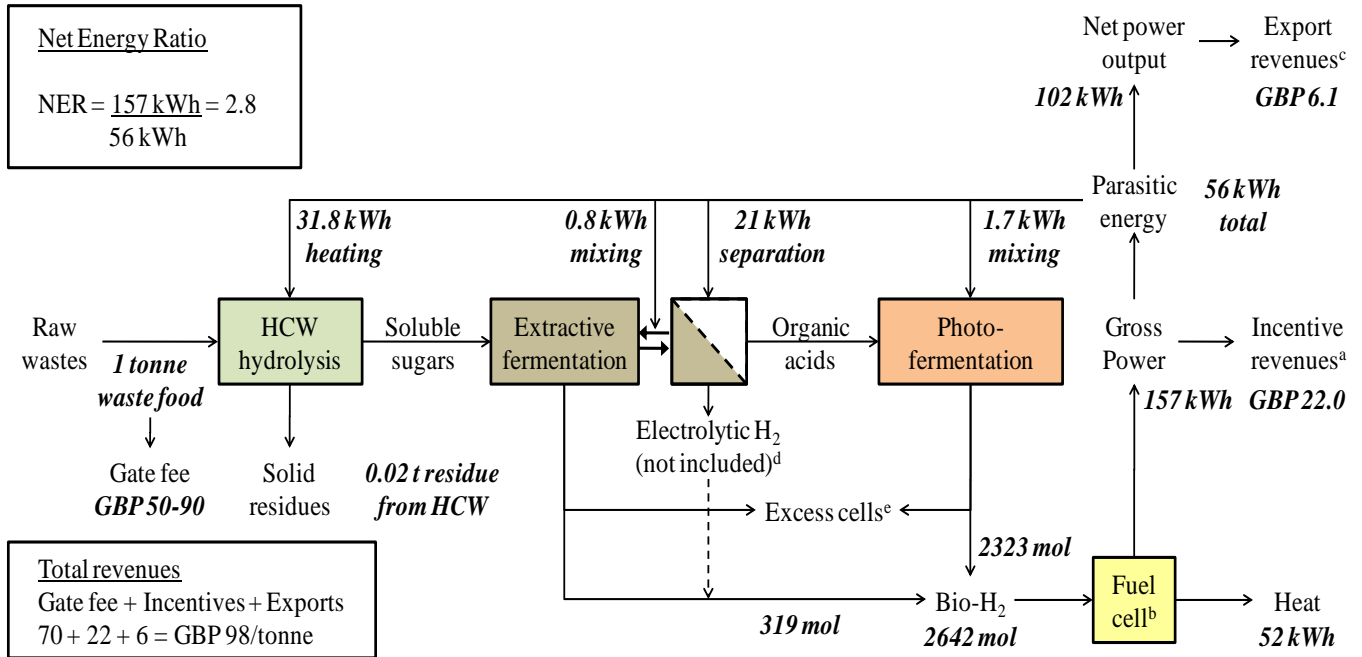


**Figure 3.** Techno-economic analysis of an integrated biohydrogen refinery (IBR) using pre-treatment by HCW and extractive fermentation.

Annotations in bold italics indicate the features of a process using wholesalers mango waste, where values are derived from the experimental data of this study. <sup>a</sup>Incentive revenues were based on current UK feed-in tariff for anaerobic digestion: GBP 0.14/kWh up to 250 kW[272]; <sup>b</sup>Fuel cell efficiency: 75%; <sup>c</sup>Approx. price of exported power: GBP 0.06/kWh; <sup>d</sup>In addition to bioH<sub>2</sub>, the IBR also produces H<sub>2</sub> via electrolysis however the yield of electrolytic H<sub>2</sub> in a full scale IBR is unclear hence only bioH<sub>2</sub> was included in this analysis. HCW: hot compressed water. <sup>e</sup>Excess *E. coli* and *R. sphaeroides* cells can be valorised via metal recovery for fuel cell manufacture.[261, 295] See also WEO8.

### VIII.5.2 Conference posters

- BGRS Symposium-poster conference. University of Birmingham, 2009. “Hydrogen production by mutant strains of *E. coli*.”  
This poster was also presented in the “Jatropha and bio-fuels congress in Mexico, 2010
- World Hydrogen Energy Conference (WHEC) 2010. Essen, Germany, 2010.
- Two posters were presented in this conference: “Hydrogen production by mutant strains of *E. coli*.” And “Towards an integrated system for bio-energy: Hydrogen production by *E. coli* and use of palladium coated waste cells por electricity generation in a fuel cell”
- World metals for catalyst convention, Argentina 2010. “Towards an integrated system for bio-energy: Hydrogen production by *E. coli* and use of palladium coated waste cells por electricity generation in a fuel cell”
- BGRS congress, Oxford 2010. “Waste into Energy” poster.
- Hybrid Materials 2011- Second International Conference on Multifunctional, Hybrid and Nanomaterials; Palais des Congrès, Strasbourg, France, March 2011  
Poster “Hydrogenation of Soybean Oil Using Bio-Pd Catalyst.”

### VIII.5.3 Conference presentations

- BGRS Symposium-talks. University of Birmingham, 2010 (awarded with the second prize).  
Talk: “Hydrogen from biomass by integration of thermochemical and biological methods”.  
Speaker: Rafael L. Orozco
- 4<sup>th</sup> World H<sub>2</sub> technologies convention, 2011, Glasgow, U.K.  
Speaker: Dr. M.D. Redwood.  
My participation consisted in assisting Dr. Redwood in the extractive fermentative experiments for the preparation of his presentation.

## **VIII.6 Appendix VIII.6 Participation in other related projects**

### **VIII.6.1 Biowaste2energy research base**

Project: “Implementation of a Volatile Fatty Acid Separator, photobioreactor and a generator for H<sub>2</sub> and energy production”.

Project leader: Dr. M.D. Redwood

My participation in this project consisted in assisting Dr. Redwood in the set-up, supervision, operation, control and data analysis in the extractive VFA experiments and photobioreactor experiments that in the latter case lasted for more than 100 days (continuous operation of the photobioreactor).

## Biowaste2energy Research Base

Mark Redwood 16/11/10

Biowaste2energy Ltd (BW2E) plans to implement a process containing 3 main elements:-

A **VFA separator** to selectively extract volatile fatty acids (VFAs) from large biogas plants.

A **photobioreactor (PBR)** to convert VFA to hydrogen gas.

A **generator**, for converting the hydrogen into electricity, so that it can be easily sold.

Research has focussed on parts 1 and 2 as biogas powered generators (part 3) are common and mixing hydrogen into the biogas stream would pose no significant technical challenge.

### *VFA separation*

The chosen technique is electrodialysis, in which the VFAs are pushed across a selective membrane by a direct current. This is a fairly sophisticated technique, used in water desalination and fine chemical production, so proof was required that that it would work in conjunction with a crude waste fed bioreactor (i.e. a biogas plant).

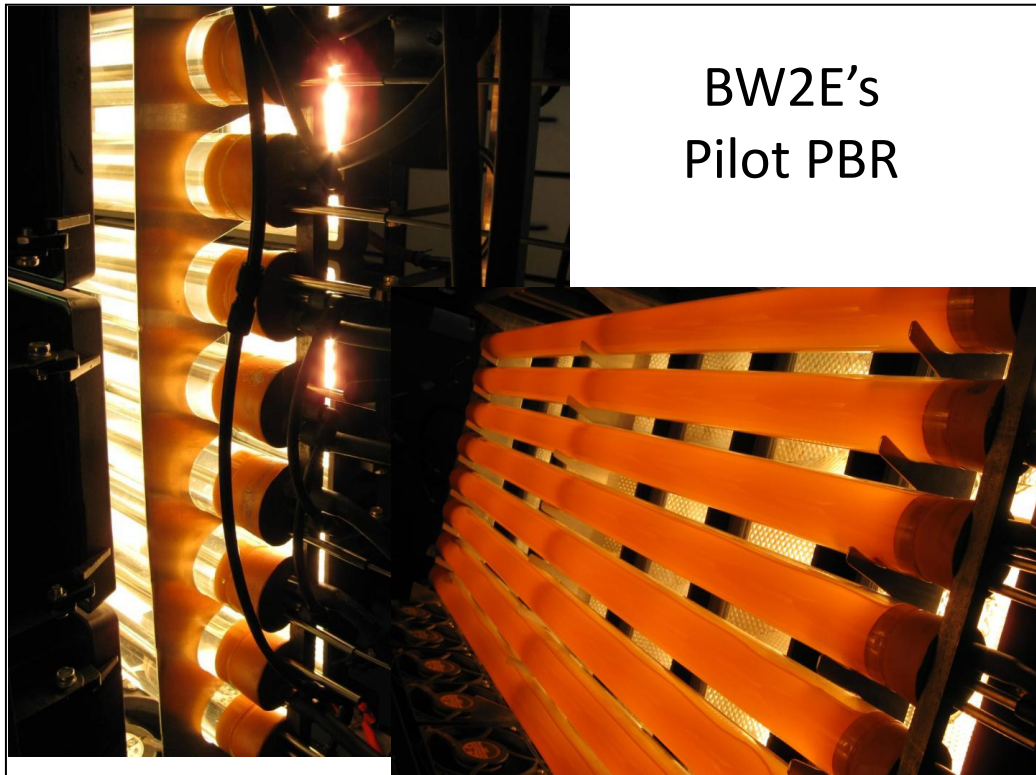
Lab scale research (funded by APOC/KTDF) demonstrated not only, that electrodialysis is capable of recovering VFA from waste fed bioreactors, but that high efficiency was maintained during long-term operation. It was also confirmed that the separated VFA solution was suitable for the photobioreactor. The results of this study are in preparation for Biotechnology Advances. It remains to prove VFA extraction from a real biogas plant.

Apparatus of VFA separation experiments



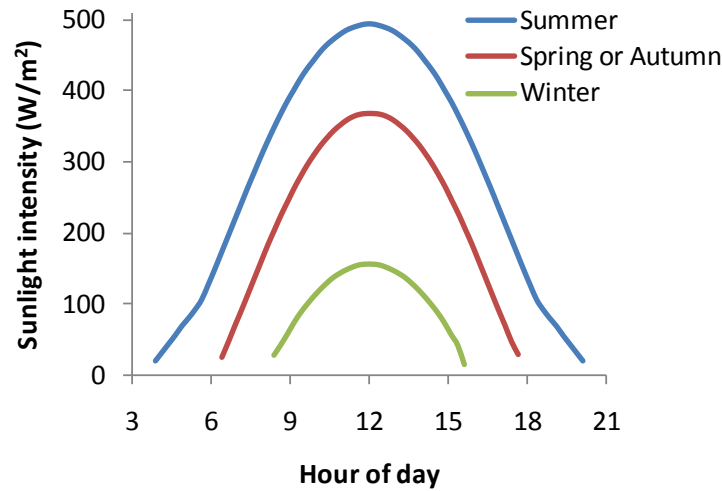
## **Photobioreactor (PBR)**

PBRs are an area of active research, now emerging as a commercial technology. The few systems commercially available are meant for algal cultivation and sub-optimal in BW2E's technology. Therefore it was necessary to design our own PBR, to prove the technique and a large laboratory PBR was constructed (funded by ModernWaste), using electric lamps to simulate sunlight.



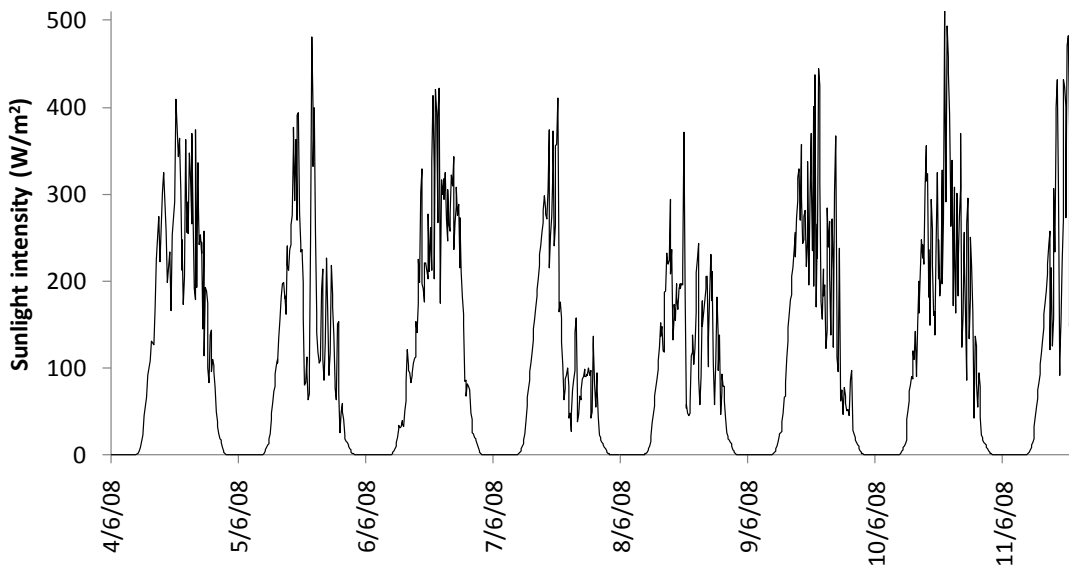
Unlike any system we know of, this PBR is unique in that the lamps can be programmed to simulate not only the intensity of sunlight, but the profile of that intensity. For example, the graph below shows how the typical profile of solar intensity changes over one day in Birmingham in four seasons.

Theoretical solar profiles for Birmingham



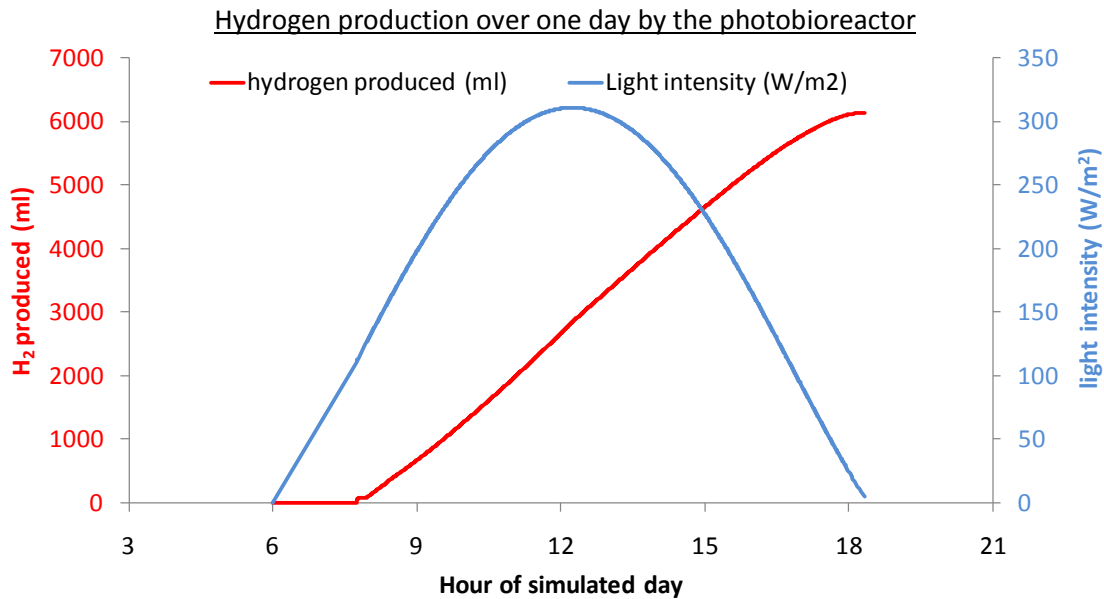
As shown in the graph, day breaks at 4-8 am, the midday sunlight peak ranges from 150-500 W/m<sup>2</sup> and sunset is at 4-8 pm, depending on the season. These profiles indicate the ‘real-sky’ taking account of average weather conditions, which reduces intensity. However, they don’t account for the variability in solar intensity due to weather, as shown below.

Examples of real sunlight profiles in Birmingham (June 2008)



The lighting system was programmed with the theoretical profile a spring/autumn day in Birmingham. The project ran for several months and called for problem-solving in several areas, particularly in the prevention of biofouling and maintaining optimal temperature. The main achievement of the study was to demonstrate the stability and reliability of the hydrogen production,

over several months of operation. The operators also gained valuable experience of running the PBR long-term. The following graph shows hydrogen production by the PBR during one simulated day.



Hydrogen production ceased completely at night and restarted about 2 hours after dawn, producing over 6 litres of gas, which was almost pure hydrogen before stopping immediately at sunset.

In these experiments, the efficiency of light conversion to hydrogen was 1.75%. It is considered that the theoretical maximum is at least 10% and we consider a 3-fold improvement to 5% to be achievable, as efficiencies of up to 8% were achieved in earlier work using a 4 litre benchtop PBR. Furthermore many accounts of similar results are reported in the literature (e.g. Akkerman et al, 2002, IJHE 27:1195).

#### Summary of technical objectives

Conceive an easily scalable photobioreactor with very low manufacturing costs.

Design and build a field trial apparatus, which closely represents a large-scale installation.

Run field trials to demonstrate expected productivity from the PBR in real sunlight with VFA fed from AD.

### **VIII.6.2 Growth of *Spirulina plantensis***

Project: “The effect of CO<sub>2</sub> on growth process of *S. plantensis* in experimental photo-incubator.”

Project leader: Professor Xu-Zhang

My participation in this one year project consisted in assisting professor Zhang in the preparation of solutions and equipment set-up during the initiation of the project and in performing the analysis of *Spirulina* growth and chlorophyll assays from the 30<sup>th</sup> of August up to date for the final stage of the project as described below.

# The Effect of CO<sub>2</sub> on the Growth Process of *S. platensis* in Experimental Photo Incubator

Xu Zhang

(School of Bioscience, University of Birmingham, August 2011)

## Abstract:

The effect of CO<sub>2</sub> on the growth of *S. platensis* was investigated in this study through batch cultures in a bench-scale photo incubator. The methods for measurement of the dry weight, chlorophyll concentration of *S. platensis* were established according to the reference. One CO<sub>2</sub> fed batch pulse-feeding technology, which could not only provide the carbon source but also maintain the pH of medium within the range of 9.5-10.5 simultaneously, was developed for the *S. platensis* culture process. Through this technology, the maximum cell concentration achieved was 14g/L within 30 days at the light intensity of 12.3W/m<sup>2</sup>. The duration could be more than one month.

**Keywords:** *S. platensis*; CO<sub>2</sub> Biofixation; photobioreactor; CO<sub>2</sub> fed batch pulse feeding; chlorophyll

## Background:

*S. platensis* are multicellular and filamentous blue-green microalgae belonging to two separate genera *S. platensis* and *Arthrospira*, which consists of about 15 species. Of these, *Arthrospira platensis* is the most common and widely available spirulina which most of the published research and public health decision refers to.

Spirulina is a primitive organism originating from 3.5 billion years ago which has established the ability to utilize carbon dioxide dissolved in seawater as a nutrient source for their reproduction. Spirulina is photosynthesizing cyanophyte (blue-green algae) that grows vigorously in strong sunshine under high temperatures and highly alkaline conditions. It grows in water, can be harvested and processed easily and has significantly high macro- and micronutrient contents.

In many countries of Africa, it is used as human food as an important source of protein and is collected from natural water, dried and eaten. It has gained considerable popularity in the health food industry and in many countries of Asia as protein supplement and human health food.

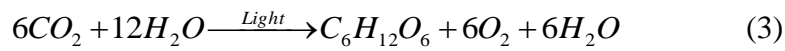
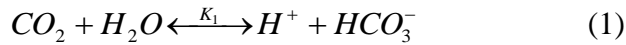
Spirulina has been used as a complementary dietary ingredient of feed for poultry and increasingly as a protein and vitamin supplement to aqua feeds.

An increase in atmospheric CO<sub>2</sub>, derived from brewery industry, poses great challenges to worldwide sustainability. The urgent need for substantive net reductions in CO<sub>2</sub> emissions to the atmosphere can be addressed via biological CO<sub>2</sub> mitigation. Microalgae, such as spirulina, have attracted a great deal of attention for CO<sub>2</sub> fixation and food production because they can convert CO<sub>2</sub> (and supplementary nutrients) into biomass via photosynthesis at much higher rates than conventional biofuel crops can.

In this work, the effect of CO<sub>2</sub> on the growth of *S. platensis* process was studied for the development of the CO<sub>2</sub> fixation process from the brewery waste gas, as well as the design of the photo-bioreactor.

## Theory

There exist two reaction mechanisms in the *S. platensis* culture process, including the CO<sub>2</sub> reversible equilibrium reaction mechanism and photosynthesis mechanism, which were shown as follows:



$$\frac{[H^+][HCO_3^-]}{[CO_2]} = K_1 \quad (4)$$

$$\frac{[H^+][CO_3^{2-}]}{[HCO_3^-]} = K_2 \quad (5)$$

Where,  $K_1 = 4.3 \times 10^{-7}$ ,  $K_2 = 5.6 \times 10^{-11}$  at 25 °C, mol/L

The *S. platensis* can consume the CO<sub>2</sub> molecular inside the solution through the photosynthesis process (equation 3). And then the above reversible chemical reaction equilibriums in the medium will move to the left side (equation 1). Thus, the pH value will increase with time during the whole culture process.

## Material and Methods:

Medium: Zarrouk's medium (based on Raouf et al. Biomass and Bioenergy 30(2006): 537-542)

**Table 1. Media: Zarrouk's medium:**

Chemicals	amount g/L
NaHCO <sub>3</sub>	16.80
K <sub>2</sub> HPO <sub>4</sub>	0.5
NaNO <sub>3</sub>	2.5
NaCl	1.00
MgSO <sub>4</sub> .7H <sub>2</sub> O	0.20
FeSO <sub>4</sub> .7H <sub>2</sub> O	0.01
K <sub>2</sub> SO <sub>4</sub>	1.00
CaCl <sub>2</sub> .2H <sub>2</sub> O	0.04
EDTA	0.08
A <sub>5</sub>	1mL

**Table 2. A<sub>5</sub> micronutrient solution**

A <sub>5</sub> micronutrient solution	Amount g/L
H <sub>3</sub> BO <sub>3</sub> (Boric acid)	2.86
MnCl <sub>2</sub> .4H <sub>2</sub> O	1.81
ZnSO <sub>4</sub> .4H <sub>2</sub> O	0.222
Na <sub>2</sub> MoO <sub>4</sub>	0.0177
CuSO <sub>4</sub> .5H <sub>2</sub> O	0.079

**Temperature:** 30 ± 1 °C,

**Initial pH:** 9.40

**Strain:** *S. platensis*

**Table 3. Strains information:**

Strain No.	Genus	Species	Authority	Former Name	
86.79	Arthrospira	Platensis	Nordstedt Gomont	<i>S. platensis</i>	
Continuous					
Divison	Class	Authentic	Medium	Axenic	Locality
Cyanobacteria	No		Spirul	Bacterial or other types of contamination	Chad Natron lake

**Sale company:** SAG (Sammlung von Algenkulturen Gottingen)

<http://epsag.uni-goettingen.de/cgi-bin/epsag/website/cgi/show-pag.cgi>

Light source: 300W lamp

Light intensity in photoincubator: Distance between light source and culture bottle: totally 88cm (with 30cm water layer and 58cm air layer) .

**Table 4. Light intensity at different experimental positions**

Position of Sensor	400-700nmλ
1 <sup>st</sup> bottle	12.3 W/m <sup>2</sup>
2 <sup>nd</sup> bottle	12.3 W/m <sup>2</sup>

**Waste CO<sub>2</sub> solution:** Solution of NaOH (~4.8 wt %) was used to wash tanks. And dump the brew-waste CO<sub>2</sub> into the NaOH- (~7.95 wt %) carbonate.

## Experimental methods

### Dry weight measurement method

Measure accurately the mass of these 3 aliquots. Take 3 centrifuge tubes, dry at 60°C. Cool in a desiccator and record empty masses. Spin down 3 aliquots, discard clear supernatants. Rinsing the samples by deionized water and then repeats the above procedure. Finally, Dry pellets at 60 °C to constant weight (at least 4 days).

### Chlorophyll assay method:

(i) Fill Ependorf tube with liquid *S. platensis* culture. (ii) Spin down cells using bench centrifuge for 5 min on high rpm (13000rpm). (iii) Carefully remove supernatant and refill tube with methanol. (iv) Shaking vigorously and leave for at least 20 min for chlorophyll extraction. (v) Spin down cell fragments using bench centrifuge for 5 min on high rpm (13000rpm). (vi) Transfer supernatant to 1\*1 cm glass cuvette. (vii) Measure absorbance at 665 and 750nm ( Spectrophotometer, Ultrospec 3300 pro, Amersham Biosciences, UK ) , if sample is too concentrated dilute it. (viii) Calculate chlorophyll concentration:

$$[\text{Chl}] (\text{Microgram/mL}) = 13.42 * (A_{665} - A_{750}) * V_{\text{methanol}} / V_{\text{sample}}. \quad (6)$$

Where, [Chl] is the concentration of chlorophyll in the sample, microgram/mL; A<sub>665</sub> and A<sub>750</sub> are the absorbance of sample at 665nm and 750nm.

V<sub>methanol</sub> is the volume of methanol; V<sub>sample</sub> is the volume of the sample.

All data of this experiment are repeated three times with repeatability error less than 10%.

### pH measurement method:

(i) Fill Ependorf tube with liquid *S. platensis* culture. (ii) Spin down cells using bench centrifuge for 5 min on high rpm (13000rpm). (iii) Carefully remove supernatant into universals and then measure the pH value by the pH meter (pH211 Microprocessor, pH Meter, HANNA instrument, UK).

### Experimental apparatus:

Figure1 shows the experimental apparatus for the experiments. Certain volume of *S. platensis* was inoculated into two 500ml glass bottles (9×5×17cm) in a fish tank. One light

source could provide the light for the photosynthesis. Air/CO<sub>2</sub> was input into the glass bottles by air pump or through cylinder

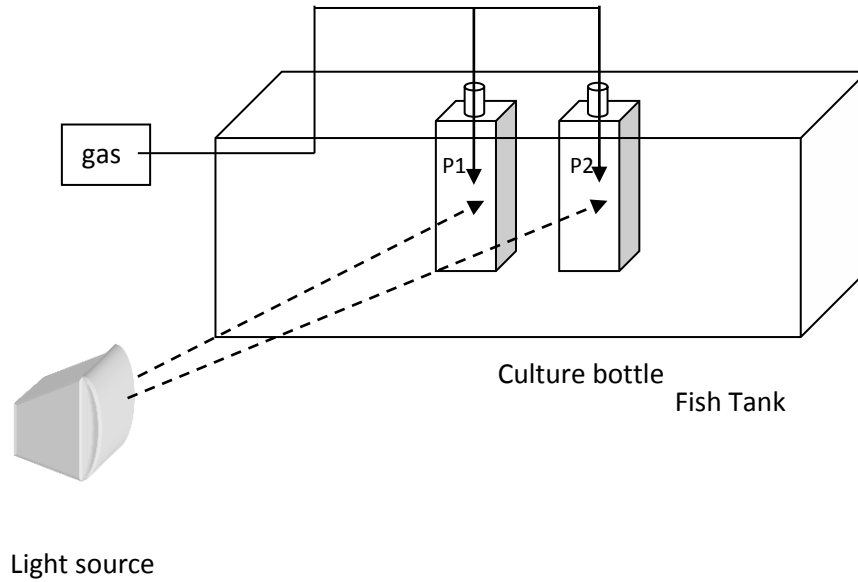
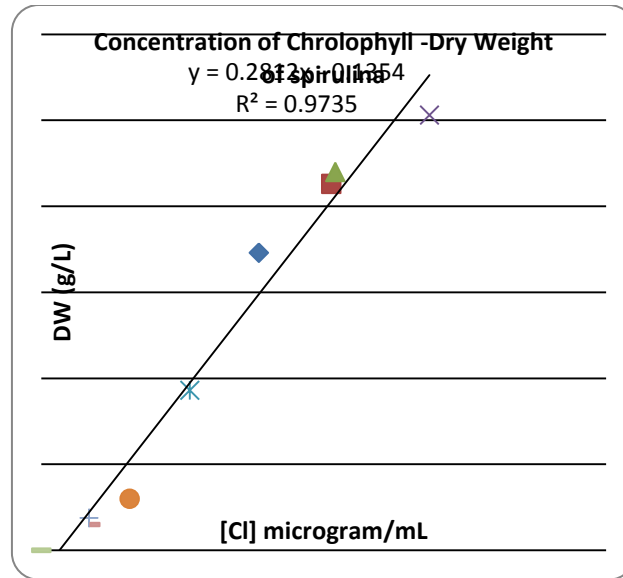


Figure 1. Experimental apparatus for the culture of *S. platensis* in the laboratory photoincubator.

## Experimental Results

### 1 The relationship between dry weight of *S. platensis* and concentration of Chlorophyll.

The experiments were carried out to determine the relationship between the dry weight of *S. platensis* and concentration of Chlorophyll for the culture under the Z-medium. Measure the dry weight of *S. plantensis* and the concentration of Chrolophyll during the culture process of non-gas bubbling culture.



**Figure 2. The relationship between dry weight of *S. platensis* and concentration of Chlorophyll**

Figure 2 shows the relationships between dry weight of *S. platensis* and concentration of chlorophyll. When the range of the average dry weight is between 0-3g/L, the following formula is obtained:

$$Y(\text{DW g/L}) = 0.281 * X([\text{Cl}] \text{ microgram/mL}) - 0.135 \quad (7)$$

Where, X is the concentration of chlorophyll (microgram/mL), Y is the average dry weight of *S. platensis* g/L.

**2 The effects of air bubbling on the growth *S. platensis* culture in laboratory photo incubator.**

The experiments were carried out to determine the importance of CO<sub>2</sub> bubbling for the culture under the Z-medium. Air bubbling culture experiments were carried out under the condition of the (1)24h light, 25ml (concentration 1.53g/L DW) inoculation, 250mL total volume.(2) air bubbling, 24h lighting, 7ml (concentration 1.53 g/L DW) inoculation, 250mL total volume. (3) non-air bubbling culture, 24h lighting, 25ml (concentration 1.53g/L DW) inoculation, 250mL total volume at position 1 and position 2, respectively.

## 2.1 The growth curves of *S. platensis* at different positions of photobioreactor.

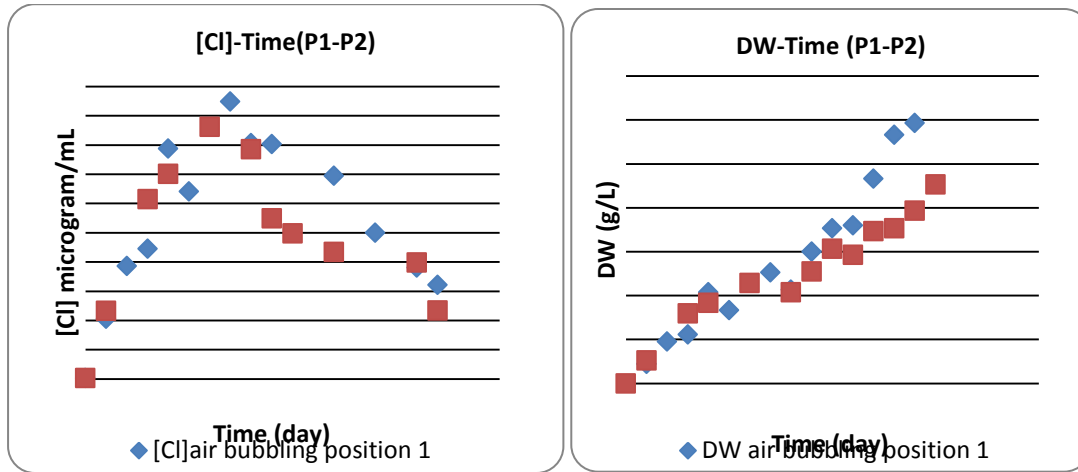


**Figure 3. Growth curves of *S. platensis* at position 1 and position 2 in the bioreactor.**

From the figure3, it is known that the two growth curves between position 1 and position 2 were similar under the condition of the air-bubbling culture. It seems that the dry weight of *S. platensis* at position1 are little higher than that of position 2 after the 12rd days culture, which maybe because of the difference in the air flowrates at these two positions. The effects of air flowrates on the growth of *S.platensis* should be investigated in the future. By the way, the concentration of chlorophyll decreased when the dry weight of *S. platensis* beyond 2-3 g/L.

## 2.2 The growth curves of *S. platensis* under condition of the bubbling and non-bubbling culture.

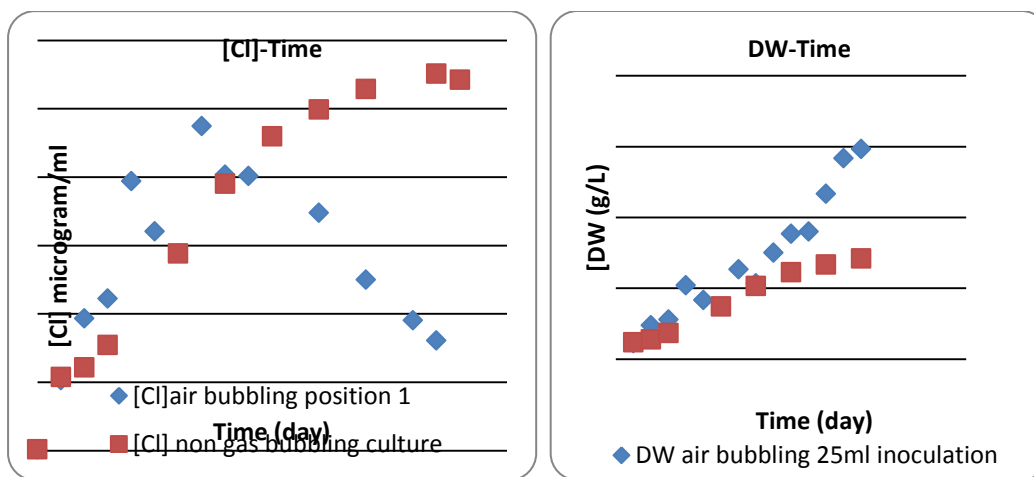


**Figure 4. The growth curve of *S. platensis* under the bubbling and non-bubbling conditions**

The figure 4 shows that the average dry weights under bubbling condition are higher than those under non-bubbling condition. Especially, the maximum concentration of bubbling is much higher than that of non-bubbling. It is mainly because the bubbling of gas could provide the internal mixing, which avoids nutrient concentration gradients. Moreover, the gas bubbling could also promote the exposure of all cells to light (especially in high density cultures), while minimizing self-shading and phototoxicity. Both the pH changed from 8.40 to 10.4 at these two different experiments within the 18 days.

However, the concentration of chlorophyll decreases when the dry weights reach about 2-3g/L after the 7 days' culture and why?

Otherwise, what is the reason that leads to the difference between the air bubbling and non-bubbling growth? More reasons should be considered, for example carbon dioxide supply, mixture, and pH adjustment etc.

### 2.3 The growth curves of *S. platensis* under the conditions of air bubbling at different inoculation volumes

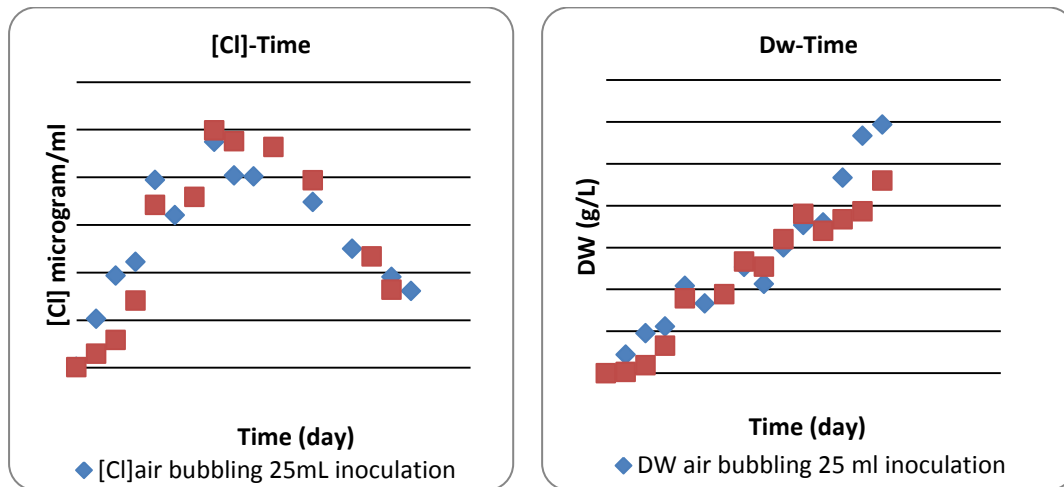


**Figure 5. The growth curves of *S. platensis* under the air-bubbling culture at 25ml and 7ml inoculation.**

From the figure 5, it is known that the two growth curves between 25ml and 7 ml inoculation are almost similar at whole process of the experiments under the condition of the air-bubbling culture. That means these two inoculation volumes would not affect the final growth results. However, the concentration of chlorophyll also decreases when the dry weights exceed 2-3 g/L.

According to the results shown in figure 3, 4, and 5, it seems that the concentration of chlorophyll could demonstrate the growth curve of the *S. platensis* well at low concentration of *S. platensis* (less than 3g/L). However, when the concentration of *S. platensis* reach a high level (more than 3g/L), the concentration of chlorophyll would decrease with the growth time, which might be due to self-shading of the high concentration of *S. platensis* that blocked the light to those algae cells inside the incubator to synthesize the chlorophyll.

### 3 The effects of CO<sub>2</sub> concentration on the growth of *S. platensis* experiments

#### 3.1 Effects of gas bubbling, which contains only N<sub>2</sub> and O<sub>2</sub>, on the growth of *S. platensis*

The experiments were carried out to determine the importance of CO<sub>2</sub> concentration for the culture under the Z-medium. The air was bubbling into NaOH solution and then into one culture bottles at position 1. One non-air bubbling culture was the control at position 2.

The dry weights of *S. priulina* during non-CO<sub>2</sub> bubbling culture process were shown in figure 6.

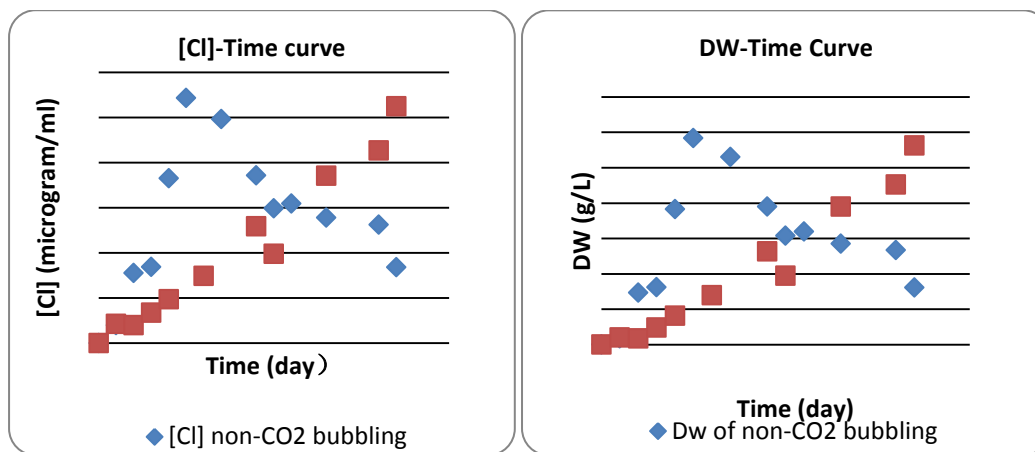


**Figure 6. The growth curve of *S. platensis* under the non-CO<sub>2</sub> bubbling culture and the control**

From the results of figure 6, it is shown that the dry weight of *S. platensis* under non-CO<sub>2</sub> bubbling culture increase within 5-6 days culture, and then decrease, which are different with that of air-bubbling culture. At this phrase, the *S. platensis* can consume the carbonate in medium, together with the higher mass transfer rate and mixing from the gas bubbling. The reason is mainly because the consumption of carbonate, which could lead to the increase of the pH value in medium, see fig 7. The pH of non-CO<sub>2</sub> bubbling culture increased from 9 to 12, which is higher than that of non-air bubbling culture. The growth of *S. platensis* will stop and the cells will be dead and broken under

this high pH condition. And then the pH decrease from 12 to 11 at the last phrase of culture. During all this process, the color of culture solution changed from green to yellow. By the way, because the concentration of *S. platensis* is low (less than 2.5 g/L), the tendency of the chlorophyll concentration is in consisting with that of dry weight of *S. platensis*.

According to the reference, photosynthesis is a reversible set of reactions, and excessive dissolved oxygen, DO (i.e. >35 mg/l), can inhibit the metabolic process of algae. In this experiment, just the nitrogen and oxygen were introduced into the cultural bottle, the accumulated DO is difficult to be stripped from medium. The results show that too much O<sub>2</sub> might be severely inhibit the the growth of *S. platensis*. The effect of O<sub>2</sub> concentration on the growth of *S. platensis* should be investigated in the near future.

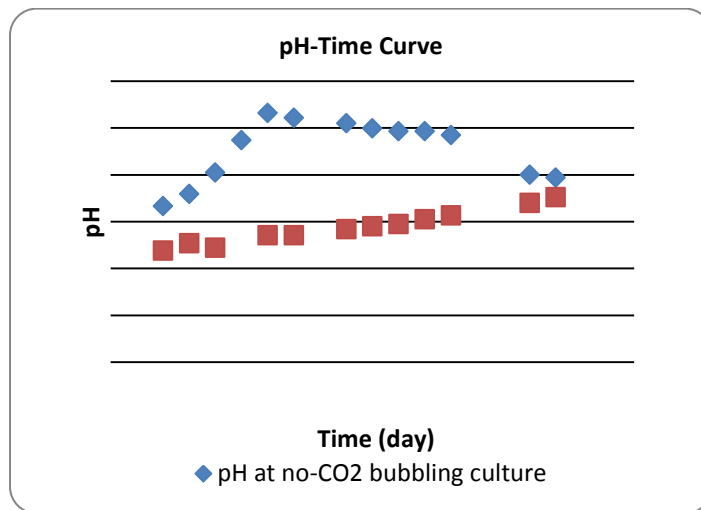


**Figure 7. The pH-time Curve of *S. platensis* under the non-CO<sub>2</sub> bubbling culture and the control**

It seems that CO<sub>2</sub> bubbling is very important as the carbon source, pH buffering, mixing and mass transfer for the growth of *S. platensis*. In addition, too much O<sub>2</sub> could also inhibit the growth of *S. platensis*.

### 3.2 Effects of continuous pure CO<sub>2</sub> bubbling on the growth of *S. platensis*

The experiments were carried out to determine the effect of the pure CO<sub>2</sub> on the growth of *S. platensis* growth process under the Z-medium. The pure CO<sub>2</sub> was bubbling into one culture bottles at position 1. One non-air bubbling culture was as control at position 2.

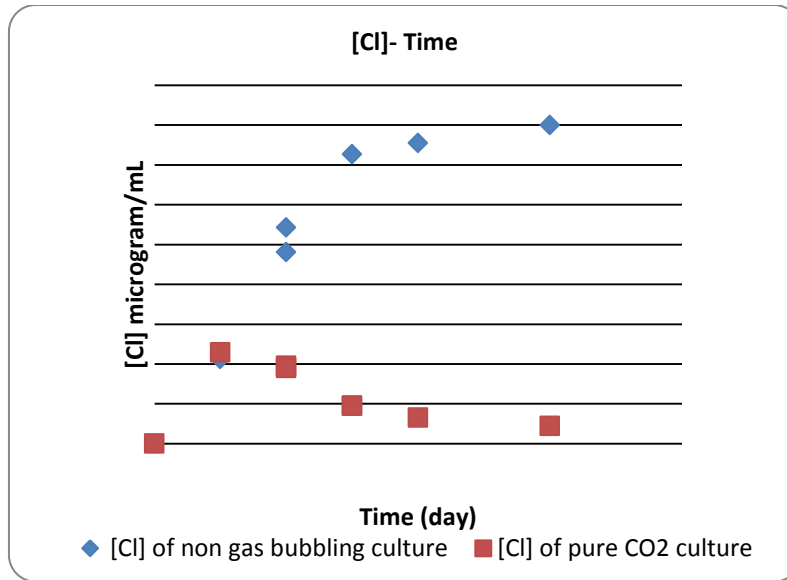


Figure 8. Growth curves of *S. platensis* under pure CO<sub>2</sub> continuous culture and the control

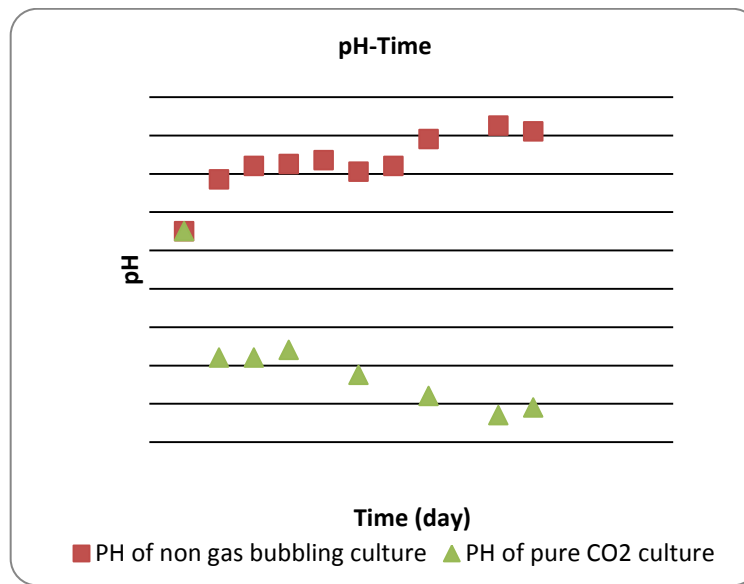


Figure 9. pH curves of *S. platensis* under pure CO<sub>2</sub> continuous culture and the control

The result of pure CO<sub>2</sub> continuous culture of *S. platensis* was shown in figure 8. Compared to the results of non-air bubbling culture, it seems that only small amount of *S. platensis* was produced at the first two days. And then, the concentration of chlorophyll of *S. platensis* decreased with the whole growth process just 6days. The reason might because the pH of medium became as low as 8.4 see figure9, which resulted from the continuous pure CO<sub>2</sub> bubbling. It also might be the change of the osmotic pressure and salinity of medium during this process. That means too much CO<sub>2</sub> would be harmful for the growth of *S. platensis*.

### 3.3 Effects of pure CO<sub>2</sub> fed batch pulse-feeding on the growth of *S. platensis*

The experiments were carried out to determine the effect of the pure CO<sub>2</sub> fed batch pulse-feeding culture on the growth of *S. platensis* growth process based on the pH adjusting strategy.

At first, pure CO<sub>2</sub> was also input into the non-air bubbling culture bottle to adjust the pH of the medium to about 8.0. And then the air was bubbling into culture bottle with pure CO<sub>2</sub> fed batch pulse-feeding to maintain the pH at the range of 9.5-10.5. One non-air bubbling culture bottle was as control.

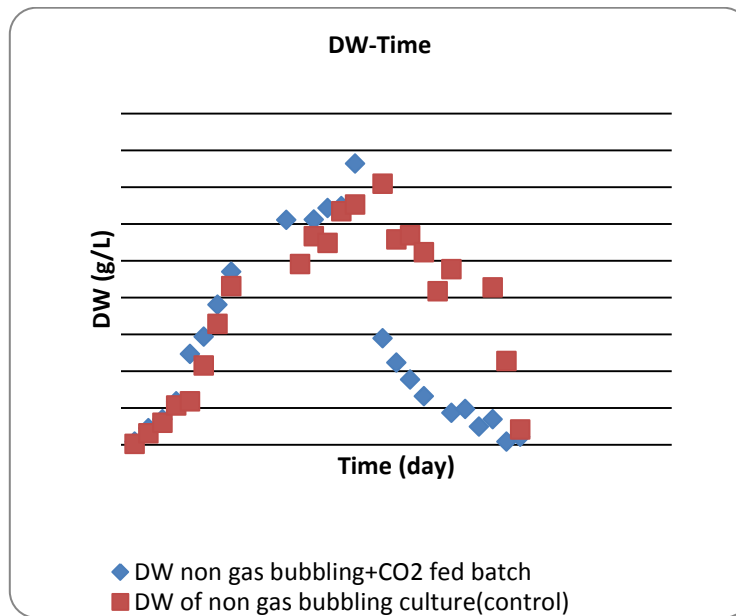
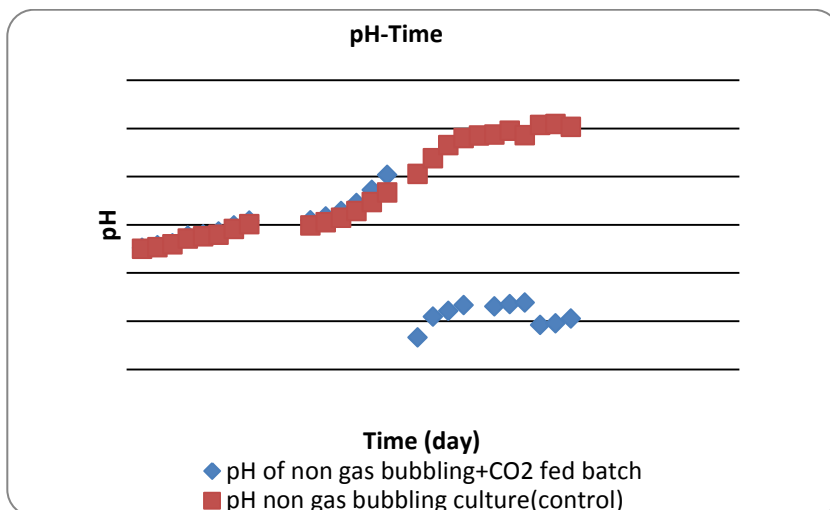
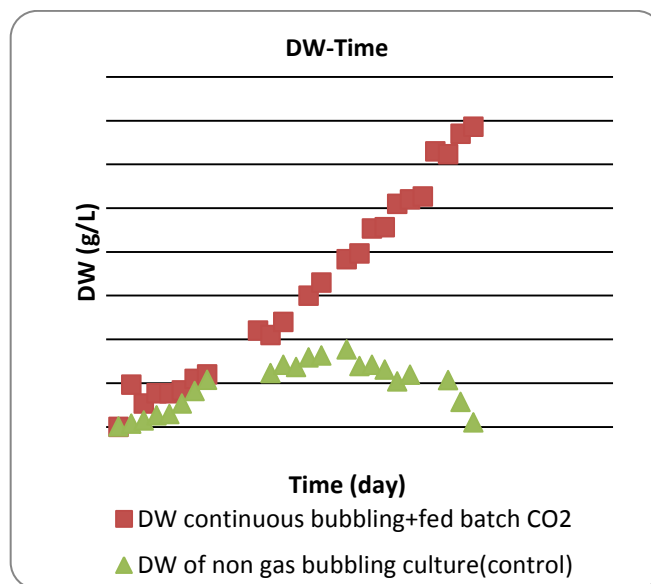


Figure 10. The growth curve of *S. platensis* under the non-gas bubbling+ fed batch CO<sub>2</sub> culture and the control



**Figure 11. The pH curve of *S. platensis* under the non-gas bubbling+ fed batch CO<sub>2</sub> culture and the control**

Figure 10 shows the growth curve of *S. platensis* under the non-air bubbling culture process. The dry weight of *S. platensis* increased firstly, and then decreased when the pH of the solution reached 12, see figure 10 and 11. That means pH value should not exceed 11 for the *S. platensis* culture. However, the DW of *S. platensis* decreased more quickly when the pH value was decreased and maintained at low as 8 by pure CO<sub>2</sub> fed batch culture. That means there is a greater negative impact of pH 8 on the growth of *S. platensis* than that of pH 12. Thus, the pH of the solution should be maintained between the ranges of 8-11.



**Figure12. The growth curve of *S. platensis* under the air continuous bubbling + CO<sub>2</sub> fed batch pulse-feeding culture and the control**

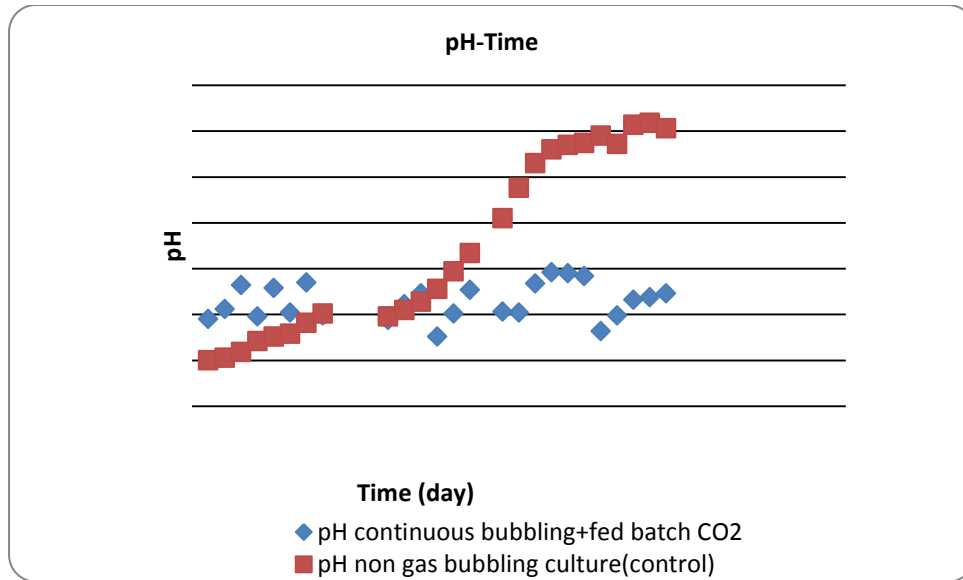


**Figure13. The pH curve of *S. platensis* under the continuous air bubbling + CO<sub>2</sub> fed batch pulse-feeding culture and the control**

Figure 13 shows that the continuous air bubbling culture with CO<sub>2</sub> fed batch pulse-feeding could maintain the pH within 9.5-10.5. It seems that the *S. platensis* grows well under these conditions with DW reached 14g/L at 29th day, see figure 12. The growth period could last for more than one month. That means it is effective to control the growth of *S. platensis* by CO<sub>2</sub>-pH adjusting strategy. Air bubbling could provide internal mixing and promote the exposure of all cells to the light, especially in the high density cultures process. CO<sub>2</sub> pulse feeding could control the pH and provide the carbon source by assuring dissolution of CO<sub>2</sub> and avoid gradients thereof; and also strip the accumulated DO, hence reducing its toxicity to *S. platensis*.

### **3.4 The effect of the reaction products of CO<sub>2</sub> and sodium hydroxide on the growth of *S. platensis*.**

Sodium carbonate was taken place by the reaction products of CO<sub>2</sub> and sodium hydroxide in one cultural bottle. One non-air bubbling cultural bottle was as control.

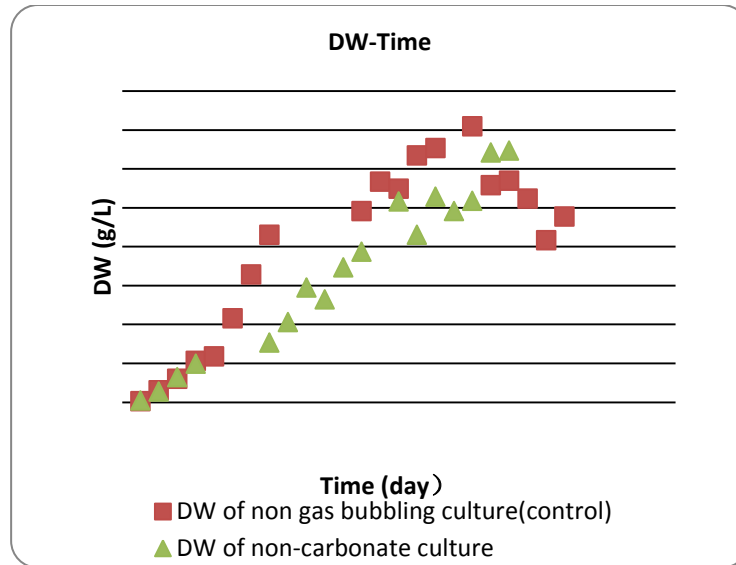


Figure14. The growth curve of *S. platensis* non-carbonate and carbonate culture

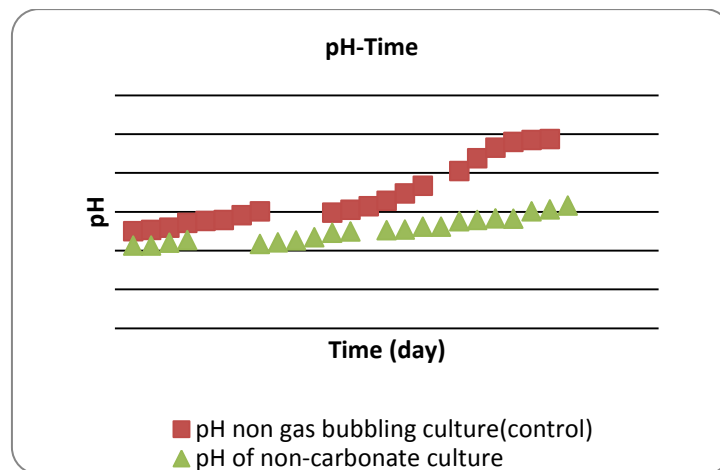


Figure 15. The pH curve of *S. platensis* non-carbonate and carbonate culture

What will happen when the sodium carbonate was taken place by the reactant product of sodium hydroxide and carbon dioxide? According to the figure 14, it seems that the growth curves of non-air bubbling culture under these two conditions were almost the similar. However, the pH values under non-carbonate culture changed slower than those of carbonate culture. That means that non-carbonate culture has greater buffering capacity than that of carbonate culture, see figure 15. Therefore, non-carbonate culture has certain advantage over the carbonate culture process.

### 3.5 Waste CO<sub>2</sub> from brewery factory culture

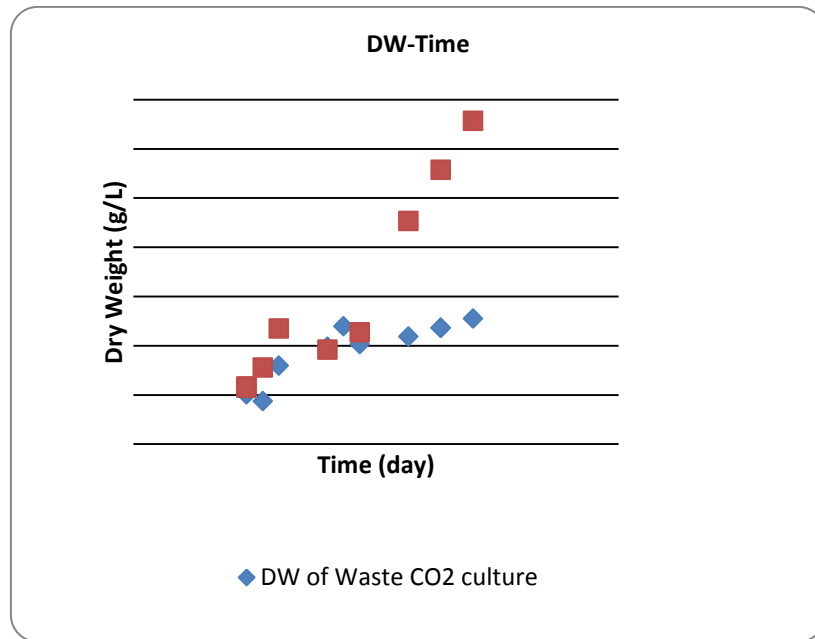


Figure 16 The growth curve of *S. platensis* in waste CO<sub>2</sub> solution culture

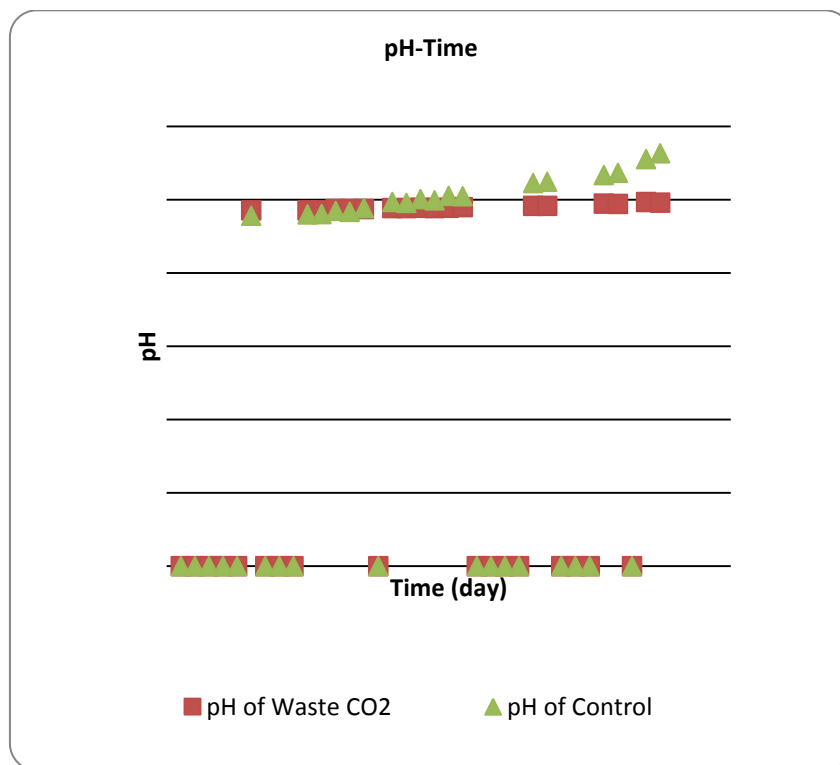


Figure 17. The pH curve of *S. platensis* in waste CO<sub>2</sub> solution culture

According to the concentration of carbonate and the initial pH of Z-medium, the waste CO<sub>2</sub>–NaOH mixture solution from brewery factory was used for the culture of Spirulina. It seems that the growth rate of spirulina in the waste CO<sub>2</sub> solution was slower than that in control, see figure 16. During the growth process, the pH of the waste CO<sub>2</sub> solution increased slower than that in the control, see figure 17. These results show that some chemicals in the waste CO<sub>2</sub> –NaOH mixture solution might inhibit the growth of Spirulin. More research work should be done to know why and how to control it. The training of the Spirulina should also be carried out to accustom the waste-CO<sub>2</sub> environment.

### **Discussion:**

The CO<sub>2</sub> bubbling could be the carbon source, pH buffering, mixing and mass transfer during the *S. platensis* growth process. Therefore, the *S. platensis* culture density could be higher under air-bubbling culture than that of non-air bubbling culture process.

The growth rates of air without CO<sub>2</sub> bubbling culture process can be significantly faster than those of non-air bubbling culture process. However, the duration of the former was shorter than the later. This is mainly due to the CO<sub>2</sub> in medium could be consumed by the *S. platensis* for its growth. The CO<sub>2</sub> gradually depleted under the non-CO<sub>2</sub> air bubbling culture process, as well as the rapid increase in pH value, which will result in the deterioration of culture environment. It is mainly due to the high efficiency of mass transfer and mixing under gas bubbling process, which enhance the growth rate of *S. platensis* and the consumption of a large amount of CO<sub>2</sub>. With the movement of equilibrium of CO<sub>2</sub> in the medium, the more H<sup>+</sup> consumed, the higher pH increased. In addition, large amount of CO<sub>2</sub> in medium were entrained by the non-CO<sub>2</sub> air bubbling culture due to the low partial pressure of CO<sub>2</sub> in the gas. All these reasons lead to the pH of the medium increased as high as 12. The deterioration of culture environment makes the growth of *S. platensis* terminated rapidly.

The carbon source in medium could be provided by the addition of pure CO<sub>2</sub> gas. On the other hand, the CO<sub>2</sub> equilibrium reaction in the medium could also be adjusted. The *S. platensis* could continue to grow under a favorable cultural environment through control the pH of 9.5-10.5 in medium.

Increased concentration of carbon source can promote the production rate of *S. platensis*. However, it is found that too high concentration of CO<sub>2</sub> could be harmful to the *S. platensis*, which maybe because of the change of the osmotic pressure and salinity in the medium. In addition, too

high concentration of CO<sub>2</sub> could drop the pH to very low level, which would be not conducive to the growth of *S. platensis*. Furthermore, the fluid shear stress from high ventilation would also do some harmful to the growth of *S. platensis*, especially the at the first one or two days of culture.

The results also proved that carbon dioxide and sodium hydroxide reaction products can replace the carbonate in medium, but also makes the solution to maintain a certain buffer capacity.

During the cultural process, the medium could be adjusted by the fed batch CO<sub>2</sub> pulse feeding technology to maintain the pH value within 9.5-10.5. Through the above measures, one *S. platensis* production process with high density and long growth cycle can be achieved.

In summary, it seems that gases introduced into cultural bottles could serve a number of purpose in *S. platensis* cultivation, including: (i) supply of CO<sub>2</sub> as sources of carbon for biomass primary and secondary metabolism; (ii) provision of internal mixing, which avoids nutrient concentration gradients; (iii) promotion of exposure of all cells to light (especially in high density cultures), while minimizing self-shading and phototoxicity; (iv) control of pH by assuring dissolution of CO<sub>2</sub> and avoid gradients thereof; and (v) stripping of accumulated DO, hence reducing its toxicity to *S. platensis*.

## Conclusions

1 The *S. platensis* growth curve can be obtained through tracking the concentration of chlorophyll. However, when the concentration of *S. platensis* became higher, this method has higher errors. The concentration of chlorophylls decreased with the increase of *S. platensis* concentration because of the self-shading among the *S. platensis* cells. The dry weight of *S. platensis* is effective at the higher concentration of *S. platensis*. Therefore, dry weight method and concentration of chlorophyll measurement should be integrated for the determination of the *S. platensis* growth curve.

2 Under the air bubbling and non-air bubbling non-gas bubbling conditions, the *S. platensis* can grow well. Moreover, the growth rates and concentration at air bubbling condition are higher than that of non-gas bubbling bubbling. However, both too high and too low CO<sub>2</sub> concentration will be harmful for the growth of the *S. platensis*. The growth characteristics of the *S. platensis* could be adjusted by CO<sub>2</sub> fed batch pulse feeding technology, which could result in the high concentration and long duration for the *S. platensis* culture.

3 The reaction products between CO<sub>2</sub> and NaOH could take the place of commercial carbonate, and also have a certain buffer capability for the culture process of *S. platensis*.

## Challenges and research needs:

Enhanced CO<sub>2</sub> level (typically well above its atmospheric level) are needed for efficient *S.platensis* growth and metabolism, and currently are major contributors to the overall cost of *S.platensis* cultivation. However, different sources of CO<sub>2</sub> and supplementary nutrients will greatly improve the overall environmental performance of *S.platensis* production. Future research should explore existing sources, such as CO<sub>2</sub> from brewery plants, for the growth of *S.platensis*.

## References:

1 Amit Kumar, Sarina Ergas, Xin Yuan, Ashish Sahu, Qiong Zhang, Jo Dewulf, F. Xavier Malcata, Herman van Langenhove, Enhanced CO<sub>2</sub> fixation and biofuel production via microalgae: recent developments and future directions, Trends in Biotechnology, 28(2010): 371-380.

2 D. Soletto, L.Binaghi, L. Ferrari, A.Lodi, J.C.M. Carvalho, M.Zilli, A. CXonverti, Effects of carbon dioxide feeding rate and light intensity on the fed-batch pulse-feeding cultivation of *Spirulina platensis* in helical photobioreactor, Biochemical Engineering Journal, 39 (2008): 369-375.

3 Amit Kumar, Xin Yuan, Ashish K Sahu, Jo Dewulf, Sarina J Ergas and Herman Van Langenhove, A hollow fiber membrane photo-bioreactor for CO<sub>2</sub> sequestration from combustion gas coupled with wastewater treatment: A process engineering approach, J Chem. Technol. Biotechnol. 2010, 85: 387-394.

4 Raquel Pedrosa Bezerra, Erika Yuliana Ortiz Montoya, Sunao Sato, Patrizia Petego, Joao Carlos Monteiro de Carvalho, Attilio Converti, Effects of light intrnsity and dilution rate on the semicontinuous cultivation of *Arthriospira (Spirulina) platensis*. A kinetic Monod-type approach, Bioresource Technology, 102 (2011), 3215-3219

5 Xin Yuan, Amit Kumar, Ashish K. Sahu, Sarina J. Ergas, Impact of ammonia concentration on *Spirulina platensis* growth in an airlift photobioreactor, Bioresource Technology, 102(2011): 3234-3239.

6 John W. Slocum JR., Roy Foster, Mike Mcguire, Wendy Conder, Robyn Frazer, John Ross, Elthon Corradini, David Lei, Stan Scott, Fermentation in the China Beer Industry, Organizational Dynamics, 2006,35(1): 32-48.

7 Feiyan Xue, Jinxin Miao, Tianwei Tan, A new strategy for liquid production by mix cultivation of *Spirulina platensis* and *Rhodotorula glutinis*, Appl. Biochem. Biotechnol. (2010)160; 498-503.

8 M. Ahsan B. Habib, Mashuda Parvin, Tim C. Huntington, Mohmmad R. Hasan, A review on culture, production and use of spirulina as food for humans and feeds for domestic animals and fish. FAO Fisheries and Aquaculture Circular No. 1034, Food and Agriculture organization of the United Nations, Rome 2008.

9 A teching module for the production of spirulina, Antenna Technologies, [www.antenna.ch](http://www.antenna.ch)

10 Feng Dao-lun, Wu Zu-cheng, Culture of Spirulina platensis in human urine for biomass production and O<sub>2</sub> evolution, Journal of Zhejiang University SCIENCE B, 2006 7(1):34-37

11 P. Kaushik, Abhishek Chauhan, In Vitro antibacterial activity of laboratory grown culture of Spirulina platensis, Indian J. Microbiol. (September 2008)48: 348-352.

12 H.Y. Lee, L.E. Erickson, S.S. Yang, Kinetics and bioenergetics of light-limited photoautotrophic growth of Spirulina platensis, Biotechnology and Bioengineering, 1987,29:832-843.

13 L. Tomaselli, G. Boldrini, M.C. Margheri, Physiological behavior of Arthrospira(Spirulina) maxima during acclimation to changes in irradiance, Journal of Applied Phycology, 1997,9:37-43.

14 A.M. Abo-Shady, S.M. Abou-Ei-Souod, Abd. Ei-Raheem, R.Ei-Shanshoury, Y.A.G. Mahmoud, Protophasts from the cyanobacterium Spirulina platensis, World Journal of Microbiology and Biotechnology, 1992,8,385-586.

15 Pierre H Ravelonandro, Dominique H Ratianarivo, Claire Joannis-Cassan, Arsene Isambert and Marson Raherimandimby, Influence of light quality and intensity in the cultivation of Spirulina platensis from Toliara (Madagascar) in a closed system, Journal of Chemical Technology and Biotechnology, 2008, 83: 842-848.

16 Basirath Raof, B.D. Kaushik, Radha Prasanna, Formulation of a low-cost medium for mass production of Spirulina, Biomass and Bioenergy, 30(2006); 537-542.

17 Carvalho, A.P. et al. (2006) Microalgal reactors: a review of enclosed systems design and performances. Biotechnol. Prog. 22, 1490-1506.

**Two photos of experiment bottles:**



## IX. REFERENCES

1. IPCC, 2011: *Summary for Policymakers. In: IPCC Special Report on Renewable Energy Sources and Climate Change Mitigation*, R.P.-M. O. Edenhofer, Y. Sokona, K. Seyboth, P. Matschoss, S. Kadner, T. Zwickel, P. Eickemeier, G. Hansen, S. Schlömer, C. von Stechow, Editor 2011, Cambridge University Press, Cambridge, United Kingdom and New York, NY, USA.
2. Blanchette Jr, S., *A hydrogen economy and its impact on the world as we know it*. Energy Policy, 2008. **36**(2): p. 522-530.
3. Davis Mike, B.F., Nemanich Gene, Katsaros Art, Ogden Joan, Niedzwiecki Alan, Serfass Jeff, *National hydrogen energy roadmap*, 2002, US Department of energy. p. 1-58.
4. Mandal TK, G.D., *Hydrogen: a future energy vector for sustainable development*. J Mech Eng Sci, 2009. **224**: p. 539-558.
5. *Climate Change 2007: Synthesis Report*, R.K.a.R. Pachauri, A. , Editor 2007, IPCC, Geneva, Switzerland.
6. Stern, N., *The economics of climate change*, 2006, HM Treasury; UK. p. 700.
7. James T. Randerson, M.V.T., Thomas J. Conway, Inez Y. Fung and Christopher B. Field, *The contribution of terrestrial sources and sinks to trends in the seasonal cycle of atmospheric carbon dioxide*. GLOBAL BIOGEOCHEMICAL CYCLES, 1997. **11**(4): p. 535-560.
8. C.D. Keeling, T.P.W., M.Wahlen and J. van der Plicht, *Interannual extremes in the rate of rise of atmospheric carbon dioxide since 1980*. Letters to Nature, 1995. **375**(22): p. 666-670.
9. Dr. Pieter Tans and Dr. Ralph Keeling, S.I.o.O.s.u.e. *Trends in atmospheric carbon dioxide*. 2011 [cited 2011 July]; Available from: <http://www.esrl.noaa.gov/gmd/ccgg/trends/>.
10. Glikson, D.A., *BEYOND 2 DEGREES CELSIUS*, 2011, Earth and paleoclimate science Australian National University. p. 1-9.
11. M Meinshausen, S.J.S., K. Calvin, J.S. Daniel, M.L.T. Kaihuma, J-F Lamarque et al., *The RCP GHG concentrations and their extensions from 1765 to 2300*, 2010. p. 48.
12. Wuebbles, D.J. and K. Hayhoe, *Atmospheric methane and global change*. Earth-Science Reviews, 2002. **57**(3-4): p. 177-210.
13. Agency, U.S.E.P., *Municipal solid waste in the United States: 2009 facts and figures*, 2010, Environmental protection agency (EPA).
14. Reichel, P.K.a.A., *THE EUROPEAN ENVIRONMENT STATE AND OUTLOOK 2010 MATERIAL RESOURCES AND WASTE*, 2010, European Environment Agency.
15. EST. *Your impact on climate change*. 2008.
16. Bates, B.C., Z.W. Kundzewicz, S. Wu and J.P. Palutikof, *Climate Change and Water*, T.P.o.t.I.P.o.C. Change, Editor 2008, IPCC Secretariat, Geneva. p. 210 pp.
17. Olsson, M., *Wheat straw and peat for fuel pellets--organic compounds from combustion*. Biomass and Bioenergy, 2006. **30**(6): p. 555-564.
18. Matsumura, Y., T. Minowa, and H. Yamamoto, *Amount, availability, and potential use of rice straw (agricultural residue) biomass as an energy resource in Japan*. Biomass & Bioenergy, 2005. **29**(5): p. 347-354.
19. Thaddeus Ezeji, Nasib Qureshi, and Hans P. Blaschek, *Butanol production from agricultural residues: Impact of degradation products on <I>Clostridium beijerinckii</I> growth and butanol fermentation*. Biotechnology and Bioengineering, 2007. **97**(6): p. 1460-1469.
20. Daniel J. Schell, N.D.H., Karel Grohmann and Ali Mohagheghi, *Changes in physical and chemical properties of pretreated wheat straw during hydrolysis with cellulose*. Biotechnology letters, 1989. **11**(10): p. 745-748.

21. Tang, D.-S., et al., *Recovery of protein from brewer's spent grain by ultrafiltration*. Biochemical Engineering Journal, 2009. **48**(1): p. 1-5.
22. Aliyu, S., Bala, Muntari, *Brewer's spent grain: A review of its potentials and applications*. African Journal of Biotechnology, 2011. **10**(3): p. 324-331.
23. Mussatto, S.I. and I.C. Roberto, *Chemical characterization and liberation of pentose sugars from brewer's spent grain*. Journal of Chemical Technology & Biotechnology, 2006. **81**(3): p. 268-274.
24. Goldemberg, J., *The Brazilian biofuels industry*. Biotechnology for Biofuels, 2008. **1**(6).
25. Levis, J.W., et al., *Assessment of the state of food waste treatment in the United States and Canada*. Waste Management, 2010. **30**(8-9): p. 1486-1494.
26. Ruihong Zhang, H.M.E.-M., Karl Hartman, Fengyu Wang, Guangqing Liu, Chris Choate, Paul Gamble, *Characterization of food waste as feedstock for anaerobic digestion*. Bioresource Technology, 2007. **98**: p. 929-935.
27. Scharff, H., A. van Zomeren, and H.A. van der Sloot, *Landfill sustainability and aftercare completion criteria*. Waste Management & Research, 2011. **29**(1): p. 30-40.
28. *Waste and recycling*. 2011; Available from: <http://www.defra.gov.uk/environment/economy/waste>.
29. (EIA), U.S.E.I.A., *Annual Energy Outlook 2011 with Projections to 2035*, 2011, U.S. Department of Energy.
30. (DECC), U.D.o.e.a.c.c. *Energy sector statistics*. 2010 [cited 2011 July]; Available from: [http://www.decc.gov.uk/en/content/cms/statistics/energy\\_stats/energy\\_stats.aspx](http://www.decc.gov.uk/en/content/cms/statistics/energy_stats/energy_stats.aspx).
31. Staniford, S. *The oil drum*. 2008; Available from: [www.theoil drum.com/node/3636](http://www.theoil drum.com/node/3636) <<http://www.theoil drum.com/node/3636>>.
32. BP. *BP Statistical Review of World Energy*. 2010 [cited 2011 15 July 2011]; Available from: [www.bp.com/statisticalreview](http://www.bp.com/statisticalreview).
33. IPCC, S.f.P.I.I.S.R.o.R.E.S.a.C., et al.
34. WRAP, *Gate fees report 2010: Comparing the cost of alternative waste treatment options*, 2010, Waste & Resources Action Programme (WRAP).
35. HyWays, *The european hydrogen roadmap*. [www.Hyways.de](http://www.Hyways.de), 2007.
36. Armaroli, N. and V. Balzani, *The Hydrogen Issue*. ChemSusChem, 2011. **4**(1): p. 21-36.
37. Stolten, D., *Hydrogen and fuel cells: Fundamentals, technologies and applications.*, ed. Wiley-VCH2010, Weinheim: Wiley-VCH Verlag GmbH & Co. KGaA.
38. Duu-Hwa Lee, D.-J.L., *Biofuel Economy and Hydrogen Competition*. *Energy & Fuels*, 2008. **22**(1): p. 177-181.
39. Tseng, P., John Lee, Paul Friley, *A hydrogen economy: opportunities and challenges*. Journal of energy, 2005. **30**: p. 2703-2720.
40. Shrikant A. Bhat, J.S., *Process intensification aspects for steam methane reforming: An overview* AIChE Journal, 2009. **55**(2): p. 408-422.
41. Tong, J., et al., *Thin and dense Pd/CeO<sub>2</sub>/MPSS composite membrane for hydrogen separation and steam reforming of methane*. Separation and Purification Technology, 2005. **46**(1-2): p. 1-10.
42. Levie, R.d., *The electrolysis of water*. Journal of Electroanalytical Chemistry, 1999. **476**: p. 92-93.
43. Holladay, J.D., et al., *An overview of hydrogen production technologies*. Catalysis Today, 2009. **139**(4): p. 244-260.
44. EERE, *Biomass a multi year program plan*, 2011, US department of energy (DOE).
45. Perlack R.D., L.L.W., Anthony F. Turhollow, Robin L. Graham, Bryce J. Stokes, Donald C. Erbach, *Biomass as Feedstock for a Bioenergy and Bioproduct industry: The Technical Feasibility of a Billion-Ton Annual Supply*. 2005.
46. Sun Ye, C.J., *Hydrolysis of lignocellulosic materials for ethanol production: a review*. Bioresource Technology, 2002. **83**: p. 1-11.

47. Kun Niu, P.C., Xu Zhang and Wen-Song Tan, *Enhanced enzymatic hydrolysis of rice straw pretreated by alkali assisted with photocatalysis technology*. J Chem Technol Biotechnol 2009. **84**: p. 1240-1245.
48. P. Alvira, E.T.-P., M. Ballesteros, M.J. Negro *Pretreatment technologies for an efficient bioethanol production process based on enzymatic hydrolysis: A review*. Bioresource Technology, 2010. **101**: p. 4851–4861.
49. Demirbas, A., *Biomass resource facilities and biomass conversion processing for fuels and chemicals*. Energy Conversion and Management, 2001. **42**(11): p. 1357-1378.
50. Yoshida T, O.Y., Matsumura Y. , *Gasification of biomass model compounds and real biomass in supercritical water*. Biomass and Bioenergy, 2004. **26**(1): p. 71-80.
51. Saqib Sohail Toor, L.R., Andreas Rudolf, *Hydrothermal liquefaction of biomass: A review of subcritical water technologies*. Energy, 2011. **36**: p. 2328-2342.
52. Mars, A.E., et al., *Biohydrogen production from untreated and hydrolyzed potato steam peels by the extreme thermophiles Caldicellulosiruptor saccharolyticus and Thermotoga neapolitana*. International Journal of Hydrogen Energy, 2010. **35**(15): p. 7730-7737.
53. Yu, Y., X. Lou, and H. Wu, *Some Recent Advances in Hydrolysis of Biomass in Hot-Compressed Water and Its Comparisons with Other Hydrolysis Methods* Energy & Fuels, 2007. **22**(1): p. 46-60.
54. Yun Yu, X.L., Hongwei Wu, *Some recent advances in hydrolysis of biomass in hot compressed water and its comparisons with other hydrolysis methods*. Energy & fuels, 2008. **22**: p. 46-60.
55. Sun, Y., et al., *Clean conversion of cellulose into fermentable glucose*. Biotechnology Advances. **27**(5): p. 625-632.
56. Yunli Ren, J.W., Zhen Liu, Yunlai Ren, Guozhi Li, *Hydrogen production from the monomeric sugars hydrolyzed from hemicellulose by Enterobacter aerogenes*, 2009.
57. McCarthy Joseph, L. and A. Islam, *Lignin Chemistry, Technology, and Utilization: A Brief History*, in *Lignin: Historical, Biological, and Materials Perspectives* 1999, American Chemical Society. p. 2-99.
58. Ni, M., et al., *An overview of hydrogen production from biomass*. Fuel Processing Technology, 2006. **87**(5): p. 461-472.
59. Devi, L., K.J. Ptasinski, and F.J.J.G. Janssen, *A review of the primary measures for tar elimination in biomass gasification processes*. Biomass and Bioenergy, 2003. **24**(2): p. 125-140.
60. Garcia, L., et al., *CO<sub>2</sub> as a gasifying agent for gas production from pine sawdust at low temperatures using a Ni/Al coprecipitated catalyst*. Fuel Processing Technology, 2001. **69**(2): p. 157-174.
61. Teramae, T., *Effect of catalysis on tar elimination and gas production from fluidized bed gasification of biomass*. Kagaku Kogaku Ronbunshu, 2007. **33**(3): p. 246-256.
62. Li, X.T., et al., *Enhanced hydrogen production from circulating fluidized bed biomass gasification by double equilibrium shift*, in *Circulating Fluidized Bed Technology VIII*, K. Cen, Editor 2005. p. 499-506.
63. Tasaka, K., T. Furusawa, and A. Tsutsumi, *Biomass gasification in fluidized bed reactor with Co catalyst*. Chemical Engineering Science, 2007. **62**(18-20): p. 5558-5563.
64. Zuberbühler, U., *Gasification of bio-mass an overview on available technologies*, in *2nd European Summer School on Renewable Motor Fuels* 2007: Warsaw, Poland.
65. E4Tech, *Review of Technologies for Gasification of Biomass and Wastes*, 2009, UK National centre for renewable energy, fuels and materials (NNFCC).
66. Lin, S.-Y., et al., *Hydrogen Production from Hydrocarbon by Integration of Water–Carbon Reaction and Carbon Dioxide Removal (HyPr–RING Method)*. Energy & Fuels, 2001. **15**(2): p. 339-343.
67. Francis S. Lau, R.Z., and David A. Bowen, *Techno-Economic Analysis of Hydrogen Production by Gasification of Biomass*, 2003, U.S. DOE Hydrogen Program Review.
68. Kruse, A. and E. Dinjus, *Hot compressed water as reaction medium and reactant: Properties and synthesis reactions*. The Journal of Supercritical Fluids, 2007. **39**(3): p. 362-380.
69. Lu, Y.J., et al., *Thermodynamic modeling and analysis of biomass gasification for hydrogen production in supercritical water*. Chemical Engineering Journal, 2007. **131**(1-3): p. 233-244.

70. Matsumura, Y., et al., *Biomass gasification in near- and super-critical water: Status and prospects*. Biomass & Bioenergy, 2005. **29**(4): p. 269-292.
71. Kruse, A., et al., *Biomass Gasification in Supercritical Water: Influence of the Dry Matter Content and the Formation of Phenols*. Industrial & Engineering Chemistry Research, 2003. **42**(16): p. 3711-3717.
72. Takeshi Furusawa, T.S., Masanari Saito, Yasuyoshi Ishiyama, Masahide Sato, Naotsugu Itoh, Noboru Suzuki, *The evaluation of the stability of Ni/MgO catalysts for the gasification of lignin in supercritical water*. Elsevier Applied Catalysis A, 2007. **327**: p. 300-310.
73. Andrew A. Peterson , F.V., Russell P. Lachance , Morgan Fröling , Michael J. Antal, Jr. and Jefferson W. Tester *Thermochemical biofuel production in hydrothermal media: A review of sub- and supercritical water technologies* Energy & environmental science, 2008. **1**: p. 32-65.
74. Yoshida, T., Y. Oshima, and Y. Matsumura, *Gasification of biomass model compounds and real biomass in supercritical water*. Biomass and Bioenergy, 2004. **26**(1): p. 71-78.
75. Lu, Y.J., et al., *Hydrogen production by biomass gasification in supercritical water: A parametric study*. International Journal of Hydrogen Energy, 2006. **31**(7): p. 822-831.
76. Potic, B., et al., *A High-Throughput Screening Technique for Conversion in Hot Compressed Water*. Industrial & Engineering Chemistry Research, 2004. **43**(16): p. 4580-4584.
77. Minowa, T., F. Zhen, and T. Ogi, *Cellulose decomposition in hot-compressed water with alkali or nickel catalyst*. Journal of Supercritical Fluids, The, 1998. **13**(1-3): p. 253-259.
78. Minowa, T.Z., F.; Ogi, T.; Varhegyi, G., *Liquefaction of cellulose in hot compressed water using sodium carbonate: products distribution at different reaction temperatures*. Journal of Chemical Engineering of Japan, 1997. **30**(1).
79. Yanik, J., et al., *Biomass gasification in supercritical water: II. Effect of catalyst*. International Journal of Hydrogen Energy, 2008. **33**(17): p. 4520-4526.
80. Kruse, A. and A. Gawlik, *Biomass Conversion in Water at 330–410 °C and 30–50 MPa. Identification of Key Compounds for Indicating Different Chemical Reaction Pathways*. Industrial & Engineering Chemistry Research, 2002. **42**(2): p. 267-279.
81. Tomoaki Minowa, Z.F., Tomoko OGI and Gabor Varhegyi, *Decomposition of cellulose and glucose in hot-compressed water under catalyst-free conditions*. Journal of chemical engineering of Japan, 1998. **31**(1): p. 131-134.
82. Kimura, T., et al., *Development of Ni catalysts for tar removal by steam gasification of biomass*. Applied Catalysis B-Environmental, 2006. **68**(3-4): p. 160-170.
83. Furusawa, T., et al., *Hydrogen production from the gasification of lignin with nickel catalysts in supercritical water*. International Journal of Hydrogen Energy, 2007. **32**(6): p. 699-704.
84. Kruse, A., *Review: Supercritical water gasification*. Biofuels, Bioprod. Bioref., 2008. **2**: p. 415-437.
85. Yoshida, Y., et al., *Comprehensive comparison of efficiency and CO<sub>2</sub> emissions between biomass energy conversion technologies--position of supercritical water gasification in biomass technologies*. Biomass and Bioenergy, 2003. **25**(3): p. 257-272.
86. Babu, B.V., *Biomass pyrolysis: a state-of-the-art review*. Biofuels, Bioproducts & Biorefining. , 2008. **2**(5): p. 393-414.
87. Demirbas, A., *Gaseous products from biomass by pyrolysis and gasification: effects of catalyst on hydrogen yield*. Energy Conversion and Management, 2002. **43**(7): p. 897-909.
88. DEMIRBAS, A., *Production of Gasoline and Diesel Fuels from Bio-materials*. Energy Sources, 2007. **29**(Part A): p. 753-760.
89. Macaskie LE, B.-P.V., Creamer NJ, Humphries AC, Mikheenko IP, Mikheenko PM, Penfold DW, Yong P., *Applications of bacterial hydrogenases in waste decontamination, manufacture of novel bionanocatalysts and in sustainable energy*. Biochem Soc Trans, 2005. **33**: p. 76-9.

90. Redwood, M.D., Marion Paterson-Beedle, Lynne E. Macaskie, *Integrating dark and light bio-hydrogen production strategies: towards the hydrogen economy*, in *Reviews in environmental science & biotechnology* 2008.
91. Tsygankov, A., *Biological generation of hydrogen*. Russian Journal of General Chemistry, 2007. **77**(4): p. 685-693.
92. Wang, J. and W. Wan, *Factors influencing fermentative hydrogen production: A review*. International Journal of Hydrogen Energy, 2009. **34**(2): p. 799-811.
93. Hawkes, F.R., et al., *Fermentative production of hydrogen from a wheat flour industry co-product*. Bioresource Technology, 2008. **99**(11): p. 5020-5029.
94. Karlsson, A., L. Vallin, and J. Ejlertsson, *Effects of temperature, hydraulic retention time and hydrogen extraction rate on hydrogen production from the fermentation of food industry residues and manure*. International Journal of Hydrogen Energy, 2008. **33**(3): p. 953-962.
95. Kapdan, I.K. and F. Kargi, *Bio-hydrogen production from waste materials*. Enzyme and Microbial Technology, 2006. **38**(5): p. 569-582.
96. Ren, N., et al., *Biohydrogen production from molasses by anaerobic fermentation with a pilot-scale bioreactor system*. International Journal of Hydrogen Energy, 2006. **31**(15): p. 2147-2157.
97. Eroglu, E., et al., *Photobiological hydrogen production by using olive mill wastewater as a sole substrate source*. International Journal of Hydrogen Energy, 2004. **29**(2): p. 163-171.
98. Davila-Vazquez, G., et al., *Fermentative biohydrogen production: trends and perspectives*. Reviews in Environmental Science and Biotechnology, 2008. **7**(1): p. 27-45.
99. Das, D. and T.N. Veziroglu, *Hydrogen production by biological processes: a survey of literature*. International Journal of Hydrogen Energy, 2001. **26**(1): p. 13-28.
100. Redwood, M.D., *Bio-hydrogen production and biomass-supported palladium catalyst for energy production and waste minimization.*, in *PhD thesis, school of biosciences* 2007, University of Birmingham, UK.
101. Gest, P.H.a.H., *H<sub>2</sub> Metabolism in the Photosynthetic Bacterium Rhodospseudomonas capsulata: Production and Utilization of H<sub>2</sub> by Resting Cells*. Journal of bacteriology, 1977. **129**(2): p. 732-739.
102. Koku Harun, E.I., Gündüz Ufuk, Yücel Meral, Türker Lemi, *Aspects of the metabolism of hydrogen production by Rhodobacter sphaeroides*. International Journal of Hydrogen Energy, 2002. **27**(11-12): p. 1315-1329.
103. Hustede, E., A. Steinbüchel, and H.G. Schlegel, *Relationship between the photoproduction of hydrogen and the accumulation of PHB in non-sulphur purple bacteria*. Applied Microbiology and Biotechnology, 1993. **39**(1): p. 87-93.
104. Lee CM, C.P., Wang CC, and Tung YC *Photohydrogen production using purple nonsulfur bacteria with hydrogen fermentation reactor effluent*. Int J Hydrogen Energy, 2002. **27**((11-12)): p. 1309-1313.
105. Tao Y, C.Y., Wu Y, He Y, Zhou Z, *High hydrogen yield from a two step process of dark and photo fermentation of sucrose*. Int J Hydrogen Energy, 2007. **32**: p. 200-206.
106. Ivanovskii RN, K.n.E., Berg IA, *The mechanism of acetate assimilation in the purple nonsulfur bacterium Rhodospirillum rubrum lacking isocitrate lyase*. Microbiology, 1997. **66**(6): p. 621-626.
107. Redwood, M.D. and L.E. Macaskie, *A two-stage, two-organism process for biohydrogen from glucose*. International Journal of Hydrogen Energy, 2006. **31**(11): p. 1514-1521.
108. Sinha, P. and A. Pandey, *An evaluative report and challenges for fermentative biohydrogen production*. International Journal of Hydrogen Energy, 2011. **36**(13): p. 7460-7478.
109. Hallenbeck, P.C., *Fundamentals of the fermentative production of hydrogen*. Water Science and Technology, 2005. **52**(1-2): p. 21-29.
110. Ghosh, P.C.H.a.D., *Advances in fermentative biohydrogen production: the way forward?* Trends in biotechnology, 2009. **27**: p. 287-297.

111. Das, D.a.V., T. Nejat, *Advances in biological hydrogen production processes*. International Journal of Hydrogen Energy, 2008. **33**(21): p. 6046-6057.
112. Hawkes, F.R., et al., *Continuous dark fermentative hydrogen production by mesophilic microflora: Principles and progress*. International Journal of Hydrogen Energy, 2007. **32**(2): p. 172-184.
113. Hallenbeck, P.C. and J.R. Benemann, *Biological hydrogen production; fundamentals and limiting processes*. International Journal of Hydrogen Energy. **27**(11-12): p. 1185-1193.
114. Ghosh, P.C.H.a.D., *Advances in fermentative biohydrogen production: the way forward?* Trends in biotechnology, 2009. **27**(5): p. 287-297.
115. Wang, J. and W. Wan, *Comparison of different pretreatment methods for enriching hydrogen-producing bacteria from digested sludge*. International Journal of Hydrogen Energy, 2008. **33**(12): p. 2934-2941.
116. Kim, S.-H. and H.-S. Shin, *Effects of base-pretreatment on continuous enriched culture for hydrogen production from food waste*. International Journal of Hydrogen Energy, 2008. **33**(19): p. 5266-5274.
117. Smith JM, V.N.H., Abbott MM. *Introduction to chemical engineering thermodynamics Introduction to chemical engineering thermodynamics*2000: New York: MacGraw-Hill.
118. Valdez-Vazquez, I., et al., *Semi-continuous solid substrate anaerobic reactors for H<sub>2</sub> production from organic waste: Mesophilic versus thermophilic regime*. International Journal of Hydrogen Energy. **30**(13-14): p. 1383-1391.
119. de Vrije, T., et al., *Glycolytic pathway and hydrogen yield studies of the extreme thermophile <i>Caldicellulosiruptor saccharolyticus</i>*. Applied Microbiology and Biotechnology, 2007. **74**(6): p. 1358-1367.
120. Wang, J. and W. Wan, *Effect of Fe<sup>2+</sup> concentration on fermentative hydrogen production by mixed cultures*. International Journal of Hydrogen Energy, 2008. **33**(4): p. 1215-1220.
121. van Niel, E.W.J., P.A.M. Claassen, and A.J.M. Stams, *Substrate and product inhibition of hydrogen production by the extreme thermophile, Caldicellulosiruptor saccharolyticus*. Biotechnology and Bioengineering, 2003. **81**(3): p. 255-262.
122. Khanal, S.K., et al., *Biological hydrogen production: effects of pH and intermediate products*. International Journal of Hydrogen Energy, 2004. **29**(11): p. 1123-1131.
123. Clark, D.P., *The fermentation pathways of Escherichia coli*. FEMS Microbiology Letters, 1989. **63**(3): p. 223-234.
124. Redwood, M.D., Iryna P. Mikheenko, Frank Sargent & Lynne Macaskie, *Dissecting the roles of Escherichia coli hydrogenases in biohydrogen production*. FEMS Microbiology Letters, 2007: p. 1-8.
125. Penfold, D.W., C.F. Forster, and L.E. Macaskie, *Increased hydrogen production by Escherichia coli strain HD701 in comparison with the wild-type parent strain MC4100*. Enzyme and Microbial Technology, 2003. **33**(2-3): p. 185-189.
126. Guwy, A.J., et al., *Fermentative biohydrogen production systems integration*. Bioresource Technology, 2011. **102**(18): p. 8534-8542.
127. DiStefano, T.D. and A. Palomar, *Effect of anaerobic reactor process configuration on useful energy production*. Water Research, 2010. **44**(8): p. 2583-2591.
128. DEFRA, *Anaerobic digestion*, U.B.s. 2007, Editor 2007.
129. Intute, *Anaerobic digestion and biogas* 2007. p. 6.
130. Splendiani, A., C. Nicoletta, and A.G. Livingston, *A novel biphasic extractive membrane bioreactor for minimization of membrane-attached biofilms*. Biotechnology and Bioengineering, 2003. **83**(1): p. 8-19.
131. Banik, R.M., et al., *Technological aspects of extractive fermentation using aqueous two-phase systems*. World Journal of Microbiology and Biotechnology, 2003. **19**(4): p. 337-348.
132. Redwood M.D., O.R.L., Majewski A.J. and Macaskie L.E., *Electro extractive fermentation for efficient biohydrogen production*. Bioresource Technology, 2011: p. In submission.

133. Miyazawa, T., et al., *Solvothermal treatment of starch for the production of glucose and maltooligosaccharides*. Journal of Materials Science, 2006. **41**(5): p. 1489-1494.
134. Yokoi, H., et al., *Microbial production of hydrogen from starch-manufacturing wastes*. Biomass and Bioenergy, 2002. **22**(5): p. 389-395.
135. Mok, W.S., M.J. Antal, and G. Varhegyi, *Productive and parasitic pathways in dilute acid-catalyzed hydrolysis of cellulose*. Industrial & Engineering Chemistry Research, 2002. **31**(1): p. 94-100.
136. Duff, S.J.B. and W.D. Murray, *Bioconversion of forest products industry waste cellulose to fuel ethanol: A review*. Bioresource Technology, 1996. **55**(1): p. 1-33.
137. Melo, E. and J.F. Kennedy, *Cellulose hydrolysis (biotechnology monographs, Vol. 3) edited by L.-T. Fan, M. M. Gharpuray and Y.-H. Lee, Springer-Verlag, Berlin, Heidelberg, New York, London, Paris and Tokyo, 1987. pp. viii + 198, price DM168.00. ISBN 3-540-17671-3. British Polymer Journal, 1988. 20(6): p. 532-532.*
138. *Bioconversion of cellulosic substances into energy, chemicals and microbial protein: symposium proceedings, held at New Delhi, February 21-23, 1977 under the auspices of the Biochemical Engineering Research Centre, Indian Institute of Technology, Delhi and the Institute of Technology, Zurich 1978*, New Delhi: Indian Institute of Technology.
139. Hatakka, A.I., *Pretreatment of wheat straw by white-rot fungi for enzymic saccharification of cellulose*. Applied Microbiology and Biotechnology, 1983. **18**(6): p. 350-357.
140. Bioprocessing of agro-residues to glucose and chemicals. VS Bisaria, A.M.-B., 1991 - Elsevier Science Publishers Ltd.
141. Cheng, C.-L., et al., *Biohydrogen production from lignocellulosic feedstock*. Bioresource Technology, 2011. **In Press, Corrected Proof**.
142. Raj Kumar, S.S., Om V. Singh, *Bioconversion of lignocellulosic biomass: biochemical and molecular perspectives*. J Ind Microbiol Biotechnol, 2008. **35**: p. 377-391.
143. Chaplin, M. *The use of enzymes in starch hydrolysis*. 2004 20 December 2004 [cited 2011 12 September 2011]; Available from: <http://www.lsbu.ac.uk/biology/enztech/starch.html>.
144. Miyazawa, T.-F., T, *Polysaccharide Hydrolysis Accelerated by Adding Carbon Dioxide under Hydrothermal Conditions*. Biotechnology Progress, 2005. **21**(6).
145. Orozco, R.L., M. D. Redwood, Leeke G.A., Bahari A., Santos R.C.D., L. E. Macaskie, *Hydrothermal hydrolysis of starch with CO<sub>2</sub> and detoxification of the hydrolysates with activated carbon for biohydrogen fermentation*. Int Journal of Hydrogen Energy, 2011. **In submission**.
146. Liu, C. and C.E. Wyman, *Partial flow of compressed-hot water through corn stover to enhance hemicellulose sugar recovery and enzymatic digestibility of cellulose*. Bioresource Technology, 2005. **96**(18): p. 1978-1985.
147. Ando, H., et al., *Decomposition Behavior of Plant Biomass in Hot-Compressed Water*. Industrial & Engineering Chemistry Research, 2000. **39**(10): p. 3688-3693.
148. Paulien Harmsen, W.H., Laura Bermudez, Robert Bakker, *Literature review of physical and chemical pretreatment processes for lignocellulosic biomass*, 2010, Wageningen UR Food & Biobased Research.
149. HALVORSON, E.J.O.A.H., *A COMPARISON OF HYDROGEN PRODUCTION FROM SUGARS AND FORMIC ACID BY NORMAL AND VARIANT STRAINS OF ESCHERICHIA COLI*. J Bacteriol., 1939. **38**(2): p. 199-220.
150. RG, S., *Formate and its role in hydrogen production in Escherichia coli*. Biochemical society transactions, 2005. **33**: p. 42-46.
151. Rich, P., *The molecular machinery of Keilin's respiratory chain*, 2003, Glynn Laboratory of Bioenergetics, Department of Biology, University College London.
152. Hewitt, C.J., et al., *A comparison of high cell density fed-batch fermentations involving both induced and non-induced recombinant Escherichia coli under well-mixed small-scale and simulated poorly mixed large-scale conditions*. Biotechnology and Bioengineering, 2007. **96**(3): p. 495-505.

153. Chaplin MF, K.J., *Dinitrosalicylic acid assay in carbohydrate analysis; a practical approach*. Oxford:IRL Press, 1986.
154. Sode K, Y.S.T.M., ed. *Metabolic engineering approaches for the improvement of bacterial hydrogen production based on Escherichia coli mixed acid fermentation*. Biohydrogen II: An Approach to Environmentally Acceptable Technology, ed. M.T.S.P.A. Miyake J2001, Pergamon, Oxford, UK. 195-204.
155. Adams, R.F.H.a.S.S., *Determination of the Carbon-Bound Electron Composition of Microbial Cells and Metabolites by Dichromate Oxidation*. Appl Environ Microbiol, 1979. **37**(2): p. 237-243.
156. Pramanik J, K.J., *Stoichiometric model of Escherichia coli metabolism: incorporation of growth-rate dependent biomass composition and mechanistic energy requirements*. Biotechnol Bioeng, 1997. **56**(4): p. 398-421.
157. Bennett, G.N. and F.B. Rudolph, *The central metabolic pathway from acetyl-CoA to butyryl-CoA in Clostridium acetobutylicum*. FEMS Microbiology Reviews, 1995. **17**(3): p. 241-249.
158. San, Y.-T.Y.a.K.-Y., *Redistribution of Metabolic Fluxes in Escherichia coli with Fermentative Lactate Dehydrogenase Overexpression and Deletion*. 1999. **1**: p. 141-152.
159. Sara Castaño-Cerezo, J.M.P., Sergio Renilla, Vicente Bernal, José L Iborra and Manuel Cánovas, *An insight into the role of phosphotransacetylase (pta) and the acetate/acetyl-CoA node in Escherichia coli*. Microbial Cell Factories, 2009. **8**: p. 19.
160. Chaplin, M.F., *Monosaccharides (section 2.2.2)*, in *Carbohydrate analysis: a practical approach*, M.F. Chaplin and J.F. Kennedy, Editors. 1986, IRL Press at Oxford University press, UK. p. 324.
161. Clerici A, C.A., Trinnaman JA, Nekhaev EV., *Survey of energy resources*. 20th ed, ed. C.A. Trimaman Judy2004: Elsevier Ltd. 1-464.
162. Dogaris, I., et al., *Hydrothermal processing and enzymatic hydrolysis of sorghum bagasse for fermentable carbohydrates production*. Bioresource Technology, 2009. **100**(24): p. 6543-6549.
163. Kamio, E., et al., *Effect of heating rate on liquefaction of cellulose by hot compressed water*. Chemical Engineering Journal, 2008. **137**(2): p. 328-338.
164. Sakaki, T., et al., *Decomposition of Cellulose in Near-Critical Water and Fermentability of the Products*. Energy & Fuels, 1996. **10**(3): p. 684-688.
165. Deguchi, S., K. Tsujii, and K. Horikoshi, *Cooking cellulose in hot and compressed water*. Chemical Communications, 2006(31): p. 3293-3295.
166. Sasaki, M., et al., *Dissolution and Hydrolysis of Cellulose in Subcritical and Supercritical Water*. Industrial & Engineering Chemistry Research, 2000. **39**(8): p. 2883-2890.
167. Sasaki, M., et al., *Cellulose hydrolysis in subcritical and supercritical water*. Journal of Supercritical Fluids, The, 1998. **13**(1-3): p. 261-268.
168. Sinağ, A., A. Kruse, and J. Rathert, *Influence of the Heating Rate and the Type of Catalyst on the Formation of Key Intermediates and on the Generation of Gases During Hydrolysis of Glucose in Supercritical Water in a Batch Reactor*. Industrial & Engineering Chemistry Research, 2003. **43**(2): p. 502-508.
169. Kamio, E., et al., *Liquefaction of cellulose in hot compressed water under variable temperatures*. Industrial & Engineering Chemistry Research, 2006. **45**(14): p. 4944-4953.
170. Orozco, R.L., M. D. Redwood, P. Yong, I. Caldelari, F. Sargent, L. E. Macaskie, *Towards an integrated system for bio-energy: hydrogen production by Escherichia coli and use of palladium-coated waste cells for electricity generation in a fuel cell*. Biotechnol Letters, 2010.
171. Zhang, T., H. Liu, and H.H.P. Fang, *Biohydrogen production from starch in wastewater under thermophilic condition*. Journal of Environmental Management, 2003. **69**(2): p. 149-156.
172. Levin, D.B., et al., *Hydrogen production by Clostridium thermocellum 27405 from cellulosic biomass substrates*. International Journal of Hydrogen Energy, 2006. **31**(11): p. 1496-1503.

173. Tirzah Y Mills, N.R.S.a.R.T.G., *Cellulosic hydrolysate toxicity and tolerance mechanisms in Escherichia coli*. Biotechnology for biofuels, 2009. **2**: p. 11.
174. Palmqvist, E. and B. Hahn-Hägerdal, *Fermentation of lignocellulosic hydrolysates. I: inhibition and detoxification*. Bioresource Technology, 2000. **74**(1): p. 17-24.
175. Hodge, D.B., et al., *Detoxification requirements for bioconversion of softwood dilute acid hydrolysates to succinic acid*. Enzyme and Microbial Technology, 2009. **44**(5): p. 309-316.
176. Saeman, J.F., J.L. Bubl, and E.E. Harris, *Quantitative Saccharification of Wood and Cellulose*. Industrial & Engineering Chemistry Analytical Edition, 2002. **17**(1): p. 35-37.
177. Sasikala, C.H., C.H.V. Ramana, and P.R. Rao, *Regulation of simultaneous hydrogen photoproduction during growth by pH and glutamate in Rhodospirillum rubrum*. International Journal of Hydrogen Energy, 1995. **20**(2): p. 123-126.
178. Dehui Yu, M.A., and Michael Jerry Antal, Jr., *Hydrogen Production by Steam Reforming Glucose in Supercritical Water*. Energy & Fuels, 1993. **7**: p. 574-577.
179. Lu, Y.J., L.J. Guo, and X.M. Zhang, *Thermodynamic modeling and analysis of hydrogen production process by biomass gasification in supercritical water*. Abstracts of Papers of the American Chemical Society, 2006. **231**: p. 9-PETR.
180. Energy, U.S.D.o., *Projected benefits of federal energy efficiency and renewable energy programs, 2007*. [http://www1.eere.energy.gov/ba/pba/gpra\\_estimates\\_fy07.html](http://www1.eere.energy.gov/ba/pba/gpra_estimates_fy07.html), 2007.
181. Milliken JoAnn, M.C.L., Sink Carl, Kung harriet, Breed Patricia, Lawson Linda et al, *Hydrogen posture plan*, 2006. p. 1-82.
182. DEFRA, *Anaerobic Digestion Strategy and Action Plan 2011*, Department for Environment, Food and Rural Affairs (DEFRA). p. 1-56.
183. Shin, H.-s. and J.-h. Youn, *Conversion of food waste into hydrogen by thermophilic acidogenesis*. Biodegradation, 2005. **16**(1): p. 33-44.
184. Palmqvist, E. and B. Hahn-Hägerdal, *Fermentation of lignocellulosic hydrolysates. II: inhibitors and mechanisms of inhibition*. Bioresource Technology, 2000. **74**(1): p. 25-33.
185. Zaldivar, J., A. Martinez, and L.O. Ingram, *Effect of selected aldehydes on the growth and fermentation of ethanologenic Escherichia coli*. Biotechnology and Bioengineering, 1999. **65**(1): p. 24-33.
186. Walker, M., et al., *Potential errors in the quantitative evaluation of biogas production in anaerobic digestion processes*. Bioresource Technology, 2009. **100**: p. 6339-6346.
187. Keweloh, H., R. Diefenbach, and H.-J. Rehm, *Increase of phenol tolerance of Escherichia coli by alterations of the fatty acid composition of the membrane lipids*. Archives of Microbiology, 1991. **157**(1): p. 49-53.
188. E.N. Miller, L.R.J., L.P. Yomano, S.W. York, K.T. Shanmugam, and L.O. Ingram, *Silencing of NADPH-Dependent Oxidoreductase Genes (yqhD and dkgA) in Furfural-Resistant Ethanologenic Escherichia coli*. Applied and Environmental Microbiology, 2009. **75**(13): p. 4315-4323.
189. Wiseloge A., T.S., Johnson D., *Biomass feedstock resources and composition*, in *Handbook on bioethanol: production and utilization*, W.C.E. (Ed), Editor 1996. p. 105-118.
190. Sato, N., et al., *Reaction Kinetics of Amino Acid Decomposition in High-Temperature and High-Pressure Water*. Industrial & Engineering Chemistry Research, 2004. **43**(13): p. 3217-3222.
191. Kruse, A., et al., *Influence of Proteins on the Hydrothermal Gasification and Liquefaction of Biomass. 1. Comparison of Different Feedstocks*. Industrial & Engineering Chemistry Research, 2005. **44**(9): p. 3013-3020.
192. Orozco R.L., R.M.D., Leeke G.A., Majewski A., Santos R.C.D. and Macaskie L.E., *Bio-hydrogen production by E. coli HD701 following hot compressed water hydrolysis of cellulose under N<sub>2</sub> and CO<sub>2</sub>*. Journal of Chemical Technology and Biotechnology, 2011: p. In submission.

193. Redwood, M.D., M. Paterson-Beedle, and L.E. Macaskie, *Integrating dark and light biohydrogen production strategies: towards the hydrogen economy*. Rev. Environ. Sci. Bio/Technol., 2009. **8**(2): p. 149-185.
194. Macaskie, L.E., et al., *Applications of bacterial hydrogenases in waste decontamination, manufacture of novel bionanocatalysts and in sustainable energy*. Biochemical Society Transactions, 2005. **33**(Pt 1): p. 76-9.
195. de Vrije, T. and P.A.M. Claassen, *Dark hydrogen fermentations*, in *Bio-methane & Bio-hydrogen*, J.H. Reith, R.H. Wijffels, and H. Barten, Editors. 2003, Dutch Biological Hydrogen Foundation: Petten, Netherlands. p. 103-123.
196. Bartacek, J., J. Zabranska, and P.N.L. Lens, *Developments and constraints in fermentative hydrogen production*. Biofuels, Bioproducts and Biorefining, 2007. **1**: p. 201–214.
197. Hallenbeck, P.C. and D. Ghosh, *Advances in fermentative biohydrogen production: the way forward?* Trends in Biotechnology, 2009. **27**(5): p. 287-297.
198. Sode, K., S. Yamamoto, and M. Tomiyama, *Metabolic engineering approaches for the improvement of bacterial hydrogen production based on Escherichia coli mixed acid fermentation*, in *Biohydrogen II : An Approach to Environmentally Acceptable Technology*, J. Miyake, T. Matsunaga, and A. San Pietro, Editors. 2001, Pergamon. p. 195-204.
199. Redwood, M.D., et al., *Dissecting the roles of E. coli hydrogenases in biohydrogen production*. FEMS Microbiology Letters, 2008. **278**: p. 48-55.
200. Warnecke, T. and R.T. Gill, *Organic acid toxicity, tolerance, and production in Escherichia coli biorefining applications*. Microbial Cell Factories, 2005. **4**: p. 25.
201. Bisailon, A., J. Turcot, and P.C. Hallenbeck, *The effect of nutrient limitation on hydrogen production by batch cultures of Escherichia coli*. International Journal of Hydrogen Energy, 2006. **31**: p. 1504-1508.
202. Show, K.Y., et al., *Critical assessment of anaerobic processes for continuous biohydrogen production from organic wastewater*. International Journal of Hydrogen Energy, 2010. **35**(24): p. 13350-13355.
203. Du, Z., H. Li, and T. Gu, *A state of the art review on microbial fuel cells: A promising technology for wastewater treatment and bioenergy*. Biotechnology Advances, 2007. **25**: p. 464–482.
204. Logan, B.E., et al., *Microbial electrolysis cells for high yield hydrogen gas production from organic matter*. Environmental Science and Technology, 2008. **42**(23): p. 8630-8640.
205. Mustacchi, R., et al., *Enhanced biotransformations and product recovery in a membrane bioreactor through application of a direct current*. Biotechnology and Bioengineering, 2005. **89**(1): p. 18-23.
206. Chukwu, U.N. and M. Cheryan, *Electrodialysis of acetate fermentation broths*. Applied Biochemistry and Biotechnology, 1999. **78**(1-3): p. 485-499.
207. Zhang, S.-T., H. Matsuoka, and K. Toda, *Production and recovery of propionic and acetic acids in electrodialysis culture of Propionibacterium shermanii*. Journal of Fermentation and Bioengineering, 1993. **75**: p. 276-282.
208. Pal, P., et al., *Process intensification in lactic acid production: A review of membrane based processes*. Chemical Engineering and Processing: Process Intensification, 2009. **48**(11-12): p. 1549-1559.
209. Schügerl, K. and J. Hubbuch, *Integrated bioprocesses*. Current Opinion in Microbiology, 2005. **8**(3): p. 294-300.
210. Xu, T.W., et al., *Application of electrodialysis to the production of organic acids: State-of-the-art and recent developments*. Journal of Membrane Science, 2007. **288**(1-2): p. 1-12.
211. Reahl, E.R. *Half a century of desalination with electrodialysis*. [www.gewater.com](http://www.gewater.com), accessed Aug 2011. 2007.
212. Xu, T.W., *Ion exchange membranes: State of their development and perspective*. Journal of Membrane Science, 2005. **263**(1-2): p. 1-29.

213. Li, H., et al., *An electrokinetic bioreactor: using direct electric current for enhanced lactic acid fermentation and product recovery*. Tetrahedron, 2004. **60**: p. 655-661.
214. Nomura, Y., M. Iwahara, and M. Hongo, *Acetic acid production by an electrodialysis fermentation method with a computerized control system*. Applied and Environmental Microbiology, 1988. **54**(1): p. 137-142.
215. Madzingaidzo, L., H. Danner, and R. Braun, *Process development and optimisation of lactic acid purification using electrodialysis*. Journal of Biotechnology, 2002. **96**(3): p. 223-239.
216. Zelic, B., et al., *Process strategies to enhance pyruvate production with recombinant Escherichia coli: From repetitive fed-batch to in situ product recovery with fully integrated electrodialysis*. Biotechnology and Bioengineering, 2004. **85**(6): p. 638-646.
217. Lugg, H., et al., *Polyhydroxybutyrate accumulation by a Serratia sp.*. Biotechnology Letters, 2008. **30**(3): p. 481-491.
218. Kyazze, G., et al., *Influence of substrate concentration on the stability and yield of continuous biohydrogen production*. Biotechnology and Bioengineering, 2006. **93**: p. 971-979.
219. Ordal, E.J. and H.O. Halvorson, *A comparison of hydrogen production from sugars and formic acid by normal and variant strains of Escherichia coli*. Journal of Bacteriology, 1939. **38**: p. 199-220.
220. Zaldivar, J. and L.O. Ingram, *Effect of organic acids on the growth and fermentation of ethanologenic Escherichia coli LY01*. Biotechnology and Bioengineering, 1999. **66**(4): p. 203-210.
221. Clark, D.P., *The fermentation pathways of Escherichia coli*. FEMS Microbiology Reviews, 1989. **5**(3): p. 223-234.
222. Yoshida, A., et al., *Efficient induction of formate hydrogen lyase of aerobically grown Escherichia coli in a three-step biohydrogen production process*. Applied Microbiology and Biotechnology, 2007. **74**: p. 754-760.
223. Gest, H., *Oxidation and evolution of molecular hydrogen by microorganisms*. Microbiology and Molecular Biology Reviews, 1954. **18**: p. 43-73.
224. Penfold, D.W., F. Sargent, and L.E. Macaskie, *Inactivation of the Escherichia coli K-12 twin arginine translocation system promotes increased hydrogen production*. FEMS Microbiology Letters, 2006. **262**: p. 135-137.
225. Orozco, R.L., et al., *Hydrothermal hydrolysis of starch with CO<sub>2</sub> and detoxification of the hydrolysates with activated carbon for bio-hydrogen fermentation*. International Journal of Hydrogen Energy, 2011. **in submission**.
226. Hewitt, C.J., et al., *Studies related to the scale-up of high-cell-density E. coli fed-batch fermentations using multiparameter flow cytometry: Effect of a changing microenvironment with respect to glucose and dissolved oxygen concentration*. Biotechnology and Bioengineering, 2000. **70**(4): p. 381-390.
227. Logan, B.E., *Extracting hydrogen and electricity from renewable resources*. Environmental Science and Technology, 2004. **38**(9): p. 161A-167A.
228. M.A., W., *Chemical Engineering Problems in Biotechnology*, ed. W. M.A. Vol. 29. 1990, Essex, England: ELSEVIER SCIENCE PUBLISHERS LTD. 370.
229. Christopher J. Hewitt, G.N.-V.C., Britta Axelsson, Caroline M. McFarlane, Alvin W. Nienow, *Studies Related to the Scale-Up of High-Cell-Density E. coli Fed-Batch Fermentations Using Multiparameter Flow Cytometry: Effect of a Changing Microenvironment with Respect to Glucose and Dissolved Oxygen Concentration*. Biotechnol Bioeng, 2000. **70**: p. 381-390.
230. Lehninger, A.L., *Biochemistry*. Second ed 1976, New York: Worth Publishers, Inc.
231. Ariane Bisailon, J.T., and Patrick C. Hallenbeck, *The Effect of Nutrient Limitation on Hydrogen Production by Escherichia coli*. International Journal of Hydrogen Energy, 2006. **31**: p. 1504-1508.
232. Madhav Prasad Pandey, C.S.K., *Lignin Depolymerization and Conversion: A Review of Thermochemical Methods*. Chemical Engineering and Technology, 2010. **34**(1): p. 29-41.

233. Casanova, O., S. Iborra, and A. Corma, *Biomass into Chemicals: Aerobic Oxidation of 5-Hydroxymethyl-2-furfural into 2,5-Furandicarboxylic Acid with Gold Nanoparticle Catalysts*. ChemSusChem, 2009. **2**(12): p. 1138-1144.
234. Wikipedia. *2,5-Furandicarboxylic acid*. 2011 13 September 2011 [cited 2011 25 September 2011]; Available from: [http://en.wikipedia.org/wiki/2,5-Furandicarboxylic\\_acid](http://en.wikipedia.org/wiki/2,5-Furandicarboxylic_acid).
235. Ribeiro, M.L. and U. Schuchardt, *Cooperative effect of cobalt acetylacetonate and silica in the catalytic cyclization and oxidation of fructose to 2,5-furandicarboxylic acid*. Catalysis Communications, 2003. **4**(2): p. 83-86.
236. Deplanche, K., *New nanocatalysts made by bacteria from metal solutions and recycling of metal wastes*, in *School of Biosciences 2009*, University of Birmingham: Birmingham, U.K.
237. James Dumesic, J.B. *Engineers develop higher-energy liquid-transportation fuel from sugar*. 2007 June 20, 2007 [cited 2011 September 25]; Available from: <http://www.physorg.com/news101566361.html>.
238. Shota Atsumi, A.F.C., Michael R. Connor, Claire R. Shen, Kevin M. Smith, Mark P. Brynildsen, Katherine J.Y. Chou, Taizo Hanai, James C. Liao, *Metabolic engineering of Escherichia coli for 1-butanol production*. Metabolic Engineering, 2008. **10**: p. 305-311.
239. Michael Malveda, T.K.a.K.Y. *Furfural*. 2011 August 2011 [cited 2011 September 25]; Available from: <http://www.sriconsulting.com/CEH/Public/Reports/660.5000/>.
240. Services, W.B.a.T., *Furfural Chemicals and Biofuels from Agriculture*, 2006, Rural Industries Research and Development Corporation: Sydney, NSW, AUSTRALIA.
241. Abo-Hashesh, M., et al., *Single stage photofermentative hydrogen production from glucose: An attractive alternative to two stage photofermentation or co-culture approaches*. Int. J. Hydrog. Energy, 2011. **In press**.
242. Afsar, N., et al., *Hydrogen productivity of photosynthetic bacteria on dark fermenter effluent of potato steam peels hydrolysate*. Int. J. Hydrog. Energy, 2011. **36**(1): p. 432-438.
243. Argun, H. and F. Kargi, *Bio-hydrogen production by different operational modes of dark and photo-fermentation: An overview*. Int. J. Hydrog. Energy, 2011. **36**(13): p. 7443-7459.
244. Avcioglu, S.G., et al., *Biohydrogen production in an outdoor panel photobioreactor on dark fermentation effluent of molasses*. International Journal of Hydrogen Energy, 2011. **In press**.
245. Chu, C.-Y., et al., *Biohydrogen production from immobilized cells and suspended sludge systems with condensed molasses fermentation solubles*. International Journal of Hydrogen Energy, 2011. **In press**.
246. Lo, Y.-C., et al., *Photo fermentative hydrogen production using dominant components (acetate, lactate, and butyrate) in dark fermentation effluents*. International Journal of Hydrogen Energy, 2011. **In press**.
247. Özgür, E., et al., *Biohydrogen production from beet molasses by sequential dark and photofermentation*. International Journal of Hydrogen Energy, 2011. **35**(2): p. 511-517.
248. Kyazze, G., et al., *Performance characteristics of a two-stage dark fermentative system producing hydrogen and methane continuously*. Biotechnology and Bioengineering, 2007. **97**(4): p. 759-770.
249. Martínez-Pérez, N., et al., *The potential for hydrogen-enriched biogas production from crops: Scenarios in the UK*. Biomass and Bioenergy, 2007. **31**(2-3): p. 95-104.
250. Kyazze, G., et al., *Influence of catholyte pH and temperature on hydrogen production from acetate using a two chamber concentric tubular microbial electrolysis cell*. International Journal of Hydrogen Energy, 2010. **35**(15): p. 7716-7722.
251. Guwy, A.J., et al., *Fermentative biohydrogen production systems integration*. Bioresour. Technol., 2011. **In press**.
252. Redwood, M.D., et al., *An integrated biohydrogen refinery: Synergy of photofermentation, extractive fermentation and hydrothermal hydrolysis of food wastes*. Environmental Science & Technology, 2011. **in submission (Aug 2011)**.

253. Chen, C.Y., et al., *Biohydrogen production using sequential two-stage dark and photo fermentation processes*. International Journal of Hydrogen Energy, 2008. **33**(18): p. 4755-4762.
254. Redwood, M.D., et al., *Electro-extractive fermentation for efficient biohydrogen production*. Bioresource Technology, 2011. **in submission**.
255. Tseng, P., J. Lee, and P. Friley, *A hydrogen economy: opportunities and challenges*. Energy, 2005. **30**(14): p. 2703-2720.
256. Claassen, P.A.M., et al., *Utilisation of biomass for for the supply of energy carriers*. Applied Microbiology and Biotechnology, 1999. **52**: p. 741-755.
257. Tao, Y., et al., *Characteristics of a new photosynthetic bacterial strain for hydrogen production and its application in wastewater treatment*. International Journal of Hydrogen Energy, 2008. **33**(3): p. 963-973.
258. Hoekema, S., et al., *A pneumatically agitated flat-panel photobioreactor with gas re-circulation: anaerobic photoheterotrophic cultivation of a purple non-sulfur bacterium*. International Journal of Hydrogen Energy, 2002. **27**(11-12): p. 1331-1338.
259. Eroğlu, E., et al., *Photobiological hydrogen production by using olive mill wastewater as a sole substrate source*. International Journal of Hydrogen Energy, 2004. **29**: p. 163-171.
260. Ormerod, J.G. and H. Gest, *Hydrogen photosynthesis and alternative metabolic pathways in photosynthetic bacteria*. Bacteriological Reviews, 1962. **26**: p. 51-66.
261. Orozco, R.L., et al., *Towards an integrated system for bio-energy: Hydrogen production by Escherichia coli and use of palladium-coated waste cells for electricity generation in a fuel cell*. Biotechnology Letters, 2010. **32**: p. 1837-1845.
262. Chaplin, M.F., *Monosaccharides*, in *Carbohydrate analysis: a practical approach*, M.F. Chaplin and J.F. Kennedy, Editors. 1986, IRL Press at Oxford University press, UK. p. 324.
263. Birch, G.G. and R.J. Priestley, *Degree of gelatinisation of cooked rice*. Starch - Stärke, 1973. **25**(3): p. 98-100.
264. Saeman, J.F., J.L. Bubl, and E.E. Harris, *Quantitative saccharification of wood and cellulose*. Industrial & Engineering Chemistry Analytical Edition, 1945. **17**(1): p. 35-37.
265. Miyazawa, T. and T. Funazukuri, *Polysaccharide hydrolysis accelerated by adding carbon dioxide under hydrothermal conditions*. Biotechnology Progress, 2005. **21**(6): p. 1782-1785.
266. Penfold, D.W. and L.E. Macaskie, *Production of H<sub>2</sub> from sucrose by Escherichia coli strains carrying the pUR400 plasmid, which encodes invertase activity*. Biotechnology Letters, 2004. **26**: p. 1879-1883.
267. Boos, W. and H. Shuman, *Maltose/maltodextrin system of Escherichia coli: transport, metabolism and regulation*. Microbiol Mol Biol Rev, 1998. **62**(1): p. 204-29.
268. Redwood, M.D., *Bio-hydrogen and biomass supported palladium catalyst for energy production and waste minimisation*. Ph.D. Thesis, 2007, University of Birmingham.
269. Akkerman, I., et al., *Photobiological hydrogen production: photochemical efficiency and bioreactor design*. International Journal of Hydrogen Energy, 2002. **27**(11-12): p. 1195-1208.
270. Rocha, J.S., M.J. Barbosa, and R.H. Wijffels, *Hydrogen production by photoheterotrophic bacteria: Culture media, yields and efficiencies*, in *Biohydrogen II : An Approach to Environmentally Acceptable Technology*, J. Miyake, T. Matsunaga, and A. San Pietro, Editors. 2001, Pergamon. p. 3-32.
271. Sasikala, C.H., C.V. Ramana, and P.R. Rao, *Regulation of simultaneous hydrogen photoproduction during growth by pH and glutamate in Rhodobacter sphaeroides O.U. 001*. International Journal of Hydrogen Energy, 1995. **20**(2): p. 123-126.
272. Anon, *Department of Energy & Climate Change (DECC). Feed-in tariffs scheme: Summary of responses to the fast-track consultation and Government response, 9 June 2011*.
273. Anon, *Waste & Resources Action Programme (WRAP). Gate Fees Report. Comparing the cost of alternative waste treatment options, July 2010*.

274. Anon, *Department of Energy and Climate Change (DECC) and Department for Environment Food and Rural Affairs (Defra). Anaerobic digestion strategy and action plan. Report number PB 13541, June 2011.*
275. Jogwar, S.S., M. Baldea, and P. Daoutidis. *Dynamics and control of reactor - Feed effluent heat exchanger networks. Paper reference WeC08.2 in Proceedings of the American Control Conference. Westin Seattle Hotel, Seattle, Washington, USA. 2008.*
276. Chen, Y.-H. and C.-C. Yu, *Design and control of heat-integrated reactors.* Industrial & Engineering Chemistry Research, 2003. **42**(12): p. 2791-2808.
277. Cumiskey, A., M. Dawson, and M. Tillotson, *Thick sludge digestion - Research, design and validation of key process unit operations.*, in *Residuals and Biosolids 2002*: Baltimore, Maryland USA.
278. Karim, K., et al., *Anaerobic digestion of animal waste: Waste strength versus impact of mixing.* Bioresource Technology, 2005. **96**(16): p. 1771-1781.
279. Lee, S.R., N.M. Cho, and W.J. Maeng, *Using the pressure of biogas created during anaerobic digestion as the source of mixing power.* Journal of Fermentation and Bioengineering, 1995. **80**(4): p. 415-417.
280. Mills, P.J., *Minimisation of energy input requirements of an anaerobic digester.* Bioresource Technology, 1979. **1**(1): p. 57-66.
281. Burgess, G. and J.G. Fernandez-Velasco, *Materials, operational energy inputs, and net energy ratio for photobiological hydrogen production.* International Journal of Hydrogen Energy, 2007. **32**: p. 1255-1234.
282. Šuri, M., et al., *Potential of solar electricity generation in the European Union member states and candidate countries.* Solar Energy, 2007. **81**(10): p. 1295-1305.
283. Levin, D.B., L. Pitt, and M. Love, *Biohydrogen production: prospects and limitations to practical application.* International Journal of Hydrogen Energy, 2004. **29**: p. 173-185.
284. Anon, *Waste & Resources Action Programme (WRAP). Gate Fees Report. Comparing the cost of alternative waste treatment options. Available from [www.wrap.org.uk](http://www.wrap.org.uk). July 2010.*
285. Sun, Q., et al., *Statistical optimization of biohydrogen production from sucrose by a co-culture of Clostridium acidisoli and Rhodobacter sphaeroides.* International Journal of Hydrogen Energy, 2010. **35**(9): p. 4076-4084.
286. Lui, H., S. Grot, and B.E. Logan, *Electrochemically assisted microbial production of hydrogen from acetate.* Environmental Science and Technology, 2005. **39**: p. 4317-4320.
287. Cheng, S. and B.E. Logan, *Sustainable and efficient biohydrogen production via electrohydrogenesis.* Proceedings of the National Academy of Sciences of the United States of America, 2007. **104**(47): p. 18871-18873.
288. Sun, M., et al., *An MEC-MR-coupled system for biohydrogen production from acetate.* Environmental Science & Technology, 2008. **42**(21): p. 8095-8100.
289. Uwe, S., *From wastewater to hydrogen: Biorefineries based on microbial fuel-cell technology.* ChemSusChem, 2008. **1**(4): p. 281-282.
290. Call, D. and B.E. Logan, *Hydrogen production in a single chamber microbial electrolysis cell lacking a membrane.* Environmental Science & Technology, 2008. **42**(9): p. 3401-3406.
291. Clauwaert, P., et al., *Combining biocatalyzed electrolysis with anaerobic digestion.* Water Science and Technology, 2008. **57**(4): p. 575-579.
292. Limmeechokchai, B. and S. Chawana, *Sustainable energy development strategies in the rural Thailand: The case of the improved cooking stove and the small biogas digester.* Renewable & Sustainable Energy Reviews, 2007. **11**(5): p. 818-837.
293. Redman, G., *National Non-Food Crops Centre (NNFCC) and The Anderson Centre. Economic assessment of anaerobic digestion technology and its suitability to UK farming and waste systems: AD cost calculator (Tool). Report number 10-010, 30 Jun 2011.*

294. MacKay, D.J.C., *Sustainable Energy - without the hot air*. Vol. ISBN 978-0-9544529-3-3. Available free online from [www.withouthotair.com](http://www.withouthotair.com). 2008: UIT Cambridge.
295. Yong, P., et al., *Biorefining of precious metals from wastes: An answer to manufacturing of cheap nanocatalysts for fuel cells and power generation via an integrated biorefinery?* *Biotechnology Letters*, 2010. **32**: p. 1821–1828.
296. Sasikala, K., et al., *Anoxygenic phototrophic bacteria : Physiology and advances in hydrogen production technology*. *Advances in Applied Microbiology*, 1995. **38**: p. 211-295.
297. Koku, H., et al., *Kinetics of biological hydrogen production by the photosynthetic bacterium Rhodobacter sphaeroides O.U. 001*. *International Journal of Hydrogen Energy*, 2003. **28**: p. 381-388.